UC Riverside

UC Riverside Electronic Theses and Dissertations

Title

Functional Analysis of CDC13 Regulation in Budding Yeast

Permalink

https://escholarship.org/uc/item/7x01z8dr

Author

Small, Vanessa Yolanda

Publication Date

2010

Peer reviewed|Thesis/dissertation

eScholarship.org Powered by the California Digital Library
University of California

UNIVERSITY OF CALIFORNIA
RIVERSIDE

Functional Analysis of *CDC13* Regulation in Budding Yeast

A Dissertation submitted in partial satisfaction
of the requirements for the degree of

Doctor of Philosophy

in

Cell, Molecular, and Developmental Biology

by

Vanessa Yolanda Small

December 2010

Dissertation Committee:
Dr. Constance Nugent, Chairperson
Dr. Katherine Borkovich
Dr. Jeff Bachant

Copyright by
Vanessa Yolanda Small
2010

The Dissertation of Vanessa Yolanda Small is approved:

_____

_____

_____

Committee Chairperson

University of California, Riverside

ACKNOWLEDGEMENTS

I would like to thank Connie for her support and patience throughout the years. I appreciate her advice and help during my Ph.D training. I also would like to thank Jeff Bachant and Katherine Borkovich for serving on my guidance committee and my dissertation committee. I would like to thank Charles Chuang, Holly Eckelhoefer, and Phoebe Chiu for their work on the projects presented in this dissertation. I would like to thank all the members in Nugent lab and the Bachant lab. They have been my family here in Riverside, and have made my graduate experience a memorable one.

I want to thank my family members and friends that have supported and encouraged me through all these years. I would like to say a special thanks to my mother Violet Small, my sisters Karlita and Francine, and my best friend Wynette Venkersammy for being always there for me. Your love and support has been invaluable during my graduate school career.

Some of the text and figures in this dissertation is a reprint of material that has been published in : Small, V., Chuang, C., & Nugent, C. (2008). Rad24 truncation, coupled with altered telomere structure, promotes *cdc13-1* suppression in S. cerevisiae. *Cell Cycle, 7*(21), 3428-3439.

ABSTRACT OF THE DISSERTATION

Functional Analysis of *CDC13* Regulation in Budding Yeast

by

Vanessa Yolanda Small

Doctor of Philosophy, Graduate Program in Cell, Molecular, and Developmental Biology
University of California, Riverside, December 2010
Dr. Constance Nugent, Chairperson

Telomeres are DNA–protein complexes that maintain the integrity of linear chromosomes. Telomeres protect the chromosome ends from being recognized as a DNA double strand break by the DNA damage checkpoint, and prevent chromosome rearrangements. Hence, telomeres are crucial to defending against genomic instability, a hallmark of cancer cells. The work presented in this dissertation will focus on the regulation of activities involving the essential telomeric DNA binding protein Cdc13. In *S. cerevisiae*, the single-strand telomere binding protein Cdc13 is important for protecting chromosome ends. Previous studies indicate a role for Cdc13 in both telomere end protection and recruitment of telomerase to the telomere. The role of *CDC13* in telomere end protection has been elucidated using the temperature sensitive allele, *cdc13-1*. In *cdc13-1* mutants the C-rich telomere strand is lost when cells are grown at high temperatures. The accumulation of single-stranded DNA at the telomere leads to a DNA damage checkpoint response and loss of cell viability. We describe a screen conducted to identify activities involved in telomere C-strand loss,

in which we identified two novel alleles of *RAD24*. Rad24 is an alternate Rfc1 subunit, and functions to load the 9-1-1 checkpoint clamp onto sites of DNA damage. In each *rad24* allele, the transposon used in the screen is inserted within the *RAD24* coding region and results in production of two amino terminal truncations of Rad24. Here, we show that an intact Rad24 amino-terminus is necessary for its checkpoint function. The *rad24-2* allele increases the frequency of obtaining *cdc13-1* cells capable of growth at high temperatures. This *rad24-2* allele combined with acquired telomere amplification facilitates growth of *cdc13-1* cells at high temperatures. The next work presented is an analysis of a Cdk1-mediated phosphorylation of Cdc13 on residue T308. Strains with a T308A mutation at that phosphorylation site had short telomeres, suggesting a role for the Cdk1- mediated phosphorylation of Cdc13 at T308 in telomerase recruitment. In the final work, we describe an analysis of the interactions between Cdc13 and the DNA polymerase α complex. The association of Cdc13 with Pol1, the catalytic subunit of the DNA polymerase α complex is proposed to recruit the conventional DNA replication to participate in C-strand synthesis of the new G-rich strand extended by telomerase. We demonstrate that the Pol1 and Cdc13 as well as Pol12 and Stn1 interact directly, and loss of these interactions using the *pol1-236* and *pol12-40* alleles results in elongated telomeres. Thus, the data shown here will provide insight on how Cdc13 functions both to protect chromosome ends and to facilitate telomere replication.

TABLE OF CONTENTS

LIST OF FIGURES

LIST OF TABLES

Chapter 1- Introduction

Discovery of telomeres - Historical overview

Telomeres are comprised of repetitive G-rich sequences which associate with specific proteins to form specialized protein- DNA structures at the ends of linear chromosomes (Blackburn, 2000). The early experiments of Barbara McClintock and Hermann Mueller were some of the first to demonstrate the presence of specialized structures which stabilized chromosome ends. Barbara McClintock observed that the ends of broken chromosomes can fuse together to form ring chromosomes. She found that these fused chromosomes would undergo subsequent breakage-fusion-bridge cycles that would further perpetuate the loss of chromosome integrity. Terminal regions were not observed at the chromosome fusion site, suggesting that the free ends of linear chromosomes are somehow protected from these fusions. (McClintock, 1942). Her contemporary, Herman Mueller mutagenized Drosophila chromosomes using x-rays and discovered that he could not recover induced chromosomal rearrangements at the chromosome end. He proposed that the free ends of chromosomes, which he termed telomeres, contained an essential gene that could not be lost (Mueller, 1938). They both concluded that the ends of linear chromosomes have properties which allow them to be distinguished from DNA double-strand breaks (DSBs) (Mueller, 1938, McClintock, 1942). Their experiments were the first to suggest the idea that telomeres act as chromosome caps, protecting chromosome ends from nucleolytic degradation, end to end fusions and inappropriate recombination.

Since the initial observations made by McClintock and Mueller, telomeres have been shown to provide several functions. This introduction chapter will cover telomere composition and structure, as well as telomere length regulation. This chapter will also discuss the roles that telomeres play in blocking the chromosome end from being recognized by the DNA damage checkpoint, and facilitating complete DNA replication, thereby maintaining the chromosome integrity.

Telomere Sequences are evolutionarily conserved

Understanding the function of telomeres was initiated with the cloning of the *Tetrahymena* telomeres in the 1980s. Experiments were conducted in which a linearized plasmid that only contained an autonomous replicating sequence (*ARS*) and a *LEU2* nutritional marker was ligated to purified terminal fragments of *Tetrahymena* rDNA chromosomes and then transformed into yeast cells (Szostak, 1982). Normally, these linearized plasmids are retained at a very low frequency. However, once *Tetrahymena* rDNA chromosome end fragments were added to the linearized plasmids, they were able to stabilize the linear pieces of DNA, demonstrating the capping function of telomeres. This capping function was specific to the sequence added to the linearized plasmid, since a *LacZ* hairpin structure created at the end of the linear plasmid did not stabilize it (Szostak, 1982). This experiment also suggested that telomere sequence was evolutionarily conserved among different species because the linearized plasmid was stable in yeast although it had *Tetrahymena* telomeres. *Tetrahymena* telomere fragments were also sequenced and revealed to consist of repetitive sequences were made up of CCCCAA/GGGGTT repeats (Szostak, 1982). Consistent with the results from the

Blackburn lab, it was later found that telomeres from different *Tetrahymena* species were also able to stabilize yeast linear plasmids (Pluta et al., 1984).

Yeast telomeres were subsequently cloned, sequenced and also found to be composed of $C_{1\text{-}3}A$ repeats (Shampay, 1984). This discovery led to the hypothesis that telomeric sequences and their function are evolutionarily conserved amongst different species (Shampay, 1984). Further supporting this hypothesis, the sequencing of telomeres in ciliates and mammals showed that they too were composed elements made up telomeric repeats, which were T_2AG_3 in mammals and T_4G_4 in *Oxytricha nova* (Allshire et al., 1989, Cross et al., 1989, Klobutcher et al., 1981).

Discovery of Telomerase

The first evidence for enzymatic activity that synthesizes the telomere was identified in *Tetrahymena* by the Blackburn lab a few years after their initial sequencing of telomeres (Greider, 1989). This group found that TTGGGG repeats were able to be added to a G-rich telomeric fragment when it was incubated with an enzyme found within *Tetrahymena* cell extract, although a priming template was not present, which suggested that the enzyme contained its own template. In addition, they showed that this enzyme activity was associated with an RNA fragment which was essential for it's activity (Greider and Blackburn, 1989). Eventually they were able to determine the sequence of the RNA, which contained a 5'-CAACCCCAA-3' motif. This suggested a mechanism in which the enzyme telomerase acts to replicate telomeric DNA using an internal RNA motif as a template to synthesize short DNA sequences (Greider and Blackburn, 1989). Sequencing of the RNA templates in *Euplotes*, yeast and humans further supported this

template mechanism (Lingner and Cech, 1994, McEachern and Blackburn, 1995, Singer and Gottsching, 1994, Feng et al., 1995). Therefore, the telomerase enzyme is understood to act as a reverse transcriptase by synthesizing short G-rich DNA sequences, using its own internal RNA subunit as a template to catalyze the addition of these telomeric repeats at the 3' overhang (Lingner et al., 1996, Lingner et al., 1997b).

Telomerase Function

In order to further understand telomerase composition and function, a genetic approach was taken to uncover genes responsible for telomerase activity *in vivo*. A genetic screen in *Saccharomyces cerevisiae* was used to identify mutations that cause the expected phenotypes for a telomerase-deficient strain, such as progressive telomere length shortening and cell senescence. These genetic screens in the yeast led to the identification of four *EST* (**E**ver **S**horter **T**elomeres) genes that displayed these telomerase-deficient phenotypes when they were mutated (Lundblad, 1989, Lendvay et al., 1996). In *Saccharomyces cerevisiae,* the components of the telomerase ribonucleoprotein (RNP) enzyme complex are encoded by the RNA subunit, *TLC1* as well as *EST1*, *EST2*, and *EST3* (Singer, 1994, Lingner et al., 1997, Hughes et al., 2000). *EST4* was later found to be an allele of the essential gene *CDC13,* and is not a component of the telomerase complex (Nugent et al., 1996).

TLC1, which encodes the RNA template used for telomeric repeat synthesis, was discovered in a screen for suppressors of telomeric silencing. The telomeres in *tlc1Δ* mutants gradually shortened as cells grew through progressive generations, which eventually led to a decrease in cell viability (Singer, 1994). Mutations that altered the

RNA template encoding by *TLC1* were incorporated into telomeric DNA *in vivo*, demonstrating that *TLC1* encodes the telomerase RNA that determines the yeast telomeric DNA sequence. *TLC1* was later found to interact with *EST1*, through co-immunoprecipitation experiments, further implicating *TLC1* as a component of the telomerase enzyme in yeast (Steiner et al., 1996).

EST1 was the first gene identified in screens for components of the telomerase enzyme, and initially was proposed to provide the telomerase catalytic function (Lundblad, 1989; Lundblad, 1990). Although, *EST1* and *TLC1* were required for telomerase activity *in vivo,* telomerase activity assays demonstrated that *EST1* was not necessary for telomerase catalytic activity *in vitro*, suggesting that *EST1* was not the catalytic subunit of telomerase (Cohn, 1995). Est1 associates with the telomeric ssDNA binding protein, Cdc13, and this Est1-Cdc13 interaction is thought to facilitate recruitment of telomerase to the telomere (Virta-Pearlman et al., 1996, Qi and Zakian, 2000, Evans and Lundblad, 2002, Pennock et al., 2001). Yeast studies have also shown that Est1 activates telomerase DNA extension activity *in vitro*, consistent with the model that *EST1* functions as a telomerase accessory factor. Immunodepletion of Est2-HA from yeast cell extracts abolished telomerase activity *in vitro*, suggesting a direct catalytic role for Est2 (Counter et al., 1997). Sequence homology between the reverse transcriptase motifs from *Euplotes* p123 and *EST2*, along with the result that telomerase activity was abolished *in vitro* in the *est2*-Δ strain, led to the conclusion that *EST2* encoded the catalytic subunit of telomerase necessary for proper telomerase function (Lendvay et al., 1996, Cohn and Blackburn, 1995, Lingner et al., 1997a). Est3 also performs a regulatory

role, as it is also crucial for telomere replication *in vivo* but not for catalysis *in vitro* (Lingner et al., 1997a). Est3 is found to associate tightly with telomerase and more recently has been suggested to be in involved in regulating telomerase nucleotide addition (Hughes et al., 2000a, Lee et al., 2010). The fourth gene identified, *EST4* was found to be an allele of the essential gene *CDC13,* which encodes a single-stranded telomere DNA binding protein that has a role in telomerase recruitment, as well as an essential function in telomere end protection (Nugent et al., 1996). Hence, Est2 and Tlc1 comprise the catalytic core of the telomerase enzyme, while Est1, Est3, and Cdc13 are regulatory factors for telomerase (reviewed in Blackburn, 2000).

Co-immuprecipitation experiments demonstrated that Tlc1 binds both Est1 and Est2 through distinct regions. Est2 binds directly to the central core of Tlc1, independent of Est1 (Livengood et al., 2002). Est1 also binds Tlc1 through a separate bulged stem-loop structure (Livengood et al., 2002, Seto et al., 2002). Accordingly, interaction between Est1 and Est2 require Tlc1, consistent with the idea that there are separate binding sites on Tlc1 for these two subunits (DeZwaan, 2009). Est1 has been shown to interact with Cdc13, and this interaction has been implicated in recruitment of telomerase to telomeres (Chandra et al., 2001, Nugent et al., 1996, Qi and Zakian, 2000). Est3 requires the Est2 subunit for telomerase association, suggesting that Est2 and Est3 interact with each other directly (Hughes, 2000a, Lee, 2010). Thus, Est3 associates with telomerase through its interaction with Est2 (Hughes et al., 2000a, Friedman et al., 2003, Lee et al., 2010). After recruitment to the telomere, the telomerase enzyme adds telomeric repeats to the 3'G-rich strand at chromosome ends (Taggart et al., 2002).

Human telomerase contains the essential RNA component *hTERC (*hTR), which is analogous to budding yeast *TLC1* and serves as a template for telomeric DNA synthesis (Cong et al., 2002). The reverse transcriptase activity is provided by the catalytic protein hTERT and is analogous to yeast Est2 (Harrington et al., 1997, Cong et al., 2002). A human *EST1* homolog, hEST1A, was shown to be associated with active telomerase and is proposed to be involved in telomerase regulation as well (Reichenbach et al., 2003). Fission yeast *Schizosaccharomyces pombe* also contains a telomerase enzyme complex with similarities to both budding yeast and human telomerase proteins. Reverse transcriptase motifs in yeast *EST2* and *Euplotes* p123 were used to identify homologs in fission yeast *S. pombe* and resulted in identification of the telomerase reverse transcriptase, Trt1 (Nakamura et al., 1997). Subsequent studies have demonstrated that a functional homolog of budding yeast *EST1,* exists in fission yeast (spEst1*)* and it is involved in telomerase recruitment and activation (Beernink et al., 2003). More recently, the *S. pombe* telomerase RNA, Ter1*,* was identified and shown to be immunoprecipitated with both Trt1 and Est1 (Webb and Zakian, 2008). Thus, the telomerase holoenzyme is conserved between highly diverse eukaryotes.

Telomerase Recruitment and Regulation

Yeast telomeres contain approximately 250 to 350 bp of $TG_{1\text{-}3}$ repeats which are maintained by telomerase (Shampay, 1984). It has been shown in yeast that telomerase does not act on every telomere in each cell cycle, but instead, preferentially extends short telomeres (Teixeira et al., 2004). When telomeres become critically short, they are no longer perform their capping function and fail to protect the chromosome end from being

recognized as a DNA double strand break, which results in activation of the DNA damage checkpoint (Blackburn, 2000, Enomoto et al., 2002, d'Adda di Fagagna et al., 2004). In fact, several of the components of the DNA damage checkpoint response pathway, such as Tel1 and Mec1, are needed for telomere maintenance (Ritchie et al., 1999, Bertuch and Lundblad, 1998). Mutating the genes encoding DNA damage response kinases *TEL1* and *MEC1* (the ATM/ATR homologs in budding yeast), causes telomeres to become short, resulting in increased telomere fusions (Craven et al., 2002). In addition, *mec1Δ tel1Δ* double mutants undergo progressive telomere shortening and eventually senescence, suggesting a role for these checkpoint genes in proper telomere length maintanence (Ritchie et al., 1999). However, telomere length is shorter in *tel1* than in *mec1* cells, suggesting a more primary role for Tel1 in telomere maintenance. Consistent with this, Tel1 is required for normal association of Est1 and Est2 with telomeres, whereas Mec1 is not (Goudsouzian et al., 2006).

Not surprisingly, components of the DNA non- homologous end joining pathway, such as the MRX (Mre11, Rad50, Xrs2) complex, are also required for telomere maintanence. Tel1 and the MRX complex are found preferentially associated with short telomeres (Sabourin et al., 2007, Hector et al., 2007). Tel1 is thought to interact and phosphorylate MRX subunits, which can then promote generation of the 3' overhang (Lisby, 2004, Mantiero et al., 2007). Processing of a 3' overhang facilitates association of telomerase with the chromosome end (Mantiero et al., 2007). The telomere association of Cdc13, a single-stranded DNA-binding protein that specifically binds TG-rich telomeric repeats, peaks in late S phase which coincides with the appearance of long 3'

overhangs and initiates a cascade of events leading to telomerase activation. It has also been reported that MRX contributes to the establishment of telomere ssDNA overhang formation in S phase (Larrivée et al., 2004). Accordingly, both Tel1 and the MRX complex increase the efficiency of telomerase association with telomeres (Takata et al., 2005, Goudsouzian et al., 2006). The cell cycle dependent association of Est1 or Est2 with telomeres is decreased in *tel1-Δ* or *mre11-Δ* cells, suggesting that these proteins function in telomerase recruitment (Takata et al., 2005, Goudsouzian et al., 2006).

The role of Cdc13 in telomerase recruitment was elucidated using the *cdc13-2* allele, which was identified by it's *EST* phenotype (*e*ver *s*horter *t*elomeres) consisting of progressive telomere shortening and delayed senescence (Nugent et al., 1996). Cdc13 has been shown to interacts with Est1 through coimmunoprecipitation experiments (Qi and Zakian, 2000). The *cdc13-2* mutant allele exhibits a phenotype similar to telomerase deficient cells, which is thought to be due to the disruption of the interaction between Cdc13 and Est1 necessary for telomerase recruitment (Pennock et al., 2001, Nugent et al., 1996). ChIP analysis from several groups has been used to assess the association of Est1 and Est2 with telomeric DNA (Taggart et al., 2002, Chan et al., 2008). Est1 has been found to associate with telomeres primarily during S phase, with a reduction in Est1 association observed when cells are in G1 (Chan et al., 2008). Est2 has been found to remain associated with telomeric chromatin throughout the cell cycle, with a peak association observed during late S phase which correlates with a peak in Est1 association with the telomere as well (Taggart et al., 2002). The peak of Est2 localization was found to be reduced in a recruitment defective *cdc13-2* mutant during late S phase, suggesting

that the recruitment of telomerase to telomeres in S-phase is dependent on the Cdc13-Est1 interaction (Taggart et al., 2002). This dependency on Cdc13 for localization is only specific for S phase, while G1 localization of Est2 is dependent on the association between yKu80 and Tlc1. It has been demonstrated that telomerase can be recruited to the telomere end through an interaction between Ku80 and the stem loop of *TLC1* by ChIP (Peterson et al., 2001, Stellwagen et al., 2003). The Ku pathway in G1 and the Cdc13 pathway in S-phase have been reported to be the only two major recruitment pathways by which telomerase is recruited to telomeres in budding yeast (Chan et al., 2008).

A different regulatory pathway is proposed for long telomeres, in which a counting mechanism is used. Rap1 is a double stranded DNA binding protein, which was found to associate with telomeric chromatin *in vivo* through chromatin immunoprecipitation experiments (Conrad et al., 1990). Rap1 binding to double-stranded DNA is thought to promote a fold-back loop structure through it's interaction with Rif1 and Rif2 (Levy and Blackburn, 2004). It has been reported that disruption of Rif1 function resulted in telomere elongation and deletion of both *RIF1* and *RIF2* resulted in a dramatic telomere lengthening. In addition, overproduction of either *RIF1* or *RIF2* decreased telomere length (Hardy et al., 1992, Wotton et al., 1997). Hence, the formation of a higher heterochromatin structure mediated by Rap1, Rif1 and Rif2 acts to inhibit telomere elongation by blocking access to the telomere end by telomerase (Marcand et al., 1997, Krauskopf et al., 1998). Previous studies conducted by the Shore lab in which an internal telomeric DNA seed adjacent to an induced DNA double strand

break (DSB) was acted on by telomerase demonstrated that targeting the Rap1 carboxyl terminus to the telomere seed reduced its length. Furthermore, the reduction in elongation was proportional to the number of Rap1 proteins targeted, such that increased Rap1 protein correlated with telomere shortening (Marcand et al., 1997). Targeting Rif1 and Rif2 to regions adjacent to the telomeric repeats also caused telomere shortening proportional to the number of tethered Rif1 or Rif2 molecules, further supporting a Rap1/Rif1/Rif2 counting mechanism that negatively regulates telomere length (Levy and Blackburn, 2004). *rif1-Δ* and *rif1-Δ* cells have telomeres that are more frequently elongated by telomerase during a cell cycle, suggesting that the Rap1/Rif1/Rif2 complex mediates the ability of telomerase to elongate telomeres (Teixeira et al., 2004). As the telomere shortens, fewer Rap1 binding sites exist to maintain the closed heterochromatin structure, which results in an open chromatin structure that may be accessed by telomerase. Taken together, these results demonstrate that Rap1 associates with Rif1 and Rif2p to regulate telomere length (Marcand et al., 1997, Levy and Blackburn, 2004).

Telomerase- independent telomere lengthening

Adjacent to the terminal TG_{1-3} repeats of telomeres, there are Y' elements and X elements, which are the more complex telomere-associated repeats (Figure 1-1). All yeast telomeres have one X element, whereas Y' elements are found only at some telomeres. Approximately two-thirds of the telomeres in haploid cells contain one or more copies of subtelomeric Y' elements (Figure 1-1). Y' elements fall in two size classes, long Y's are 6.7 kb and short Y' elements are 5.2 kb. Multiple Y' elements form directly repeating arrays which are separated by short stretches of telomeric TG_{1-3} DNA. Lastly,

all yeast telomeres contain an approximately 475 bp conserved 'core' X element. TG_{1-3} sequences are found between some X and Y' elements (Figure 1-1) (Pryde et al., 1997). In cells lacking telomerase, telomeres become critically short and cells eventually enter crisis. Yeast cells can generate survivors at low frequency that maintain telomeres by a recombination-dependent mechanism (Lundblad and Blackburn, 1993). Two types of these survivors have been identified. Type I survivors amplify Y' elements and type II amplify the TG_{1-3} repeats (Figure 1-1) (Chen et al., 2001). Both types of survivors are dependent on *RAD52*, indicating the telomere maintenance in telomerase-deficient cells requires homologous recombination. Two independent pathways defined by *RAD50* and *RAD51* promote the generation of survivors. The *RAD51* pathway involves *RAD51*, *RAD54* and *RAD57* while the *RAD50* pathway involves three subunits of MRX complex *RAD50*, *XRS2* and *MRE11*. Deletion of both *RAD50* and *RAD51* prevents the generation of survivors in telomerase deficient cells. Mutations in the telomerase RNA, *TLC1*, were combined with single and double mutations in the recombination pathways to investigate the role of *RAD59* and the *RAD50* and *RAD51* epistasis groups in telomere maintenance. These experiments demonstrated that *tlc1 rad50* and *tlc1 rad59* mutants generated predominantly type I survivors, while the *tlc1 rad51, tlc1 rad54*, and *tlc1 rad57* mutants generated only type II survivors (Chen et al., 2001).

Telomeres prevent genome instability

Genomic instability refers to the accumulation of mutations and chromosomal rearrangements which has been shown to promote genetic abnormalities, and play an important role in cancer cell formation (Bailey and Murnane, 2006, Murnane, 2006).

Loss of telomere function has been reported to have several different outcomes in various model organisms, such as loss of the telomeric 3'- overhang, resection of the C-rich strand, increased levels of recombination at chromosome ends, chromosomes fusion , cell cycle arrest and cell death (Verdun and Karlseder, 2007) . For example, loss of *TRF2*, a mammalian duplex telomeric DNA binding protein with roles in telomere protection and telomere length regulation, caused a significant increase in of telomere fusions in mammalian cells (van Steensel and Smogorzewska, 1998). In human cells, removal of TRF2 from telomeres resulted in deprotection of chromosome ends and premature senescence (Smogorzewska and De Lange, 2002). In Saccharomyces *cerevisiae*, loss of a single telomere causes a prolonged, but transient, cell-cycle arrest. However, cells recovered from the arrest without repairing the damaged chromosome, with many cells eventually losing the chromosome. Telomere elimination also led to an increase in chromosome loss, demonstrating that yeast telomeres are also essential for maintaining chromosome stability (Sandell and Zakian, 1993). Hence, telomeres are essential in preventing chromosome ends from being recognized and processed as DNA double strand breaks. In human cells, telomeres play a crucial role in protecting cells from the chromosome instability that can promote tumor formation, further demonstrating the importance of maintaining telomere integrity (Deng et al., 2008).

Telomere Chromatin Organization

Telomere end protection or capping is maintained through the interaction of the linear ends of DNA with specialized proteins that bind and physically protect the chromosome end. Telomere associated proteins which contributed to the capping

function of telomeres were first studied in *Oxytricha nova (O. nova*). Experiments demonstrated that a telomere end binding protein (TEBP) specifically bound single stranded G_4T_4 repeats (Gottschling and Cech, 1984, Gottschling and Zakian, 1986, Price and Cech, 1987, Horvath et al., 1998). *O. nova* TEBP is made up of a 56-kDa α subunit that binds the single-strand telomeric DNA and a 41-kDa β subunit that weakly binds DNA but affects the ability of the α subunit to interact with the DNA. TEBP α/β forms a stable complex with the telomeric DNA which both protects the DNA from nucleolytic degradation and inhibits elongation by telomerase (Gottschling and Zakian, 1986, Froelich-Ammon et al., 1998). The crystal structure of TEBP demonstrated that the 3′-end of the telomeric DNA was buried within the protein complex, suggesting that the TEBP proteins established telomere capping by physically sequestering the chromosome ends (Horvath et al., 1998, Classen et al., 2001). Thus, the telomere structure discovered in *Oxytricha nova* was the first evidence for a specialized chromatin structure established by telomeric DNA binding proteins that promoted telomere protection and capping.

Mammalian telomeres form a t-loop structure

Studies in mammalian cells have suggested a different telomere structure, in which the terminal G-rich single-stranded 3'- overhang invades the adjacent double-stranded telomeric DNA, resulting in a lariat structure, known as a telomeric loop or "t-loop" (Griffith et al., 1999) (Figure 1-2a). The displaced region is called the displacement loop or "D-loop", which is similar to the strand invasion structure found during homologous recombination (Figure 1-2a). Experiments where telomere DNA sequence from Hela cells was incubated with an *E. coli* single-stranded binding protein were

performed to visualize the t-loop microscopically *in vitro* (Griffith et al., 1999). Hence, the t-loop is proposed to be a structure which sequesters the chromosome ends to protect them and provides a mechanism by which mammalian chromosome ends would be protected (de Lange, 2004).

Several proteins associate with the T-loop to stabilize this structure at the telomere, which together are termed the shelterin complex. In addition to promoting telomere capping function, components of shelterin regulate telomere replication through telomerase by both promoting and inhibiting telomerase activity (de Lange, 2005, Wang et al., 2007, Palm and De Lange, 2008). The shelterin complex is comprised of TRF1, TRF2, RAP1, TIN2, POT1 and TPP1 (Figure 1-2b). This six protein complex contains both double stranded and single stranded DNA binding proteins, which together, stabilize and protect the chromosome end. Two shelterin subunits, TRF1 and TRF2, bind to the double-stranded telomeric TTAGGG sequences. POT1 binds to single-stranded telomeric DNA sequences. These three proteins are held together by TIN2 and TPP1, which promotes formation of the shelterin complex (de Lange, 2009) (Figure 1-2b).

The first mammalian telomeric protein identified, TRF1, was purified based on its affinity for double-stranded TTAGGG telomere repeats *in vitro* (Zhong et al., 1992, Chong et al., 1995). TRF2 was identified as a TRF1 paralog in the protein database (Bilaud et al., 1997, Broccoli et al., 1997). Both TRF1 and TRF2 form homodimers and directly interact with telomeric DNA to promote formation of the t-loop (Bilaud et al., 1997, Bianchi et al., 1997, Broccoli et al., 1997, König et al., 1998). In the human cells, TRF1 binds the dsDNA via its *MYB* domains to facilitate t-loop formation (Bianchi et al.,

1997, König et al., 1998, Hanaoka et al., 2005). TRF2 is proposed to stabilize the DNA junction formed by the invasion of the 3' overhang into the adjacent internal duplex DNA, and has been shown to promote the generation of t-loop structures *in vitro* (Griffith et al., 1999, Stansel et al., 2001, Yoshimura et al., 2004, Poulet et al., 2009) (Figure 1-2b). Both TRF1 and TRF2 function to protect telomeres against checkpoint recognition and recombination (van Steensel and Smogorzewska, 1998, Smogorzewska et al., 2000, Martínez et al., 2009). Embryonic stem (ES) cells that were conditionally deleted for *TRF1* were shown to have normal increased telomere-telomere fusions and multi-telomeric signals, indicating that loss of TRF1 resulted in increased chromosomal aberrations (Okamoto et al., 2008). Mouse embryonic fibroblasts deleted for *TRF1* showed a large increase in the DNA damage foci at telomeres, activation of ATM/ATR checkpoint and cell cycle arrest, demonstrating that TRF1 protects telomeres from eliciting a DNA damage response (Martínez et al., 2009). TRF2 is also essential for telomere capping and conditional deletion of *TRF2* in mouse embryonic fibroblasts (MEFs) led to chromosome end-to-end fusions and severe proliferative defects (van Steensel and Smogorzewska, 1998, Celli and De Lange, 2005). Loss of TRF2 leads to activation of the DNA damage checkpoint at telomeres in mouse or human cells with DNA damage foci appearing at chromosome ends, indicating that TRF2 represses the DNA damage checkpoint response at telomeres and protects chromosome ends from being recognized as DNA double strand breaks (Celli and De Lange, 2005, Karlseder et al., 1999, Takai et al., 2003). Both TRF1 and TRF2 are mammalian telomeric repeat-binding factors that promote t-loop formation which protects the chromosome end, and

hides the telomere terminus.

TRF1 was found to interact with TIN2 through yeast two-hybrid screens and a TIN2 knockdown removed TRF1 from telomeres (Kim, 1999 et al., Ye et al., 2004b, Palm and De Lange, 2008). However, it was later found that TIN2 interacts with TRF2 through co-immunoprecipitation, Far-Western assays, and two-hybrid assays. Furthermore, TRF2 localization to the telomere is also reduced by a TIN2 knockdown, indicating that TIN2 interacts with both TRF1 and TRF2 at the telomere (Ye et al., 2004a). Reduction of TIN2 via siRNA knockdown promotes formation of abnormal telomere structures and induces apoptosis in human tumor cells, indicating that TIN2 is required to maintain chromosome integrity as well (Kim et al., 2008). TIN2 interacts with TPP1 and POT1, which is thought to facilitate the recruitment of the single-stranded telomeric DNA binding proteins to telomeres (Liu et al., 2004a, Ye et al., 2004a). Stabilization of telomeres is facilitated by TIN2 connecting TRF1 and TRF2 with TPP1 and POT1 (Liu et al., 2004a, Ye et al., 2004a, Palm and De Lange, 2008) (Figure 1-2b).

TRF2 was found to interact with RAP1 through yeast two-hybrid screens (Li et al., 2000). RAP1, which does not directly bind DNA, associates with TRF2 to bind DNA and regulate telomere length (Li et al., 2000). Although, loss of RAP1 did not cause telomere fusions, or DNA damage foci, it was found that RAP1 repressed telomere recombination in TRF2 deficient mouse embryonic fibroblasts, suggesting that RAP1 functions at mouse telomeres to inhibit telomerase-independent telomere maintenance (Sfeir et al., 2010).

TPP1 (previously called TIN1, PTOP, and PIP1) and was discovered in searches for proteins associated with TIN2 (Houghtaling et al., 2004, Liu et al., 2004b, Ye et al., 2004b). The interaction between single stranded DNA and double stranded DNA binding proteins in shelterin is bridged by TIN2 and TPP1 (Figure 1-2b). TPP1 forms a heterodimer with POT1, and depletion of TPP1 prevents POT1a and POT1b localization to telomeric, thus the TPP1-POT1 interaction increases the affinity of POT1 for telomeric single-stranded DNA (Guo et al., 2007, Wang et al., 2007, Xin et al., 2007). Knockdown of *TPP1* in MEFs elicited a cell cycle arrest, cellular senescence, and a DNA damage checkpoint response at telomeres (Guo et al., 2007). Hence, *TPP1* also functions in promoting chromosome end protection in mammalian cells.

POT1 is a conserved single-stranded telomere DNA binding protein found in humans that was identified based on sequence homology to *S. pombe*, POT1 (Baumann and Cech, 2001, Palm and De Lange, 2008). POT1 binds the single-stranded telomeric DNA 3′ overhang and interacts with the complex of shelterin proteins at the telomere (Loayza and De Lange, 2003). TRF1 functions with POT1, to negatively regulate telomere length (Colgin et al., 2003, Loayza and De Lange, 2003, Kelleher et al., 2005) It has also been shown that POT1 negatively effects telomerase activity *in vitro* and the DNA binding activity of POT1 is also required for telomerase inhibition (Kelleher et al., 2005, Palm and DeLange, 2008). Knock out of human *POT1* leads to chromosome fusion and genome instability (Veldman et al., 2004). Deletion of the two mouse genes, *POT1a* and *POT1b,* results in a DNA damage response, as evidenced by DNA damage foci at telomeres (Hockemeyer et al., 2006). MEFs deleted for *POT1a* resulted in

enhanced chromosomal instability, and tumor formation in a p53-deficient background, demonstrating that *POT1a* is crucial for the suppression of tumor formation and telomere integrity (Wu et al., 2006). Thus, POT1 is the telomeric single-stranded DNA binding protein necessary for chromosome end protection in mammalian cells.

Telomere structure in *S. pombe*

Telomeres in *Schizosaccharomyces pombe* associate with a protein complex that is similar in many ways to the mammalian shelterin complex (de Lange, 2009). In this complex, Pot1 associates with the TPP1 homolog, Tpz1 (Miyoshi et al., 2008). The double stranded telomeric DNA binding protein, Taz1, is similar to the human TRF proteins and interacts with the conserved Rap1 protein at fission yeast telomeres to inhibit telomere recombination (Miller and Cooper, 2003, Ferreira and Cooper, 2001, Subramanian et al., 2008). Poz1 serves a function similar to Tin2 and connects the Tpz1/Pot1 dimer to Taz1/Rap1, thus connecting the single-stranded and double-stranded telomeric DNA regions (Miyoshi et al., 2008). Hence, telomere structure is understood to be closely conserved with the human t-loop model.

Telomere structure in *S. cerevisiae*

The proposed telomere structure in *S. cerevisiae* is such that telomeric DNA is bound by single-stranded and double-stranded telomeric DNA binding proteins which facilitate the telomeric chromatin to "fold back", and contact subtelomeric regions, thus establishing a heterochromatin structure that functions to protect chromosome ends (de Bruin et al., 2000, de Bruin et al., 2001) (Figure 1-3). Unlike the t-loop structure in humans, the fold-back loop has not been visualized microscopically. Instead, the structure

has been proposed from information gathered from genetic experiments testing the activation or repression of genes proximal to telomeres (de Bruin et al., 2000, de Bruin et al., 2001). These experiments showed that a gene with its own enhancer positioned 2 kilobases downstream, was only activated when the reporter was linked to a telomere, suggesting that telomere looping had occurred (de Bruin et al., 2001).

Rap1 is telomeric double stranded DNA binding protein in yeast that is thought to mediate the "fold-back" structure. Rap1 was first identified as a transcriptional regulator, but was later found to associate with both telomeric DNA and subtelomeric chromatin *in vivo* (Shore and Nasmyth, 1987, Conrad et al., 1990, Strahl-Bolsinger et al., 1997) (Figure 1-3). The crystal structure of Rap1 revealed that it can bind telomere $C_{1\text{-}3}A$ repeats through its two Myb -like domains to change the DNA conformation (Wright et al., 1992, Konig et al., 1996, Del Vescovo et al., 2004). Some temperature sensitive alleles of Rap1 have been shown to cause telomere shortening, while other Rap1 mutations cause long telomeres, suggesting a role for Rap1 in telomere length regulation (Lustig et al., 1990, Krauskopf and Blackburn, 1998). This "fold-back" structure is also thought to be vital to the counting mechanism which regulates telomere length as previously discussed. The proposed "fold-back" model places the end of the telomere inward toward the back onto the subtelomeric regions to form a heterochromatin structure, thus capping the chromosome end and promoting a "closed" telomere state (Strahl-Bolsinger et al., 1997, Grunstein, 1998) (Figure 1-3). As telomeres shorten, Rap1 binding sites are lost, and the fold-back structure is disrupted into a more open state, thus allowing telomerase access to the chromosome end (Marcand et al., 1997).

The fold-back structure may promote telomere capping, as loss of Rap1 function through a conditional degron allele (*rap1-Δ*) led to telomere end to end fusions (Pardo et al., 2005). In addition to Rap1, the Sir2, Sir3, and Sir4 may also facilitate higher order telomere structure. Evidence to support this comes from the observation that Sir2, Sir3, and Sir4 proteins are found at both telomeres and associated with histones in subtelomeric regions (Strahl-Bolsinger et al., 1997). The Sir proteins that interact with Rap1 are also capable of contacting the subtelomeric nucleosomal arrays, promoting a folded chromatin structure (Smith et al., 2003). This is consistent with the idea that the Rap1 and the Sir proteins bound to the terminal telomeric $TG_{1\text{-}3}$ repeats "fold back" to interact with internal histones, creating a higher order structure to protect the chromosome end.

In *S. cerevisiae,* the 3' G-rich overhang at telomeres is protected by a three protein complex comprised of Cdc13–Stn1–Ten1, named CST (Petreaca et al., 2006, Gao et al., 2007) (Figure 1-3). Cdc13 is the telomeric single stranded DNA binding protein in *S. cerevisiae* required for chromosome end protection (Garvik et al., 1995, Lin and Zakian, 1996, Nugent et al., 1996). The role of *CDC13* in telomere end protection has been elucidated using the temperature sensitive allele, *cdc13-1*. *cdc13-1* mutant strains grow normally when kept at permissive temperatures of 25^{o}C and below, however, when raised to non-permissive temperatures, cells rapidly lose viability (Garvik et al., 1995; Lydall and Weinert, 1995, Nugent et al., 1996). Analysis of *cdc13-1* mutants grown at the non-permissive temperature by two dimensional gel electrophoresis and quantitative PCR amplification show that *cdc13-1* cells accumulate single stranded DNA specifically on

the 3' G-rich end, which extended up to 50 kilobases from the telomere (Garvik et al., 1995, Booth et al., 2001). This single stranded DNA is a strong activator of the DNA damage checkpoint, and *cdc13-1* mutants arrest as large-budded cells, eventually leading to cell death (Garvik et al., 1995, Lydall and Weinerrt, 1995, Nugent et al., 1996). Hence, *CDC13* functions to cap chromosome ends by protecting them from nucleolytic degradation (Lydall and Weinert, 1995, Booth et al., 2001). Cdc13 interacts with two other proteins, Stn1 and Ten1 to protect the chromosome end (Grandin et al., 1997, Grandin et al., 2001b). Stn1 was isolated from a screen for high copy suppressors of the *cdc13-1* allele, and permitted growth of *cdc13-1* cells at 30^{o}C (Grandin et al., 1997). Ten1 was isolated in a separate screen as a high copy suppressor of *stn1-13,* a temperature sensitive allele of *STN1* (Grandin, 2001). Mutant alleles of both *stn1* and *ten1* have been identified which acquire telomeric ssDNA and activate the DNA damage checkpoint (Petreaca et al., 2007, Xu et al., 2009). Thus, it is proposed that Stn1 and Ten1 form a complex with Cdc13 which functions to protect chromosome ends from nucleolytic degradation and DNA damage checkpoint activation (Petreaca et al., 2006, Xu et al., 2009, Gao et al., 2007).

The CST complex was initially thought to be unique to budding yeast, although functionally similar to the POT1–TPP1 interaction found in mammalian cells. However, recent studies have reported Stn1 and Ten1 homologs in several organisms that contain POT1 complexes, and have implicated Stn1 and Ten1 in telomere capping (Martín et al., 2007, Song et al., 2008). In fact, a mammalian CTC1 (conserved telomere maintenance component 1), STN1 and TEN1 complex has been identified which was shown to bind to

single-stranded DNA as a trimeric complex and localize to telomeres in Hela cells (Miyake et al., 2009). Loss of telomere protection as measured by DNA damage foci demonstrated that STN1/POT1-knockdown cells had an increase in DNA damage foci compared to either single knockdown, suggesting that POT1 and CST play redundant roles in telomere protection. Potential structural similarities have been reported between Stn1 and Rpa2, a component of the replication protein A (RPA) complex (Gao et al., 2007). Replication protein A (RPA) is a nonspecific ssDNA-binding complex comprised of Rpa1, Rpa2 and Rpa3 that mediates various DNA metabolic processes throughout the genome (Wold, 1997). It was recently shown that the N-terminal OB fold-like domain of Stn1 was able to function in place of the Rpa2 OB fold (Gao et al., 2007). Similar to the interaction between Rpa2 and Rpa3, the N terminus of Stn1 interacts with Ten1 *in vitro* and *in vivo* (Sun et al., 2009). Furthermore, the human homolog of *STN1*, initially identified as *OBFC1* (OB Fold-containing Protein 1), has been found to associate with telomeric ssDNA and the shelterin component, TPP1 (Wan et al., 2009). Taken together, these suggest the CST complex may represent a telomere specific RPA complex that functions in parallel to the POT1-containing complex, although the exact function of CST at mammalian telomeres is not completely understood.

Comparison of end protection modes

The telomere structure discovered in architecture *Oxytricha nova* is the most basic model for a specialized chromatin structure established by telomeric DNA binding proteins that promotes telomere protection and capping. In this structure, the 3′-end of the telomeric DNA is buried within the TEBP α/β protein complex to physically sequester

the ends of the telomeric DNA within the protein complex, and in this way these proteins protect the chromosome end. The telomere structure in human cells is similar to that found in *O.nova* in that the chromomsome end is sequestered within a protein complex in both organisms. However, the proposed "t-loop" structure in humans is more complex, and dependent on the six protein shelterin complex to facilitate t-loop formation, instead of a protein dimer. TEBP α/β is distantly related to Pot1 and its binding partner Tpp1 in the shelterin complex, suggesting that the mechanism of telomere end protection has been conserved evolutionarily (Baumann and Cech, 2001, Wang et al., 2007, Xin et al., 2007).

The fold-back model in yeast is a combination of the structures proposed for *Oxytricha nova* and humans, in that the telomeric chromatin folds back to contact subtelomeric regions and the terminal end is protected by the single stranded DNA binding activity of Cdc13 (de Bruin et al., 2001, de Bruin et al., 2000). The model proposed for the telomere structure in *S. cerevisiae* is different from humans, in that the most terminal 3' end is not proposed to invade the duplex DNA, but instead contacts are made by interacting DNA binding proteins.

G_2/M DNA Damage checkpoint

In order to ensure proper transmission of genetic information and to guard against heritable mutations, cells must be able to detect, respond to, and repair any DNA damage that may cause genome instability. The appearance of DNA damage signals the cell to arrest cell cycle progression at the G_2/M checkpoint, giving the cell more time to repair what might otherwise be a fatal DNA lesion (Weinert and Hartwell, 1988, Weinert and Hartwell, 1993). The checkpoint pathways utilize three main groups of protein to

translate a DNA damage signal into subsequent cell cycle arrest and repair of the damaged DNA (Nyberg et al., 2002). The first group is sensor proteins which recognize damaged DNA and their role is to initiate the downstream signal cascade. Transducer proteins relay and amplify the damage signal from the sensors by phosphorylating other downstream targets. Effector proteins are usually the most downstream proteins targeted, and are regulated to convert the damage signal into forms of regulation that control transduction, promote repair, and induce cell cycle arrest (Humpal et al., 2009, Harrison and Haber, 2006).

In *S. cerevisiae*, arresting the cell cycle at G2/M in response to DNA damage has been shown to be dependent on *MEC1, RAD9, RAD24, RAD17, RAD53* and *MEC3* (Lydall and Weinert, 1995, Lydall and Weinert, 1997). In budding yeast, the G2/M DNA damage checkpoint response pathway is activated by the PI3-like kinase, Mecl after initial processing at the site of a DSB (Weinert et al., 1994) (Figure 1-4). Single – stranded DNA (ssDNA) is a potent activator of the DNA damage checkpoint and those proteins which detect damage. Studies in yeast have shown that the nuclease activities of the MRX complex (*MRE11, RAD50 and XRS2)* and Exo1 are needed to create ssDNA at a DSB (Nakada et al., 2004). Tel1 is a kinase that serves redundant roles with Mec1 (Sanchez et al., 1996, Mantiero et al., 2007). Tel1 localizes to DNA double strand breaks via an interaction with the Mre11p/Rad50p/Xrs2p complex (MRX) (Nakada et al., 2003, Falck et al., 2005). Tel1 has been shown to phosphorylate the MRX complex through its interaction with Xrs2 to activate the downstream signal cascade necessary for arrest (D'Amours and Jackson 2001). Furthermore, it was found that Mre11 function was

required for an effective cell cycle arrest response, suggesting that the MRX complex is specifically required for the generation of ssDNA necessary for checkpoint activation in respond to DSBs (Grenon et al., 2001). The ssDNA generated at a DSB does not remain naked in the cell, but instead is bound by the ssDNA–binding protein complex called replication protein A (RPA) (Wold, 1997).

Mec1 plays an essential role in the DNA damage checkpoint response. Using a system which generates a single site-specific double-strand break at the *MAT* locus, it was shown via chromatin immunoprecipitation that Mec1 can recognize and directly bind a DSB in yeast (Kondo et al., 2001, Melo et al., 2001, Dubrana et al., 2007). Mec1 kinase activity requires the cofactor Ddc2, as Mec1 foci formation following DNA damage was dependent on Ddc2 (Dubrana et al., 2007) (Figure 1-4). The binding of RPA to ssDNA at a DSB is thought to be necessary for Mec1/Ddc2 recruitment. Accordingly, the Elledge group has shown that decreasing RPA at an induced DSB reduced Ddc2 binding, despite ssDNA being equivalent both with and without RPA (Zou et al., 2003b). In addition, the yeast checkpoint deficient RPA mutant, *rfa1-t11,* is defective in recruiting both Ddc2 and Ddc1 to ssDNA at DNA damage sites *in vivo* (Zou et al., 2003a, Zou et al., 2003b). Mec1 foci formation at an induced DSB and checkpoint activation was also diminished in the *rfa1-t11* strain, directly implicating RPA in Mec1-Ddc2 recruitment to a DSB (Dubrana et al., 2007). The Mec1/Ddc2 complex has also been shown to localize to a DSB using ChIP and immunofluorescence (Paciotti et al., 2000, Rouse et al., 2000, Melo et al., 2001). Mec1 association with a DSB has also been demonstrated not to be dependent on either *RAD9* or *RAD24,* suggesting that these proteins are recruited to a

DSB independently of each other (Kondo et al., 2001, Melo et al., 2001) (Figure 1-4). Hence, Mec1/Ddc2 kinase complex is thought to act as the central regulator of checkpoint signaling, and is required for most known phosphorylation events that occur following DNA damage, including the phosphorylation of key cell cycle targets (Weinert, 1998).

In addition to the Mec1/Ddc2 complex being recruited to DNA lesions, the Rad24-RFC clamp loading complex is also recruited to DNA damage sites (Kondo et al., 2001, Melo et al., 2001). During DNA replication, the processivity factor for DNA polymerase is a doughnut-shaped homotrimeric complex termed the proliferating cell nuclear antigen (PCNA) (Waga and Stillman, 1998, Majka and Burgers, 2004). PCNA is loaded onto primed DNA by the replication factor C (RFC) complex, a heteropentamer made up of RFC1-5 that is aptly termed the "clamp loader" (Waga and Stillman, 1998, Majka and Burgers, 2004). Rad24 interacts with the small subunits of the replication factor C (RFC) complex (Rfc2, Rfc3, Rfc4, and Rfc5) and forms a specialized complex related to the RFC complex (Shimomura et al., 1998, Green et al., 2000, Naiki et al., 2000). Ddc1, Mec3, and Rad17 are structurally similar to the proliferating cell nuclear antigen (PCNA), and they form a trimeric doughnut-like clamp complex (Venclovas et al., 2000). The Rad24-RFC clamp loader complex loads the Rad17/Mec3/Ddc1 sliding clamp onto sites of DNA damage (Melo et al., 2001, Majka and Burgers, 2003, Griffith et al., 2002) (Figure 1-4). RPA has been also shown to stimulate the binding of the checkpoint clamp loader complex DNA *in vitro,* suggesting that the Rad24-Rfc2-5 clamp loader complex recognizes DNA damage by interacting with RPA-coated ssDNA to associate with damage sites (Zou et al., 2003a).

Several lines of evidence suggest that Mec1 and Ddc1 are recruited to sites near the HO-induced DSB through distinct mechanisms (Kondo et al., 2001, Dubrana et al., 2007). Mec1 was shown to phosphorylate the Ddc1 and Mec3 subunits of the checkpoint clamp and this phosphorylation was important for proper checkpoint function (Paciotti et al., 2001, Paciotti et al., 1998). Ddc1 phosphorylation after DNA damage was also dependent on *RAD24*, suggesting that Ddc1 functions downstream of both *MEC1* and *RAD24* (Paciotti et al., 1998). Association of Ddc1 with an induced DSB was detected in *rad9*Δ mutants as well as in *mec1*Δ mutants. However, this association is lost in *rad24*Δ or *rad17Δ* mutants, consistent with the observation that *DDC1* functions in the same checkpoint pathway as *RAD24*. Similarly, Mec1 association with a DSB in a *ddc1*Δ mutant was not affected, indicating that the association of Ddc1 to an induced DSB is dependent on *RAD24* and *RAD17,* but not on *RAD9* or *MEC1* (Kondo et al., 2001) (Figure 1-4). After being loaded, the Ddc1/Rad17/Mec3 complex recruits Mec1 substrates, allowing Mec1 to phosphorylate targets of the DNA damage checkpoint signal transduction cascade (Melo et al., 2001).

In addition to phosphorylation of the checkpoint clamp, Mec1 has been shown to phosphorylate a conserved motif on histone H2A. Although, the motif itself is not necessary for Mec1-dependent cell-cycle arrest, it is important for viability in the presence of DNA damaging agents (Downs et al., 2000). Lastly, it has been demonstrated that phosphorylation of H2A is required for efficient DNA double-strand break repair by non-homologous end joining, suggesting that H2A plays a role in

organizing chromatin structure in response to DNA damage to facilitate repair (Downs et al., 2000).

Rad9 functions as a transducer protein to amplify the damage signal from the Mec1 and Tel1 upstream kinases to their downstream effector targets, such as Rad53 and Chk1. After Mec1 phosphorylates Rad9, Rad9 can associate with Rad53 which promotes the autophosphorylation of Rad53 (Gilbert et al., 2001) (Figure 1-4). Phosphorylated Rad53 dissociates from Rad9 and transmits the damage signals to further downstream targets. Once Rad53 is activated it can phosphorylate downstream targets, such as Dun1, which function to arrest the cell cycle and activate repair of DNA damage (Allen et al., 1994). Rad9 activates a separate branch of the checkpoint response through association with Chk1, in response to DNA damage (Sanchez, 1999). After activation Chk1 can phosphorylate Pds1 directly which contributes to the G_2/M cell cycle arrest (Sanchez et al., 1999). Rad9 has been found to contain domains that specifically interact with Rad53 or Chk1, which permits Rad9 to modulate activation of two distinct signaling pathways (Schwartz et al., 2002, Blankley and Lydall, 2004) (Figure 1-4).

Control of resection at native telomeres

Single-stranded DNA is also generated at the telomere in a cell cycle dependent manner. Native telomeres of budding yeast end in a short 3' G-rich overhang of approximately 10–15 nucleotides (Larrivée et al., 2004). During conventional replication, lagging-strand synthesis occurs on the G-rich strand running 5′ to 3′ toward the end of the chromosome, and removal of the primer on the newly synthesized C-rich strand will result in a short 3′ G-rich overhang. Leading-strand synthesis is thought to

produce a blunt end, yet it has been reported that 3' G-rich overhangs occur on both the leading- strand and the lagging-strand ends of a linear plasmid (Wellinger et al., 1996). In addition, these G- rich overhangs are detected in cells lacking telomerase activity, suggesting that the blunt ends resulting from leading-strand synthesis are processed, presumably by a nuclease, to generate 3' overhangs (Dionne and Wellinger, 1996, Wellinger et al., 1996). Yeast studies using native in-gel hybridization to detect telomeric ssDNA have demonstrated that telomeres acquired longer 3' G-rich overhangs in late S phase, after conventional replication had occurred (Wellinger et al., 1993a, Wellinger et al., 1993b). Inhibition of Cdk1 activity resulted in loss of ssDNA signal in late S-phase at native telomeres, indicating that the nuclease activity which processes native telomeres during late S-phase is regulated by Cdk1 (Vodenicharov and Wellinger, 2006). The MRX complex has been shown to play a role in the formation of this cell cycle dependent 3' G-rich overhang. The G-rich overhangs in *mre11Δ* mutants were found to be shorter in length, indicating that although the MRX complex contributes to overhang formation (Larrivée et al., 2004).

Resection occurs at unprotected telomeres

Telomeres that become deprotected accumulate ssDNA damage, which is a potent activator of the DNA damage checkpoint. *CDC13* functions to cap chromosome ends by protecting them from nucleolytic degradation (Lydall et al., 1995, Booth et al., 2001). Interestingly, when telomere capping activities are inactivated, such as in *cdc13-1* mutants, checkpoint genes have also been shown to play a role in single stranded DNA generation at unprotected telomeres. *rad9Δ* and *rad24Δ* mutants are defective for cell

cycle arrest in response to *cdc13-1* damage, yet *RAD24* seems to contribute to ssDNA production and *RAD9* inhibits ssDNA production (Lydall and Weinert, 1995). Analysis of single-stranded DNA accumulation using a filter-binding assay to detect telomeric ssDNA demonstrated that the checkpoint gene *RAD9* limits single-stranded production at telomeres, as *cdc13-1 rad9Δ* exhibit higher levels of ssDNA. *RAD24* seems to contribute to the excessive single-stranded DNA accumulation in *cdc13-1* cells, as *cdc13-1 rad24Δ* exhibit lower levels of ssDNA (Lydall and Weinert, 1995). Furthermore, death of *cdc13-1 rad9* cells is due to the degradation controlled by *RAD24*, since *cdc13-1 rad9Δ rad24Δ* cells have better viability. In addition to Rad24, the exonuclease Exo1, contributes to telomeric ssDNA accumulation in *cdc13-1* mutants (Maringele and Lydall, 2002, Zubko et al., 2004). However, it has been shown that *cdc13-1 rad24Δ exo1Δ* cells still generated detectable levels of ssDNA at telomeres, indicating that additional nuclease activity was present. Hence, it is proposed that the sliding clamp loaded by the Rad24 complex is required to anchor a yet unidentified exonuclease, termed ExoX (Zubko et al., 2004).

The end replication problem

Although telomeres and their associated proteins are required to maintain chromosome end protection, it is necessary to allow telomerase access to the telomeric DNA sequence in order to complete telomere replication. Hence, the telomeric chromatin structures maintained throughout the cell cycle must be disrupted during DNA replication. The known DNA polymerases all synthesize genetic information in the 5'to 3' direction. They require a primer with 3' hydroxyl group in order to synthesis the

template. This primer then gets removed once synthesis has been primed and initiated. Replication of linear chromosome ends becomes problematic for cells due to the priming that is necessary in order to initiate synthesis (Watson, 1972, Olovnikov, 1973). In theory, the leading strand can be continuously synthesized to the end of chromosome. However, the lagging strand is synthesized in short, individually primed Okazaki fragments. The RNA primers are removed, the resulting gaps are filled in by DNA polymerase and the fragments are connected by DNA ligase. The removal of the most terminal RNA primer leaves a single-stranded 3' overhang at the chromosome end (Chakhparonian and Wellinger, 2003). Hence, the daughter DNA synthesized by lagging strand synthesis is shorter than parental DNA, while the daughter DNA synthesized by leading strand synthesis is the same length as the parental template DNA and has a blunt end. Processing of the blunt end resulting from leading strand synthesis to form a 3' overhang will result in a chromosome end that is shorter than the original template (Cech et al., 1997). Without a mechanism to compensate for the loss of sequence, chromosomes will gradually lose terminal sequence as cells continue to proliferate. As telomeres shorten, they lose the ability to provide a protective chromosome cap, eventually leading to cell cycle arrest, chromosome instability or cell death (Chakhparonian and Wellinger, 2003).

Timing of telomere replication

An evolutionarily conserved mechanism exists to compensate for this progressive loss of terminal sequence, which is accomplished through the activity of the enzyme telomerase (Blackburn, 2000). Semi- conservative replication is conducted during S

phase of the cell cycle and initiation of replication is controlled in respect to both location and time by replication origins, which contain autonomous replication sequence elements (ARSs). Telomeric sequence has been implicated in determining the timing of activation of subtelomeric ARSs. It has been shown that a circular plasmid containing telomeric TG_{1-3} repeats and an ARS initiated replication early, but if the plasmid is linearized so that it contains telomeres, the ARS fired late (Ferguson and Fangman, 1992). The conserved subtelomeric Y' element contains its own ARS (Chan, 1983). Using density transfer experiments and microarray analysis, it has been reported that this Y' ARS replicates in late S phase (Stevenson and Gottsching, 1999, Raghuraman et al., 2001). Consistent with this, the Blackburn lab demonstrated that the Y' ARS fires at the same time as an established late firing origin, *ARS501*, using two- dimensional gel electrophoresis gel analysis (Makovets et al., 2004). Taken together, these results indicate that telomeres are replicated late in S-phase, presumably after the majority of semi-conservative replication has been initiated.

In addition, analysis of yeast telomere replication intermediates demonstrated that the single-stranded G-rich 3' overhang is extended up to 30 bases in late S-phase, after the replication fork had reached the telomere (Wellinger et al., 1993a; Wellinger et al., 1993b). These G-tails can still form in a cell-cycle- dependent manner in a telomerase deficient cell, suggesting that an exonuclease resects the C-rich strands to generate elongated 3' overhangs late in S-phase (Wellinger et al., 1996; Dionne and Wellinger, 1996). These G-tails are thought to be a substrate that telomerase can act on to extend the telomere end, which is subsequently filled in by the conventional DNA replication

machinery (Lingner et al., 1995, Wellinger et al., 1996). Using non-denaturing Southern hybridization and two-dimensional agarose gel electrophoresis, it was shown that formation of an elongated G-tail on a linearized plasmid only occurred if the plasmid contained an origin of replication (Dionne and Wellinger, 1998). These results suggest that the generation of G-tails at the telomeres at the end of S-phase is dependent on the passage of a replication fork (Dionne and Wellinger, 1998). Telomeres on a minichromsome containing an ARS were found to be elongated by telomerase, while the elongation of telomeres on a minichromosome lacking the ARS was suppressed, which is consistent with the idea that replication fork passage promotes telomere extension by telomerase (Dionne and Wellinger, 1998, Marcand et al., 2000). Taken together, these data suggests a coordinated mechanism between conventional replication and telomere replication by telomerase.

C-strand synthesis is coordinated between telomerase and DNA polymerase alpha

C-strand fill-in synthesis refers to the mechanism by which the conventional DNA replication machinery, the DNA polymerase α/ primase complex, is used in telomere replication to generate the telomeric 5' C-strand once telomerase has extended the 3' G-strand (Greider et al., 1996) (Figure 1-5). Studies using the ciliate *Euplotes crassus* provide the first direct evidence for coordination between telomerase -dependent extension of the G-strand with DNA polymerase α -dependent synthesis of the corresponding C-strand. During the sexual stage of the life cycle in *Euplotes*, a large amount of telomeres are generated without simultaneous DNA replication which provided a unique opportunity to study the role of DNA polymerase in telomeric C-strand

synthesis (Prescott, 1994). In these experiments, the DNA polymerase inhibitor aphidicolin was used to inhibit DNA polymerase during the stage when *de novo* telomere addition occurred. Cells treated with aphidicolin resulted in lengthening of G-strands and an increase in heterogeneity of the C-strand length. Taken together, these results suggest that G- and C strand synthesis are coordinated with each other, and this regulation involves DNA polymerase α function (Fan and Price, 1997).

Furthermore, evidence supporting the coordination between G-strand and C-strand synthesis has been provided by yeast studies conducted in the Gottschling lab. These experiments take advantage of a system in which the *ADE2* gene, a telomere seed consisting of 81 base pairs of telomeric DNA repeats and a HO endonuclease cleavage site adjacent to telomere seed were inserted into left arm of Chromosome VII. Cleavage at the HO site exposes the telomere repeats, which can then be used by telomerase for *de novo* telomere addition (Diede and Gottsching, 1999). Using conditional alleles for essential replication proteins, these studies showed that *in vivo* telomere addition was specifically dependent on the main replicative polymerases *CDC17/POL1* (DNA polymerase α catalytic subunit), *POL2* (DNA polymerase δ catalytic subunit), as well as *PRI2* (DNA primase subunit), as loss of these genes reduces the addition of telomere repeats *in vivo* (Diede and Gottsching, 1999). These results indicate that the DNA polymerase α-primase complex does indeed participate in telomerase-mediated telomere addition and suggests that complete telomere replication requires telomerase to extend the G-rich DNA strand and DNA polymerase α to subsequently synthesize the complementary C-rich strand (Figure 1-5).

In addition, mutations in replication components such as Cdc17/Pol1, Pol12 (regulatory B subunit of DNA pol α), or Cdc44/RFC1 (large subunit of replication factor C) have been shown to exhibit a telomere lengthening phenotype, suggesting that filling in the complementary C-rich strand by DNA polymerase inhibits further telomere elongation (Carson and Hartwell, 1985, Grossi et al., 2004, Adams et al., 1996). A temperature sensitive allele of Pol1, *pol1-17*, has elongated telomeres which are accompanied by an increase in the length of the G-strand overhang (Adams Martin et al., 2000). It was also found that telomere addition required the activity of the cyclin-dependent kinase, *CDK1* (Frank et al., 2006). Cdk1 activity was required for the generation of 3′ single-strand overhangs at both native and de novo telomeres. Thus, Cdk1 activity is proposed to control the timing of telomere elongation by regulating the single-strand overhang at chromosome ends (Frank et al., 2006). Recent studies have also implicated the Cdk1-dependent phosphorylation of Cdc13 in the interaction between Cdc13 and Est1, suggesting a role for Cdk1 in telomerase recruitment (Li et al., 2009).

Telomere capping proteins interact with telomerase and DNA polymerase alpha

In addition to the requirements for *in vivo* telomere addition, protein-protein interactions have been uncovered which are thought to facilitate recruitment of both telomerase and DNA polymerase α to the telomere (Shore and Bianchi, 2009). Disruption of the interaction between the DNA replication machinery and telomere maintanence proteins alters telomere length. Cdc13 has also been shown to interact with Pol1, the DNA Polymerase α catalytic subunit, as well as and Est1, the regulatory subunit of telomerase through two-hybrid and biochemical techniques (Qi and Zakian, 2000).

Telomere lengthening was observed in the *pol1-236 and cdc13-50* alleles, which were found to disrupt the Cdc13-Pol1 interaction, suggesting that this interaction provides negative regulation of telomere length (Qi and Zakian, 2000). This interaction is proposed to be responsible for DNA polymerase α recruitment to the telomere to conduct fill-in synthesis and inhibit further telomere elongation by telomerase (Qi and Zakian, 2000).

In addition, Stn1 interacted with Pol12 through both yeast two hybrid and biochemical assays (Grossi et al., 2004, Petreaca et al., 2006). Furthermore, *pol12-216 stn1-13* double mutants are synthetic lethal, suggesting a potential functional interaction between Stn1 and Pol12 (Grossi et al., 2004). These associations between telomere capping proteins and replication proteins further supports the idea that the Cdc13, Stn1, and Ten1 complex coordinately regulates telomerase access with recruitment of the DNA polymerase α complex to the telomere to participate in fill-in synthesis of the C-strand (Qi and Zakian, 2000, Chandra et al., 2001). Interactions between telomerase and DNA polymerase α have been observed in organisms other than budding yeast as well. Telomerase was shown physically associate with the lagging-strand replication machinery through an interaction with DNA primase in *Euplotes crassus* (Ray et al., 2002). In *Schizosaccharomyces pombe,* it was shown that mutations in the *pol α* subunit of DNA polymerase α caused telomerase dependent long telomeres (Dahlén et al., 2003). Furthermore, DNA polymerase α was found to associate with telomerase *in vivo*, although whether this interaction is direct is unknown (Dahlén et al., 2003). Taken together, these data suggest that interactions between the DNA polymerase complex and

telomerase together coordinate telomerase-mediated extension of the G-strand with fill-in synthesis of the complementary C-strand.

As I've discussed in this overview, in budding yeast the Cdc13 protein has been shown to play essential roles in capping telomeres and in recruiting telomerase during telomere replication. However, how Cdc13 modulates its various activities and its functions in relation with Stn1 and Ten1 is not yet clear. The work presented in this thesis will attempt to elucidate some of the key issues not yet understood about Cdc13 function. Although it has been shown that Cdc13 protects the chromosome end from degradation by nucleases, all the nuclease acitivites present at unprotected telomeres in *cdc13-1* cells have not yet been identified (Garvik et al., 1995, Lydall and Weinert, 1995, Nugent et al., 1996, Booth et al., 2001). In Chapter 2, we describe a screen conducted in an attempt to identify activities involved in telomere C-strand loss at uncapped telomeres in *cdc13-1* cells. The screen resulted in the identification of two novel alleles of *RAD24*. Each *rad24* allele, results in the production of two amino terminal truncations of Rad24. We show that an intact Rad24 amino-terminus is necessary for its checkpoint function. The *rad24-2* allele combined with telomere amplification facilitated the growth of *cdc13-1* cells at high temperatures and *rad24-2* increased the frequency of obtaining temperature resistant *cdc13-1* cells.

Cdc13 facilitates the elongation of telomeres by telomerase through an interaction with the telomerase subunit, Est1 (Chandra et al., 2001, Taggart et al., 2002). Dr. Nugent observed that Cdc13 was phosphorylated during late S-phase, the time when telomeres are expected to be replicated. In Chapter 3, we focused on identifying the kinase

responsible for this phosphorylation and determining its functional significance. We demonstrate that Cdc13 is phosphorylated by Cdk1 on residue T308. Loss of the phosphorylation site through a T308A mutation resulted in telomere shortening, suggesting a role for the Cdk1- mediated phosphorylation in telomerase recruitment. The phosphorylation of Cdc13 also promoted interaction with the 14-3-3 protein, Bmh1, which may be involved in regulating the protein stability of Cdc13.

In addition to interacting with telomerase, Cdc13 has been shown to associate with Pol1 of the DNA polymerase α-primase complex. The Cdc13- Pol1 interaction is thought to coordinate telomere extension of the G-strand by telomerase with fill-in synthesis of the C-strand by DNA polymerase α. Furthermore, Stn1 has been shown to interact with the Pol12 subunit of DNA polymerase α as well (Grossi et al., 2004, Petreaca et al., 2006). However, it has not been directly shown that the Cdc13- Pol1 and Stn1-Pol12 interactions serve to recruit DNA polymerase α to the telomere. In Chapter 4, we investigate the functional significance of the Cdc13- Pol1 and Stn1-Pol12 interactions in telomere length regulation. We show that the interactions between Cdc13 and Pol1 and between Stn1 and Pol12 are direct. Analysis of a *pol1-236 pol12-40* double mutant, which has both these interactions disrupted, shows that loss of the Cdc13- Pol1 and Stn1-Pol12 interactions result in elongated telomere length, consistent with the idea that these interactions negatively regulate telomerase extension length. The major conclusions from the studies presented in this thesis supports the idea that Cdc13 makes independent contributions to both telomere end protection and telomere length regulation by forming different protein complexes.

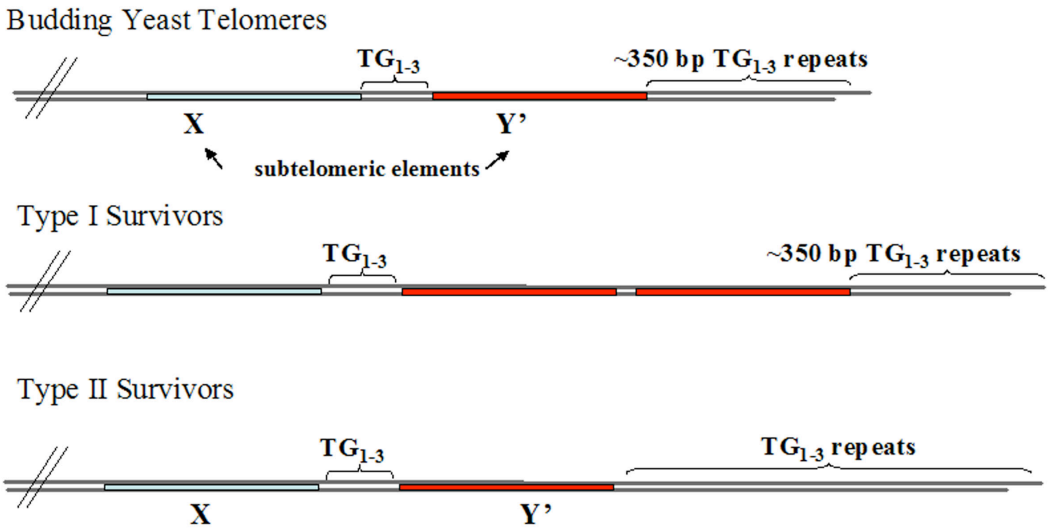

Figure 1-1 Budding yeast telomeres contain conserved sequence. *S. cerevisiae* telomeres contain approximately 250 to 350 bp of terminal TG_{1-3} repeats. All yeast telomeres contain a 475 bp conserved X element. Approximately two-thirds of the telomeres in haploid cells contain one or more copies of subtelomeric Y' elements. TG_{1-3} sequences are found between some X and Y' elements. In cells lacking telomerase, telomeres become critically short and cells eventually enter crisis. Yeast cells can generate survivors at low frequency that maintain telomeres by a recombination-dependent mechanism. Two types of these survivors have been identified. Type I survivors amplify Y' subtelomeric elements and Type II amplify the TG_{1-3} repeats.

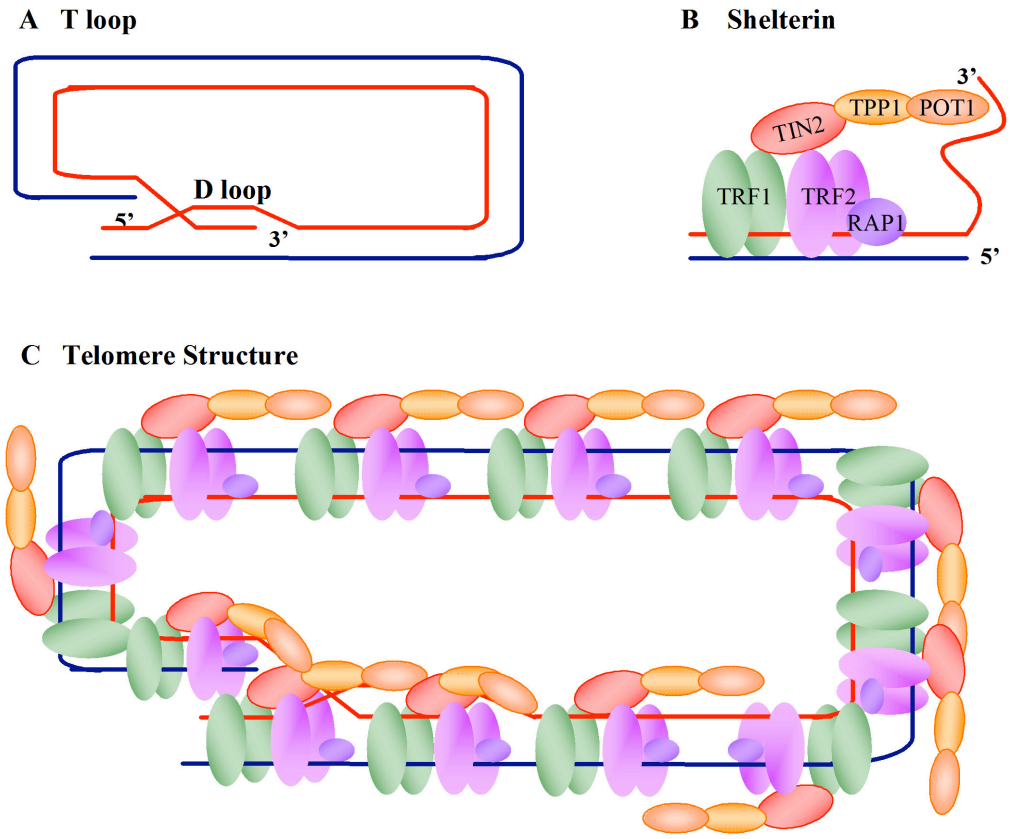

Figure 1-2 Mammalian Telomere Structure A. Mammalian telomeres are composed of long stretches of the repetitive sequence TTAGGG that form a lariat structure, the t-loop, which results from the strand invasion of the 3' single-stranded overhang into the adjacent telomeric dsDNA region. This displaced region is referred to as the d- loop. B. The t-loop is stabilized by the telomere-specific protein complex, shelterin. The shelterin complex is comprised of TRF1, TRF2, RAP1, TIN2, TPP1 and POT1. TRF1 and TRF2 bind to the telomeric dsDNA, while POT1 interacts with single-stranded telomeric DNA. TIN2 and TPP1 connect POT1 to TRF1 and TRF2. TRF2 also bind Rap1. C. Shelterin binds the majority of the double-stranded telomeric DNA, and POT1 associates with single-stranded telomeric DNA either at the 3' overhang or in the D loop. Shelterin and the t-loop structure together stabilize and protect the chromosome end from unwanted repair events

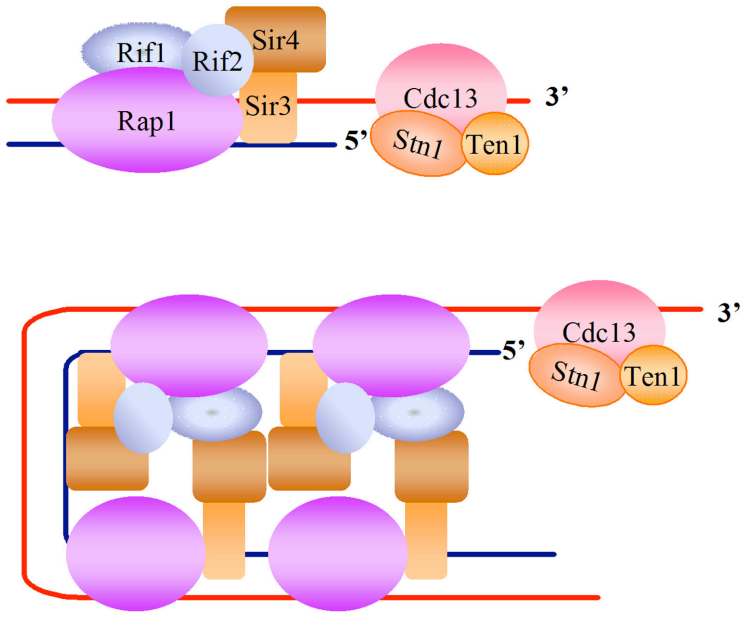

Figure 1-3 Yeast Telomere Structure
In budding yeast, the telomeric DNA is packaged in a non-nucleosomal DNA–protein complex. Duplex telomeric DNA is covered by of Rap1 protein that interact either with a Sir complex, which is involved in the formation of subtelomeric heterochromatin, or with a Rif complex, which negatively controls telomere elongation.

Figure 1-4 DNA Damage Checkpoint
In *S. cerevisiae*, the Mec1/Ddc2 complex has also been shown to localizes to a DSB following resection by MRX. The Rad24-RFC clamp loading complex is also recruited to DNA damage sites and loads the sliding checkpoint clamp onto sites of DNA damage. The Ddc1/Rad17/Mec3 complex recruits Mec1 substrates, such as Rad9, allowing Mec1 to phosphorylate targets of the DNA damage checkpoint signal transduction. After Mec1 phosphorylates Rad9, Rad9 can associate with Rad53 which promotes the autophosphorylation of Rad53. Phosphorylated Rad53 dissociates from Rad9 and transmits the damage signals to further downstream targets. Once Rad53 is activated it can phosphorylate targets such as Dun1 and Cdc5, which function to arrest the cell cycle and activate repair of DNA damage. Rad9 activates a separate branch of the checkpoint response through association with Chk1, in response to DNA damage. After activation, Chk1 can phosphorylate Pds1 directly, which contributes to the G2/M cell cycle arrest.

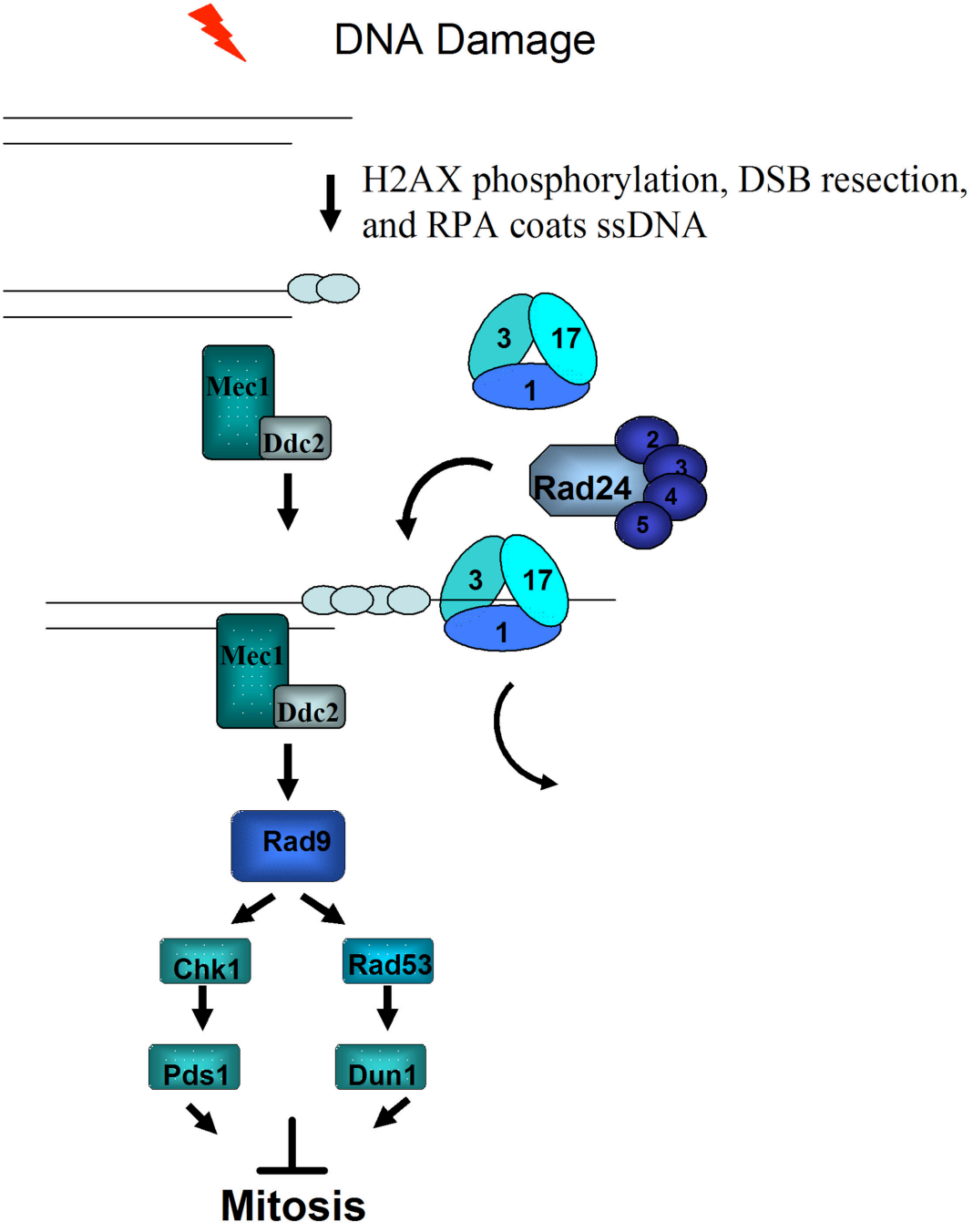
DNA Damage
H2AX phosphorylation, DSB resection, and RPA coats ssDNA
3
17
1
Mec1
Ddc2
2
3
4
5
Rad24
3
17
1
Mec1
Ddc2
Rad9
Chk1
Rad53
Pds1
Dun1
Mitosis

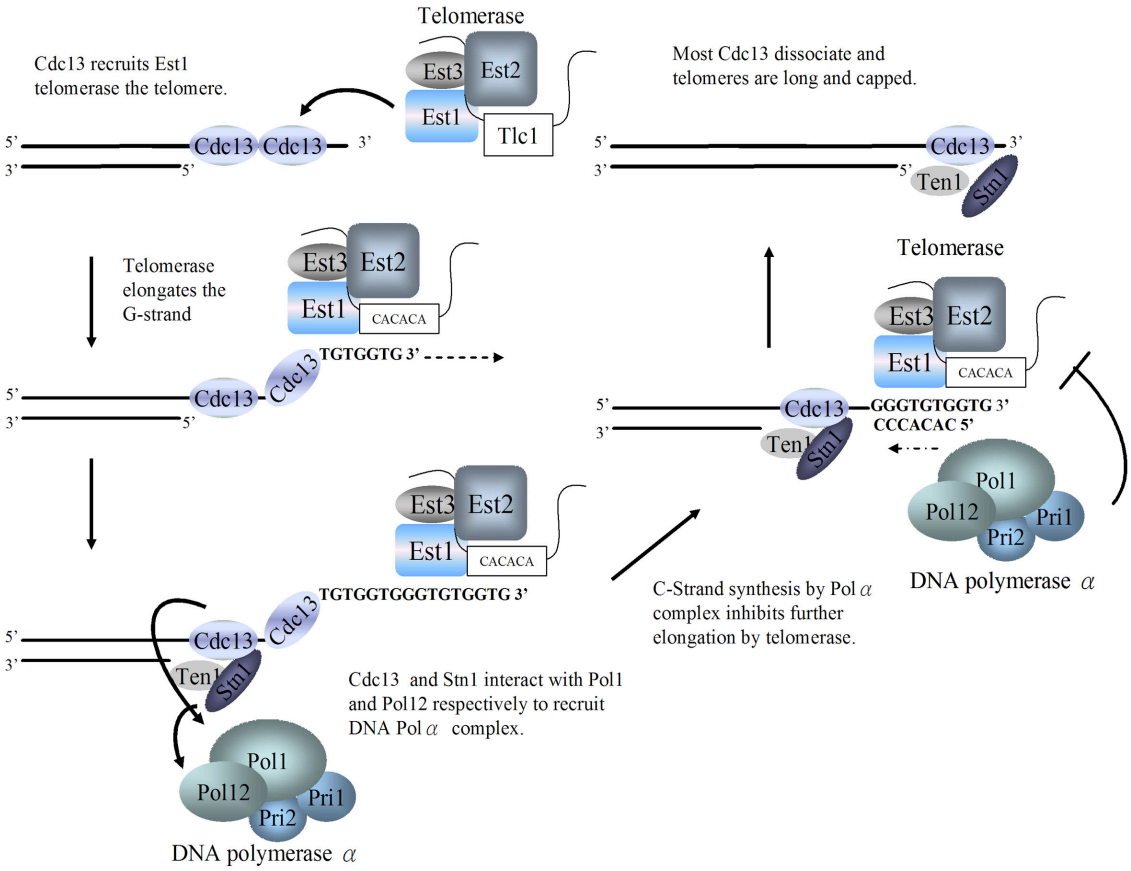

Figure 1-5 Telomere replication in budding yeast The telomere end is processed by MRX complex. Cdc13 binding to the telomere blocks further exonucleolytic degradation. Cdc13 also recruits Est1, which activates telomerase. Cdc13 and Stn1 then recruit the DNA polymerase α. DNA Polymerase α synthesizes the complementary C-strand, and acts as a negative feedback loop on telomerase activity.

References

Adams, A. & Holm, C. 1996. Specific DNA Replication Mutations Affect Telomere Length In Saccharomyces Cerevisiae. *Mol Cell Biol,* 16, 4614-20.

Adams Martin, A., Dionne, I., Wellinger, R. & Holm, C. 2000. The Function Of DNA Polymerase Alpha At Telomeric G Tails Is Important For Telomere Homeostasis. *Mol Cell Biol,* 20, 786-96.

Allen, J., Zhou, Z., Siede, W., Friedberg, E. & Elledge, S. 1994. The Sad1/Rad53 Protein Kinase Controls Multiple Checkpoints and DNA Damage-Induced Transcription In Yeast. *Genes Dev,* 8, 2401-15.

Allshire, R., Dempster, M. & Hastie, N. 1989. Human Telomeres Contain At Least Three Types Of G-Rich Repeat Distributed Non-Randomly. *Nucleic Acids Res,* 17, 4611-27.

Bailey, S. & Murnane, J. 2006. Telomeres, Chromosome Instability And Cancer. *Nucleic Acids Res,* 34, 2408-17.

Baumann, P. & Cech, T. 2001. Pot1, The Putative Telomere End-Binding Protein In Fission Yeast And Humans. *Science,* 292, 1171-5.

Beernink, H., Miller, K., Deshpande, A., Bucher, P. & Cooper, J. 2003. Telomere Maintenance In Fission Yeast Requires An Est1 Ortholog. *Curr Biol,* 13, 575-80.

Bertuch, A. & Lundblad, V. 1998. Telomeres And Double-Strand Breaks: Trying To Make Ends Meet. *Trends Cell Biol,* 8, 339-42.

Bianchi, A., Smith, S., Chong, L., Elias, P. & De Lange, T. 1997. Trf1 Is A Dimer And Bends Telomeric Dna. *Embo J,* 16, 1785-94.

Bilaud, T., Brun, C., Ancelin, K., Koering, C., Laroche, T. & Gilson, E. 1997. Telomeric Localization Of Trf2, A Novel Human Telobox Protein. *Nat Genet,* 17, 236-9.

Blackburn, E. 2000. Telomere States And Cell Fates. *Nature,* 408, 53-6.

Blankley, R. & Lydall, D. 2004. A Domain Of Rad9 Specifically Required For Activation Of Chk1 In Budding Yeast. *J Cell Sci,* 117, 601-8.

Booth, C., Griffith, E., Brady, G. & Lydall, D. 2001. Quantitative Amplification Of Single-Stranded DNA (QAOS) Demonstrates that *cdc13-1* Mutants Generate ssDNA In A Telomere To Centromere Direction. *Nucleic Acids Res,* 29, 4414-22.

Broccoli, D., Smogorzewska, A., Chong, L. & De Lange, T. 1997. Human Telomeres Contain Two Distinct Myb-Related Proteins, Trf1 And Trf2. *Nat Genet,*17, 231-5.

Carson, M. & Hartwell, L. 1985. Cdc17: An Essential Gene That Prevents Telomere Elongation In Yeast. *Cell,* 42, 249-57.

Cech, T., Nakamura, T. & Lingner, J. 1997. Telomerase Is A True Reverse Transcriptase. A Review. *Biochemistry (Mosc),* 62, 1202-5.

Celli, G. B. & De Lange, T. 2005. Dna Processing Is Not Required For Atm-Mediated Telomere Damage Response After Trf2 Deletion. *Nat Cell Biol,* 7, 712-8.

Chakhparonian, M. & Wellinger, R. 2003. Telomere Maintenance And DNA Replication: How Closely Are These Two Connected? *Trends Genet,* 19, 439-46.

Chan, A., Boulé, J. & Zakian, V. 2008. Two Pathways Recruit Telomerase To Saccharomyces Cerevisiae Telomeres. *Plos Genet,* 4, E1000236.

Chan, C. & Tye, B. 1983. Organization Of DNA Sequences And Replication Origins At Yeast Telomeres. *Cell,* 33, 563-73.

Chandra, A., Hughes, T. R., Nugent, C. I. & Lundblad, V. 2001. Cdc13 Both Positively And Negatively Regulates Telomere Replication. *Genes Dev,* 15, 404-14.
Chen, Q., Ijpma, A. & Greider, C. 2001. Two Survivor Pathways That Allow Growth In The Absence Of Telomerase Are Generated By Distinct Telomere Recombination Events. *Mol Cell Biol,* 21, 1819-27.
Chong, L., Van Steensel, B., Broccoli, D., Erdjument-Bromage, H., Hanish, J., Tempst, P. & De Lange, T. 1995. A Human Telomeric Protein. *Science,* 270, 1663-7.
Classen, S., Ruggles, J. & Schultz, S. 2001. Crystal Structure Of The N-Terminal Domain Of Oxytricha Nova Telomere End-Binding Protein Alpha Subunit Both Uncomplexed And Complexed With Telomeric Ssdna. *J Mol Biol,* 314, 1113-25.
Cohn, M. & Blackburn, E. 1995. Telomerase In Yeast. *Science,* 269, 396-400.
Colgin, L., Baran, K., Baumann, P., Cech, T. & Reddel, R. 2003. Human Pot1 Facilitates Telomere Elongation By Telomerase. *Curr Biol,* 13, 942-6.
Cong, Y., Wright, W. & Shay, J. 2002. Human Telomerase And Its Regulation. *Microbiol Mol Biol Rev,* 66, 407-25, Table Of Contents.
Conrad, M., Wright, J., Wolf, A. & Zakian, V. 1990. Rap1 Protein Interacts With Yeast Telomeres In Vivo: Overproduction Alters Telomere Structure And Decreases Chromosome Stability. *Cell,* 63, 739-50.
Counter, C., Meyerson, M., Eaton, E. & Weinberg, R. 1997. The Catalytic Subunit Of Yeast Telomerase. *Proc Natl Acad Sci U S A,* 94, 9202-7.
Craven, R., Greenwell, P., Dominska, M. & Petes, T. 2002. Regulation Of Genome Stability By Tel1 And Mec1, Yeast Homologs Of The Mammalian Atm And Atr Genes. *Genetics,* 161, 493-507.
Cross, S., Allshire, R., Mckay, S., Mcgill, N. & Cooke, H. 1989. Cloning Of Human Telomeres By Complementation In Yeast. *Nature,* 338, 771-4.
D'adda Di Fagagna, F., Teo, S. & Jackson, S. 2004. Functional Links Between Telomeres And Proteins Of The Dna-Damage Response. *Genes Dev,* 18, 1781-99.
D'amours, D. & Jackson, S. 2001. The Yeast Xrs2 Complex Functions In S Phase Checkpoint Regulation. *Genes Dev,* 15, 2238-49.
Dahlén, M., Sunnerhagen, P. & Wang, T. 2003. Replication Proteins Influence The Maintenance Of Telomere Length And Telomerase Protein Stability. *Mol Cell Biol,* 23, 3031-42.
De Bruin, D., Kantrow, S., Liberatore, R. & Zakian, V. 2000. Telomere Folding Is Required For The Stable Maintenance Of Telomere Position Effects In Yeast. *Mol Cell Biol,* 20, 7991-8000.
De Bruin, D., Zaman, Z., Liberatore, R. & Ptashne, M. 2001. Telomere Looping Permits Gene Activation By A Downstream UAS In Yeast. *Nature,* 409, 109-13.
De Lange, T. 2004. T-Loops And The Origin Of Telomeres. *Nat Rev Mol Cell Biol,* 5, 323-9.
De Lange, T. 2005. Shelterin: The Protein Complex That Shapes And Safeguards Human Telomeres. *Genes Dev,* 19, 2100-10.
De Lange, T. 2009. How Telomeres Solve The End-Protection Problem. *Science,* 326, 948-52.
Del Vescovo, V., De Sanctis, V., Bianchi, A., Shore, D., Di Mauro, E. & Negri, R. 2004.

Distinct Dna Elements Contribute To Rap1p Affinity For Its Binding Sites. *J Mol Biol,* 338, 877-93.
Deng, Y., Chan, S. & Chang, S. 2008. Telomere Dysfunction and Tumour Suppression: The Senescence Connection. *Nat Rev Cancer,* 8, 450-8.
Dezwaan, D. & Freeman, B. 2009. The Conserved Est1 Protein Stimulates Telomerase DNA Extension Activity. *Proc Natl Acad Sci U S A,* 106, 17337-42.
Diede, S. J. & Gottschling, D. E. 1999. Telomerase-Mediated Telomere Addition In Vivo Requires DNA Primase And Dna Polymerases Alpha And Delta. *Cell,* 99, 723-33.
Dionne, I. & Wellinger, R. 1996. Cell Cycle-Regulated Generation Of Single-Stranded G-Rich Dna In The Absence Of Telomerase. *Proc Natl Acad Sci U S A,* 93, 13902-7.
Dionne, I. & Wellinger, R. 1998. Processing Of Telomeric DNA Ends Requires The Passage Of A Replication Fork. *Nucleic Acids Res,* 26, 5365-71.
Downs, J., Lowndes, N. & Jackson, S. 2000. A Role For Saccharomyces Cerevisiae Histone H2A In Dna Repair. *Nature,* 408, 1001-4.
Dubrana, K., Van Attikum, H., Hediger, F. & Gasser, S. 2007. The Processing Of Double-Strand Breaks And Binding Of Single-Strand-Binding Proteins Rpa And Rad51 Modulate The Formation Of Atr-Kinase Foci In Yeast. *J Cell Sci,* 120, 4209-20.
Enomoto, S., Glowczewski, L. & Berman, J. 2002. Mec3, Mec1, And Ddc2 Are Essential Components of a Telomere Checkpoint Pathway Required For Cell Cycle Arrest During Senescence In Saccharomyces Cerevisiae. *Mol Biol Cell,* 13, 2626-38.
Evans, S. & Lundblad, V. 2002. The Est1 Subunit Of Saccharomyces Cerevisiae Telomerase Makes Multiple Contributions To Telomere Length Maintenance. *Genetics,* 162, 1101-15.
Falck, J., Coates, J. & Jackson, S. 2005. Conserved Modes Of Recruitment Of Atm, Atr And Dna-Pkcs To Sites Of Dna Damage. *Nature,* 434, 605-11.
Fan, X. & Price, C. 1997. Coordinate Regulation Of G- And C Strand Length During New Telomere Synthesis. *Mol Biol Cell,* 8, 2145-55.
Feng, J., Funk, W., Wang, S., Weinrich, S., Avilion, A., Chiu, C., Adams, R., Chang, E., Allsopp, R. & Yu, J. 1995. The RNA Component Of Human Telomerase. *Science,* 269, 1236-41.
Ferguson, B. & Fangman, W. 1992. A Position Effect On The Time Of Replication Origin Activation In Yeast. *Cell,* 68, 333-9.
Ferreira, M. & Cooper, J. 2001. The Fission Yeast Taz1 Protein Protects Chromosomes From Ku-Dependent End-To-End Fusions. *Mol Cell,* 7, 55-63.
Frank, C., Hyde, M. & Greider, C. 2006. Regulation of Telomere Elongation by the Cyclin-Dependent Kinase Cdk1. *Mol Cell,* 24, 423-32.
Friedman, K., Heit, J., Long, D. & Cech, T. 2003. N-Terminal Domain Of Yeast Telomerase Reverse Transcriptase: Recruitment of Est3p To The Telomerase Complex. *Mol Biol Cell,* 14, 1-13.
Froelich-Ammon, S., Dickinson, B., Bevilacqua, J., Schultz, S. & Cech, T. 1998. Modulation of Telomerase Activity By Telomere DNA-Binding Proteins In Oxytricha. *Genes Dev,* 12, 1504-14.
Gao, H., Cervantes, R., Mandell, E., Otero, J. & Lundblad, V. 2007. Rpa-Like Proteins Mediate Yeast Telomere Function. *Nat Struct Mol Biol,* 14, 208-14.

Garvik, B., Carson, M. & Hartwell, L. 1995. Single-Stranded Dna Arising At Telomeres In Cdc13 Mutants May Constitute A Specific Signal For The Rad9 Checkpoint. *Mol Cell Biol,* 15, 6128-38.
Gilbert, C., Green, C. & Lowndes, N. 2001. Budding Yeast Rad9 is an ATP-Dependent Rad53 Activating Machine. *Mol Cell,* 8, 129-36.
Gottschling, D. & Cech, T. 1984. Chromatin Structure of The Molecular Ends Of Oxytricha Macronuclear DNA: Phased Nucleosomes And A Telomeric Complex. *Cell,* 38, 501-10.
Gottschling, D. & Zakian, V. 1986. Telomere Proteins: Specific Recognition and Protection Of The Natural Termini Of Oxytricha Macronuclear Dna. *Cell,* 47, 195-205.
Goudsouzian, L., Tuzon, C. & Zakian, V. 2006. S. Cerevisiae Tel1p And Mre11p Are Required For Normal Levels Of Est1p And Est2p Telomere Association. *Mol Cell,* 24, 603-10.
Grandin, N., Damon, C. & Charbonneau, M. 2001. Ten1 Functions in Telomere End Protection and Length Regulation in Association With Stn1 And Cdc13. *Embo J,* 20, 1173-83.
Grandin, N., Reed, S. & Charbonneau, M. 1997. Stn1, A New Saccharomyces Cerevisiae Protein, Is Implicated In Telomere Size Regulation In Association With Cdc13. *Genes Dev,* 11, 512-27.
Green, C., Erdjument-Bromage, H., Tempst, P. & Lowndes, N. 2000. A Novel Rad24 Checkpoint Protein Complex Closely Related To Replication Factor C. *Curr Biol,* 10, 39-42.
Greider, C. 1996. Telomere Length Regulation. *Annu Rev Biochem,* 65, 337-65.
Greider, C. & Blackburn, E. 1989. A Telomeric Sequence In The RNA Of Tetrahymena Telomerase Required For Telomere Repeat Synthesis. *Nature,* 337, 331-7.
Grenon, M., Gilbert, C. & Lowndes, N. 2001. Checkpoint Activation In Response To Double-Strand Breaks Requires The Mre11/Rad50/Xrs2 Complex. *Nat Cell Biol,* 3, 844-7.
Griffith, J., Comeau, L., Rosenfield, S., Stansel, R., Bianchi, A., Moss, H. & De Lange, T. 1999. Mammalian Telomeres End In A Large Duplex Loop. *Cell,* 97, 503-14.
Griffith, J., Lindsey-Boltz, L. & Sancar, A. 2002. Structures Of The Human Rad17-Replication Factor C And Checkpoint Rad 9-1-1 Complexes Visualized By Glycerol Spray/Low Voltage Microscopy. *J Biol Chem,* 277, 15233-6.
Grossi, S., Puglisi, A., Dmitriev, P., Lopes, M. & Shore, D. 2004. Pol12, The B Subunit of DNA Polymerase Alpha, Functions In Both Telomere Capping And Length Regulation. *Genes Dev,* 18, 992-1006.
Grunstein, M. 1998. Yeast Heterochromatin: Regulation Of Its Assembly And Inheritance By Histones. *Cell,* 93, 325-8.
Guo, X., Deng, Y., Lin, Y., Cosme-Blanco, W., Chan, S., He, H., Yuan, G., Brown, E. & Chang, S. 2007. Dysfunctional Telomeres Activate An ATM-ATR-Dependent DNA Damage Response To Suppress Tumorigenesis. *Embo J,* 26, 4709-19.
Hanaoka, S., Nagadoi, A. & Nishimura, Y. 2005. Comparison Between Trf2 And Trf1 Of Their Telomeric Dna-Bound Structures and DNA-Binding Activities. *Protein Sci,* 14, 119-30.

Hardy, C., Sussel, L. & Shore, D. 1992. A Rap1-Interacting Protein Involved In Transcriptional Silencing And Telomere Length Regulation. *Genes Dev,* 6, 801-14.
Harrington, L., Zhou, W., Mcphail, T., Oulton, R., Yeung, D., Mar, V., Bass, M. & Robinson, M. 1997. Human Telomerase Contains Evolutionarily Conserved Catalytic And Structural Subunits. *Genes Dev,* 11, 3109-15.
Harrison, J. & Haber, J. 2006. Surviving the Breakup: The DNA Damage Checkpoint. *Annu Rev Genet,* 40, 209-35.
Hector, R., Shtofman, R., Ray, A., Chen, B., Nyun, T., Berkner, K. & Runge, K. 2007. Tel1p Preferentially Associates With Short Telomeres To Stimulate Their Elongation. *Mol Cell,* 27, 851-8.
Henson, J., Neumann, A., Yeager, T. & Reddel, R. 2002. Alternative Lengthening Of Telomeres in Mammalian Cells. *Oncogene,* 21, 598-610.
Hockemeyer, D., Daniels, J., Takai, H. & De Lange, T. 2006. Recent Expansion Of The Telomeric Complex In Rodents: Two Distinct Pot1 Proteins Protect Mouse Telomeres. *Cell,* 126, 63-77.
Horvath, M., Schweiker, V., Bevilacqua, J., Ruggles, J. & Schultz, S. 1998. Crystal Structure of the *Oxytricha nova* Telomere End Binding Protein Complexed With Single Strand DNA. *Cell,* 95, 963-74.
Houghtaling, B., Cuttonaro, L., Chang, W. & Smith, S. 2004. A Dynamic Molecular Link between the Telomere Length Regulator Trf1 and the Chromosome End Protector Trf2. *Curr Biol,* 14, 1621-31.
Hughes, T., Evans, S., Weilbaecher, R. & Lundblad, V. 2000a. The Est3 Protein Is A Subunit Of Yeast Telomerase. *Curr Biol,* 10, 809-12.
Hughes, T., Weilbaecher, R., Walterscheid, M. & Lundblad, V. 2000b. Identification of The Single-Strand Telomeric DNA Binding Domain of the *Saccharomyces cerevisiae* Cdc13 Protein. *Proc Natl Acad Sci U S A,* 97, 6457-62.
Humpal, S., Robinson, D. & Krebs, J. 2009. Marks To Stop The Clock: Histone Modifications And Checkpoint Regulation in the DNA Damage Response. *Biochem Cell Biol,* 87, 243-53.
Ira, G., Pellicioli, A., Balijja, A., Wang, X., Fiorani, S., Carotenuto, W., Liberi, G., Bressan, D., Wan, L., Hollingsworth, N., Haber, J. & Foiani, M. 2004. DNA End Resection, Homologous Recombination And DNA Damage Checkpoint Activation Require Cdk1. *Nature,* 431, 1011-7.
Karlseder, J., Broccoli, D., Dai, Y., Hardy, S. & De Lange, T. 1999. P53- and ATM-Dependent Apoptosis Induced By Telomeres Lacking Trf2. *Science,* 283, 1321-5.
Kelleher, C., Kurth, I. & Lingner, J. 2005. Human Protection Of Telomeres 1 (Pot1) Is A Negative Regulator Of Telomerase Activity In Vitro. *Mol Cell Biol,* 25, 808-18.
Kim, S., Davalos, A., Heo, S., Rodier, F., Zou, Y., Beausejour, C., Kaminker, P., Yannone, S. & Campisi, J. 2008. Telomere Dysfunction and Cell Survival: Roles For Distinct Tin2-Containing Complexes. *J Cell Biol,* 181, 447-60.
Kim, S., Kaminker, P. & Campisi, J. 1999. Tin2, a New Regulator of Telomere Length In Human Cells. *Nat Genet,* 23, 405-12.
Klobutcher, L., Swanton, M., Donini, P. & Prescott, D. 1981. All Gene-Sized Dna Molecules In Four Species Of Hypotrichs Have The Same Terminal Sequence And An

Unusual 3' Terminus. *Proc Natl Acad Sci U S A,* 78, 3015-9.
Kondo, T., Wakayama, T., Naiki, T., Matsumoto, K. & Sugimoto, K. 2001. Recruitment Of Mec1 And Ddc1 Checkpoint Proteins To Double-Strand Breaks Through Distinct Mechanisms. *Science,* 294, 867-70.
Konig, P., Giraldo, R., Chapman, L. & Rhodes, D. 1996. The Crystal Structure Of The DNA-Binding Domain Of Yeast Rap1 In Complex With Telomeric DNA. *Cell,* 85, 125-36.
Krauskopf, A. & Blackburn, E. 1998. Rap1 Protein Regulates Telomere Turnover In Yeast. *Proc Natl Acad Sci U S A,* 95, 12486-91.
König, P., Fairall, L. & Rhodes, D. 1998. Sequence-Specific DNA Recognition By The Myb-Like Domain of The Human Telomere Binding Protein Trf1: A Model For The Protein-Dna Complex. *Nucleic Acids Res,* 26, 1731-40.
Larrivée, M., Lebel, C. & Wellinger, R. 2004. The Generation of Proper Constitutive G-Tails On Yeast Telomeres is Dependent on the MRX Complex. *Genes Dev,* 18, 1391-6.
Lee, J., Mandell, E., Rao, T., Wuttke, D. & Lundblad, V. 2010. Investigating The Role Of The Est3 Protein In Yeast Telomere Replication. *Nucleic Acids Res*.
Lendvay, T., Morris, D., Sah, J., Balasubramanian, B. & Lundblad, V. 1996. Senescence Mutants Of Saccharomyces Cerevisiae With A Defect In Telomere Replication Identify Three Additional *EST* Genes. *Genetics,* 144, 1399-412.
Levy, D. & Blackburn, E. 2004. Counting Of Rif1p And Rif2p On Saccharomyces Cerevisiae Telomeres Regulates Telomere Length. *Mol Cell Biol,* 24, 10857-67.
Li, B., Oestreich, S. & De Lange, T. 2000. Identification Of Human Rap1: Implications For Telomere Evolution. *Cell,* 101, 471-83.
Li, S., Makovets, S., Matsuguchi, T., Blethrow, J., Shokat, K. & Blackburn, E. 2009. Cdk1-Dependent Phosphorylation Of Cdc13 Coordinates Telomere Elongation During Cell-Cycle Progression. *Cell,* 136, 50-61.
Lin, J. & Zakian, V. 1996. The Saccharomyces Cdc13 Protein Is A Single-Strand TG1-3 Telomeric Dna-Binding Protein In Vitro That Affects Telomere Behavior *in vivo*. *Proc Natl Acad Sci U S A,* 93, 13760-5.
Lingner, J. & Cech, T. 1996. Purification of Telomerase From Euplotes Aediculatus: Requirement Of A Primer 3' Overhang. *Proc Natl Acad Sci U S A,* 93, 10712-7.
Lingner, J., Cech, T., Hughes, T. & Lundblad, V. 1997a. Three Ever Shorter Telomere (*EST*) Genes Are Dispensable for *in vitro* Yeast Telomerase Activity. *Proc Natl Acad Sci U S A,* 94, 11190-5.
Lingner, J., Hendrick, L. & Cech, T. 1994. Telomerase RNAs Of Different Ciliates Have A Common Secondary Structure and a Permuted Template. *Genes Dev,* 8, 1984-98.
Lingner, J., Hughes, T., Shevchenko, A., Mann, M., Lundblad, V. & Cech, T. 1997b. Reverse Transcriptase Motifs In The Catalytic Subunit Of Telomerase. *Science,* 276, 561-7.
Lisby, M. & Rothstein, R. 2004. Dna Damage Checkpoint And Repair Centers. *Curr Opin Cell Biol,* 16, 328-34.
Liu, D., Safari, A., O'connor, M., Chan, D., Laegeler, A., Qin, J. & Songyang, Z. 2004. Ptop Interacts With Pot1 and Regulates Its Localization To Telomeres. *Nat Cell Biol,* 6, 673-80.

Livengood, A., Zaug, A. & Cech, T. 2002. Essential Regions of *Saccharomyces cerevisiae* Telomerase RNA: Separate Elements For Est1p And Est2p Interaction. *Mol Cell Biol,* 22, 2366-74.
Loayza, D. & De Lange, T. 2003. Pot1 as a Terminal Transducer of Trf1 Telomere Length Control. *Nature,* 423, 1013-8.
Lundblad, V. & Blackburn, E. 1990. RNA-Dependent Polymerase Motifs in Est1: Tentative Identification of a Protein Component of an Essential Yeast Telomerase. *Cell,* 60, 529-30.
Lundblad, V. & Blackburn, E. 1993. An Alternative Pathway For Yeast Telomere Maintenance Rescues Est1- Senescence. *Cell,* 73, 347-60.
Lundblad, V. & Szostak, J. 1989. A Mutant with a Defect in Telomere Elongation Leads To Senescence in Yeast. *Cell,* 57, 633-43.
Lustig, A., Kurtz, S. & Shore, D. 1990. Involvement Of The Silencer And Uas Binding Protein Rap1 In Regulation Of Telomere Length. *Science,* 250, 549-53.
Lydall, D. & Weinert, T. 1995. Yeast Checkpoint Genes in DNA Damage Processing: Implications For Repair and Arrest. *Science,* 270, 1488-91.
Lydall, D. & Weinert, T. 1997. G2/M Checkpoint Genes of *Saccharomyces cerevisiae*: Further Evidence For Roles in DNA Replication And/Or Repair. *Mol Gen Genet,* 256, 638-51.
Majka, J. & Burgers, P. 2003. Yeast Rad17/Mec3/Ddc1: A Sliding Clamp For The DNA Damage Checkpoint. *Proc Natl Acad Sci U S A,* 100, 2249-54.
Majka, J. & Burgers, P. 2004. The Pcna-Rfc Families of DNA Clamps And Clamp Loaders. *Prog Nucleic Acid Res Mol Biol,* 78, 227-60.
Makovets, S., Herskowitz, I. & Blackburn, E. 2004. Anatomy and Dynamics Of DNA Replication Fork Movement In Yeast Telomeric Regions. *Mol Cell Biol,* 24, 4019-31.
Mantiero, D., Clerici, M., Lucchini, G. & Longhese, M. 2007. Dual Role For Saccharomyces Cerevisiae Tel1 in the Checkpoint Response To Double-Strand Breaks. *Embo Rep,* 8, 380-7.
Marcand, S., Brevet, V., Mann, C. & Gilson, E. 2000. Cell Cycle Restriction Of Telomere Elongation. *Curr Biol,* 10, 487-90.
Marcand, S., Gilson, E. & Shore, D. 1997. A Protein-Counting Mechanism for Telomere Length Regulation in Yeast. *Science,* 275, 986-90.
Maringele, L. & Lydall, D. 2002. Exo1-Dependent Single-Stranded DNA at Telomeres Activates Subsets Of DNA Damage And Spindle Checkpoint Pathways in Budding Yeast Yku70delta Mutants. *Genes Dev,* 16, 1919-33.
Martín, V., Du, L., Rozenzhak, S. & Russell, P. 2007. Protection of Telomeres By A Conserved Stn1-Ten1 Complex. *Proc Natl Acad Sci U S A,* 104, 14038-43.
Martínez, P., Thanasoula, M., Muñoz, P., Liao, C., Tejera, A., Mcnees, C., Flores, J., Fernández-Capetillo, O., Tarsounas, M. & Blasco, M. 2009. Increased Telomere Fragility And Fusions Resulting From Trf1 Deficiency Lead To Degenerative Pathologies And Increased Cancer In Mice. *Genes Dev,* 23, 2060-75.
Mcclintock, B. 1942. The Fusion of Broken Ends Of Chromosomes Following Nuclear Fusion. *Proc Natl Acad Sci U S A,* 28, 458-63.
Mceachern, M. & Blackburn, E. 1995. Runaway Telomere Elongation Caused By

Telomerase Rna Gene Mutations. *Nature,* 376, 403-9.
Melo, J., Cohen, J. & Toczyski, D. 2001. Two Checkpoint Complexes Are Independently Recruited To Sites Of DNA Damage *in vivo*. *Genes Dev,* 15, 2809-21.
Miller, K. & Cooper, J. 2003. The Telomere Protein Taz1 Is Required To Prevent And Repair Genomic Dna Breaks. *Mol Cell,* 11, 303-13.
Miyake, Y., Nakamura, M., Nabetani, A., Shimamura, S., Tamura, M., Yonehara, S., Saito, M. & Ishikawa, F. 2009. Rpa-Like Mammalian Ctc1-Stn1-Ten1 Complex Binds To Single-Stranded Dna And Protects Telomeres Independently Of The Pot1 Pathway. *Mol Cell,* 36, 193-206.
Miyoshi, T., Kanoh, J., Saito, M. & Ishikawa, F. 2008. Fission Yeast Pot1-Tpp1 Protects Telomeres And Regulates Telomere Length. *Science,* 320, 1341-4.
Muller, H. J. (1938). The Remaking Of Chromosomes. *Collecting Net* 13(8):182-198.
Murnane, J. 2006. Telomeres and Chromosome Instability. *Dna Repair (Amst),* 5, 1082-92.
Naiki, T., Shimomura, T., Kondo, T., Matsumoto, K. & Sugimoto, K. 2000. Rfc5, In Cooperation with Rad24, Controls DNA Damage Checkpoints Throughout The Cell Cycle In Saccharomyces Cerevisiae. *Mol Cell Biol,* 20, 5888-96.
Nakada, D., Hirano, Y. & Sugimoto, K. 2004. Requirement Of The Mre11 Complex And Exonuclease 1 For Activation Of The Mec1 Signaling Pathway. *Mol Cell Biol,* 24, 10016-25.
Nakada, D., Matsumoto, K. & Sugimoto, K. 2003. ATM-Related Tel1 Associates With Double-Strand Breaks Through An Xrs2-Dependent Mechanism. *Genes Dev,* 17, 1957-62.
Nakamura, T., Morin, G., Chapman, K., Weinrich, S., Andrews, W., Lingner, J., Harley, C. & Cech, T. 1997. Telomerase Catalytic Subunit Homologs From Fission Yeast And Human. *Science,* 277, 955-9.
Negrini, S., Ribaud, V., Bianchi, A. & Shore, D. 2007. DNA Breaks Are Masked By Multiple Rap1 Binding In Yeast: Implications For Telomere Capping And Telomerase Regulation. *Genes Dev,* 21, 292-302.
Nugent, C. I., Hughes, T. R., Lue, N. F. & Lundblad, V. 1996. Cdc13p: A Single-Strand Telomeric DNA-Binding Protein with A Dual Role In Yeast Telomere Maintenance. *Science,* 274, 249-52.
Nyberg, K., Michelson, R., Putnam, C. & Weinert, T. 2002. Toward Maintaining The Genome: DNA Damage And Replication Checkpoints. *Annu Rev Genet,* 36, 617-56.
Okamoto, K., Iwano, T., Tachibana, M. & Shinkai, Y. 2008. Distinct Roles of Trf1 In The Regulation of Telomere Structure and Lengthening. *J Biol Chem,* 283, 23981-8.
Olovnikov, A. 1973. A Theory Of Marginotomy. The Incomplete Copying Of Template Margin in Enzymic Synthesis Of Polynucleotides and Biological Significance Of The Phenomenon. *J Theor Biol,* 41, 181-90.
Paciotti V, Clerici M, Scotti M, Lucchini G & Mp., L. 2001. Characterization of Mec1 Kinase-Deficient Mutants And Of New Hypomorphic Mec1 Alleles Impairing Subsets Of The DNA Damage Response Pathway. *Mol Cell Biol,* 21, 3913-3925.
Paciotti, V., Clerici, M., Lucchini, G. & Longhese, M. 2000. The Checkpoint Protein Ddc2, Functionally Related to *S. Pombe* Rad26, Interacts With Mec1 and Is Regulated

By Mec1-Dependent Phosphorylation In Budding Yeast. *Genes Dev,* 14, 2046-59.
Paciotti, V., Lucchini, G., Plevani, P. & Longhese, M. 1998. Mec1p Is Essential For Phosphorylation Of The Yeast DNA Damage Checkpoint Protein Ddc1p, Which Physically Interacts With Mec3p. *Embo J,* 17, 4199-209.
Palm, W. & De Lange, T. 2008. How Shelterin Protects Mammalian Telomeres. *Annu Rev Genet,* 42, 301-34.
Pardo, B. & Marcand, S. 2005. Rap1 Prevents Telomere Fusions By Nonhomologous End Joining. *Embo J,* 24, 3117-27.
Pennock, E., Buckley, K. & Lundblad, V. 2001. Cdc13 Delivers Separate Complexes To The Telomere For End Protection And Replication. *Cell,* 104, 387-96.
Peterson, S., Stellwagen, A., Diede, S., Singer, M., Haimberger, Z., Johnson, C., Tzoneva, M. & Gottschling, D. 2001. The Function Of A Stem-Loop In Telomerase Rna Is Linked To The Dna Repair Protein Ku. *Nat Genet,* 27, 64-7.
Petreaca, R., Chiu, H., Eckelhoefer, H., Chuang, C., Xu, L. & Nugent, C. 2006. Chromosome End Protection Plasticity Revealed By Stn1p and Ten1p Bypass Of Cdc13p. *Nat Cell Biol,* 8, 748-55.
Petreaca, R., Chiu, H. & Nugent, C. 2007. The Role of Stn1p In Saccharomyces Cerevisiae Telomere Capping Can Be Separated From Its Interaction With Cdc13p. *Genetics,* 177, 1459-74.
Pluta, A., Dani, G., Spear, B. & Zakian, V. 1984. Elaboration of Telomeres In Yeast: Recognition And Modification Of Termini From Oxytricha Macronuclear Dna. *Proc Natl Acad Sci U S A,* 81, 1475-9.
Poulet, A., Buisson, R., Faivre-Moskalenko, C., Koelblen, M., Amiard, S., Montel, F., Cuesta-Lopez, S., Bornet, O., Guerlesquin, F., Godet, T., Moukhtar, J., Argoul, F., Déclais, A., Lilley, D., Ip, S., West, S., Gilson, E. & Giraud-Panis, M. 2009. Trf2 Promotes, Remodels and Protects Telomeric Holliday Junctions. *Embo J,* 28, 641-51.
Prescott, D. 1994. The Dna Of Ciliated Protozoa. *Microbiol Rev,* 58, 233-67.
Price, C. & Cech, T. 1987. Telomeric DNA-Protein Interactions of Oxytricha Macronuclear Dna. *Genes Dev,* 1, 783-93.
Pryde, F., Gorham, H. & Louis, E. 1997. Chromosome Ends: All the Same Under Their Caps. *Curr Opin Genet Dev,* 7, 822-8.
Qi, H. & Zakian, V. A. 2000. The Saccharomyces Telomere-Binding Protein Cdc13p Interacts With Both The Catalytic Subunit Of DNA Polymerase Alpha And The Telomerase-Associated Est1 Protein. *Genes Dev,* 14, 1777-88.
Raghuraman, M., Winzeler, E., Collingwood, D., Hunt, S., Wodicka, L., Conway, A., Lockhart, D., Davis, R., Brewer, B. & Fangman, W. 2001. Replication Dynamics of The Yeast Genome. *Science,* 294, 115-21.
Ray, S., Karamysheva, Z., Wang, L., Shippen, D. & Price, C. 2002. Interactions Between Telomerase And Primase Physically Link The Telomere and Chromosome Replication Machinery. *Mol Cell Biol,* 22, 5859-68.
Reichenbach, P., Höss, M., Azzalin, C., Nabholz, M., Bucher, P. & Lingner, J. 2003. A Human Homolog Of Yeast Est1 Associates With Telomerase And Uncaps Chromosome Ends When Overexpressed. *Curr Biol,* 13, 568-74.
Ritchie, K., Mallory, J. & Petes, T. 1999. Interactions of Tlc1 (Which Encodes The Rna

Subunit Of Telomerase), Tel1, And Mec1 In Regulating Telomere Length in the Yeast *Saccharomyces cerevisiae*. *Mol Cell Biol,* 19, 6065-75.
Rouse, J. & Jackson, S. 2000. Lcd1: An Essential Gene Involved In Checkpoint Control And Regulation Of The Mec1 Signalling Pathway In Saccharomyces Cerevisiae. *Embo J,* 19, 5801-12.
Sabourin, M., Tuzon, C. & Zakian, V. 2007. Telomerase And Tel1p Preferentially Associate With Short Telomeres In S. Cerevisiae. *Mol Cell,* 27, 550-61.
Sanchez, Y., Bachant, J., Wang, H., Hu, F., Liu, D., Tetzlaff, M. & Elledge, S. 1999. Control of The DNA Damage Checkpoint By Chk1 And Rad53 Protein Kinases Through Distinct Mechanisms. *Science,* 286, 1166-71.
Sanchez, Y., Desany, B., Jones, W., Liu, Q., Wang, B. & Elledge, S. 1996. Regulation Of Rad53 by the ATM-Like Kinases Mec1 And Tel1 In Yeast Cell Cycle Checkpoint Pathways. *Science,* 271, 357-60.
Sandell, L. & Zakian, V. 1993. Loss of A Yeast Telomere: Arrest, Recovery, And Chromosome Loss. *Cell,* 75, 729-39.
Schwartz, M., Duong, J., Sun, Z., Morrow, J., Pradhan, D. & Stern, D. 2002. Rad9 Phosphorylation Sites Couple Rad53 to the *Saccharomyces cerevisiae* DNA Damage Checkpoint. *Mol Cell,* 9, 1055-65.
Seto, A., Livengood, A., Tzfati, Y., Blackburn, E. & Cech, T. 2002. A Bulged Stem Tethers Est1p to Telomerase RNA in Budding Yeast. *Genes Dev,* 16, 2800-12.
Shampay, J., Szostak, J. & Blackburn, E. DNA Sequences Of Telomeres Maintained In Yeast. *Nature,* 310, 154-7.
Shay, J., Zou, Y., Hiyama, E. & Wright, W. 2001. Telomerase and Cancer. *Hum Mol Genet,* 10, 677-85.
Shimomura, T., Ando, S., Matsumoto, K. & Sugimoto, K. 1998. Functional and Physical Interaction Between Rad24 And Rfc5 in the Yeast Checkpoint Pathways. *Mol Cell Biol,* 18, 5485-91.
Shore, D. & Bianchi, A. 2009. Telomere Length Regulation: Coupling DNA End Processing To Feedback Regulation Of Telomerase. *Embo J,* 28, 2309-22.
Shore, D. & Nasmyth, K. 1987. Purification And Cloning Of A DNA Binding Protein From Yeast That Binds To Both Silencer And Activator Elements. *Cell,* 51, 721-32.
Singer, M. & Gottschling, D. 1994. Tlc1: Template RNA Component Of Saccharomyces Cerevisiae Telomerase. *Science,* 266, 404-9.
Smith, C., Smith, D., Derisi, J. & Blackburn, E. 2003. Telomeric Protein Distributions and Remodeling Through The Cell Cycle In Saccharomyces Cerevisiae. *Mol Biol Cell,* 14, 556-70.
Smogorzewska, A. & De Lange, T. 2002. Different Telomere Damage Signaling Pathways in Human And Mouse Cells. *Embo J,* 21, 4338-48.
Smogorzewska, A., Van Steensel, B., Bianchi, A., Oelmann, S., Schaefer, M., Schnapp, G. & De Lange, T. 2000. Control of Human Telomere Length By Trf1 And Trf2. *Mol Cell Biol,* 20, 1659-68.
Song, X., Leehy, K., Warrington, R., Lamb, J., Surovtseva, Y. & Shippen, D. 2008. Stn1 Protects Chromosome Ends In Arabidopsis Thaliana. *Proc Natl Acad Sci U S A,* 105, 19815-20.

Stansel, R., De Lange, T. & Griffith, J. 2001. T-Loop Assembly In Vitro Involves Binding Of Trf2 Near The 3' Telomeric Overhang. *Embo J,* 20, 5532-40.
Steiner, B., Hidaka, K. & Futcher, B. 1996. Association of The Est1 Protein With Telomerase Activity In Yeast. *Proc Natl Acad Sci U S A,* 93, 2817-21.
Stellwagen, A., Haimberger, Z., Veatch, J. & Gottschling, D. 2003. Ku Interacts With Telomerase RNA to Promote Telomere Addition at Native And Broken Chromosome Ends. *Genes Dev,* 17, 2384-95.
Stevenson, J. & Gottschling, D. 1999. Telomeric Chromatin Modulates Replication Timing Near Chromosome Ends. *Genes Dev,* 13, 146-51.
Strahl-Bolsinger, S., Hecht, A., Luo, K. & Grunstein, M. 1997. Sir2 And Sir4 Interactions Differ In Core And Extended Telomeric Heterochromatin In Yeast. *Genes Dev,* 11, 83-93.
Subramanian, L., Moser, B. & Nakamura, T. 2008. Recombination-Based Telomere Maintenance Is Dependent On Tel1-Mrn And Rap1 And Inhibited By Telomerase, Taz1, And Ku In Fission Yeast. *Mol Cell Biol,* 28, 1443-55.
Sun, J., Yu, E., Yang, Y., Confer, L., Sun, S., Wan, K., Lue, N. & Lei, M. 2009. Stn1-Ten1 Is An Rpa2-Rpa3-Like Complex At Telomeres. *Genes Dev,* 23, 2900-14.
Szostak, J. & Blackburn, E. 1982. Cloning Yeast Telomeres on Linear Plasmid Vectors. *Cell,* 29, 245-55.
Taggart, A., Teng, S. & Zakian, V. 2002. Est1p As A Cell Cycle-Regulated Activator Of Telomere-Bound Telomerase. *Science,* 297, 1023-6.
Takai, H., Smogorzewska, A. & De Lange, T. 2003. DNA Damage Foci At Dysfunctional Telomeres. *Curr Biol,* 13, 1549-56.
Takata, H., Tanaka, Y. & Matsuura, A. 2005. Late S Phase-Specific Recruitment of Mre11 Complex Triggers Hierarchical Assembly Of Telomere Replication Proteins In Saccharomyces Cerevisiae. *Mol Cell,* 17, 573-83.
Teixeira, M., Arneric, M., Sperisen, P. & Lingner, J. 2004. Telomere Length Homeostasis Is Achieved Via a Switch Between Telomerase- Extendible And -Nonextendible States. *Cell,* 117, 323-35.
Van Steensel, B., Smogorzewska, A. & De Lange, T. 1998. Trf2 Protects Human Telomeres From End-To-End Fusions. *Cell,* 92, 401-13.
Veldman, T., Etheridge, K. & Counter, C. 2004. Loss Of hPot1 Function Leads To Telomere Instability and a Cut-Like Phenotype. *Curr Biol,* 14, 2264-70.
Venclovas, C. & Thelen, M. 2000. Structure-Based Predictions Of Rad1, Rad9, Hus1 And Rad17 Participation In Sliding Clamp And Clamp-Loading Complexes. *Nucleic Acids Res,* 28, 2481-93.
Verdun, R. & Karlseder, J. 2007. Replication And Protection Of Telomeres. *Nature,* 447, 924-31.
Virta-Pearlman, V., Morris, D. & Lundblad, V. 1996. Est1 has the Properties of a Single-Stranded Telomere End-Binding Protein. *Genes Dev,* 10, 3094-104.
Vodenicharov, M. & Wellinger, R. 2006. DNA Degradation At Unprotected Telomeres In Yeast Is Regulated By The Cdk1 (Cdc28/Clb) Cell-Cycle Kinase. *Mol Cell,* 24, 127-37.
Waga, S. & Stillman, B. 1998. The DNA Replication Fork In Eukaryotic Cells. *Annual*

Review Of Biochemistry, 67, 721-751.
Wan, M., Qin, J., Songyang, Z. & Liu, D. 2009. Ob Fold-Containing Protein 1 (Obfc1), A Human Homolog of Yeast Stn1, Associates With Tpp1 and is Implicated In Telomere Length Regulation. *J Biol Chem,* 284, 26725-31.
Wang, F., Podell, E., Zaug, A., Yang, Y., Baciu, P., Cech, T. & Lei, M. 2007. The Pot1-Tpp1 Telomere Complex Is A Telomerase Processivity Factor. *Nature,* 445, 506-10.
Watson, J. 1972. Origin Of Concatemeric T7 Dna. *Nat New Biol,* 239, 197-201.
Weinert, T. 1998. DNA Damage And Checkpoint Pathways: Molecular Anatomy And Interactions With Repair. *Cell,* 94, 555-8.
Weinert, T. & Hartwell, L. 1988. The Rad9 Gene Controls The Cell Cycle Response To Dna Damage In Saccharomyces Cerevisiae. *Science,* 241, 317-22.
Weinert, T. & Hartwell, L. 1993. Cell Cycle Arrest of Cdc Mutants and Specificity of The Rad9 Checkpoint. *Genetics,* 134, 63-80.
Weinert, T., Kiser, G. & Hartwell, L. 1994. Mitotic Checkpoint Genes in Budding Yeast and The Dependence Of Mitosis On DNA Replication And Repair. *Genes Dev,* 8, 652-65.
Wellinger, R., Ethier, K., Labrecque, P. & Zakian, V. 1996. Evidence For A New Step In Telomere Maintenance. *Cell,* 85, 423-33.
Wellinger, R., Wolf, A. & Zakian, V. 1993a. Origin Activation And Formation Of Single-Strand TG1-3 Tails Occur Sequentially In Late S Phase On A Yeast Linear Plasmid. *Mol Cell Biol,* 13, 4057-65.
Wellinger, R., Wolf, A. & Zakian, V. 1993b. Saccharomyces Telomeres Acquire Single-Strand TG1-3 Tails Late In S Phase. *Cell,* 72, 51-60.
Wold, M. S. 1997. Replication Protein A: A Heterotrimeric, Single-Stranded Dna-Binding Protein Required For Eukaryotic DNA Metabolism. *Annual Review Of Biochemistry,* 66, 61-92.
Wotton, D. & Shore, D. 1997. A Novel Rap1p-Interacting Factor, Rif2p, Cooperates With Rif1p To Regulate Telomere Length in *Saccharomyces Cerevisiae*. *Genes Dev,* 11, 748-60.
Wright, J., Gottschling, D. & Zakian, V. 1992. Saccharomyces Telomeres Assume A Non-Nucleosomal Chromatin Structure. *Genes Dev,* 6, 197-210.
Wu, L., Multani, A., He, H., Cosme-Blanco, W., Deng, Y., Deng, J., Bachilo, O., Pathak, S., Tahara, H., Bailey, S., Behringer, R. & Chang, S. 2006. Pot1 Deficiency Initiates DNA Damage Checkpoint Activation And Aberrant Homologous Recombination At Telomeres. *Cell,* 126, 49-62.
Xin, H., Liu, D., Wan, M., Safari, A., Kim, H., Sun, W., O'connor, M. & Songyang, Z. 2007. Tpp1 Is A Homologue Of Ciliate Tebp-Beta And Interacts With Pot1 To Recruit Telomerase. *Nature,* 445, 559-62.
Xu, L., Petreaca, R., Gasparyan, H., Vu, S. & Nugent, C. 2009. Ten1 Is Essential For Cdc13-Mediated Telomere Capping. *Genetics*.
Ye, J. & De Lange, T. 2004. Tin2 Is A Tankyrase 1 Parp Modulator In The Trf1 Telomere Length Control Complex. *Nat Genet,* 36, 618-23.
Ye, J., Donigian, J., Van Overbeek, M., Loayza, D., Luo, Y., Krutchinsky, A., Chait, B. & De Lange, T. 2004. Tin2 Binds Trf1 And Trf2 Simultaneously and Stabilizes The Trf2

Complex On Telomeres. *J Biol Chem,* 279, 47264-71.
Yoshimura, S., Maruyama, H., Ishikawa, F., Ohki, R. & Takeyasu, K. 2004. Molecular Mechanisms Of Dna End-Loop Formation By Trf2. *Genes Cells,* 9, 205-18.
Zhong, Z., Shiue, L., Kaplan, S. & De Lange, T. 1992. A Mammalian Factor That Binds Telomeric TTAGGG Repeats *in vitro*. *Mol Cell Biol,* 12, 4834-43.
Zou, L. & Elledge, S. 2003. Sensing Dna Damage Through Atrip Recognition Of Rpa-Ssdna Complexes. *Science,* 300, 1542-8.
Zou, L., Liu, D. & Elledge, S. 2003. Replication Protein A-Mediated Recruitment And Activation of Rad17 Complexes. *Proc Natl Acad Sci U S A,* 100, 13827-32.
Zubko, M., Guillard, S. & Lydall, D. 2004. Exo1 and Rad24 Differentially Regulate Generation of ssDNA At Telomeres of *Saccharomyces cerevisiae cdc13-1* Mutants. *Genetics,* 168, 103-15.

Chapter 2

Rad24 truncation, coupled with altered telomere structure, promotes *cdc13-1* suppression in *S. cerevisiae*

Introduction

Telomeres are the physical ends of linear chromosomes, typically comprising short repetitive G-rich sequences in association with specific proteins that promote protection of the chromosome ends from nuclease degradation and fusion. Telomeres also function to distinguish the chromosome end from a DNA double strand break. When DNA damage in the form of DSB is detected, the cell usually responds by arresting cell cycle progression and repairing the break. In G_1, telomeres that become uncapped are repaired using non-homologous end joining (Ferreira et al., 2004). If deprotection occurs in cells that are in S/G_2 phase, uncapped chromosome ends are degraded 5' to 3', which creates single-stranded regions that facilitate subsequent strand invasion and homologous recombination (Vodenicharov and Wellinger, 2006). Extensive degradation and inappropriate recombination often results in genomic instability due to loss of critical genetic information from chromosome ends. Chromosome end to end fusions at uncapped telomeres often lead to breakage-fusion-bridge cycles resulting in loss of genomic integrity as well (McEachern and Haber, 2006, Murnane, 2006).

Cdc13 is critical for maintaining the proper capping function of telomeres in budding yeast (Lin and Zakian, 1996, Nugent et al., 1996). It has been well documented that at restrictive temperature in *cdc13-1* cells, the C-rich strand undergoes resection and the terminal regions of chromosomes become excessively single-stranded (Garvik et al., 1995; Lydall and Weinert, 1995; Lydall and Weinert, 1997). Two dimensional gel electrophoresis and quantitative PCR analysis of *cdc13-1* mutants grown at the non-

permissive temperature demonstrated that *cdc13-1* cells accumulate single stranded DNA specifically on the 3' G-rich end, which extended up to 50 kilobases from the telomere toward the centromere (Garvik et al., 1995, Booth et al., 2001). Cdc13 protein prevents this resection from occurring with the aid of Stn1 and Ten1, which have been shown to interact with Cdc13 (Petreaca et al., 2007, Grandin et al., 1997, Grandin et al., 2001b). Stn1 has been isolated from a screen of high copy suppressors of *cdc13-1,* and allowed growth of *cdc13-1* cells up to 30^{o}C (Grandin et al., 1997). Ten1 was isolated in a screen as a high copy suppressor of the temperature sensitive *stn1-13* allele and over expression of Ten1 enhances the ability of *STN1* to suppress *cdc13-1* (Grandin et al., 2001b). Several *stn1* and *ten1* mutants have also been found to exhibit single stranded DNA at telomeres and arrest at the DNA damage checkpoint in a Rad9 dependent fashion similar to the *cdc13-1* allele. Thus, it is proposed that Cdc13, Stn1 and Ten1 form the C-S-T complex that mediates chromosome end protection, which may similarities with the single-stranded DNA binding complex RPA (Gao et al., 2007).

To further understand how telomeres promote chromosome capping, it is necessary to understand the activities that occur at the chromosome end when telomeres become unprotected. The cell usually recognizes and processes uncapped telomeres as DNA damage through the DNA damage response pathways, one of which is the DNA damage checkpoint at G2/M. Recognition and processing of DNA double-strand breaks is similar to the processing which occurs at uncapped telomeres (Lydall et al., 2003).

MRE11 is a 3′-5′ exonuclease and single-stranded endonuclease that together with *RAD50* and *XRS2,* comprises the MRX complex which has been shown to contribute to

the processing of DNA ends at DSBs in mitotic recombination,and nonhomologous end joining (NHEJ) (Paull et al., 1998, Haber et al., 1998). The MRX complex is required for nonhomologous end-joining in yeast and mutations that abolish Mre11 nuclease endo- and exonuclease activities activity result in accumulation of unresected meiotic DSBs and sporulation failure (Tsubouchi and Ogawa, 1998, Furuse et al., 1998, Moreau et al., 1999). Although Mre11 3′-5′ exonuclease polarity is opposite to the expected 5' to 3' nuclease polarity necessary for DSB resection, NHEJ is defective in Δ*mre11*, Δ*rad50*, and Δ*xrs2* strains, and end-joining between linear DNA ends is reduced, indicating a role for MRX in DSB processing (Moore and Haber, 1996, Boulton and Jackson, 1998). In addition to DSB repair, the Mre11 complex is required for checkpoint responses after DSB induction, since Mre11 function was specifically required for proper cell cycle arrest in response to an induced DSB. This indicates that the Mre11 complex is required in the DSB processing that is necessary for proper DNA damage checkpoint activation (Grenon et al., 2001, D'Amours and Jackson, 2001, D'Amours and Jackson, 2002). Null mutations of *rad50* and *xrs2* result in slower resection of HO-induced DSBs, but they do not abolish DSB processing, suggesting additional nuclease activities can act on DSBs *in vivo* (Ivanov et al., 1994, Moreau et al., 2001).

MRX is thought to act in concert with other nuclease activities to process DNA ends at DSBs. MRX allows resection of DSBs by acting in collaboration with the endonuclease Sae2 protein (Clerici et al., 2005, Clerici et al., 2006, Lengsfeld, 2007). It has also been reported that the processing of the DNA ends by exonucleases at a single induced DSB was dependent on the activity of the major cyclin-dependent kinase in

budding yeast, Cdk1 (Cdc28/Clb2 in yeast) (Ira et al., 2004, Huertas et al., 2008). Cdk1 activity is needed for DSB processing to phosphorylate Sae2 on Ser267, suggesting that proper DSB resection is an important regulated step which requires several nucleases (Ira et al., 2004, Huertas et al., 2008). Sae2 and MRX have been proposed to form an early intermediate that initiates the 5′ degradation of a DSB end, which may then processed by Exo1 to generate longer tracts of ssDNA (Mimitou et al., 2008, Zhu et al., 2008, Mimitou et al., 2009). Exo1 is a 5′-3′ dsDNA exonuclease and flap-endonuclease, which exerts its nuclease function in the resection of DNA ends of DSBs, as well as in mismatch repair and homologous recombination (Fiorentini et al., 1997; Tsubouchi et al., 2000; Bolderson et al., 2010). Overexpression of *EXO1* was shown to partially rescue the mitotic DNA repair defects of *mre11*Δ strains, indicating that Exo1 is capable of some DSB processing in the absence of MRX (Moreau et al., 2001). Furthermore, studies in yeast have shown that the Mre11 complex and Exo1 collaborate to create ssDNA at an induced DSB ends and promote Mec1 association with DSBs, suggesting that they are involved in creating the ssDNA signal recognized by the DNA damage checkpoint (Nakada et al., 2004).

Chromosome ends and DSBs are similar to each other in that both are resected by 5′-3′ exonucleases to generate ssDNA overhangs (Wellinger et al., 1993). Native telomeres of budding yeast end in a short 3’ G-rich overhang of approximately 10–15 nucleotides for most of the cell cycle, but their length increases transiently in late S phase during the time that telomere replication takes place (Larrivée et al., 2004, Wellinger et al., 1993). The MRX complex has been shown to play a role in the formation of this cell

cycle dependent telomeric 3' G-tail overhang (Diede and Gottschling, 2001, Larrivée et al., 2004) . The G-rich overhangs in *mre11Δ* mutants were shorter in length, indicating that the MRX complex contributes to overhang formation (Larrivée et al., 2004). However, disruption of MRX function does not completely abolish this G tail, suggesting that redundant nucleolytic activities are involved in the processing of native telomeres (Larrivée et al., 2004). Studies assessing resection of the C-rich strand at a short telomere seed adjacent to an induced DSB was shown to be reduced in *mre11Δ, sae2Δ,* and *exo1Δ* mutants (Bonetti et al., 2009). The cell cycle-dependent control generation of G-strand overhangs formation and telomere elongation is mediated Cdk1, which targets Sae2 for phosphorylation. Taken together, these results demonstrate that many of the same factors that process the DNA ends of DSBs are also necessary for processing native telomere ends (Vodenicharov and Wellinger, 2006, Frank et al., 2006, Huertas et al., 2008).

Although the Mre11, Rad50, Xrs2 (MRX) complex influences the processing of DSBs, it is not required for resection occurring at uncapped telomeres in *cdc13-1* mutants (Zubko et al., 2004, Foster et al., 2006). Exo1 has been shown to contribute to C strand resection at uncapped telomeres role when cells are defective for telomerase or Cdc13 function (Maringele and Lydall, 2002, Bertuch and Lundblad, 2004, Zubko et al., 2004). In addition to regulating C-strand resection at both a DSB and native telomeres, Cdk1 has been shown to regulate degradation leading to loss of the C-rich strand in *cdc13-1* uncapped telomeres (Vodenicharov and Wellinger, 2006, Frank et al., 2006). Although Sae2 has been identified as a Cdk1 target which regulates resection at DSBs and

telomeres, critical Cdk1-regulated activities that occur specifically at uncapped telomeres in *cdc13-1* cells remain to be elucidated (Huertas et al., 2008, Bonetti et al., 2009).

In an attempt to identify genes responsible for the activities that occur at telomeres that have become unprotected, we undertook a screen to identify extragenic suppressors of the *cdc13-1* temperature sensitivity. At high temperatures, *cdc13-1* cells accumulate single-stranded telomeric DNA damage which activates the DNA damage checkpoint response and cells arrest at G2/M phase (Garvik et al., 1995, Lydall and Weinert, 1995, Lydall and Weinert, 1997). Use of the conditional *cdc13-1* allele to disrupt telomere capping is advantageous because its maximum permissive temperature of 25°C is low, while the DNA damage checkpoint is activated at higher temperatures. Loss of the DNA damage checkpoint acts as an extragenic suppressor of *cdc13-1* cells and the maximum permissive temperature is increased in the double mutants. Hence, when the DNA damage checkpoint is inactivated, *cdc13-1* cells can proliferate and maintain viability at 30°C (Weinert and Hartwell, 1993, Lydall and Weinert, 1995, Lydall and Weinert, 1997, Garvik et al., 1995).

In the screen for extragenic suppressors of *cdc13-1*, two classes of suppressor mutations were expected. The first being mutations in genes that coded for the activities which result in the accumulation of telomeric single stranded DNA in *cdc13-1* cells, and the second would be mutations in genes involved in the DNA damage checkpoint. It has been proposed that Rad24, Rad17 and Mec3 controlled the activity of a 3' to 5' exonuclease that degraded the C- strand since *rad24Δ* mutants had decreased ssDNA, while Rad9 inhibited the exonuclease because *rad9Δ* cells accumulated ssDNA (Lydall

and Weinert, 1995). Previous experiments have shown Exo1 (a 5' to 3 exonuclease) and Rad24 (the G2/M checkpoint clamp loader) to contribute to production of single-stranded telomeric DNA in *cdc13-1* cells, since *cdc13-1 rad24Δ* and *cdc13-1 exo1Δ* cells have reduced subtelomeric single-stranded DNA (Lydall and Weinert, 1995, Maringele and Lydall, 2002, Larrivée et al., 2004, Zubko et al., 2004). However, ssDNA was still produced in *cdc13-1 rad24Δ exo1Δ* strains, suggesting additional activity occurred at *cdc13-1* uncapped telomeres which has been attributed to a yet unidentified nuclease termed ExoX (Lydall and Weinert, 1995, Booth et al., 2001, Zubko et al., 2004).

A screen, using an mTn3-transposon insertion mutagenesis strategy, was conducted before I joined the lab and resulted in identification of two alleles of the DNA checkpoint clamp loader, *RAD24*. Rad24 replaces the RFC1 subunit of the Replication Factor C pentameric complex, to form the checkpoint clamp loader complex which binds and loads the 9-1-1 checkpoint clamp (hRad9, hHus1, hRad) onto DNA lesions, thus playing a key role in the DNA damage checkpoint (Majka and Burgers, 2003, Majka et al., 2004, Green et al., 2000). In yeast, the 9-1-1 clamp is formed by Ddc1, Mec3, and Rad17, which promotes checkpoint signaling and DSB repair activities (Jia et al., 2004, Melo et al., 2001, Kondo et al., 2001). In each *rad24* allele, a transposon inserted within the *RAD24* coding region resulted in the expression of different carboxyl terminal portions of Rad24, in which the amino-terminus was truncated (*rad24-2*) or deleted (*rad24-3*). Initial characterization of the *rad24* alleles showed that *rad24-2* was a stronger suppressor than *rad24-3*, allowing growth of *cdc13-1* mutants up to 36°C. The *rad24-3* allele, on the other hand, showed suppression phenotypically similar to *rad24-Δ*,

allowing growth up to 30°C. The ability of *rad24-2* to allow growth of *cdc13-1* mutants up to 36°C was interesting, and suggested that a truncated protein was produced from the *rad24-2* allele which provided a mechanism of suppression distinct from one occurring in the *rad24-Δ* and *rad24-3* alleles, which only allow growth of *cdc13-1* cells up to 30°C. In this chapter, the hypothesis that the protein produced from the *rad24-2* was functionally distinct from Rad24 and the mechanism for the enhanced suppression of *cdc13-1* by *rad24-2* was investigated.

Here, we show that an intact amino-terminus is necessary for proper Rad24 checkpoint function. Upon further analysis of *rad24-2,* we found that the *rad24-2* allele alone was not sufficient to provide the extent of suppression that was previously observed at 36°C, indicating that additional factors were modifying the suppression. Although the initial *cdc13-1 rad24-2* strains grew at 36°C, the extent of suppression associated with *rad24-2* weakened in serial backcrosses, and *cdc13-1* segregants from these crosses showed a modest increase in temperature resistance. Moreover, a *RAD24* plasmid suppressed the checkpoint defect in the initial *cdc13-1 rad24-2* strain, whereas the temperature resistance was only partially suppressed. Our investigation into the mechanism allowing the *cdc13-1 rad24-2* cells to grow at 36˚C suggests that the telomere structure adopted in these strains contributes to the observed suppression phenotype. In particular, we have found that the telomeric DNA in *cdc13-1 rad24-2* cells is amplified and more heterogeneous compared to wild-type telomeres. These data suggest that the $TG_{1\text{-}3}$ amplification observed in this strain contributes to the suppression phenotype. Reconstruction of the *rad24-2* allele in a strain with normal telomeres demonstrated that

rad24-2 increased the frequency of obtaining *cdc13-1* cells capable of growth at high temperatures relative to the *rad24-Δ* allele. Our hypothesis is that the Rad24-2 truncation protein affects telomere structure or recombination in a manner distinct from *rad24-Δ*.

Materials and Methods

Yeast manipulations

Standard techniques were followed in handling the yeast strains. Yeast strains used in this study are listed in Table 1. Yeast plasmids and oligos used in this study are listed in Table 2 and Table 3, respectively.

Viability Testing

To plate dilutions of yeast cells, serial ten-fold dilutions of equivalent starting concentrations of cell cultures were performed in micro-titer dishes, "stamped" onto solid media, and grown at the indicated temperatures.

Strain construction

To epitope tag the wild-type and mutant Rad24 proteins; a cassette encoding 13 copies of the c-myc epitope followed by the HIS3 gene from pFA6a-13MycHis3MX6 was PCR amplified using oligos CO147 and CO148. The PCR product was integrated at the end of the *RAD24* open reading frame in wild-type (hC160), *rad24-2* (hc341) and *rad24-3* (hc342) haploid strains. Both Southern blot and PCR analysis were used to verify the correct integration of the myc-13x sequence.

To re-create the *rad24-2* allele, an 8.7 kb PCR fragment encompassing the transposon integration sites within the *rad24-2* ORF was amplified with the Expand polymerase mix

(Roche) using the primers CO117 and CO118 (Primer sequences are shown in Table 2-3). Genomic DNA from the strain hC647 was used as the template for the PCR. Following transformation of the PCR fragment into *cdc13-1/+* diploids and selection on Leu- media, the correct integrants were confirmed by PCR analysis.

Western Blot analysis

Rad24-myc13x, Rad24-2myc13x, and Rad24-3myc13x strains were incubated at 23°C in YPD to an OD600 of 0.8 and protein extracts were prepared. For each sample, 300 µg of protein was loaded on a 10% SDS-PAGE gel. After transfer, the membrane was probed with a 9E10 α-myc antibody (Covance). The blot was then stripped and re-probed with a α-tubulin antibody (clone YOL 1/34, Accurate Chemical and Scientific) as a loading control. A wild-type strain (hC160) was used as the negative control.

Rad53 phosphorylation shift

For exposure to MMS, 50 mls of cells at OD600 0.5 were incubated in 0.1% MMS for 2 hours. For UV exposure, strains were spread on solid media in 150mm plates, exposed to 80J/m2 UV light using a UV Stratalinker 2400 (Stratagene), and after 30 min. recovery the cells were harvested by scraping. The strains containing *cdc13-1* were shifted to 36°C for four hours to induce DNA damage. Protein extracts were prepared by bead-beating cells in 20% TCA. For each lysate, 300 µg was loaded on a 8% 30:0.39 acrylamide : bis-acrylamide SDS-PAGE gel. After transfer, membranes were probed with α-Rad53 goat polyclonal primary (sc-6749) antibody and bovine anti-goat secondary (sc-2350) antibody (Santa Cruz).

Southern Blot analysis

Yeast genomic DNA was isolated according to a previously published protocol (Lundblad and Szostak, 1989). The DNA was digested overnight with either XhoI or with AluI, HaeIII, HinfI, and MspI. A conserved XhoI site is located within the subtelomeric Y' elements; the AluI, HaeIII, HinfI, and MspI enzymes each have 4bp recognition sites which are not present within the telomere repeat sequence. After running the digested DNA on a 1.3% agarose gel and transferring to a nylon membrane (Hybond XL, Amersham), a [32P] -dGT/CA probe or [32P] –Y' probe was used to detect telomere fragments.

Pulse Field Gel Electrophoresis

Agarose plugs containing the chromosomal DNA were prepared as described by the manufacturer's protocol (Bio-Rad) and resolved on a 1% agarose gel using the CHEF-DR III system (Bio-Rad) at 5.5V/cm for 24 hours at 14°C, with an initial switch time of 60 seconds, and final switch time of 120 seconds. Standard southern blotting technique probed with a [32P] -dGT/CA probe was used to analyze the chromosomes.

Temperature resistant colony analysis

Cultures were inoculated from single colonies, and grown 1-2 days at 23°C in YPD. Cell density was determined using a hemocytometer. From each culture, a calculated 250 cells were plated on YPD and incubated at 23°C, and either 500,000 cells were plated on YPD and incubated at 36°C. Colonies were counted after 4 days of incubation. 27 independent cultures were tested for *cdc13-1 rad24-Δ*, and 31 cultures tested for *cdc13-1 rad24-2*. The strains tested were haploids from dCN318, dCN319, dCN343 and DVL202 diploids.

Results

Two alleles of *RAD24* were identified in a screen for extragenic suppressors of *cdc13-1* temperature sensitivity.

When I initially joined the lab, characterization of alleles identified in a screen for suppressors of *cdc13-1* temperature sensitivity was being conducted. The purpose of this screen was to identify the gene responsible for the single stranded DNA generated in *cdc13-1* cells at elevated temperatures. The screen was conducted by Charles Chuang and utilized a yeast genomic library containing mTn-lacZ/*LEU2* transposon insertions. A linearized yeast genomic library containing random insertions of an mTn-lacZ/*LEU2* transposon was transformed into *cdc13-1* cells and grown at the restrictive temperature of 30°C. Temperature resistant colonies were then mated with a wild-type haploid, and the tetrads in which *cdc13-1* temperature sensitivity and the mTn-lacZ/*LEU2* insertion were tightly linked were further analyzed. The insertion site of the transposon was identified by integrating a linearized plasmid into sequences within the transposon, and then selecting for the *URA3* marker on the plasmid. Sequences adjacent to the insertion site were then recovered following ligation of genomic DNA fragments (Small et al., 2008). Sequence analysis, also conducted by Charles Chuang, revealed that both the suppressors contained the transposon inserted at different sites within the *RAD24* coding region (Small et al., 2008). The *rad24-2* allele was a strong suppressor of temperature sensitivity and permitted growth up to 36°C, while the other suppressor identified, *rad24-3*, allowed growth up to 32°C (Figure 2-1). Previous studies have found that *rad24-1* and *rad24-Δ* suppress *cdc13-1* up to 30°C, but neither allele provided the level of suppression

observed in *cdc13-1 rad24-2* cells (Lydall and Weinert, 1995, Weinert et al., 1994). Hence, it was important to determine the nature of the Rad24 protein being expressed from these alleles.

When I initially started work on this project, the location of the transposon insertion within the *rad24-2* and *rad24-3* alleles was known through sequence analysis, but the effect of the transposon on Rad24 protein production was unclear. In the *rad24-2* allele, the transposon is inserted following nucleotide 189 in the *RAD24* open reading frame (Figure 2-2a). The orientation of the transposon is reversed in *rad24-3* and is inserted after nucleotide 388 (Figure 2-2a). Rad24 contains a conserved AAA+ domain, common to PCNA clamp loaders, located between amino acids 104-250, which is needed for ATP binding (Figure 2-2a) (Naiki et al., 2000). Analysis of a Rad24-K115E mutant shows that ATP binding is required Rad24's checkpoint clamp loading function (Majka et al., 2004). In both alleles, very short peptide fragments are encoded by *RAD24* before the gene is disrupted by the insertion. The *rad24-2* allele encodes the first 63 amino acids, while *rad24-3* encodes the first 129 amino acids. The ability of *cdc13-1 rad24-2* cells to grow at higher temperature than either the *cdc13-1 rad24-3* strain or *cdc13-1 rad24-Δ* suggests that the *rad24-2* allele provides suppression that is distinct from the suppression provided by the null allele.

Our hypothesis was that sequences within the integrated transposon in *rad24-2* or *rad24-3* could act as a promoter for transcription of the remainder of the *RAD24* gene, allowing portions of the Rad24 C- terminus to be translated (Figure 2-2a). The first methionine that could potentially initiate translation downstream of the transposon in the

rad24-2 allele is at residue 95, and the first methionine downstream of the integration site for *rad24-3* is at residue 163 (Figure 2-2a) (Small et al., 2008). To test whether protein was being expressed from the mutant alleles, a myc-epitope tag was integrated in-frame at the *RAD24, rad24-2, and rad24-3* C- terminus (Figure 2-2b). Interestingly, Rad24 protein was produced from both the *rad24-2* and *rad24-3* alleles (Figure 2-2b). The presence of truncated proteins corresponding to the expected sizes for translated products initiated at Met95 and Met163 at approximately 62 kD and 55kD in *rad24-2*, and with Met163 and Met178 at approximately 55kD and 53kD in *rad24-3* suggest that sequences within the transposon were able to act as a promoter for transcription from both methionines for the remainder of the *RAD24* gene following the insertion (Figure 2-2b). Furthermore, the Rad24-3myc$_{13x}$ protein appears to be expressed at a lower level than the Rad24-myc$_{13x}$ and Rad24-2myc$_{13x}$ proteins. Thus, the truncated protein being produced from the *rad24-2* allele could potentially account for the increased viability of *cdc13-1 rad24-2* at higher temperatures.

The *rad24-2* and *rad24-3* alleles are both checkpoint deficient.

The larger Rad24 protein fragment produced from the *rad24-2* allele keeps both the AAA+ module between residues 104-250, and the hydrophobic clamp binding domain between residues 166-170 fully intact (Figure 2-2a) (Majka and Burgers, 2004, Venclovas et al., 2002). However, the protein fragment produced from the *rad24-3* allele was expected not to maintain proper *RAD24* function, because the AAA+ motif was disrupted in this mutant. Hence, our hypothesis was that the larger Rad24 protein fragment produced from the *rad24-2* allele, which included amino acids 95-659, would

retain proper Rad24 function in checkpoint responses. Once it was found that truncated proteins were being produced from the *rad24* alleles, it was important to test whether the *rad24-2* and *rad24-3* alleles retain normal Rad24 function in the DNA Damage Checkpoint response. Therefore, we examined cell viability of these strains to determine the ability of the *rad24-2* and *rad24-3* cells to repair DNA damage after exposure to different DNA damaging agents. Both the *rad24-2* and *rad24-3* alleles are sensitive to UV treatment, to the same extent observed in the *rad24-Δ* strain (Figure 2-3a). In contrast to wild-type cells, each of the *rad24* strains loses viability when exposed to 75mM hydroyurea (HU), with the *rad24-2* strain showing slightly more sensitivity than the *rad24-Δ* strain (Figure 2-3b). Lastly, wild-type cells exposed to 0.025% methyl methanesulfonate (MMS) were able to maintain normal viability after 4 hours, while *rad24-2*, and *rad24-3* cells all rapidly lose viability similar to *rad24-Δ* cells (Figure 2-3c). Thus, *rad24-2* and *rad24-3* mutants behave similarly to *rad24-Δ* cells, suggesting that they are defective for checkpoint function.

Next we examined the DNA damage checkpoint activation by assessing the response of the central checkpoint kinase Rad53 to multiple types of damage. After activation of the S-phase or DNA damage checkpoint, Rad53 becomes phosphorylated and displays a strong electrophoretic mobility shift (Alcasabas et al., 2001). It has previously been shown that Rad53 phosphorylation is dependent on *RAD9* and loss of *RAD24* function impairs the mobility shift of Rad53 (Pellicioli et al., 2001, Sanchez et al., 1999). Shifting *cdc13-1* cells to 36°C leads to activation of the DNA damage checkpoint as demonstrated by the strong Rad53 mobility shift that depends on *RAD9*

(Figure 2-4a). In *cdc13-1 rad24Δ* cells, Rad53 phosphorylation is no longer detected. This loss of Rad53 phosphorylation is also observed in the *cdc13-1 rad24-2* and *cdc13-1 rad24-3* strains (Figure 2-4a).

In addition, the checkpoint response of the *rad24* strains to other types of DNA damage was also examined, because the *rad24* mutants may reduce the level of ssDNA in *cdc13-1*, which could in turn reduce the damage signal to the checkpoint. After MMS or UV treatment both the *rad24-2* and *rad24-3* strains respond similar to the *rad24-Δ* strain, with a partial mobility shift of Rad53 (Figure 2-4b). Phleomycin is a DNA damaging agent that catalyzes double-strand breaks (Nakada et al., 2003). Interestingly, Rad53 phosphorylation is observed in the *rad9-Δ, rad24-Δ, rad24-2* and *rad24-3* strains following phleomycin treatment, suggesting that this type of DNA damage does not specifically the DNA damage checkpoint and may also activate other checkpoints in which Rad53 phosphorylated, such as the S-phase checkpoint (Figure 2-4c). Taken together, these data indicate that *rad24-2* and *rad24-3* are both deficient for proper checkpoint activation.

It has been previously shown that single-stranded DNA is reduced in *cdc13-1 rad24-Δ* cells grown at high temperatures, suggesting that Rad24 regulates an exonucleolytic function at telomeres (Lydall and Weinert, 1995, Booth et al., 2001). Although both the *rad24-2* and *rad24-3* alleles appear to be deficient for their DNA damage checkpoint function, our hypothesis was that the *rad24-2* allele was distinct from the null allele and the phenotypically null *rad24-3* allele with respect to regulating the metabolism of telomere DNA. Hence, we tested whether the improved temperature

resistance of the *rad24-2* strain correlated with changes in telomere structure such as the amount of single stranded DNA, and telomere length. An in-gel hybridization analysis done by Charles Chuang demonstrated that while the median accumulation of ssTG is reduced in each *cdc13-1 rad24* strain relative to *cdc13-1*, there is no difference among the *rad24-Δ, rad24-2* and *rad24-3* strains (data not shown) (Small et al., 2008). Thus, our comparison of single-stranded DNA among these strains does not reveal an obvious suppression of the single-stranded DNA characteristic of *cdc13-1* strains correlating with the temperature resistance observed in the *cdc13-1 rad24-2* strain.

Under certain conditions, cells can survive in the complete absence of *CDC13* (Zubko et al., 2006, Larrivée et al., 2006, Petreaca et al., 2006). The ability of cells to survive without Cdc13 is enhanced by the loss of DNA damage checkpoint function, particularly in combination with deletions of genes encoding nucleases such as *EXO1,* which can contribute to telomere resection (Zubko et al., 2004, Zubko et al., 2006). In addition, while telomere recombination per se is not sufficient for *CDC13*-independent growth, combined with checkpoint deficiencies, the ability to grow independently of *CDC13* function is likely to be stimulated (Larrivée et al., 2006, Petreaca et al., 2006). Since our examination of the *rad24-2* checkpoint and telomere resection phenotypes did not reveal any substantial differences from the *rad24-Δ* allele, we next analyzed the telomere structure in *cdc13-1 rad24-2* mutants at the high temperatures, to test our hypothesis that structural changes had occurred at the telomere that would account for the increased temperature resistance of the suppressed mutant strain. First, we examined the *Xho*I telomere restriction fragments in strains that were grown at either 23°C or at

30°C (Figure 2-5a). The restriction enzyme *Xho* I cuts yeast DNA in the sub-telomeric Y' repeat, generating a terminal restriction fragment in wild-type yeast strains of ~1.3 kb, ~350-500 bp representing the terminal poly TG $_{1\text{-}3}$ tract (Walmsley, 1985). Interestingly, this Southern blot shows evidence of telomere repeat recombination in the strains that were derived from the dCN149 *cdc13-1* /+ *rad24-2* /+ diploid (Figure 2-5a). Not only are additional restriction fragments observed in these strains but also the intensity of the higher molecular weight restriction fragments is increased relative to the intensity of the terminal telomere fragment (in brackets) (Figure 2-6a, *rad24-2** and *cdc13-1 rad24-2** lanes). There was no evidence for telomere rearrangements in the *rad24-3* strains (Figure 2-6a, *rad24-3* lanes). An additional outcross of the rearranged *cdc13-1 rad24-2* strain resulted in telomere rearrangements not only in *cdc13-1 rad24-2* cells, but also in "wildtype", *rad24-2,* and *cdc13-1* haploids derived from the same diploid strain (dCN155) (Figure 2-6b, compare wildtype with *wildtype**, *rad24-2**, *cdc13-1 rad24-2 **, and *cdc13-1** lanes). The *rad24-Δ* strains show some amplification of a Y' subtelomeric element, but this amplification was present in the diploid that the *rad24- Δ* was originally created in (data not shown). The telomeres in the *cdc13-1* haploid used for the screen show no evidence of recombination (Figure 2-7a, *cdc13-1* lane and Figure 2-12 right panel, *cdc13-1* lane).

The pattern of telomere recombination in the *rad24-2* strains is reminiscent of that observed in strains that amplify their $TG_{1\text{-}3}$ repeats through a Rad50-dependent homologous recombination pathway (Lundblad and Blackburn, 1993, Teng and Zakian, 1999, Grandin et al., 2001a, Chen et al., 2001). To show that longer tracts of telomere

repeats are indeed present in the *rad24-2* strains, the yeast genomic DNA was digested with a combination of restriction enzymes (*Alu*I, *Hae*III, *Hinf*I and *Msp*I) that cut multiple sites within the telomere Y' sequences but not within the TG_{1-3} repeat sequences. The telomere repeats fragments observed in *rad24-2* strains are distinct high molecular weight species, in contrast to the shorter tracts of telomere repeats found in normal wild-type cells (in brackets) (Figure 2-6a). Backcrossing the rearranged *cdc13-1 rad24-2* strain also resulted in amplified TG_{1-3} repeats in wildtype, *rad24-2,* and *cdc13-1* haploids from the same cross (Figure 2-6a, *wildtype*,*, *rad24-2**, and *cdc13-1** lanes).To further characterize the telomeric amplification present in the *rad24-2* strains, we examined the *Xho*I telomere restriction fragments in strains that were grown at either 23°C or at 30°C and probed with subtelomeric Y' probe. Wild-type telomeres exhibited the expected sizes for long Y' and short Y' elements at 6.7 kb and 5.2 kb, respectively (Figure 2-6b, wildtype lane). Southern blots show that the subtelomeric Y' element composition in *rad24-2* strains was distinctly different from wildtype cells, and displayed multiple additional Y' bands, indicating amplification of Y' elements had occured as well (Figure 2-6b compare wildtype lanes to *rad24-2** and *cdc13-1 rad24-2** lanes). Such altered restriction fragment patterns of telomeric DNA are characteristic of those found in telomerase deficient survivors, and in *cdc13-1 mec3- Δ* or *cdc13-1 rad24- Δ exo1- Δ* temperature resistant strains, suggesting the *rad24-2* allele may promote the acquisition of chromosomal alterations (Teng and Zakian, 1999, Foster et al., 2006, Zubko and Lydall, 2006, Grandin et al., 2001).

Finally, to assess whether the TG_{1-3} repeats amplification occurs across the genome, we used pulsed field gel electrophoresis (PFGE) to separate whole chromosomes and then compared the intensity of telomere probe hybridization to the chromosomes. A Southern Blot of the chromosomes with a telomere probe showed much stronger hybridization to the chromosomes in the *cdc13-1 rad24-2* strain as compared with all of the other strains (Figure 2-7a). Ethidium bromide (EtBr) staining of the pulsed-field gel did not show large differences in the total amount of chromosomal DNA present in the gel, indicating that the TG-repeats are indeed amplified in the *cdc13-1 rad24-2* strain (Figure 2-7b). One of the *cdc13-1 rad24-2* samples also showed poor resolution of its individual chromosomes on the EtBr stained gel, consistent with a conclusion that the chromosomes have a recombination or replication structure that is interfering with migration through the gel (Figure 2-7b). Once the blot was stripped and probed with a subtelomeric Y' probe, chromosomes in the *cdc13-1 rad24-2* strain showed much stronger hybridization with to the Y' probe compared with all of the other strains, indicating that Y' elements were amplified as well (Figure 2-7c). From these data we conclude that the *cdc13-1 rad24-2* strain, but not the *cdc13-1 rad24-3* strain, has amplified TG_{1-3} repeats. Together, these data support the hypothesis that *rad24-2* supports *cdc13-1* growth at higher temperatures than *rad24-Δ* because *rad24-2* promotes the amplification of telomere repeats.

Heritable telomere structure may promote temperature resistance of *cdc13-1 rad24-2* cells.

If the *rad24-2* allele is sufficient to promote the growth of *cdc13-1* at 36°C, then following a cross of a temperature resistance *cdc13-1 rad24-2* with a wild-type strain, *cdc13-1 rad24-2* double mutant segregants should retain their ability to grow at 36°C. Furthermore, it is expected that the resulting haploids from this diploid would inherit a mix of normal and recombined telomeres from the parental strains. In order to test our hypothesis that the inherited recombined telomeres contributed to the suppression of temperature sensitivity in *cdc13-1 rad24-2* cells, we tested the temperature sensitivity of the *cdc13-1 rad24-2* haploids in successive generations from back-crosses of the *cdc13-1 rad24-2* strain with a wild-type haploid (Figure 2-8a). Interestingly, the degree of temperature resistance of the *cdc13-1 rad24-2* strains is diminished in each successive cross. The *cdc13-1 rad24-2** strains from the first cross (from diploid dCN149) show much better growth at 36°C than the *cdc13-1 rad24-2*** haploids from the third outcross, which even show reduced growth at 34°C. These data are consistent with the interpretation that instead of *rad24*-2 being sufficient for *cdc13-1* growth at 36°C, a non-Mendelian factor, such as telomere amplification, improves the suppression mediated by *rad24-2.*

Testing the hypothesis that telomere amplification contributed to the temperature resistance of *cdc13-1 rad24-2* required determining the ability of telomere amplification to promote growth of *cdc13-1.* Two approaches were taken to address this. First, the ability of the *cdc13-1* haploids obtained from dCN149 to grow above the *cdc13-1*

maximum permissive temperature of 25°C was tested. As shown in Figure 2-8b, after propagating the *cdc13-1** strains at 23°C and then plating serial dilutions at a range of temperatures, there is a modest improvement in *cdc13-1** growth at 28°C. The extent to which the growth improved at 28°C was variable among the *cdc13-1** strains, and in no case were the cells able to grow well above 28°C. In addition, the *cdc13-1*** strains (from the second out-cross) did not show improved growth relative to *cdc13-1* strains (data not shown).

To test the hypothesis that an altered telomere structure alone was sufficient to promote growth of *cdc13-1* cells, *est2Δ* type II survivors were crossed to *cdc13-1* cells and the ability of *cdc13-1* haploids segregants obtained from this diploid to grow above the *cdc13-1* maximum permissive temperature of 25°C was tested. Fast-growing colonies of senescing telomerase defiecent cells were found to predominately generate type II recombination survivors when grown in liquid cultures at high temperatures (Grandin and Charbonneau, 2003). As shown in Figure 2-9a, propagating *est2Δ* strains to select for fast-growing telomerase-deficient survivors resulted in an amplified telomeric repeats structure characteristic of type II survivors. This *est2Δ* type II survivor strain was crossed with a *cdc13-1* strain that, once sporulated, gave rise to haploid strains that had inherited mix of normal and recombined telomeres (Figure 2-9a). After *cdc13-1** haploids from that diploid strain were grown at 23°C to saturation in liquid media and serial dilutions were plated at a range of temperatures, there was a modest improvement in *cdc13-1** growth at 28°C (Figure 2-9b). This further demonstrates that altered telomere structure alone can promote growth of *cdc13-1* strains at higher temperatures.

The second approach was to test whether introduction of *RAD24* on a *CEN* plasmid into the *cdc13-1 rad24-2* strain was sufficient to fully complement the checkpoint defect and temperature resistant growth in the strain. Significantly, while the UV resistance of these cells improved to wild-type levels, a population of the cells retained the ability to grow up to 30-32°C (Figure 2-10). Both of these experiments indicate that the amplified telomere repeats do contribute to *cdc13-1* suppression, consistent with the hypothesis that long or rearranged telomeres have a reduced requirement for *CDC13* capping function (Vodenicharov and Wellinger, 2006, Negrini et al., 2007). While the telomere TG_{1-3} amplification in these strains is not sufficient to mediate strong suppression of *cdc13-1,* we conclude that it is likely to contribute to the suppression observed in the *cdc13-1 rad24-2* isolate.

Promotion of *cdc13-1* suppression is similar in *rad24-2* and *rad24-Δ* strains.

Since the amplified telomeres are heritable, recreating the *rad24-2* allele in diploids that have normal telomeres allowed us to test the hypothesis that the *rad24-2* mutation itself promoted telomere recombination. Instead of mating, transformation of a PCR fragment was used to construct the *rad24-2* mutation in two diploid strains that are heterozygous for *cdc13-1* and have normal telomeres (dCN293, DVL144). A DNA fragment encompassing the mTn3 insertion cassette and flanking *rad24-2* sequences was transformed into each diploid, replacing one *RAD24* allele. The strains derived from the re-created allele are denoted with an "R". Examining the *cdc13-1 rad24-2 R* strains obtained from these diploids reveals that their temperature sensitivity is similar to *cdc13-1 rad24-Δ* strains (Figure 2-11a). Therefore, the recreated *rad24-2* allele is not sufficient

for growth of *cdc13-1* cells beyond ~30°C. In addition, the *rad24-2* and *rad24-2R* strains are both as sensitive to UV damage as the *rad24-Δ* (Figure 2-11b), confirming that the *rad24-2* allele was responsible for the checkpoint deficient phenotype. Finally, unlike our starting *cdc13-1 rad24-2* strain, the telomeres in the *rad24-2 R* strains from either yeast background analyzed did not show evidence of TG-repeat recombination (Figure 2-12). Thus, it is possible that the telomere recombination in the original isolate occurred independently of the *rad24-2* mutation.

Since *rad24-2 R* is not sufficient for *cdc13-1* growth at high temperatures, we next tested the hypothesis that the frequency of obtaining temperature resistant *cdc13-1* colonies is increased in *rad24-2* strains as compared to *rad24-Δ* strains. Using *cdc13-1 rad24-Δ* and *cdc13-1 rad24-2 R* haploids that had never previously been exposed to temperatures above 23°C, liquid cultures from single colonies were grown at 23°C, and cells were plated at both 23°C and 34°-36°C. The plating efficiency at 23°C for each culture was determined, and the fraction of cells capable of growth at 34°-36°C was calculated (Figure 2-13). Interestingly, the analysis showed that, in comparison with *cdc13-1 rad24-Δ* cells, there is a small, but statistically significant, increase in the fraction of *cdc13-1 rad24-2* cells that are able to form colonies at high temperature. Analysis of the telomeres in the temperature resistant (TR) colonies that arose did not show evidence for immediate induction of a particular telomere rearrangement in the *rad24-2* strain concomitant with growth at high temperature (Figure 2-14). Similar to previous observations with *cdc13-1 rad24-Δ* strains, many of the cultures showed no apparent alteration in their telomere restriction fragments, and among the colonies tested,

cdc13-1 revertants appeared rarely (data not shown) (Zubko and Lydall, 2006). However, it remains possible that *rad24-2* does alter telomere metabolism in a subtle way that our experiments have not detected.

Discussion

In an attempt to identify genes involved C-strand degradation after telomere end protection has been lost, a transposon mutagenesis screen was conducted for extragenic suppressors of *cdc13-1* temperature sensitivity. Two new alleles of *RAD24* were identified, which both contained an insertion of the mTn3 transposon within the *RAD24* coding region. Complete deletion of *RAD24* has been previously shown to provide a modest suppression of *cdc13-1* temperature sensitivity, due to inactivation of the DNA damage checkpoint (Lydall and Weinert, 1995).

In addition to its role in the DNA damage checkpoint, Rad24 has been found to also affect the amount of ssDNA that is generated in *cdc13-1* cells, suggesting an undefined role for the checkpoint clamp-loader complex in telomere resection (Lydall and Weinert, 1995). The robust suppression of *cdc13-1* observed in our initial isolate of *cdc13-1 rad24-2* suggested that the *rad24-2* allele could potentially be used to give insight into the activities that control telomere resection once capping has been lost in *cdc13-1* cells. Unfortunately, when the *rad24-2* allele was reconstructed in a naïve *cdc13-1* strain that had not previously been exposed to high temperatures, we found that the *rad24-2* allele alone was not sufficient to promote *cdc13-1* growth at 36°C. Therefore, we conclude that our initial *cdc13-1 rad24-2* isolate had acquired an additional alteration that allowed growth at higher temperature when combined with

rad24-2. Consistent with this idea, consecutive outcrossing of our initial isolate revealed an additional trait segregating through the cross in a non-Mendelian manner that could influence the temperature sensitivity of *cdc13-1* strains.

Loss of *RAD24* has been previously shown to enhance the frequency of *cdc13-1* cells becoming capable of forming a colony at 36°C, although lack of Rad24 does not strongly suppress *cdc13-1* temperature sensitivity (Zubko and Lydall, 2006). The rate of *cdc13-1* temperature resistant colony formation is further enhanced by the absence of the *EXO1*, suggesting that reduced telomere resection promotes *cdc13-1* viability (Zubko and Lydall, 2006). After prolonged propagation, telomeres in the temperature resistant *cdc13-1 rad24-Δ exo1-Δ* or *cdc13-1 mec3-Δ* strains become rearranged, and contain a pattern of restriction fragments that is observed in strains in which the TG_{1-3} repeats have been amplified (Zubko and Lydall, 2006, Grandin et al., 2001a). Intriguingly, the initial *cdc13-1 rad24-2* strain isolated from our screen had acquired similar telomere amplification, and this rearrangement of the telomeric DNA contributes to the ability of these cells to maintain viability at increased temperatures. Thus, the temperature resistance observed in our initial *cdc13-1 rad24-2* strain resulted from a fortuitous coselection of a clone with both *rad24-2* and telomere amplification. These amplified telomeres were then inherited in the subsequent diploids that were created, and we show that it is likely that the altered telomeres contribute to the *cdc13-1* suppression.

Given these observations, a key issue that remains to be addressed is whether *rad24-2* is in any sense phenotypically distinct from a *rad24*-Δ allele. Examination of naïve *cdc13-1 rad24-2* strains, demonstrated that the *rad24-2* mutation does not directly

stimulate TG_{1-3} repeat amplification. However, the finding that *cdc13-1* temperature resistant colonies arise more frequently in *rad24-2* strains compared to *rad24-Δ* strains indicates that the *rad24-2* allele is functionally distinct from the null, although in a potentially subtle manner. Although the *rad24-2* allele is recessive, the expressed protein fragments may interfere with an aspect of telomere metabolism that increases the likelihood of uncapped *cdc13-1* cells acquiring changes that allow it to grow at higher temperatures. Multiple Rad24 protein fragments are potentially produced from the *rad24-2* locus, which includes the 63 amino acid N-terminal fragment, and carboxyl-terminal fragments initiating from methionine 95 and 163. These carboxyl-terminal portions of the protein are likely to be expressed from a transcript that is initiated by a promoter within the transposon. The conserved AAA+ domain , which is necessary for ATP hydrolysis, is predicted to be contained within the largest Rad24-2 fragment initiating at methionine 95, but will be absent in the truncation product that starts with methionine 163. The ability of either truncation to bind the checkpoint clamp, the RFC subunits, or to ATP has not been tested. Even though these Rad24 truncations do not maintain their checkpoint function, they could still potentially interfere with telomere processing and/or recombination pathways. Loss of Rad24 function (*rad24-Δ)* has been shown to impair recombination from templates with limited homology, which is likely related to the delayed processing of DSBs in *rad24-Δ* cells (Aylon and Kupiec, 2003). Thus, the Rad24-2 protein fragments may facilitate the acquirement of telomeric modifications that promote *cdc13-1* growth at elevated temperatures.

Interestingly, a somewhat analogous Rad17 mutant was analyzed in *Mus musculus*, where a mutation in the 5' portion of the gene was shown to lead to the production of a truncated protein lacking the 78 amino-terminal residues in the mice ES cells, but not in the mRad17$^{5'\Delta/5'\Delta}$ MEFs (Budzowska et al., 2004). Alignment of the mouse and yeast homologs reveals that this mRad17 mutant includes 42 additional amino terminal residues as compared to the *S. cerevisiae* Rad24-2 Δ1-94 N-terminal truncation. ES cells expressing this mutant protein were competent for the S and G_2 checkpoint functions, but were sensitive to genotoxic stress. In addition, it was found that some DNA repair processes were impaired, such as the homologous recombination processes required for gene replacement (Budzowska et al., 2004). Based on these findings, a further analysis of how Rad24 affects processing, and recombination of DNA ends should be of considerable interest.

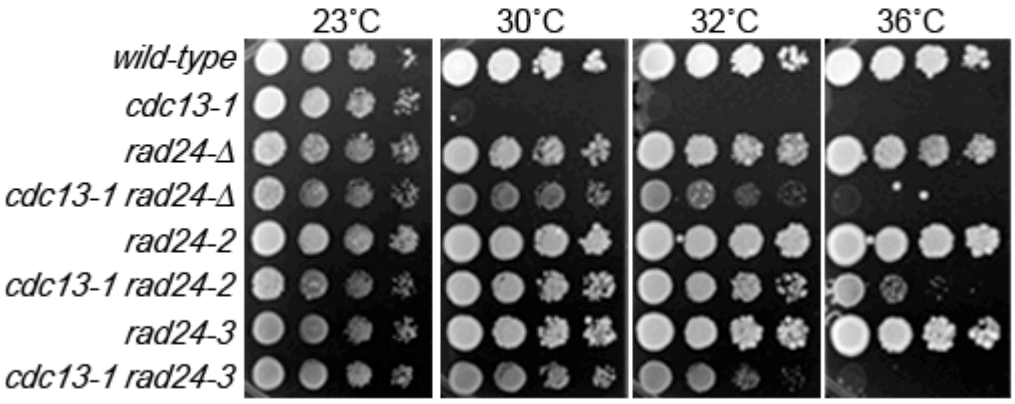

Figure 2-1 Suppression of *cdc13-1* by truncated *rad24-2* and *rad24-3* alleles. Comparison of suppression of *cdc13-1* temperature sensitivity by *rad24-Δ*, *rad24-2* and *rad24-3* compared at different temperatures. Cultures were grown to saturation in YPD at 23°C and used to prepare tenfold serial dilutions which were stamped onto YPD plates, and incubated at indicated temperatures for three to five days. Strains: wild-type (hC160), *cdc13-1* (hC188), *rad24-Δ* (hC344), *rad24-Δ cdc13-1* (hC350), *rad24-2* (hC340), *rad24-2 cdc13-1* (hC346), *rad24-3* (hC342), and *rad24-3 cdc13-1* (hC348).

Figure 2-2 Truncated proteins are expressed from both the *rad24-2* and *rad24-3* alleles. A. Maps of *Rad24* gene (upper panel), *rad24-2* (middle panel) and *rad24-3* (lower panel) alleles. For both alleles, the transposon is integrated at the endogenous *RAD24* locus within the coding region. The transposon is inserted following nucleotide 189 in the *rad24-2 allele* and following nucleotide 388 in *rad24-3*. The orientation of the transposable cassette is reversed in the two alleles. The *rad24-2* allele is predicted to produce amino acids 1-63 from its native promoter; following the transposon, it has the potential to translate from amino acid 95 to the end of the protein, residue 659. The *rad24-3* allele encodes amino acids 1-129 prior to its disruption, with the potential to translate the remainder of Rad24 from residue 163. B. Truncated proteins are expressed from both the *rad24-2* and *rad24-3* alleles. Western blot of myc epitope tagged Rad24 proteins. 300 µg of each total protein lysate was loaded on a 10% SDS-PAGE gel. Membranes were probed with a 9E10 α- myc antibody. The blot was then stripped and re-probed with an α - tubulin antibody, as a loading control. The α - myc panel on the right is from a separate experiment, where the amount of total protein lysate loaded was not equivalent. This panel was not re-probed with α- tubulin. Strains: wild-type (hC160), *RAD24myc18x* (hC770), *RAD24myc18x cdc13-1* (hC1073), *rad24-2myc18x* (hC771), *rad24-2myc18x cdc13-1* (hC1074), *rad24-3myc18x* (hC772), and *rad24-3myc18x cdc13-1* (hC1075).

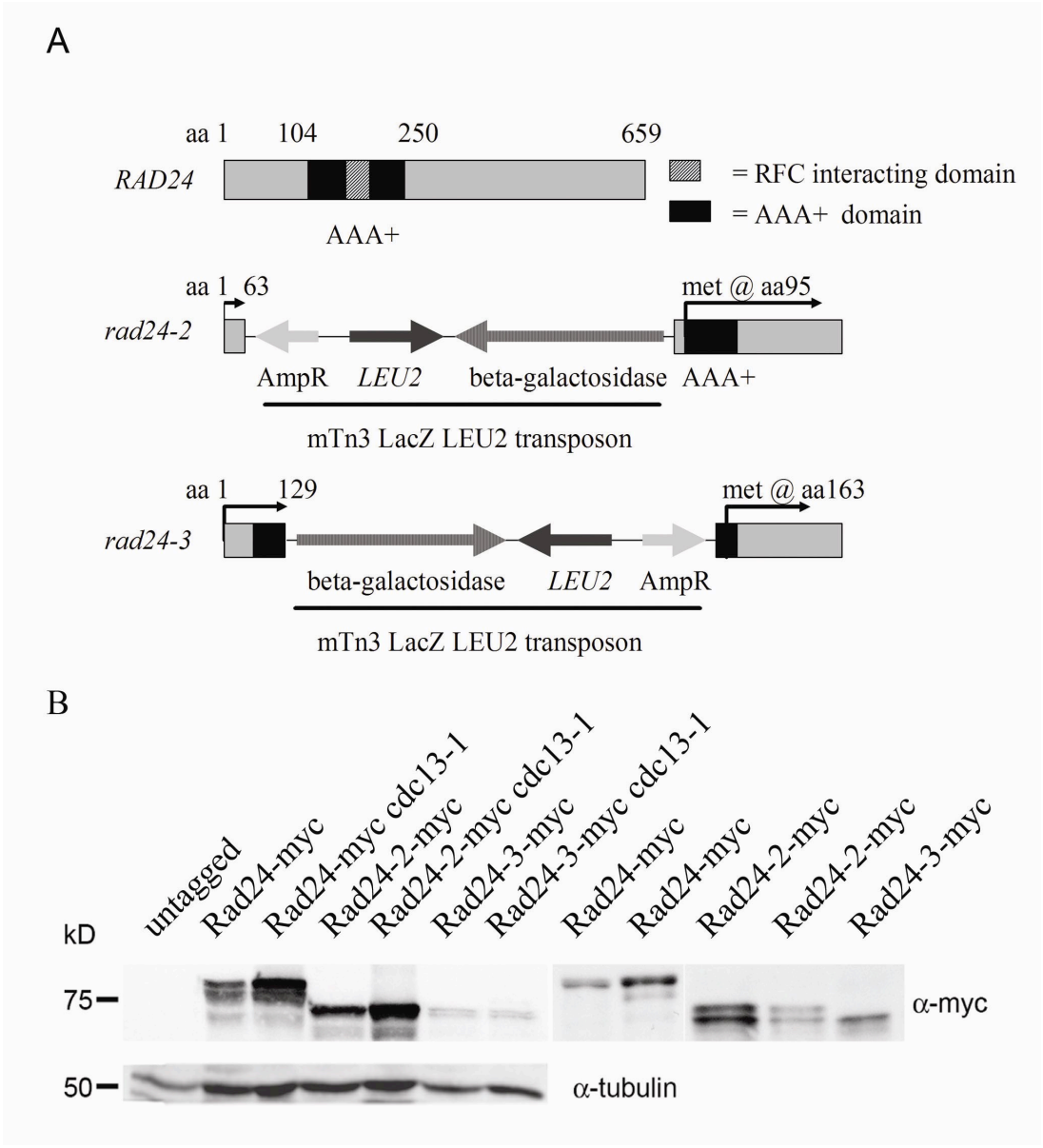
A
aa 1
104
250
659
RAD24
= RFC interacting domain
= AAA+ domain
AAA+
aa 1 63
met @ aa95
rad24-2
AmpR
LEU2
beta-galactosidase
AAA+
mTn3 LacZ LEU2 transposon
aa 1
129
met @ aa163
rad24-3
beta-galactosidase
LEU2
AmpR
mTn3 LacZ LEU2 transposon
B
kD
untagged
Rad24-myc
Rad24-myc cdc13-1
Rad24-2-myc
Rad24-2-myc cdc13-1
Rad24-3-myc
Rad24-3-myc cdc13-1
Rad24-myc
Rad24-myc
Rad24-2-myc
Rad24-2-myc
Rad24-3-myc
75
50
α-myc
α-tubulin

Figure 2-3 The amino terminal portion of Rad24 is essential for its checkpoint function. A. Sensitivity of *rad24::mTn3* strains to UV irradiation is similar to *rad24*-Δ. Strains were grown to saturation in YPD and ten-fold serial dilutions were spotted onto YPD media. One plate was irradiated with 75 J/m^2 of UV. Plates were incubated at 23°C for 5 days. B. Sensitivity of *rad24::mTn3* strains to HU is similar to *rad24*-Δ. Strains were grown to saturation in YPD and ten-fold serial dilutions were spotted onto YPD or YPD media containing 75 mM hydroyurea.. Plates were incubated at 23°C for 5 days. C. Viability of *rad24* mutant strains drops following exposure to 0.1% MMS. Data shown was provided by Charles Chuang. Cells were arrested in G1 with alpha factor, and then released into 0.1% MMS. At each time point, cells were plated for single colonies, which were counted after 3 days at 30°C. Strains: wild-type (hC160), *cdc13-1* (hC188), *rad24-Δ* (hC344), *rad24-Δ cdc13-1* (hC350), *rad24-2* (hC341), *rad24-2 cdc13-1* (hC346), *rad24-3* (hC343), and *rad24-3 cdc13-1* (hC348).

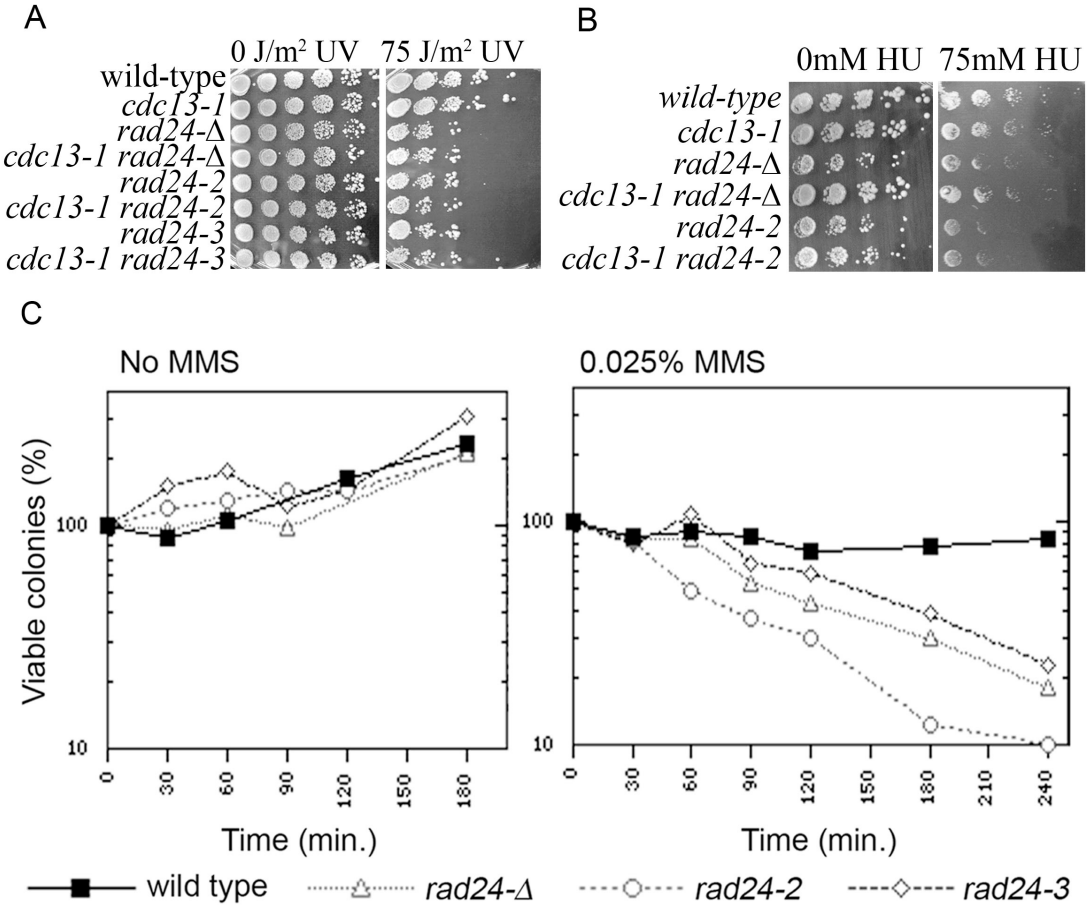
A
0 J/m2 UV
75 J/m2 UV
wild-type
cdc13-1
rad24-Δ
cdc13-1 rad24-Δ
rad24-2
cdc13-1 rad24-2
rad24-3
cdc13-1 rad24-3
B
0mM HU
75mM HU
wild-type
cdc13-1
rad24-Δ
cdc13-1 rad24-Δ
rad24-2
cdc13-1 rad24-2
C
No MMS
0.025% MMS
Viable colonies (%)
100
10
0
30
60
90
120
150
180
210
240
Time (min.)
wild type
rad24-Δ
rad24-2
rad24-3

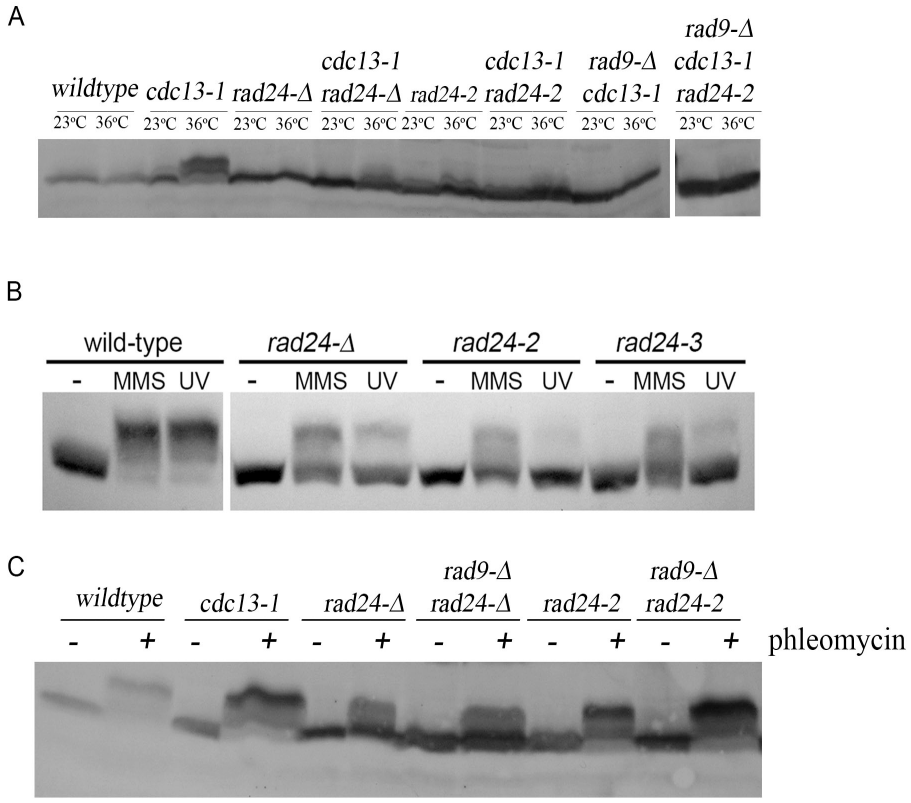

Figure 2- 4 Phosphorylation of Rad53 by DNA damage is diminished in all *rad24* strains. A. *rad24* alleles show similar deficiencies in Rad53 phosphorylation in response to *cdc13-1* loss of function. Cells were grown at 23°C to an OD600 of 0.5, then the culture was split, with half shifted to 36°C for 4 hours. The Western blot was probed with anti-Rad53 (Santa Cruz). B. Phosphorylation of Rad53 by MMS and UV damage is diminished in all *rad24* strains. Western blot of Rad53 in untreated, MMS treated (0.1 % for 2 hrs), or UV irradiated (80 J/m2) cells. All lanes were on the same gel. C. *rad24* alleles show similar abilities to phosphorylate Rad53 in response to DNA damage caused by phleomycin treatment (0.1 % for 4 hrs). Cells were grown at 23°C to an OD600 of 0.5, then the culture was split, with half treated with phleomycin for 4 hours. Strains: wild-type (hC160), *cdc13-1* (hC188), *rad9-Δ cdc13-1* (hC400), *rad24-Δ cdc13-1* (hC350), *rad24-2 cdc13-1* (hC654), *rad24-3 cdc13-1* (hC665).

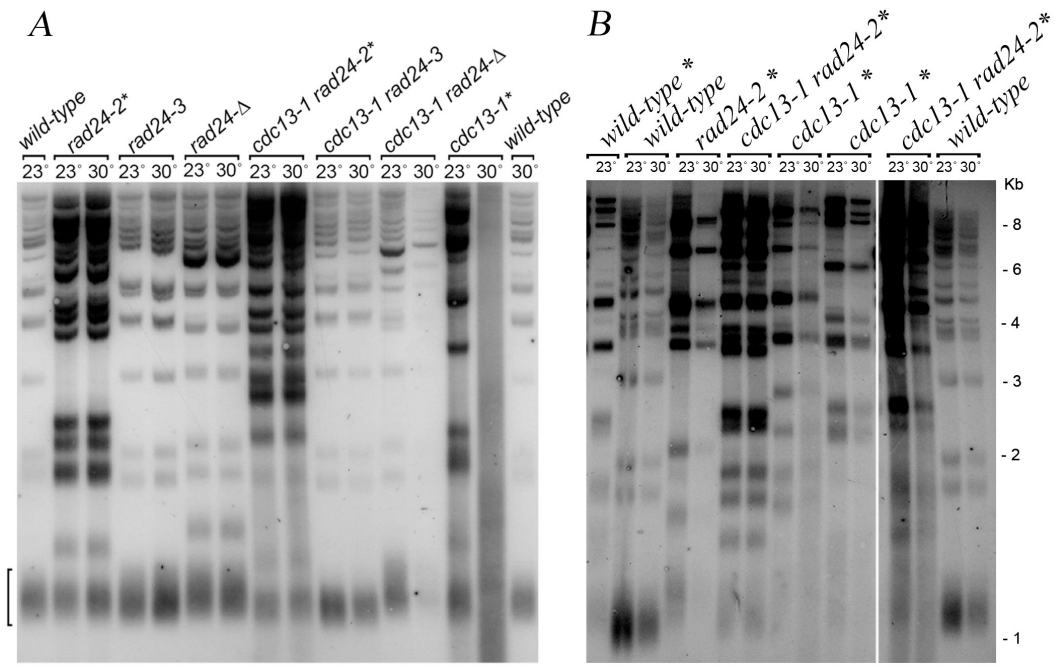

Figure 2- 5 *cdc13-1 rad24-2* strains acquire amplified telomere repeats.

A. Southern Blot analysis comparing telomere restriction fragments from single and double mutant *rad24* strains grown at 23°C and 30°C. Genomic DNA was prepared from the indicated yeast strains, digested with *Xho*I, fractionated through 1% agarose, transferred to a nylon membrane, hybridized with a [32P]-dGT/CA probe, and exposed on film. Strains marked with an asterisk are from the first outcross of the original *cdc13-1 rad24-2* mutant isolate from dCN149. Data shown was provided by Charles Chuang and Dr. Constance Nugent. Strains: wild-type (hC160), *rad24-2** (hC657), *rad24-3* (hC343), *rad24-Δ* (hC344), *cdc13-1 rad24-2** (hC654), *rad24-3 cdc13-1* (hC348) *rad24-Δ cdc13-1* (hC350), *cdc13-1** (hC649). B. Southern Blot analysis comparing telomere restriction fragments from single and double mutant *rad24* strains grown at 23°C and 30°C prepared as described in A. Strains marked with asterisk are from the second outcross of the *cdc13-1 rad24-2* mutant isolate obtained from dCN155 diploid strain. Strains: wild-type (hC160), wild-type* (hC658), *rad24-2** (hC657), *cdc13-1 rad24-2** (hC654, hC655), *cdc13-1*** (hC649, hC653).

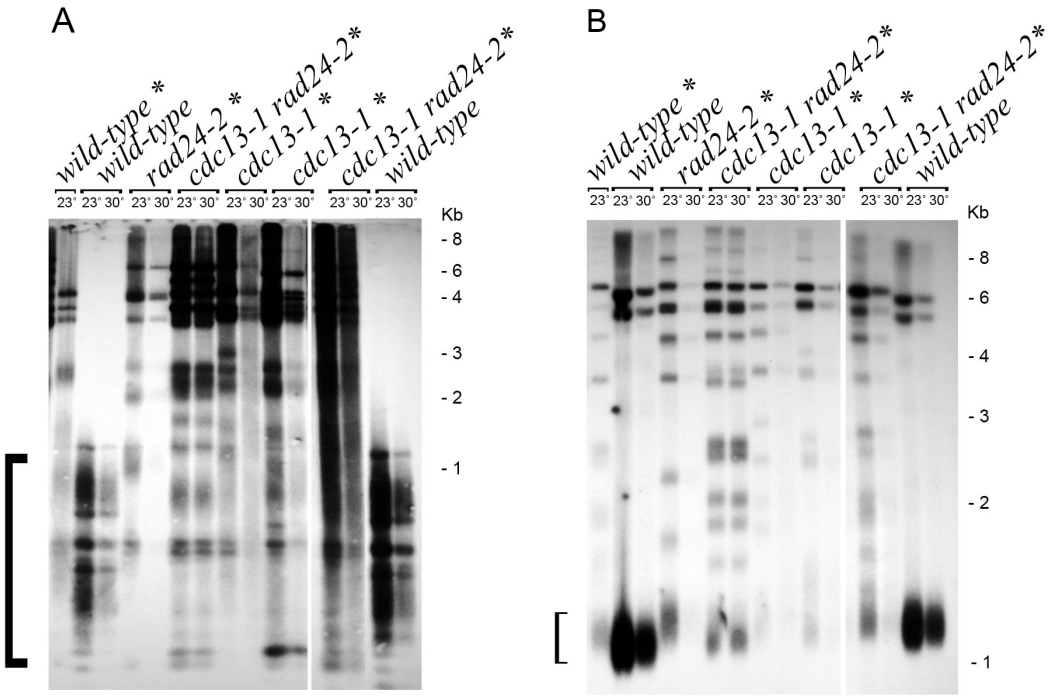

Figure 2-6 *cdc13-1 rad24-2* strain has acquired telomere repeats reminiscent of telomerase – deficient Type II survivors. A. Southern Blot analysis of yeast genomic DNA digested with *Alu*I, *Hae*III, *Hinf*I, and *Msp*I, Genomic DNA was digested with a mixture restriction enzymes that each have 4-bp recognition sequences which are not present in telomere repeats. The digested DNA was run on a 1.3% agarose gel, transferred to a nylon membrane and hybridized to a [32P]-dGT/CA probe. The bracket indicates the terminal repeat fragment size in wild-type cells. B. Southern Blot analysis comparing telomere restriction fragments from single and double mutant *rad24* strains grown at 23°C and 30°C. Genomic DNA was prepared from the indicated yeast strains, digested with *Xho*I, fractionated through 1% agarose, transferred to a nylon membrane, hybridized with a [32P]-subtelomeric Y' probe, and exposed on film. Strains marked with an asterisk are from the second outcross of the original *cdc13-1 rad24-2* mutant isolate derived from dCN155 diploid strain. Strains: wild-type (hC160), wild-type* (hC658), *rad24-2** (hC657), *cdc13-1 rad24-2** (hC654, hC655), *cdc13-1** (hC649, hC653).

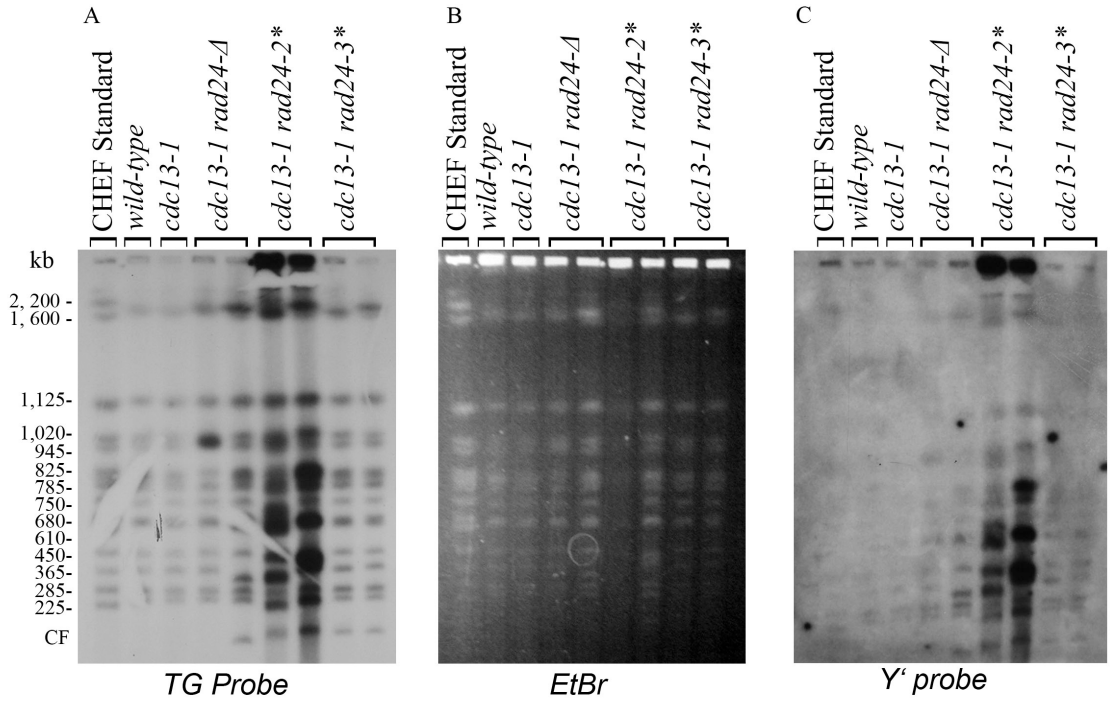

Figure 2- 7 Telomere repeat amplification acquired in *cdc13-1 rad24-2* strain is present on multiple chromosomes. Analysis of telomeric repeat amplification by pulsed-field gel electrophoresis. Chromosomes of the indicated strains were prepared for CHEF-gel analysis from strains that were grown at 23°C. A. Southern blot of CHEF-gel, probed with [^{32}P]-dGT/CA. B. Ethidium Bromide stained agarose CHEF-gel. C. Southern blot of CHEF-gel, probed with [32P]-Y' sequence. *S. cerevisiae* chromosome standards (BioRad) were loaded in the first lane of the gel, with sizes indicated on the left. CF refers to a chromosome fragment present in some of the strain backgrounds used. Strains: wild-type (hC160), *cdc13-1* (hC188), *rad24-Δ cdc13-1* (hC350, hC351), *cdc13-1 rad24-2* (hC346, hC655), *cdc13-1 rad24-3* (hC346, hC665).

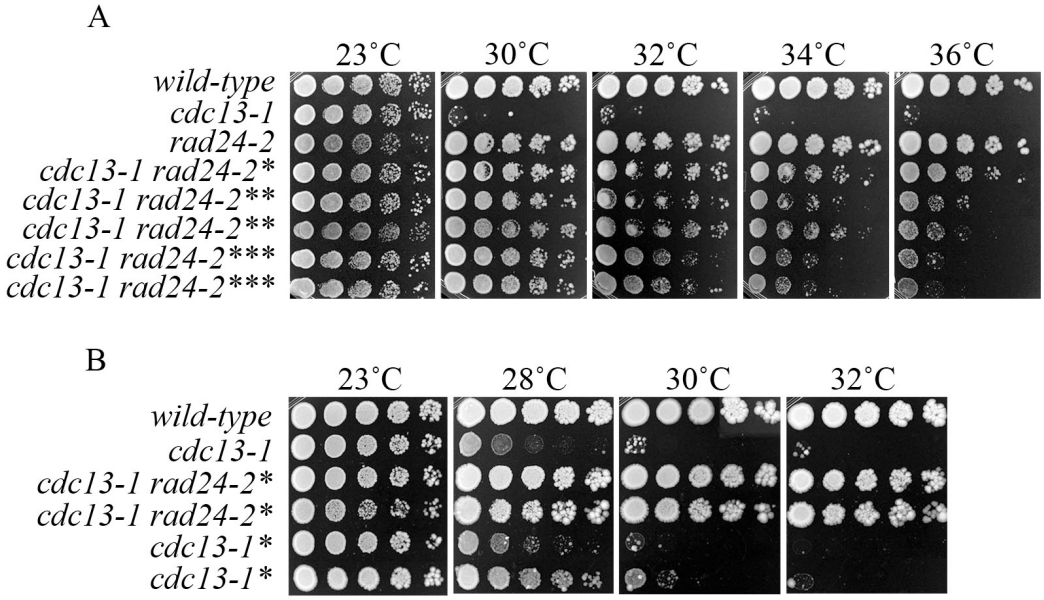

Figure 2- 8 Modifier of *cdc13-1* growth inherited in cross.

A. *cdc13-1 rad24-2* mutants show decreased temperature resistance with each successive cross. Haploid *cdc13-1 rad24-2* strains were obtained through dissection of diploids that were created through serial matings of *cdc13-1 rad24-2* with wild-type cells. Cultures of the indicated strains were grown at 23°C, and ten-fold serial dilutions were then stamped onto YPD, incubating for 3-5 days at the indicated temperatures. To denote the generation from which a strain is derived, we added one asterisk to indicate the F1 generation, two asterisks for the F2, etc. Strains were maintained at 23°C throughout the crosses. **B.** *cdc13-1* strains from backcrossed diploids are less temperature sensitive. Strains were grown at 23°C and serial 10-fold dilutions were stamped onto YPD plates, and incubated at indicated temperatures. Plates were incubated 3-5 days before being photographed. The two *cdc13-1** and *cdc13-1 rad24-2** strains are independent spores from the first backcross of *cdc13-1 rad24-2* (dCN149). Strains: wild-type (hC160), *cdc13-1* (hC188), *rad24-2* (hC340), *cdc13-1 rad24-2** (hC346), *cdc13-1 rad24-2*** (hC1436, hC1437), *cdc13-1 rad24-2**** (hC1438, hC1439), *cdc13-1**(hC653, hC656).

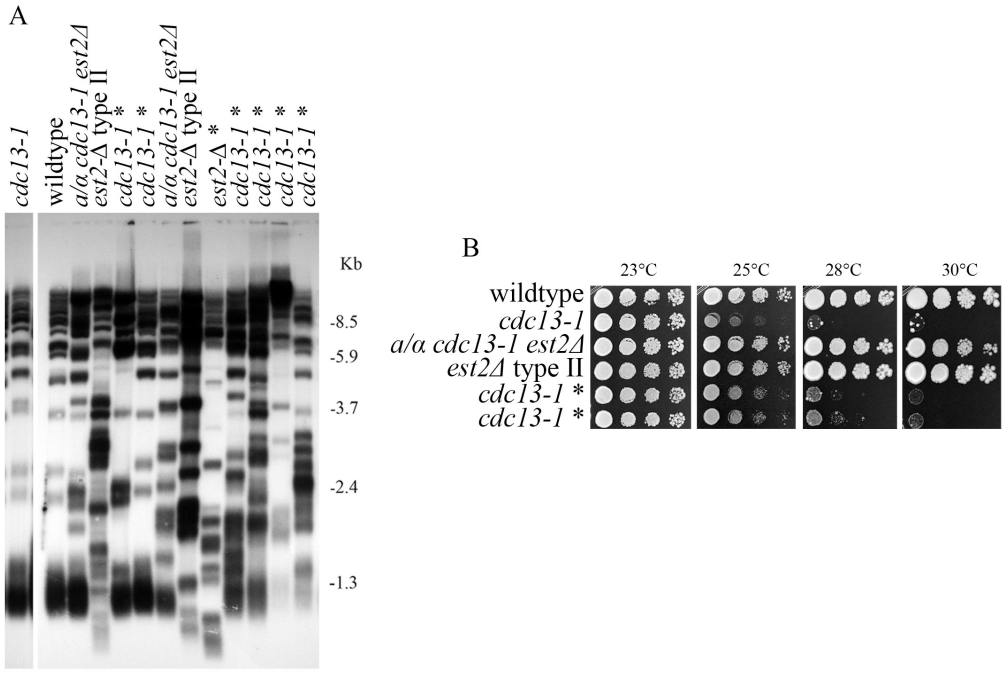

Figure 2- 9 *cdc13-1* haploids from *cdc13-1 est2Δ* type II survivor diploids have acquired moderate temperature resistance.

A. Southern Blot analysis comparing telomere restriction fragments of *cdc13-1* haploids from a homozygous *cdc13-1 est2-Δ* diploid strain grown at 23°C. Genomic DNA was prepared from the indicated yeast strains, digested with *Xho*I, fractionated through 1% agarose, transferred to a nylon membrane, hybridized with a [32P]- [^{32}P]-dGT/CA telomere probe, and exposed on film. *est2-Δ* type II cells were crossed with a *cdc13-1* to create the *cdc13-1 est2-Δ* type II diploid strain (dCN497) shown. Strains marked with an asterisk indicate the strains derived from the *cdc13-1 est2-Δ* type II dCN497 diploid strain. B. Strains were grown at 23°C and serial 10-fold dilutions were stamped onto YPD plates, and incubated at indicated temperatures. Plates were incubated 3-5 days before being photographed. The *cdc13-1** strains are independent spores from the *cdc13-1 est2-Δ* diploid. Strains: wild-type (hC160), *cdc13-1* (hC188), a/α *cdc13-1 est2-Δ* (dCN497), *est2-Δ* type II (hC2173), *cdc13-1** (hC1823), *cdc13-1** (hC1824).

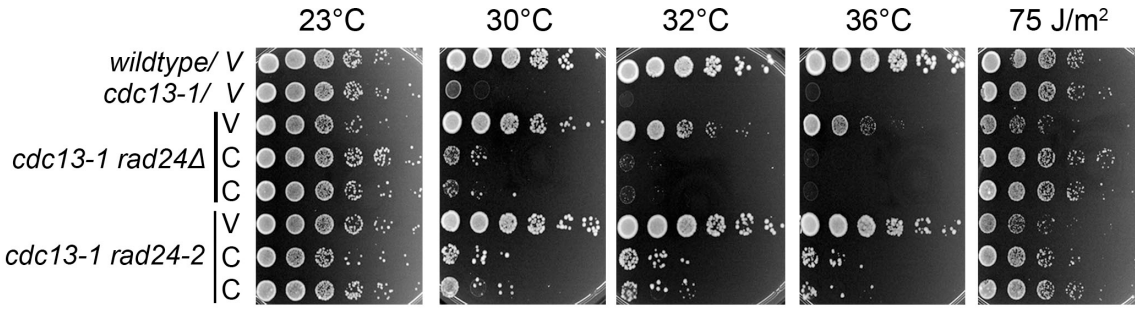

Figure 2- 10 p*RAD24* fully complements *cdc13-1 rad24-2* UV sensitivity but not temperature resistant growth. wild-type, *cdc13-1* , *cdc13-1 rad24-Δ* and *cdc13-1 rad24-2* strains were transformed with either vector denoted as "V" (pRS424) or pWL4 (*RAD24 TRP1 CEN*) denoted as "C". Serial 10-fold dilutions were stamped onto Trp- media, with one plate exposed to 75 J/m2 of UV. Cells were grown at the indicated temperatures for 3-5 days. The UV-exposed plate was grown at 23°C. Strains: wild-type/pRS424 (hC2174), *cdc13-1*/pRS424 (hC2175), *cdc13-1 rad24-Δ/* pRS424 (hC2176), *cdc13-1 rad24-Δ/*pWL4 (hC2177), *cdc13-1 rad24-2**/pRS424 (hC2178), *cdc13-1 rad24-2**/ pWL4 (hC2179).

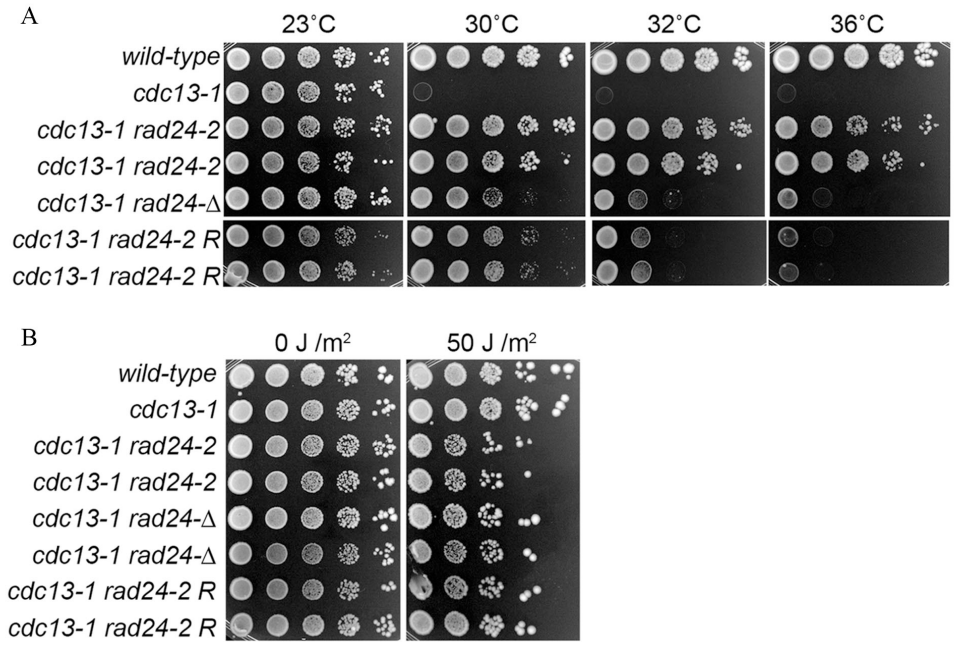

Figure 2- 11 *rad24-2* allele is not sufficient for *cdc13-1* growth at 36°C.

A. Reconstructing the *rad24-2* mutation in a strain not previously exposed to high temperature reveals a similar extent of *cdc13-1* suppression as mediated by *rad24-Δ*. A region surrounding the mTn3 integration site in *rad24-2* was transformed into a *cdc13-1/+* diploid strain replacing one wild-type *RAD24* allele. Strains marked with an "R" (reconstructed) were obtained from this diploid (dCN343). Cells were cultured at 23°C, and ten-fold serial dilutions were stamped on plates and incubated at the indicated temperatures. The cells in the figure were on the same plates. B. *rad24-2 R* strains show similar UV sensitivity as *rad24-Δ*. Serial 10-fold dilutions of the strains from (A) were stamped onto plates, and exposed to 50 J/m2 of UV. Plates were incubated at 23°C for five days. Strains shown: wild-type (hC160), *cdc13-1* (hC188), *cdc13-1 rad24Δ* (hC350, hC351), *cdc13-1 rad24-2* (hC346, hC347), *cdc13-1 rad24-2 R* (hC1542, hC1544).

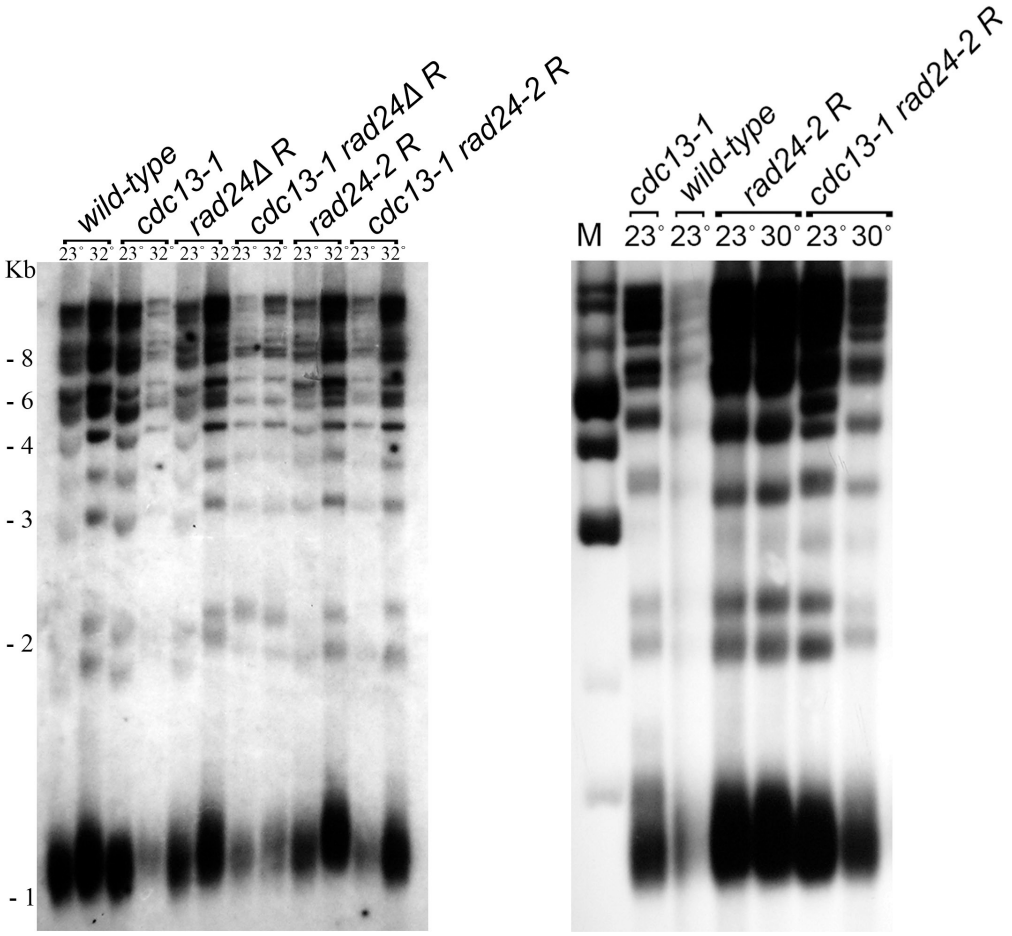

Figure 2- 12 Telomeres in *rad24-2 R* strains do not show TG-repeat recombination. Southern blot of telomere restriction fragments in the recreated *rad24-2* allele. Left panel shows reconstructed alleles derived from dCN318 and dCN319 the CRY background. Right panel shows haploid *rad24-2* and *cdc13-1 rad24-2* strains were derived from dCN343, in the W303 background. All strains were maintained at 23°C prior to this experiment. Single colonies were inoculated in liquid YPD and grown to saturation at either 23°C or 30°C. Genomic DNA was digested with *Xho*I and fractionated through 1% agarose. Following transfer to a nylon membrane the blot was probed with [32P]-dGT/CA and exposed to film for 1 day. Strains in CRY background: wildtype (CRY1), *cdc13-1* (hC31), *rad24Δ* (hC1506), *cdc13-1 rad24Δ* (hC1507), *cdc13-1 rad24-2* (hC1508), *cdc13-1 rad24-2 R* (hC1509). Strains in W303 background: wildtype (hC160), *cdc13-1* hC188), *rad24-2* (hC1543), *cdc13-1 rad24-2* (hC1542).

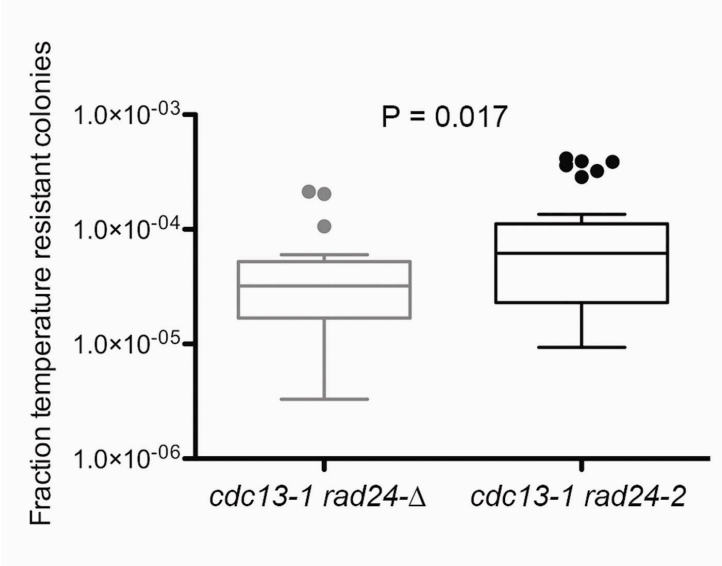

Figure 2-13 Promotion of *cdc13-1* suppression is increased in *rad24-2* compared to *rad24-Δ* strains. Fluctuation analysis of *cdc13-1 rad24-Δ* and *cdc13-1 rad24-2* R strains. Single colonies were inoculated into 5 ml of YPD, incubated at 23°C for 1-2 days, and cell density was determined using a hemocytometer. Cells were plated at a density of 250 cells per plate at 23°C and 500,000 cells per plate at 34°-36°C. 27 cultures were tested for *cdc13-1 rad24- Δ,* and 31 cultures were tested for *cdc13-1 rad24-2.* The data was analyzed using an unpaired Student's test with Welch's correction (calculated and plotted using with GraphPad Prism software). The data set for the *cdc13-1 rad24-2* cells showed a higher level of variance than the data set for the *cdc13-1 rad24-Δ* cells. The box plots are diagrammed with whiskers that extend 1.5 times the interquartile range; the dots are the outliers. Similar results were obtained for the naïve *cdc13-1 rad24-2R* strains for the two different genetic backgrounds that were tested. This data shows that the number of cells that are able to form a colony at high temperature is significantly increased in the *cdc13-1 rad24-2* strain relative to the *cdc13-1 rad24- Δ* strain. Strains: *cdc13-1 rad24- Δ* (hC1507, hC350), *rad24-2 cdc13-1* (hC1509, hC1542).

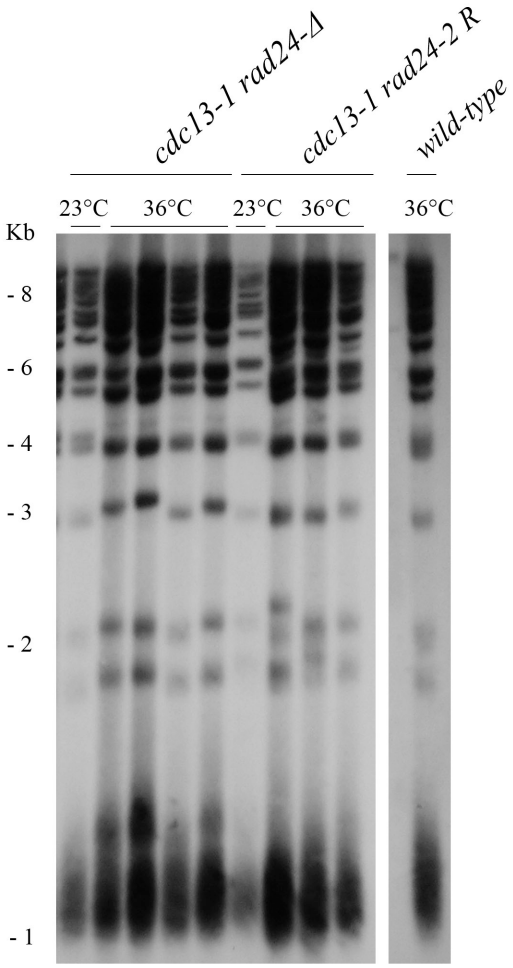

Figure 2- 14 Telomeres in temperature resistant *cdc13-1 rad24-2 R* strains do not show TG-repeat recombination. Southern blot of telomere restriction fragments in the recreated *rad24-2* allele. Haploid *cdc13-1 rad24Δ* and *cdc13-1 rad24-2* temperature resistant colonies from the fluctuation analysis shown in Figure 2-13 were inoculated in liquid YPD and grown to saturation at 36°C. Single colonies of *cdc13-1 rad24Δ* and *cdc13-1 rad24-2* strains were also grown at 23°C as a control. Single colonies of wildtype cells were grown to saturation in liquid YPD at 36°C as well. Genomic DNA was digested with *Xho*I and fractionated through 1% agarose. Following transfer to a nylon membrane the blot was probed with [32P]-dGT/CA and exposed to film for 1 day. Strains: wildtype (hC160), *cdc13-1 rad24Δ* (hC350), *cdc13-1 rad24-2 R* (hC1542).

Table 2-1 Yeast Strains used in Chapter 2

Strain	Relevant Genotype	Reference
CRY1	*MATa ade2-1 trp1-1 ura3-1 leu2-3,112 his3-11,15 can1-100*	Elledge
dVL 144	*MATa/* α *cdc13-1ts TRP1* *CDC13 trp1-Δ1*	Lundblad
dVL 202	*MATa/* α *cdc13-1ts rad24-Δ::kanMX2 rad9-Δ::TRP1* *CDC13 RAD24 RAD9*	Lundblad
dCN 149	*MATa/*α *cdc13-1ts rad24-2::LEU2* *CDC13 RAD24*	This study
dCN 293	*MATa/*α *cdc13-1ts* *CDC13*	This study
dCN 318	*MAT a/*α *cdc13-1ts rad24-Δ R ::kan MX2* *CDC13 RAD24*	This study
dCN 319	*MAT a/*α *cdc13-1ts rad24-2 R:: LEU2* *CDC13 RAD24*	This study
dCN 343	*MAT a/* α *cdc13-1ts rad24-2 R:: LEU2 TRP1* *CDC13 RAD24 trp1-Δ1*	This study
dCN 497	*MAT a/* α *cdc13-1ts est2-Δ ::URA3* *CDC13 EST2*	This study
hC 31	*MATa cdc13-1ts* *ade2-1 trp1-1 ura3-1 leu2-3,112 his3-11,15 can1-100*	Elledge
hC 56	*MATα est2Δ::URA3* *ura3-52 ade2-101 lys2-801 leu2-Δ1 trp1-Δ1 his3-Δ200*	
hC 160	*MATa* *ura3-52 ade2-101 lys2-801 leu2-Δ1 trp1-Δ1 his3-Δ200*	Lundblad
hC 188	*MATa cdc13-1ts* *ura3-52 ade2-101 lys2-801 leu2-Δ1 trp1-Δ1 his3-Δ200*	Petrecea
hC 340	*MATa rad24-2::LEU2 CF*[a] *ura3-52 ade2-101 lys2-801 leu2-Δ1 trp1-Δ1 his3-Δ200*	This study
hC 341	*MATα rad24-2::LEU2 CF*[a] *ura3-52 ade2-101 lys2-801 leu2-Δ1 trp1-Δ1 his3-Δ200*	This study
hC 342	*MATa rad24-3::LEU2 CF*[a] *ura3-52 ade2-101 lys2-801 leu2-Δ1 trp1-Δ1 his3-Δ200*	This study
hC 344	*MATa rad24Δ::kanMX2* *ura3-52 ade2-101 lys2-801 leu2-Δ1 trp1-Δ1 his3-Δ200*	This study
hC 346	*MATa cdc13-1ts rad24-2::LEU2* *ura3-52 ade2-101 lys2-801 leu2-Δ1 trp1-Δ1 his3-Δ200*	This study
hC 348	*MATa cdc13-1ts rad24-3::LEU2* *ura3-52 ade2-101 lys2-801 leu2-Δ1 trp1-Δ1 his3-Δ200*	This study
hC 350	*MATa cdc13-1ts rad24-Δ::kanMX2* *ura3-52 ade2-101 lys2-801 leu2-Δ1 trp1-Δ1 his3-Δ200*	This study

hC 351	*MATα cdc13-1ts rad24-Δ::kanMX2 ura3-52 ade2-101 lys2-801 leu2-Δ1 trp1-Δ1 his3-Δ200*	This study
hC 649	*MATα cdc13-1* CF*[a] *ura3-52 ade2-101 lys2-801 leu2-Δ1 trp1-Δ1 his3-Δ200*	This study
hC 654	*MATa cdc13-1 rad24-2*:: LEU2 ura3-52 ade2-101 lys2-801 leu2-Δ1 trp1-Δ1 his3-Δ200*	This study
hC 657	*MATa rad24-2*:: LEU2 ura3-52 ade2-101 lys2-801 leu2-Δ1 trp1-Δ1 his3-Δ200*	This study
hC 658	*MATα ura3-52 ade2-101 lys2-801 leu2-Δ1 trp1-Δ1 his3-Δ200* CF*[a]	This study
hC 770	*MATa RAD24-myc$_{13x}$::HIS3 ura3-52 ade2-101 lys2-801 leu2-Δ1 trp1-Δ1 his3-Δ200*	This study
hC 771	*MATα rad24-2myc$_{13x}$::HIS3 ura3-52 ade2-101 lys2-801 leu2-Δ1 trp1-Δ1 his3-Δ200*	This study
hC 772	*MATa rad24-3myc$_{13x}$::HIS3 ura3-52 ade2-101 lys2-801 leu2-Δ1 trp1-Δ1 his3-Δ200*	This study
hC 1073	*MATα cdc13-1 RAD24-myc$_{13x}$::HIS3 CF*[a] *ura3-52 ade2-101 lys2-801 leu2-Δ1 trp1-Δ1 his3-Δ200*	This study
hC 1074	*MATα cdc13-1 rad24-2myc$_{13x}$::HIS3 CF*[a] *ura3-52 ade2-101 lys2-801 leu2-Δ1 trp1-Δ1 his3-Δ200*	This study
hC 1075	*MATα cdc13-1 rad24-3myc$_{13x}$::HIS3 CF*[a] *ura3-52 ade2-101 lys2-801 leu2-Δ1 trp1-Δ1 his3-Δ200*	This study
hC 1433	*MATa cdc13-1 rad24Δ*::kanMX2 ura3-52 ade2-101 lys2-801 leu2-Δ1 trp1-Δ1 his3-Δ200*	This study
hC 1436	*MATα cdc13-1rad24-2*:: LEU2 ura3-52 ade2-101 lys2-801 leu2-Δ1 trp1-Δ1 his3-Δ200*	This study
hC 1437	*MATa cdc13-1rad24-2**:: LEU2 ura3-52 ade2-101 lys2-801 leu2-Δ1 trp1-Δ1 his3-Δ200*	This study
hC 1438	*MATα cdc13-1rad24-2***:: LEU2 ura3-52 ade2-101 lys2-801 leu2-Δ1 trp1-Δ1 his3-Δ200*	This study
hC 1439	*MATα cdc13-1rad24-2***:: LEU2 ura3-52 ade2-101 lys2-801 leu2-Δ1 trp1-Δ1 his3-Δ200*	This study
hC 1441	*MATα cdc13-1rad24-3*:: LEU2 ura3-52 ade2-101 lys2-801 leu2-Δ1 trp1-Δ1 his3-Δ200*	This study
hC 1506	*MATa rad24Δ R::kanMX2 ade2-1 trp1-1 ura3-1 leu2-3,112 his3-11,15 can1-100*	This study
hC 1507	*MAT α cdc13-1 rad24Δ R::kanMX2 ade2-1 trp1-1 ura3-1 leu2-3,112 his3-11,15 can1-100*	This study
hC 1508	*MATa rad24-2 R:: LEU2 ade2-1 trp1-1 ura3-1 leu2-3,112 his3-11,15 can1-100*	This study
hC 1509	*MAT α cdc13-1 rad24-2 R:: LEU2 ade2-1 trp1-1 ura3-1 leu2-3,112 his3-11,15 can1-100*	This study
hC 1542	*MATa cdc13-1ts rad24-2 R::LEU2 ade2-1 trp1-1 ura3-1 leu2-3,112 his3-11,15 can1-100*	This study

hC 1543	*MATa rad24-2 R::LEU2*	This study
hC 1544	*MATa cdc13-1ts rad24-2 R::LEU2 ade2-1 trp1-1 ura3-1 leu2-3,112 his3-11,15 can1-100*	This study
hC2173	*MATα est2Δ::URA3* type II telomeres *ura3-52 ade2-101 lys2-801 leu2-Δ1 trp1-Δ1 his3-Δ200*	This study
hC2174	*MATa ura3-52 ade2-101 lys2-801 leu2-Δ1 trp1-Δ1 his3-Δ200* / pRS424	This study
hC2175	*MATa cdc13-1ts/* pRS424 *ura3-52 ade2-101 lys2-801 leu2-Δ1 trp1-Δ1 his3-Δ200*	This study
hC2176	*MATa cdc13-1ts rad24-Δ::kanMX2/* pRS424 *ura3-52 ade2-101 lys2-801 leu2-Δ1 trp1-Δ1 his3-Δ200*	This study
hC2177	*MATa cdc13-1ts rad24-Δ::kanMX2/* pWL4 *ura3-52 ade2-101 lys2-801 leu2-Δ1 trp1-Δ1 his3-Δ200*	This study
hC2178	*MATa cdc13-1ts rad24-2::LEU2 /* pRS424 *ura3-52 ade2-101 lys2-801 leu2-Δ1 trp1-Δ1 his3-Δ200*	This study
hC2179	*MATa cdc13-1ts rad24-2::LEU2 /* pWL4 *ura3-52 ade2-101 lys2-801 leu2-Δ1 trp1-Δ1 his3-Δ200*	This study
hC2180	*$_{MATa}$ cdc13-1ts rad24-2 R::LEU2 ura3-52 ade2-101 lys2-801 leu2-Δ1 trp1-Δ1 his3-Δ200*	This study
hC2181	*$_{MATα}$ cdc13-1ts rad24-2 R::LEU2/* pRS424 *ura3-52 ade2-101 lys2-801 leu2-Δ1 trp1-Δ1 his3-Δ200*	This study
hC2182	*MATα cdc13-1ts rad24-2 R::LEU2/* pWL4 *ura3-52 ade2-101 lys2-801 leu2-Δ1 trp1-Δ1 his3-Δ200*	This study

CF[a] : [*ura3:TRP1 SUP11 CEN4 D8B*]; asterisk (*) indicates number of successive backcrosses. Strains marked with an "R" (reconstructed allele) were obtained from diploids dCN 318, dCN 319 and dCN 343.

Table 2-2 Plasmids used in chapter 2

Plasmid	Gene	Reference
Longtine #12	pFA6a-13MycHis3MX6	(Longtine et al., 1998)
pRS424	2μ *TRP1*	T. Weinert
pWL4	*pRS424-$_{NATIVE}$ RAD24*	T. Weinert

Table 2-3 Primers used in chapter 2

Oligo	Sequence	Reference
CO117	TTTCTCGAGTTGTCCTGTCTGAATGATATGGAT	C. Nugent
CO118	TTTCTCGAGCTGCAGATTTCCTGGGGTTTTCTCGT	C. Nugent

CO147	GCGCCAGTTATCAGTGAGTCCCTTTCAGATTCAG ATCTGGAAATACTC CGGATCCCCGGGTTAATTAA	C. Nugent
CO148	AGATTTGTGTGGAATATTTCCTGGGGTTTTCTCGT CAAATTTAAAGAG GAATTCGAGCTCGTTTAAAC	C. Nugent

References

Alcasabas, A., Osborn, A., Bachant, J., Hu, F., Werler, P., Bousset, K., et al. (2001). Mrc1 transduces signals of DNA replication stress to activate Rad53. *Nat Cell Biol, 3*(11), 958-965.

Aylon, Y., & Kupiec, M. (2003). The checkpoint protein Rad24 of *Saccharomyces cerevisiae* is involved in processing double-strand break ends and in recombination partner choice. *Mol Cell Biol, 23*(18), 6585-6596.

Bertuch, A., & Lundblad, V. (2004). *EXO1* contributes to telomere maintenance in both telomerase-proficient and telomerase-deficient *Saccharomyces cerevisiae*. *Genetics, 166*(4), 1651-1659.

Bolderson, E., Tomimatsu, N., Richard, D., Boucher, D., Kumar, R., Pandita, T., et al. (2010). Phosphorylation of Exo1 modulates homologous recombination repair of DNA double-strand breaks. *Nucleic Acids Res, 38*(6), 1821-1831.

Bonetti, D., Martina, M., Clerici, M., Lucchini, G., & Longhese, M. (2009). Multiple pathways regulate 3' overhang generation at *S. cerevisiae* telomeres. *Mol Cell, 35*(1), 70-81.

Booth, C., Griffith, E., Brady, G., & Lydall, D. (2001). Quantitative amplification of single-stranded DNA (QAOS) demonstrates that *cdc13-1* mutants generate ssDNA in a telomere to centromere direction. *Nucleic Acids Res, 29*(21), 4414-4422.

Boulton, S., & Jackson, S. (1998a). Components of the Ku-dependent non-homologous end-joining pathway are involved in telomeric length maintenance and telomeric silencing. *EMBO J, 17*(6), 1819-1828.

Boulton, S., & Jackson, S. (1998b). Components of the Ku-dependent non-homologous end-joining pathway are involved in telomeric length maintenance and telomeric silencing. *EMBO J, 17*(6), 1819-1828.

Budzowska, M., Jaspers, I., Essers, J., de Waard, H., van Drunen, E., Hanada, K., et al. (2004). Mutation of the mouse Rad17 gene leads to embryonic lethality and reveals a role in DNA damage-dependent recombination. *EMBO J, 23*(17), 3548-3558.

Chen, Q., Ijpma, A., & Greider, C. (2001). Two survivor pathways that allow growth in the absence of telomerase are generated by distinct telomere recombination events. *Mol Cell Biol, 21*(5), 1819-1827.

Clerici, M., Mantiero, D., Lucchini, G., & Longhese, M. (2005). The Saccharomyces cerevisiae Sae2 protein promotes resection and bridging of double strand break ends. *J Biol Chem, 280*(46), 38631-38638.

Clerici, M., Mantiero, D., Lucchini, G., & Longhese, M. (2006). The *Saccharomyces cerevisiae* Sae2 protein negatively regulates DNA damage checkpoint signalling. *EMBO Rep, 7*(2), 212-218.

D'Amours D, & SP., J. (2001). The yeast Xrs2 complex functions in S phase checkpoint regulation. *Genes Dev, 15*(17), 2238-2249.
D'Amours, D., & Jackson, S. (2002). The Mre11 complex: at the crossroads of DNA repair and checkpoint signalling. *Nat Rev Mol Cell Biol, 3*(5), 317-327.
Diede, S., & Gottschling, D. (2001). Exonuclease activity is required for sequence addition and Cdc13p loading at a de novo telomere. *Curr Biol, 11*(17), 1336-1340.
Ferreira, M., Miller, K., & Cooper, J. (2004). Indecent exposure: when telomeres become uncapped. *Mol Cell, 13*(1), 7-18.
Fiorentini, P., Huang, K., Tishkoff, D., Kolodner, R., & Symington, L. (1997). Exonuclease I of *Saccharomyces cerevisiae* functions in mitotic recombination in vivo and in vitro. *Mol Cell Biol, 17*(5), 2764-2773.
Foster, S., Zubko, M., Guillard, S., & Lydall, D. (2006). MRX protects telomeric DNA at uncapped telomeres of budding yeast *cdc13-1* mutants. *DNA Repair (Amst), 5*(7), 840-851.
Furuse, M., Nagase, Y., Tsubouchi, H., Murakami-Murofushi, K., Shibata, T., & Ohta, K. (1998). Distinct roles of two separable in vitro activities of yeast Mre11 in mitotic and meiotic recombination. *EMBO J, 17*(21), 6412-6425.
Gao, H., Cervantes, R., Mandell, E., Otero, J., & Lundblad, V. (2007). RPA-like proteins mediate yeast telomere function. *Nat Struct Mol Biol, 14*(3), 208-214.
Garvik, B., Carson, M., & Hartwell, L. (1995). Single-stranded DNA arising at telomeres in cdc13 mutants may constitute a specific signal for the *RAD9* checkpoint. *Mol Cell Biol, 15*(11), 6128-6138.
Grandin, N., & Charbonneau, M. (2003). The Rad51 pathway of telomerase-independent maintenance of telomeres can amplify TG_{1-3} sequences in *yku* and *cdc13* mutants of Saccharomyces cerevisiae. *Mol Cell Biol, 23*(11), 3721-3734.
Grandin, N., Damon, C., & Charbonneau, M. (2001a). Cdc13 prevents telomere uncapping and Rad50-dependent homologous recombination. *EMBO J, 20*(21), 6127-6139.
Grandin, N., Damon, C., & Charbonneau, M. (2001b). Ten1 functions in telomere end protection and length regulation in association with Stn1 and Cdc13. *EMBO J, 20*(5), 1173-1183.
Grandin, N., Reed, S., & Charbonneau, M. (1997). Stn1, a new *Saccharomyces cerevisiae* protein, is implicated in telomere size regulation in association with Cdc13. *Genes Dev, 11*(4), 512-527.
Green, C., Erdjument-Bromage, H., Tempst, P., & Lowndes, N. (2000). A novel Rad24 checkpoint protein complex closely related to replication factor C. *Curr Biol, 10*(1), 39-42.
Grenon, M., Gilbert, C., & Lowndes, N. (2001). Checkpoint activation in response to double-strand breaks requires the Mre11/Rad50/Xrs2 complex. *Nat Cell Biol, 3*(9), 844-847.
Haber, J. (1998). The many interfaces of Mre11. *Cell, 95*(5), 583-586.
Huertas, P., Cortés-Ledesma, F., Sartori, A., Aguilera, A., & Jackson, S. (2008). *CDK* targets Sae2 to control DNA-end resection and homologous recombination. *Nature, 455*(7213), 689-692.

Ira, G., Pellicioli, A., Balijja, A., Wang, X., Fiorani, S., Carotenuto, W., et al. (2004). DNA end resection, homologous recombination and DNA damage checkpoint activation require CDK1. *Nature, 431*(7011), 1011-1017.
Ivanov, E., Sugawara, N., White, C., Fabre, F., & Haber, J. (1994). Mutations in *XRS2* and *RAD50* delay but do not prevent mating-type switching in *Saccharomyces cerevisiae*. *Mol Cell Biol, 14*(5), 3414-3425.
Jia, X., Weinert, T., & Lydall, D. (2004). Mec1 and Rad53 inhibit formation of single-stranded DNA at telomeres of Saccharomyces cerevisiae *cdc13-1* mutants. *Genetics, 166*(2), 753-764.
Kondo, T., Wakayama, T., Naiki, T., Matsumoto, K., & Sugimoto, K. (2001). Recruitment of Mec1 and Ddc1 checkpoint proteins to double-strand breaks through distinct mechanisms. *Science, 294*(5543), 867-870.
Larrivée, M., LeBel, C., & Wellinger, R. (2004). The generation of proper constitutive G-tails on yeast telomeres is dependent on the MRX complex. *Genes Dev, 18*(12), 1391-1396.
Lengsfeld, B., Rattray, A., Bhaskara, V., Ghirlando, R., & Paull, T. (2007). Sae2 is an endonuclease that processes hairpin DNA cooperatively with the Mre11/Rad50/Xrs2 complex. *Mol Cell, 28*(4), 638-651.
Lin, J., & Zakian, V. (1996). The Saccharomyces *CDC13* protein is a single-strand TG_{1-3} telomeric DNA-binding protein in vitro that affects telomere behavior in vivo. *Proc Natl Acad Sci U S A, 93*(24), 13760-13765.
Longtine, M., McKenzie, A.R., Demarini, D., Shah, N., Wach, A., Brachat, A., et al. (1998). Additional modules for versatile and economical PCR-based gene deletion and modification in *Saccharomyces cerevisiae*. *Yeast, 14*(10), 953-961.
Lundblad, V., & Blackburn, E. (1993). An alternative pathway for yeast telomere maintenance rescues *est1-Δ* senescence. *Cell, 73*(2), 347-360.
Lundblad, V., & Szostak, J. (1989). A mutant with a defect in telomere elongation leads to senescence in yeast. *Cell, 57*(4), 633-643.
Lydall, D. (2003). Hiding at the ends of yeast chromosomes: telomeres, nucleases and checkpoint pathways. *J Cell Sci, 116*(20), 4057-4065.
Lydall, D., & Weinert, T. (1995). Yeast checkpoint genes in DNA damage processing: implications for repair and arrest. *Science, 270*(5241), 1488-1491.
Lydall, D., & Weinert, T. (1997). G2/M checkpoint genes of *Saccharomyces cerevisiae*: further evidence for roles in DNA replication and/or repair. *Mol Gen Genet, 256*(6), 638-651.
Majka, J., Chung, B., & Burgers, P. (2004). Requirement for ATP by the DNA damage checkpoint clamp loader. *J Biol Chem, 279*(20), 20921-20926.
Maringele, L., & Lydall, D. (2002). *EXO1*-dependent single-stranded DNA at telomeres activates subsets of DNA damage and spindle checkpoint pathways in budding yeast yku70Delta mutants. *Genes Dev, 16*(15), 1919-1933.
McEachern, M., & Haber, J. (2006). Break-induced replication and recombinational telomere elongation in yeast. *Annu Rev Biochem, 75*, 111-135.
Melo, J., Cohen, J., & Toczyski, D. (2001). Two checkpoint complexes are independently recruited to sites of DNA damage in vivo. *Genes Dev, 15*(21), 2809-2821.

Mimitou, E., & Symington, L. (2008). Sae2, Exo1 and Sgs1 collaborate in DNA double-strand break processing. *Nature, 455*(7214), 770-774.
Mimitou, E., & Symington, L. (2009). DNA end resection: many nucleases make light work. *DNA Repair (Amst), 8*(9), 983-995.
Moore, J., & Haber, J. (1996). Cell cycle and genetic requirements of two pathways of nonhomologous end-joining repair of double-strand breaks in Saccharomyces cerevisiae. *Mol Cell Biol, 16*(5), 2164-2173.
Moreau, S., Ferguson, J., & Symington, L. (1999). The nuclease activity of Mre11 is required for meiosis but not for mating type switching, end joining, or telomere maintenance. *Mol Cell Biol, 19*(1), 556-566.
Moreau, S., Morgan, E., & Symington, L. (2001). Overlapping functions of the Saccharomyces cerevisiae Mre11, Exo1 and Rad27 nucleases in DNA metabolism. *Genetics, 159*(4), 1423-1433.
Murnane, J. P. (2006). Telomeres and chromosome instability. *DNA Repair (Amst), 5*(9-10), 1082-1092.
Naiki, T., Shimomura, T., Kondo, T., Matsumoto, K., & Sugimoto, K. (2000). Rfc5, in cooperation with Rad24, controls DNA damage checkpoints throughout the cell cycle in *Saccharomyces cerevisiae*. *Mol Cell Biol, 20*(16), 5888-5896.
Nakada, D., Hirano, Y., & Sugimoto, K. (2004). Requirement of the Mre11 complex and exonuclease 1 for activation of the Mec1 signaling pathway. *Mol Cell Biol, 24*(22), 10016-10025.
Nakada, D., Matsumoto, K., & Sugimoto, K. (2003). ATM-related Tel1 associates with double-strand breaks through an Xrs2-dependent mechanism. *Genes Dev, 17*(16), 1957-1962.
Negrini, S., Ribaud, V., Bianchi, A., & Shore, D. (2007). DNA breaks are masked by multiple Rap1 binding in yeast: implications for telomere capping and telomerase regulation. *Genes Dev, 21*(3), 292-302.
Nugent, C. I., Hughes, T. R., Lue, N. F., & Lundblad, V. (1996). Cdc13p: a single-strand telomeric DNA-binding protein with a dual role in yeast telomere maintenance. *Science, 274*(5285), 249-252.
Paull, T., & Gellert, M. (1998). The 3' to 5' exonuclease activity of Mre11 facilitates repair of DNA double-strand breaks. *Mol Cell, 1*(7), 969-979.
Pellicioli, A., Lee, S., Lucca, C., Foiani, M., & Haber, J. (2001). Regulation of Saccharomyces Rad53 checkpoint kinase during adaptation from DNA damage-induced G2/M arrest. *Mol Cell, 7*(2), 293-300.
Petreaca, R., Chiu, H., Eckelhoefer, H., Chuang, C., Xu, L., & Nugent, C. (2006). Chromosome end protection plasticity revealed by Stn1p and Ten1p bypass of Cdc13p. *Nat Cell Biol, 8*(7), 748-755.
Petreaca, R., Chiu, H., & Nugent, C. (2007). The role of Stn1p in *Saccharomyces cerevisiae* telomere capping can be separated from its interaction with Cdc13p. *Genetics, 177*(3), 1459-1474.
Sanchez, Y., Bachant, J., Wang, H., Hu, F., Liu, D., Tetzlaff, M., et al. (1999). Control of the DNA damage checkpoint by Chk1 and Rad53 protein kinases through distinct mechanisms. *Science, 286*(5442), 1166-1171.

Small, V., Chuang, C., & Nugent, C. (2008). Rad24 truncation, coupled with altered telomere structure, promotes cdc13-1 suppression in *S. cerevisiae*. *Cell Cycle, 7*(21), 3428-3439.
Teng, S., & Zakian, V. (1999). Telomere-telomere recombination is an efficient bypass pathway for telomere maintenance in *Saccharomyces cerevisiae*. *Mol Cell Biol, 19*(12), 8083-8093.
Tsubouchi, H., & Ogawa, H. (1998). A novel mre11 mutation impairs processing of double-strand breaks of DNA during both mitosis and meiosis. *Mol Cell Biol, 18*(1), 260-268.
Tsubouchi, H., & Ogawa, H. (2000). Exo1 roles for repair of DNA double-strand breaks and meiotic crossing over in Saccharomyces cerevisiae. *Mol Biol Cell, 11*(7), 2221-2233.
Venclovas, C., Colvin, M., & Thelen, M. (2002). Molecular modeling-based analysis of interactions in the RFC-dependent clamp-loading process. *Protein Sci, 11*(10), 2403-2416.
Vodenicharov, M., & Wellinger, R. (2006). DNA degradation at unprotected telomeres in yeast is regulated by the *CDK1* (Cdc28/Clb) cell-cycle kinase. *Mol Cell, 24*(1), 127-137.
Vodenicharov, M., & Wellinger, R. (2007). The cell division cycle puts up with unprotected telomeres: cell cycle regulated telomere uncapping as a means to achieve telomere homeostasis. *Cell Cycle, 6*(10), 1161-1167.
Weinert, T., & Hartwell, L. (1993). Cell cycle arrest of cdc mutants and specificity of the RAD9 checkpoint. *Genetics, 134*(1), 63-80.
Weinert, T., Kiser, G., & Hartwell, L. (1994). Mitotic checkpoint genes in budding yeast and the dependence of mitosis on DNA replication and repair. *Genes Dev, 8*(6), 652-665.
Wellinger, R., Wolf, A., & Zakian, V. (1993). Saccharomyces telomeres acquire single-strand TG_{1-3} tails late in S phase. *Cell, 72*(1), 51-60.
Zhu, Z., Chung, W., Shim, E., Lee, S., & Ira, G. (2008). Sgs1 helicase and two nucleases Dna2 and Exo1 resect DNA double-strand break ends. *Cell, 134*(6), 981-994.
Zubko, M., Guillard, S., & Lydall, D. (2004). Exo1 and Rad24 differentially regulate generation of ssDNA at telomeres of Saccharomyces cerevisiae *cdc13-1* mutants. *Genetics, 168*(1), 103-115.
Zubko, M., & Lydall, D. (2006). Linear chromosome maintenance in the absence of essential telomere-capping proteins. *Nat Cell Biol, 8*(7), 734-740.

Chapter 3

Functional Analysis of Cdc13 Phosphorylation in Budding Yeast

Introduction

Throughout most of the cell cycle, telomeres are maintained in a capped conformation that prevents chromosome end fusions, inappropriate recombination, and degradation. However, during DNA replication of the chromosome end the conformation of telomeres must transiently open to allow the replication machinery and telomerase to access the two parental DNA strands to copy the DNA and subsequently reestablish the telomere cap after replication is completed (de Bruin et al., 2001, Loayza and de Lange, 2004). The structure at the telomere formed by telomeric DNA sequences and the associated proteins are likely to be regulated in order to respond to changes that occur as cells progress through the cell cycle. Exactly how activities at the telomere are controlled through the cell cycle at the molecular level is not yet not completely understood.

In *S. cerevisiae*, Cdc13 binds single-stranded telomeric DNA (ssDNA) and functions in both telomere end protection and regulating telomerase activity (Chandra, et al., 2001, Lin and Zakian, 1996, Nugent, et al., 1996). Cdc13 is required for chromosome end protection only in proliferating cells, and not when cells are blocked in G_1 phase (Vodenicharov and Wellinger, 2006). Accordingly, Cdc13 association with telomeres varies through the cell cycle, with a peak in telomere association during late S phase, corresponding to a time when telomeres are undergoing DNA replication (Chan, et al., 2008, Diede and Gottschling, 1999, Marcand, et al., 2000, Taggart, et al., 2002). Cdc13 recruits telomerase to the telomere through association with Est1 (Chan, et al., 2008, Evans and Lundblad, 1999, Taggart, et al., 2002). Est1 association with telomeres is cell cycle regulated, with a peak association also occurring in late S phase through G2 phase

(Osterhage, et al., 2006, Taggart, et al., 2002). Previous studies have shown that telomere elongation by telomerase is restricted to late S to G2 phases as well (Diede and Gottschling, 1999, Marcand, et al., 2000). The time when telomere elongation occurs correlates with the binding of Est1 and Cdc13 in late S and G2 phase, suggesting that the assembly of a active telomerase complex at the telomeres is restricted to late S to G2 phases of the cell cycle (Taggart, et al., 2002). Interestingly, phosphorylated forms of Cdc13 were observed during late S phase, accumulating until anaphase and in cells arrested with nocodozole at G2/M phase (C. Nugent, data not shown). This phosphorylation event of Cdc13 correlates with the time that telomerase is active at the telomere (Diede and Gottschling, 1999, Marcand, et al., 2000, Vodenicharov and Wellinger, 2006). These correlations suggest that Cdc13 phosphorylation may be functionally significant with respect to Cdc13 association at the telomere, or recruitment of telomerase to the telomere.

Cdc13 contains several putative phosphorylation sites that could be targeted by kinases *in vivo*. Initial experiments conducted by Dr. Nugent to identify the kinase responsible for Cdc13 phosphorylation ruled out several known kinases. The phosphorylation shift of Cdc13 did not appear to be dependent on the kinase activity of *MEC1, TEL1,* and *RAD53*, as the presence of the Cdc13 phosphorylation shift was not affected in these mutant backgrounds (C. Nugent, data not shown). One kinase that remained a potential candidate is the major regulator of the cell cycle, Cdk1 (also called Cdc28). Cdk1 associates with various cyclins to control cell cycle progression by phosphorylating various protein substrates (Ubersax et al., 2003). The CDK family of

kinases has a preference for phosphorylation of serine in SP motifs or threonine in TP motifs (Ubersax, et al., 2003). Seven of these motifs were identified in Cdc13. Cdc13 contains one full Cdk1 consensus phosphorylation site (S/T*-P-x-K/R) at T308, and six additional minimal Cdk1 consensus phosphorylation sites (T*/P or S*/P) located throughout the protein at S110, S336, S460, S650, S708 and S711 (Figure 3-1a). Cdc13 also contains a Mec1/Tel1 consensus site at S306, and it was previously reported that Cdc13 was phosphorylated by Mec1 at this site (Tseng, et al., 2006, Tseng, et al., 2009) (Figure 3-1a). Interestingly, Cdk1 activity has been implicated in the processing of telomeric DNA. In budding yeast, the G-rich overhang to which Cdc13 binds is short (about 13 bases) throughout most of the cell cycle but becomes longer (more than 30 nucleotides) around late S to G2 phases (Dionne and Wellinger, 1996, Larrivée, et al., 2004, Wellinger, et al., 1993). It has been demonstrated that Cdk1 is required for the generation of this extended 3' single-strand overhang (Frank, et al., 2006, Vodenicharov and Wellinger, 2006). Given the correlation between increased Cdc13 binding in late S-phase and the requirement for Cdk1 to generate longer 3' single-strand overhangs during late S to G2 phases, it is possible that Cdk1 may be involved in regulating Cdc13's activities at the telomere. Thus, we were interested in whether Cdc13 may be directly phosphorylated by Cdk1 at one or more of the phosphorylation sites located within Cdc13.

Here, the hypothesis that Cdk1 is responsible for phosphorylation of Cdc13, and that this phosphorylation is relevant to how Cdc13 functions in telomere maintenance is investigated. The functional relevance of the Cdc13 phosphorylation was studied through

identification of *in vivo* phosphorylation sites and phenotypic analysis of telomeres in yeast strains containing mutations at the phosphorylation sites. In this study, we demonstrate that Cdc13 is a substrate of the Cdk1 kinase. Cdc13 is phosphorylated at threonine 308 in the telomerase recruitment domain and is a direct substrate for Cdk1 as demonstrated by an *in vitro* kinase assay. Phosphorylation defective mutants were shown to have slightly shortened telomere lengths. Therefore, we suggest that Cdk1 phosphorylation of Cdc13 promotes telomere elongation by telomerase.

Materials and Methods

Yeast manipulations

Standard techniques were followed in handling the yeast strains. Genotypes of yeast strains used in this study are listed in Table 3-1. Plasmids used in this study are listed in Table 3-2. All yeast strains were cultured according to standard laboratory protocols in YPD media (2% glucose, 1% yeast extract, 2% peptone) or selective synthetic complete media (2% glucose, 1% yeast nitrogen base, supplemented with all amino acids except those which were being selected for).

Plasmid Construction

Plasmids used in this study are listed in Table 3-2. To produce *GST-cdc13*^{T308A} (pCN470), the pCN335 plasmid (p*cdc13*$_{18x}$*myc*-^{T308A}) was digested with XhoI and SacII to release a 2301bp fragment containing the T308A mutation. Next, pPC19 (*GST-CDC13*) was digested with XhoI and SacII and the 6925bp fragment released from this restriction digest was ligated to the 2301bp fragment from the pCN335 digest using T4

Quick Ligase (New England Biolabs). To produce *pAS1-cdc13*$^{1\text{-}450\ T308A}$ (pCN473), plasmid pCN335 (p*cdc13*$_{18x}$*myc*-^{T308A}) was digested with BsmI and MluI, which released a 518bp fragment containing the T308A mutation. pVL587 (*pAS1-CDC13*$^{1\text{-}450}$) was digested with BsmI and MluI and the 7894bp fragment released from this restriction digest was ligated to the 518bp fragment from the pCN335 digest using T4 Quick Ligase (New England Biolabs) A similar strategy was used to create pCN474 (*pAS1-cdc13*$^{1\text{-}450\ S306A\ T308A}$). pCN339 (p*cdc13*$_{18x}$*myc*-^{T308A}) was digested with BsmI and MluI and the 518bp fragment released containing both the S308A and T308A mutations was ligated to the 7894bp fragment released from the BsmI and MluI restriction digest of pVL587 (*pAS1-CDC13*$^{1\text{-}450}$).

Site-directed mutagenesis

Site-directed mutagenesis was performed using the Quickchange Site-directed mutagenesis Kit to create *cdc13*^{T308A} mutation (Stratagene, La Jolla CA). Plasmid pVL1086 was mutated with mutagenic primer CO191 to yield pCN335 (T308A). Plasmid pVL1086 was mutated with CO195 to yield pCN339 (S306A T308A). Primers used in this study are listed in Table 3-3. PCR reaction conditions were 95˚C for 3 min, 30 cycles of 95˚C for 1 min, 55˚C for 1 min and 68˚C for 6 min, followed by 68˚C for 20 min. PCR products were digested with Dpn1 to remove the parental DNA before being transformed into XL10-Gold ultra competent cells (Stratagene). These *cdc13* mutants were constructed and verified by Holly Eckelhoefer.

To generate the T711A mutation, plasmid pVL1086 was mutated using mutagenic primers CO406 and CO407 and Phusion high-fidelity DNA polymerase (New England

Biolabs) to create pCN461. The *cdc13*$^{S306A\ T308A\ T711A}$ triple mutant was created using mutagenic primers CO406 and CO407 on pCN339 to yield pCN468. The mutagenic primers used are presented in Table 3-3. PCR reaction conditions were 94˚C for 3 min, 16 cycles of 94˚C for 1 min, 45˚C for 1 min and 68˚C for 16 min, followed by 68˚C for 1 hour. PCR products were digested with Dpn1 to remove the parental DNA before being transformed into chemically competent DH5α cells. Mutations were verified by restriction digests and sequencing.

Phosphorylation Shift

A 50ml culture of each strain with an O.D. 600 of .6 to .8 was arrested with 50 µl of a 1mg/ml stock of nocodazole. Cells were then grown at 30°C to allow for G2/M arrest. After 3 hours, cells were pelleted at 3,000g for 5 mins. Cell pellets were resuspended in 300 µl 20% TCA supplemented with protease inhibitors (leupeptin, aprotinin, benzamidine, PMSF, and pepstatin) and phosphatase inhibitors (NaF and NaV). Cells were lysed by Biospec mini-bead beater with 5 times of 1 minute-beating. 2 minute incubation on ice was performed between each beating. Lysates were transferred to new tubes by poking hole in the screw-cap tube and briefly spinning into new tubes. Lysates were pelleted by 2 minute spinning at 12,000g in a cold centrifuge, and the TCA supernatant was removed. The pellet was resuspended in 100 µl 1M Tris base, and 100 µl Buffer A with protease inhibitors. 100 µl of 20% SDS and 60 µl 6x Laemmli Sample buffer were added to each sample. 75 µl of each sample was heated for 5 minutes at 95°C, pelleted and was separated on a 6% 30:0.39 acrylamide/ bisacrylamide gel. After

transfer, Western blots were probed with a 9E10 α-myc antibody (Covance). A wild-type strain (hC160) was used as the negative control.

GST Fusion Protein Expression

GST-CDC13 (pPC19), *GST-cdc13T308A* (pCN470), or *GST* (pPC20) plasmid were transformed into BL21 *E.coli* cells. 5 ml cultures of cells carrying each plasmid were grown at 37˚C overnight and inoculated into 50 ml fresh LB medium next day. After O.D. reached 0.3-0.4, cells were switched to 16˚C. GST and GST-Cdc13p expression was induced by 1mM IPTG (Fisher Scientific, Tustin, CA) for 8 hours. Bacterial cells were pelleted in cold centrifuge at 3000g for 30 minutes. Pelleted cells were resuspended in 1.5 ml lysis buffer (50 mM potassium phosphate, pH7.8, 400 mM NaCl, 100 mM KCl, 10% glycerol, 0.5% Triton X-100 and 10 mM imidazole) and frozen (-80˚C) and thawed (37˚C) for three times. Samples were then sonicated 12 seconds for three times with a 2 minute incubation on ice between each sonication. After sonication, samples were pelleted in the cold centrifuge at 12,000g for 20 minutes. 1ml of protein supernatants was incubated with 25 µl Glutathione Sepharose 4B beads (Amersham) at 4°C for 30 min in LSBT buffer with protease inhibitors to purify GST proteins.

***in vitro* Kinase Assay**

To obtain Cdk1/Clb2-HA complexes, 50 ml cultures of Clb2-HA cells (JBY12) were arrested with nocodozole for 3 hours, and pelleted at 3000g for 5 minutes. Cells were resuspended in 500 µl buffer A (25 mM HEPES at pH 7.5, 5 mM $MgCl_2$, 50 mM KCl, 10% glycerol and 1% Triton-X) supplemented with protease inhibitors (leupeptin, aprotinin, benzamidine, PMSF, and pepstatin). Samples were transferred to 2 ml screw-

cap tube with 500 µl glass beads and lysed with a mini-bead beater (Biospec Products, Bartlesville, OK) by 6 times of 1 minute-beating. Each sample was incubated for two minutes on ice between each beating. Triton X-100 was added into the supernatant to the final concentration of 0.5%. Lysates were transferred to new tubes by poking hole in the screw-cap tube and briefly spinning into new tubes. Lysates were clarified by spinning for two minutes at 12,000g in a cold centrifuge. Crude extracts were transferred into new tubes and quantified using Bradford assay (Bio-Rad, Hercules, CA). Samples containing 1mg of Clb2-HA protein extract, was incubated with 4µl of anti-HA (12CA5; Roche, Indianapolis, IN) at 4°C for 2 hours in 1 ml LBST buffer (20 mM HEPES–NaOH at pH 7.9, 100 mM NaCl, 2.5 mM $MgCl_2$, 0.1 mM EDTA, 0.05% NP-40 and 0.2% Triton X-100) with protease inhibitors. 40 µl Protein A/G beads (Santa Cruz Biotechnology) were added and incubated at 4°C for two hours. Beads were washed in LSBT buffer and resuspended in 40µl of cold Kinase Buffer (20mM Tris pH 7.5, 7.5mM $MgCl_2$).

GST fusion proteins immobilized to GST beads were washed once with LSBT buffer. GST pull-down products were then incubated at 37°C for 1 hour with 20µl of the Clb2-HA IP bead-resuspension described above, 1µl 4mM ATP and 1µl γ-^{32}-P ATP (Perkin Elmer). 1µg histone H1 (New England Biolabs) was used as Cdk1 substrate as a positive control. Reactions were stopped by addition of 8µl of 6x LSB. Kinase reactions were separated on a 10% SDS-PAGE gels and then analyzed by Western Blotting probed with anti-GST (Amersham, Piscataway, NJ) before being exposed to a phosphoimager screen for five days (Typhoon Imager).

Viability Testing

To plate dilutions of yeast cells, serial ten-fold dilutions of cell cultures were performed in microtiter dishes, "stamped" onto solid media, and grown at the appropriate temperatures. To create strains with Cdc13 phosphorylation defective alleles, a *cdc13-Δ::kanMX2 (hC1238)* strain carrying p*CDC13* (pVL438) marked with *URA3* was transformed individually with p*cdc13*^{T308A} (pCN335), p*cdc13* $^{S306A\ T308A}$ (pCN339), p*cdc13*^{T711A} (pCN460), or p*cdc13* $^{S306A\ T308A\ T711A}$ (pCN468) plasmids marked with *LEU2*. Transformed cells were then struck out onto 5-FOA media to shuffle out complementing *CDC13* plasmid. 5 ml cultures of each strain were grown in –Leu media for 3 days. Serial ten-fold dilutions were made of each strain in a 96-well plate, and stamped onto -Leu plates. Plates were incubated at the indicated temperature for 3-5 days.

Southern Blotting

Genomic DNA was prepared as previously described (Lundblad and Szostak, 1989) from a *cdc13-Δ::kanMX2/*p*CDC13 (hC1238), cdc13-Δ::kanMX2/*p*cdc13*^{T308A} *(hC1233), cdc13-Δ::kanMX2/* p*cdc13* $^{S306A\ T308A}$ (*hC1245*), *cdc13-Δ::kanMX2/* p*cdc13*^{T711A} *(hC1937),* or *cdc13-Δ::kanMX2/* p*cdc13* $^{S306A\ T308A\ T711A}$ *(hC1936)* strain. XhoI digested DNA was electrophoresed through 0.8% agarose gel and transferred to nylon membrane (Hybond XL, Amersham, Piscataway, NJ). The membranes were probed with poly dGT/CA, which was labeled with ^{32}P using the Megaprime DNA labeling kit to detect telomere fragments (Amersham, Piscataway, NJ). The blots were then washed and exposed to X-ray film.

Two-hybrid Assay

pJ694A strain (*MATa trp1 leu2 ura3 his3 gal4Δ gal80Δ LYS2::GAL1-HIS3 GAL2-ADE2 met2::GAL7-lacZ)* was used in two hybrid system. This strain uses three reporter genes to test protein interaction (James et al., 1996). Strains transformed with either p*CDC13*$^{1\text{-}481}$ (pVL587), p*CDC13* $^{1\text{-}481\ T308A}$ (pCN473), or p*CDC13* $^{1\text{-}481\ S306AT308A}$ (pCN474) and *BMH1* (pVL1389) were propagated on selective media lacking leucine and tryptophan. Cultures were grown in 5 ml -leu -trp media for 3 days, then 10-fold serial dilutions were stamped onto -leu -trp, -leu -trp -ade, and -leu -trp -his plates supplemented with 1 mM of 3-aminotriazole (3-AT), to analyze reporters. Plates were incubated at 30˚C for 3 days. The parallel experiment was performed in the positive control, strains transformed with p*TOP2* (pMN2) and p*SGS1* $^{434\text{-}792}$ (pMN4) (Watt, et al., 1995).

Results

Cdc13 phosphorylation is dependent upon Cdk1 consensus sites in vivo

Once it was determined that Cdc13 was phosphorylated, we wanted to examine which sites were targeted by the kinase. Our hypothesis was that one or more of the Cdk1 consensus phosphorylation sites in Cdc13 were targeted *in vivo* (Figure 3-1a). To determine if the Cdc13 electrophoretic mobility shift is the result of phosphorylation of Cdc13 at one or more of the Cdk1 consensus sites, we generated Myc-tagged *CDC13* alleles on plasmids with the phosphorylation sites mutated. Using site-directed mutagenesis, we mutated the threonines and serines in the Cdk1p consensus phosphorylation sites to non-phosphorylatable alanine residues. SDS-PAGE and Western blot analysis were used to analyze the various *cdc13* mutant proteins. A mutation in the full Cdk1 consensus site at threonine 308 was generated by Holly Eckelhoefer prior to my working on the project. The T308A mutation was also combined with a S306A mutation at the Mec1/Tel1 consensus site to remove any potential contribution to the mobility shift due to a phosphorylation event at the S306 site. I generated two additional mutant alleles at the minimal Cdk1 consensus sites located near the Cdc13 DNA binding domain at S708 and T711 once I started working on the project. These sites were chosen first because they were adjacent to the region of Cdc13 that makes contact with telomeric DNA. The phosphorylation site mutant plasmids were separately transformed into a *cdc13Δ::LYS2*/ p*CDC13-URA3* (hC1238) strain. In yeast, growth of cells expressing *URA3* is inhibited in the presence of the drug 5-Fluoroorotic acid, (5FOA). Therefore, transformed yeast strains were struck onto plates containing 5FOA to select for loss of

the wild-type *CDC13* complementing plasmid. These transformants were grown then to log phase in -Leu media to select for the mutant plasmids. Compared to cells transformed with a wild type *CDC13-18xmyc* plasmid, p*cdc13*^{T308A}*18xmyc* transformants showed a loss of the electrophoretic mobility shift on Western blots (Figure 3-1b). Individual S708A and T711A mutations generated at the minimal phosphorylation sites had no effect on the Cdc13 phosphorylation shift. Proper resolution of Cdc13 phosphorylated species proved technically difficult, but we consistently saw loss of the Cdc13 phosphorylation only when the T308A mutation was present. This result suggests that the threonine residue 308 is phosphorylated *in vivo* and contributes to the Cdc13 phosphorylation shift we observed.

CDK1 phosphorylates GST-Cdc13 in vitro

The abolishment of the Cdc13 electrophoretic mobility shift in the T308A mutant suggested that Cdc13 was phosphorylated at this site by Cdk1 *in vivo*. However, it was not clear whether Cdc13 was a direct substrate for Cdk1 kinase activity. To determine whether Cdc13 is a direct substrate of Cdk1, we tested whether Cdk1 could phosphorylate Cdc13 by conducting an *in vitro* kinase assay. We used purified recombinant GST-Cdc13 from *E. coli* as a substrate for Cdk1 in our kinase assays (Figure 3-2a). GST-Cdc13 and GST-Cdc13^{T308A} was induced in BL21 *E. coli* cells with 200mM IPTG for 8 hours to obtain sufficient levels of Cdc13 protein for use in our kinase assays (Figure 3-2a). The GST-Cdc13 and GST-Cdc13^{T308A} protein produced was purified from bacterial lysate by incubation with GST beads. In order to obtain Cdk1 activity, we purified Cdk1 protein from yeast extracts. Active Cdk1 associates with the regulatory

cyclin, Clb2, during G2/M (Miller and Cross, 2001). We used an epitope tagged version of Clb2 to purify Cdk1 activity from yeast extracts. Clb2-HA yeast cells were arrested in G_2/M with nocodazole, the time during the cell cycle where Cdk1-Clb2 complexes are most abundant (Miller and Cross, 2001). Cdk1-Clb2-HA complexes were immunoprecipitated with an anti-HA antibody from protein extracts of these cells and incubated under *in vitro* kinase conditions in the presence of γ-^{32}-P ATP and GST-Cdc13, GST-Cdc13^{T308A}, GST or histone H2A (Figure 3-2b). The reactions were subjected to SDS–PAGE and autoradiography (Figure 3-2b). GST-Cdc13 was robustly phosphorylated by Cdk1-Clb2, whereas neither GST alone nor GST-Cdc13^{T308A} proteins showed any detectable phosphorylation by Cdk1. These data indicate that Cdc13 is indeed a direct substrate of Cdk1 *in vitro* and the phosphorylation of Cdc13 by Cdk1 is abolished if threonine 308 is mutated. Taken together, we conclude that Cdk1 phosphorylates Cdc13 at T308 *in vivo*.

cdc13^{T308A} mutants retain normal cell viability

If the *in vivo* function of the Cdk1-mediated Cdc13 phosphorylation is to regulate recruitment of telomerase then it is possible that mutants defective for this phosphorylation would exhibit a phenotype similar to, but not as severe as, a telomerase-deficient strain. To test the hypothesis that the Cdk1 phosphorylation of Cdc13 is involved in regulating Cdc13's activities at the telomere, we first analyzed whether mutations in these phosphorylation sites would affect the growth of yeast strains. To identify a growth phenotype associated with the p*cdc13^{T308A}18xmyc* allele we tested whether this plasmid could complement a *CDC13* null mutant, *cdc13Δ::LYS2*.

cdc13Δ::LYS2/ p*CDC13-URA3* (hC1238) cells were transformed with p*CDC1318xmyc -LEU2* or p*cdc13*^{T308A}*18xmyc -LEU2*. In addition, two different mutant alleles were transformed and analyzed for a change in cell viability phenotype: a Cdc13$^{S306A\ T308A}$ mutant in which both the Mec1 and Cdk1 consensus sites are mutated to non-phosphorylatable alanines (p*cdc13*$^{S306A\ T308A}$ *18xmyc*), and a Cdc13$^{S306A\ T308A\ T711A}$ mutant where the Mec1 and Cdk1 consensus sites plus a minimal consensus site near the DNA binding domain are mutated (p*cdc13*$^{S306A\ T308A\ T711A}$*18xmyc*). These mutants were used to assess whether a decrease in cell viability phenotype would be observed when several potential phosphorylation sites are removed. Telomerase-deficient cells usually senesce after approximately 50-100 generations (Lundblad and Blackburn, 1993). Yeast cells transformed with the mutant plasmids were grown on plates containing 5FOA to select for loss of the wild-type *CDC13* complementing plasmid. Colonies that arose on 5FOA were grown in liquid –Leu media. Each passage of a single yeast colony allows for approximately 25 generations (Lundblad and Blackburn, 1993). Although we did not do successive streakouts of single colonies in this experiment, we estimate that the cells would have likely gone through ~30-35 generations, enough to start to display a senescent phenotype. 10-fold serial dilutions of these strains were stamped onto -Leu selective plates to maintain selection for the transformed plasmid. p*cdc13*^{T308A}*18xmyc* was able to fully complement the *CDC13* null mutation, suggesting that the *cdc13*^{T308A} allele does not confer a senescent phenotype (Figure 3-3). Cdc13$^{S306A\ T308A}$ and Cdc13$^{S306A\ T308A\ T711A}$ mutants also did not display any change in viability (Figure 3-3). Therefore, although the T308 residue is necessary for the phosphorylation mobility shift

observed on Western blots, mutation of this phosphorylation site does not result in reduced viability with continued propagation that would be suggestive of senescence.

Cdc13 phosphorylation is not needed in the absence of Ku

The yKu70/80 heterodimer has been shown to bind telomeres *in vivo* and to make contributions to maintaining both telomere integrity and telomere length that are distinct from Cdc13. In the absence of yKu70 or yKu80 function, telomeres are significantly shorter than wild-type telomeres (Boulton and Jackson, 1996, Porter, et al., 1996), and terminate with long single-stranded G-tails (Gravel, et al., 1998, Polotnianka, et al., 1998). yKu80 has also been shown to interact with the telomerase RNA subunit, *TLC1*, and mutations in either *TLC1* (*tlc1Δ48*) or *yKU80* (*yku80-135i*) that disrupt this interaction eliminate Est2 association with the telomere in G1 and early S phase (Chan, et al., 2008, Fisher, et al., 2004, Peterson et al., 2001, Stellwagen, et al., 2003). It has been shown that the binding of Est2 to the telomere is eliminated when both the yKu80-Tlc1 and the Cdc13-Est1 recruitment pathways are abolished (Chan, et al., 2008). Taken together, these data suggest that yKu70/80 functions in regulating telomere length by promoting telomerase recruitment in a manner independent of Cdc13. Importantly, strains that lack either telomerase or Cdc13-capping function are lethal when combined with *yku70*Δ or *yku80*Δ (Nugent, et al., 1998), providing a way to test whether mutations in *cdc13* affect either its roles in telomere length or integrity.

If the Cdk1-mediated phosphorylation of Cdc13 is required for telomerase recruitment, then it possible that telomere recruitment defects in *yku80Δ* cells would be further compromised when the *cdc13*^{T308A} allele is combined with the *yku80Δ* mutation,

potentially causing a senescent-like phenotype. Here, we examined whether the cell viability of *yku80Δ* mutants would be exacerbated by loss of the Cdk1-mediated phosphorylation on Cdc13. In this experiment, *yku80Δ cdc13Δ/ pCDC13* double mutants were transformed with *LEU2*-marked plasmids encoding Cdc13myc, Cdc13myc^{T308A}, and Cdc13myc $^{S306A\ T308A}$. Transformed yeast cells were grown in liquid –Leu media to maintain the transformed plasmid, and 10-fold serial dilutions of these cultures were stamped onto -Leu selective plates (Figure 3-4a) and onto –Leu 5FOA plates to select for loss of the wild-type *CDC13* complementing plasmid (Figure 3-4b). Neither the *cdc13*^{T308A} or *cdc13* $^{S306A\ T308A}$ mutations reduced cell viability of the *yku80Δ* strain, as the viability of the *cdc13* mutant alleles was similar to wild-type cells (Figure 3-4b). These results suggest that loss of the Cdk1-mediated phosphorylation on T308 in Cdc13 in combination with *yku80* does not result in reduced cell viability that would be suggestive of a senescent phenotype.

Loss of Cdc13 phosphorylation causes modest telomere shortening

The *cdc13-2* allele is thought to specifically affect the telomerase recruitment function of Cdc13 since telomerase association with the telomere was reduced in *cdc13-2* mutants (Chan, et al., 2008). Cells containing the *cdc13-2* mutation exhibit a telomere replication defect and senescent phenotype similar to that of a strain that is deficient for telomerase, indicating a role for Cdc13 in positively regulating telomere length (Nugent, et al., 1996). To test the hypothesis that Cdk1-mediated Cdc13 phosphorylation was involved in telomerase recruitment, we assessed whether telomere length was reduced in the *cdc13*^{T308A} mutant by performing Southern blot analysis. A *cdc13Δ::LYS2* (hC1238)

haploid yeast strain carrying a *URA3* marked *CDC13* plasmid was transformed with a plasmid encoding either *CDC13-18xmyc* or *cdc13^{T308A}18xmyc*. In addition, three different mutant alleles were transformed and analyzed for a telomere length phenotype: a Cdc13 ^{T711A} mutant (p*cdc13^{T711A}18xmyc*), in which one of the minimal Cdk1 consensus site near the DNA binding domain is mutated, a Cdc13$^{S306A\ T308A}$ mutant in which both the Mec1 and Cdk1 consensus sites are mutated (p*cdc13$^{S306\ T308A}$ 18xmyc*), and a Cdc13$^{S306A\ T308A\ T711A}$ mutant where the Mec1 and Cdk1 consensus sites plus the minimal consensus site were mutated. These mutants were used to assess whether a more severe telomere length phenotype would be observed when several potential phosphorylation sites are removed. Again, transformed strains were grown on plates containing 5FOA to select for loss of the wild-type *CDC13* complementing plasmid. The telomere length of cultures inoculated from individual colonies was measured after successive streak-outs, corresponding to approximately 25, 50, 75, and 100 generations.

Southern blot hybridization using a telomere probe showed that the single mutation at residue T308 to A was sufficient to cause telomere shortening compared to wild-type cells (Figure 3-5, compare *CDC13* lane to *T308A* lanes). The *cdc13^{T308A}* mutation resulted in telomere shortening of approximately 60 $\pm$ 20 bp. This telomere shortening had largely taken place by 25 generations following loss of *CDC13* plasmid, and telomeres do not become progressively shorter with increasing generations. Moreover, the S306A T308A mutation conferred shorter telomeres as well, similar to the short telomere lengths observed in T308A cells (Figure 3-5, compare S306A T308A with T308A lanes). The telomeres in *cdc13 $^{S306A\ T308A\ T711A}$* cells maintained telomere lengths

similar to wild-type length (Figure 3-5, compare S306A T308A T711A with wild-type lanes). The T711A mutation alone did not affect telomere length, as telomeres from *cdc13*^{T711A} mutants were similar in length to wild-type telomeres (Figure 3-5, compare *CDC13* lane to *T711A* lanes). Since the *cdc13*^{T308A} mutation results in telomere length reduction *in vivo*, this suggests that the Cdk1-mediated phosphorylation at threonine 308 in Cdc13 may be necessary for normal telomere length regulation.

Cdc13 interaction with the 14-3-3 protein, Bmh1, is phosphorylation dependent

Previously a yeast two-hybrid assay using the N-terminus of Cdc13 (Cdc13$^{1-450}$) was conducted to identify new Cdc13 binding partners (C. Nugent). The portion of Cdc13 used as bait in the screen contained the major Cdk1 phosphorylation site at T308. The 14-3-3 protein, Bmh1, was found to interact weakly with Cdc13 (Figure 3-6). Budding yeast contain two 14-3-3 proteins, Bmh1 and Bmh2, which specifically bind to proteins involved in cell signaling, metabolism, and cell cycle regulation in a phosphorylation-dependent manner (Bruckmann et al., 2007, Kakiuchi et al., 2007). To further investigate the molecular function of Cdc13 phosphorylation, a yeast two hybrid assay was used to determine whether the interaction with Bmh1 was phosphorylation dependent. Consistent with observations by Dr. Nugent, the Cdc13$^{1-450}$ interaction with Bmh1 can activate all three two hybrid reporters (Figure 3-6). We observe an interaction between pAS and Bmh1, suggesting that there was background activation of the reporters in this assay. However, when the *cdc13*^{T308A} or the *cdc13*$^{S306A\ T308A}$ mutant was used as bait, the observed Bmh1 interaction was abolished, suggesting that the Cdc13-Bmh1 interaction is dependent on Cdc13 phosphorylation by Cdk1.

Discussion

In an effort to determine the functional relevance of Cdc13 phosphorylation, we sought to pinpoint the major Cdc13 phosphorylation site *in vivo*. We also wanted to identify the kinase responsible for this phosphorylation event. Lastly, we attempt to characterize any apparent phenotypes present in the phosphorylation defective mutants. We demonstrate that Cdc13 is phosphorylated by Cdk1 *in vivo* and the major phosphorylation site is threonine 308. The T308 site is within the defined telomerase recruitment domain of Cdc13 (Pennock et al., 2001). We have observed the phosphorylation to be cell-cycle dependent (C. Nugent, data not shown), which occurs during late S to G2/M phase of the cell cycle. Consistent with our results, two other groups observed that Cdc13 is phosphorylated in late S and Cdk1 mediates phosphorylation in a cell-cycle dependent manner (Li et al., 2009, Tseng, et al., 2009). Coincidentally, this window in the cell cycle corresponds to the time in which the telomerase complex is recruited to telomeres (Taggart et al., 2002, Chan et al., 2008).

Previous studies of Cdc13 phosphorylation demonstrated that Cdc13 was phosphorylated by Mec1/Tel1 at serine 306 (Tseng, et al., 2006). This site was a major phosphorylation site for both the Mec1 and Tel1 kinase, as a S306A mutation abolished *in vitro* phosphorylation (Tseng, et al., 2006, Tseng, et al., 2009). This particular modification of Cdc13 was hard to resolve with traditional SDS-PAGE, and was instead analyzed using 2D gel electrophoresis (Tseng, et al., 2006). Consistent with this, we did not observe any change in the electrophoretic shift of Cdc13 when this S306 phosphorylation site was mutated in our lab. It has been proposed that the negative

charges provided by the Mec1/Tel1 and Cdk1 phosphorylation events together provide an optimal surface for Est1 interaction, however this has never been actually shown (Tseng, et al., 2009). Although the need for both Mec1/Tel1 and Cdk1 phosphorylation events together have not been shown to be required for Cdc13-Est1 interaction, Tel1 has been shown to be necessary for normal amounts of Est1 and Est2 at telomeres, suggesting that Tel1 may function in the recruitment of telomerase complex to telomeres (Goudsouzian, et al., 2006).

Given that Cdc13 is phosphorylated at threonine 308 *in vivo*, we thought that this phosphorylation may be needed for some aspect of Cdc13's function in telomerase recruitment to the telomere. If this Cdk1-mediated phosphorylation was essential for maintaining telomere length or integrity, then perhaps we would observe decreased viability in our *cdc13*^{T308A} mutant, however this was not the case. Combining the T308A nonphosphorylatable mutation with a serine 306 to alanine mutation at the proposed Mec1 phosphorylation site or the threonine T711 to A near the DNA binding domain also did not reduce cell viability. In addition, the *cdc13*^{T308A} did not appear to exarcerbate the defects in *yku80Δ* cells, since *yku80Δ cdc13*^{T308A} double mutants maintain normal growth. Consistent with these findings, it was shown that combining the *cdc13*^{T308A} mutation with *yku80Δ* did not result in additive or synergistic telomere shortening (Li, et al., 2009). Taken together, we conclude that Cdc13's function in telomerase recruitment is not completely disrupted by loss of the Cdk1- dependent phosphorylation at threonine 308.

Analysis of telomere length in the phosphorylation defective T308A mutant revealed that these cells undergo modest telomere shortening. This reduction in telomere

length suggests that the phosphorylation of Cdc13 may be important in the telomerase recruitment. In addition, we find that the telomeres in *cdc13* $^{S306A\ T308A\ T711A}$ cells maintained telomere lengths similar to wild-type length, suggesting that the T711A mutation may rescue the telomere shortening. It is possible that the phosphorylation at T711 affects negative regulation of telomerase, although in an otherwise wild-type strain, it appears that this mutation is not sufficient to lead to telomere elongation. The *cdc13-5* allele is a truncation that eliminates the portion of Cdc13 that interacts with Stn1, and has been shown to result in telomere lengthening. The telomere elongation in *cdc13-5* mutants is proposed to be due to loss of the Cdc13-Stn1 interaction, which provides negative regulation on telomerase (Chandra, et al., 2001). It is possible that the phosphorylation on T711 may promote the interaction with Stn1. The Blackburn lab published data suggesting that the role of Cdc13 T308 phosphorylation is to regulate the recruitment of the telomerase complex to telomeres by competing with the Stn1-Ten1 complex during telomere elongation (Li, et al., 2009). It is possible that the phosphorylation on T711 may promote the interaction with Stn1, thereby providing negative regulation on telomerase. Accordingly, the Blackburn lab published data suggesting that the role of Cdc13 phosphorylation is to regulate the recruitment of the telomerase complex to telomeres by competing with the Stn1-Ten1 complex during telomere elongation (Li, et al., 2009). It would be interesting to test the model that two different phosphorylation events are involved in the proposed toggling of Cdc13 interactions with Est1 and Stn1. It is possible that different phosphorylation events could be involved in the model suggested by the Blackburn lab, with phosphorylastion at T308

affecting Est1 association and phosphorylation at T711 affecting Stn1 association. Thus, it would be good to test impact of the T711A mutation on the Cdc13-Stn1 interaction. In addition, it is not known whether Cdk1 is the kinase responsible for T711 phosphorylation or if both the T308 and T711 sites are phosphorylated sequentially. Hence, further characterization of the phosphorylation at T711 would be of interest.

Telomere elongation in the *de novo* telomere addition assay developed by Diede and Gottschling requires a functional telomerase (Diede and Gottschling, 1999). *De novo* telomere addition also requires the interaction between Cdc13 and Est1, since *cdc13-2* cells are deficient in telomere elongation (Diede and Gottschling, 1999). Although we found that $cdc13^{T308A}$ mutants have shorter telomeres, it has been reported that $cdc13^{T308A}$ mutants can still perform *de novo* telomere addition despite loss of the phosphorylation at T308, suggesting that the Est1 present at the telomere in the T308A mutant is sufficient for telomerase recruitment (Li, et al., 2009, Tseng, et al., 2009). The ability of the $cdc13^{S306A\ T308A}$ to perform *de novo* telomere addition has not been tested and it would be of interest to determine if this mutant is deficient for telomere addition. If the $cdc13^{S306A\ T308A}$ mutant would not be able to perform *de novo* telomere addition, then this would support the idea that both the Mec1/Tel1 and Cdk1 phosphorylation events together provide an optimal surface for Est1 interaction.

Lastly, we found that loss of Cdc13 phosphorylation affected its interaction with the 14-3-3 protein, Bmh1. Previous studies using genomics and proteomics approaches found that Bmh1 is involved with the post-transcriptional regulation of several *S. cerevisiae* proteins. These studies suggest a role for Bmh1 binding in protein synthesis

and degradation (Bruckmann, et al., 2007, Bruckmann, et al., 2004). Cdc13 phosphorylation has also been implicated in regulating Cdc13 protein stability, since *cdc13*^{T308A} cells treated with cycloheximide (to turn off the protein translation of Cdc13) maintained a longer protein half life relative to wild-type or *cdc13*^{T308D} strains (Tseng, et al., 2009). In addition, there was an increase in the levels of the Cdc13^{T308A} protein even without cycloheximide treatment at a nocodozole arrest, suggesting that the Cdc13 protein is maintained in a cell cycle-dependent manner (Tseng, et al., 2009). Cdc13 protein has been previously shown to be degraded rapidly (Vodenicharov and Wellinger, 2006). Thus, it is possible Cdc13 phosphorylation could regulate protein stability, with the interaction between Cdc13 and Bmh1 reducing the stability of Cdc13.

The *bmh1Δ* mutation was identified as a genetic suppressor of the temperature sensitive *cdc13-1* allele and allowed growth of *cdc13-1* cells up to 27.5°C (Downey et al., 2006). The *cdc13-1* allele has been shown to decrease Cdc13 protein stability (Gardner, et al., 2005). This suppression of *cdc13-1* by *bmh1Δ* is consistent with the idea that Bmh1 may decrease the protein stability of Cdc13. It is possible that the Cdc13-Bmh1 phosphorylation dependent interaction plays a role in telomere length regulation. Hence, it would be of interest to determine the effect (if any) that a *bmh1Δ* mutation would have on telomere length in the *cdc13*^{T308A} mutant. The *bmh1Δ* alone does not change telomere length (Grandin and Charbonneau, 2008). However, if Bmh1 is directly involved in Cdc13 protein degradation, then it is possible that the *bmh1Δ* mutation could restore the short telomeres in *cdc13*^{T308A} cells to wildtype length.

Our data that the Cdc13-Bmh1 interaction is dependent on Cdc13 phosphorylation suggests that there may be a biological significance for Cdc13- Bmh1 interaction, rather than the relatively weak interaction being a false positive in the yeast two-hybrid assay. Although the phosphorylation mimetic *cdc13*^{T308D} was not tested in the yeast two hybrid assay, it is unlikely that this change would restore interaction with Bmh1, since replacement of threonine 308 with aspartic acid or with glutamic acid to provide a negative charge similar to phosphorylation failed to rescue the telomere shortening phenotype (Li, et al., 2009, C. Nugent, unpublished observations). This was taken to mean that the phosphorylation itself, rather than the negative charge associated with the phosphorylation event, was important for Cdc13 function. It is possible that this would be the case for the phosphorylation-dependent interaction between Cdc13 and Bmh1. Future work should be aimed at elucidating the exact molecular mechanisms by which the Cdc13 association with Bmh1 (potentially at the telomere) is controlled throughout the cell cycle.

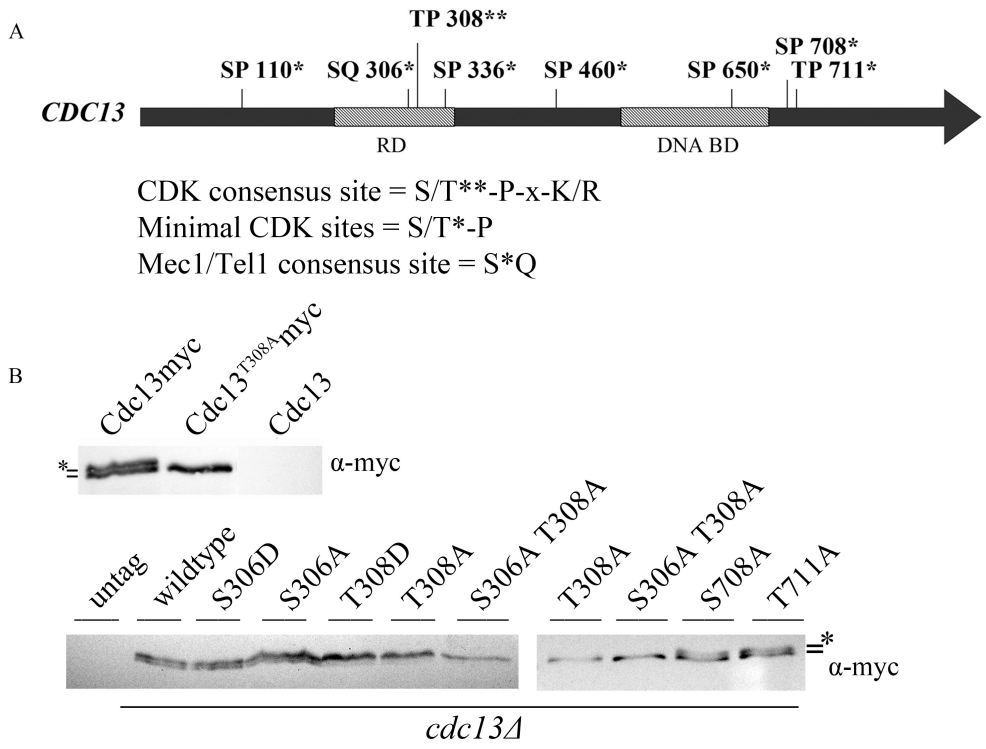

Figure 3-1 Cdc13 phosphorylation is dependent upon Cdk1 consensus sites in vivo. A. Schematic diagram of Cdc13 illustrates its domain structure and potential serine or threonine (S/T) phosphorylation sites. The telomerase recruitment domain (RD) which includes amino acids 190-340 and DNA-binding domain (DBD) which spans amino acids 557-694 are shown. B. T308A is the major phosphorylation site of Cdc13. Cdc13myc and Cdc13 phosphorylation site mutants were at G2/M with nocodozole for 3 hours. Cells were lysed in 20% TCA, separated on 6% 30:0.39 acrylamide/ bisacrylamide SDS–PAGE and analyzed by Western blot analysis using with α-myc antibody. Hyper-phosphorylated Cdc13 are marked with an asterisk. T308A mutation is sufficient to abolish Cdc13 electrophoretic mobility shift. The data in the top of panel B provided by Holly Eckelhoefer. The data in the bottom of panel B shows data from two independent experiments. Bottom left panel shows 6 minute exposure to film and bottom right panel shows 4 minute film exposure. Strains: *CDC13* (hC160), *cdc13Δ::LYS2/ pCDC13myc* (hC1238), *cdc13Δ::LYS2/ pcdc13^{S306D}myc* (hC1240), *cdc13Δ::LYS2/ pcdc13^{S306A}myc* (hC1239), *cdc13Δ::LYS2/ pcdc13^{T7308D}myc* (hC1236), *cdc13Δ::LYS2/ pcdc13^{T308A}myc* (hC1233), *cdc13Δ::LYS2/ pcdc13$^{S306A\ T308A}$ myc* (hC1245), *cdc13Δ::LYS2/ pcdc13^{S708A}*myc (hC1238 transformed with *pcdc13^{S708A}* (pCN460), *cdc13Δ::LYS2/ pcdc13^{T711A}myc* (hC1937).

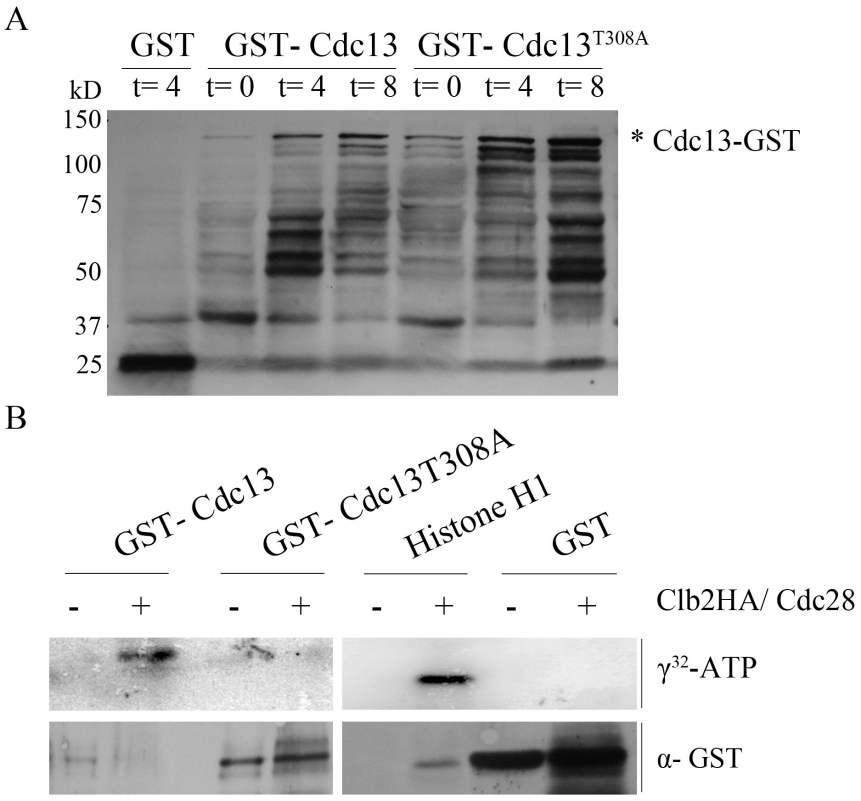

Figure 3-2 Cdc13 is phosphorylated by Cdk1 in vitro.
Cdk1 phosphorylates GST-Cdc13 in vitro. A. IPTG induction of GST (pPC20), GST-CDC13 (pPC19), GST-Cdc13^{T308A} (pCN470) from BL21 cells. Strains were induced with IPTG for 4 or 8 hours and 50µl of each sample was separated on 10% SDS-PAGE and analyzed by Western blot with α-GST antibody. GST proteins were detected by α-HA antibody after exposure to film for 4 minutes. B. Cdk1-mediated phosphorylation of GST-Cdc13 in vitro. Clb2-HA3 strain (JBY12) was arrested with nocodazole and Cdk1/Clb2-HA3 complexes were immunoprecipitated from protein extracts using an α-HA antibody (12CA5). 1ml of GST-Cdc13, GST-Cdc13T308A and GST protein produced after an 8 hour induction in BL21 cells were purified by pull-down with 25µl GST beads. GST-Cdc13, GST-Cdc13T308A or GST pull-down products, were then incubated at 37°C for 1 hour with 20µl of Clb2-HA IP, 1µl 4mM ATP and 1µl γ-^{32}-P ATP protein. These kinase reactions were analyzed on 10% SDS–PAGE and western blotted with α- GST antibody. Phosphorylated proteins were detected by autoradiography after exposure to phosphoimager screen. Cdk1 substrate histone H1 was used a positive control. Top panels: Autoradiograph after a 5 day exposure. Bottom panels: α- GST Western Blot showing the amount of substrate proteins that went into the assay. Bottom left panel shows 6 minute exposure to film and bottom right panel shows 2 minute film exposure.

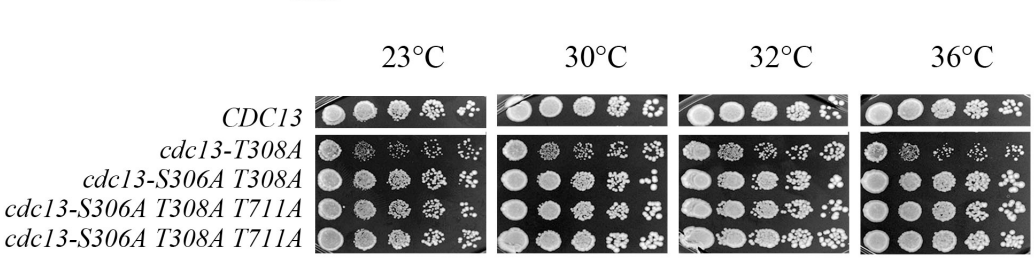

Figure 3-3 Viability of *cdc13* mutant strains compared at different temperatures. Phosphorylation consensus site mutants retain normal viability. Cultures were grown to saturation in –Leu media at 23°C and used to prepare tenfold serial dilutions which were stamped onto-Leu plates, and incubated at indicated temperatures for three to five days. Strains: *cdc13Δ::LYS2/ pCDC13* (hC1238), *cdc13Δ::LYS2/ pcdc13* ^{T308A} (hC1233), *cdc13Δ::LYS2/ pcdc13* $^{S306A\ T308A}$ (hC1245), *cdc13Δ::LYS2/ pcdc13* $^{S306A\ T308A\ T711A}$ (hC1936).

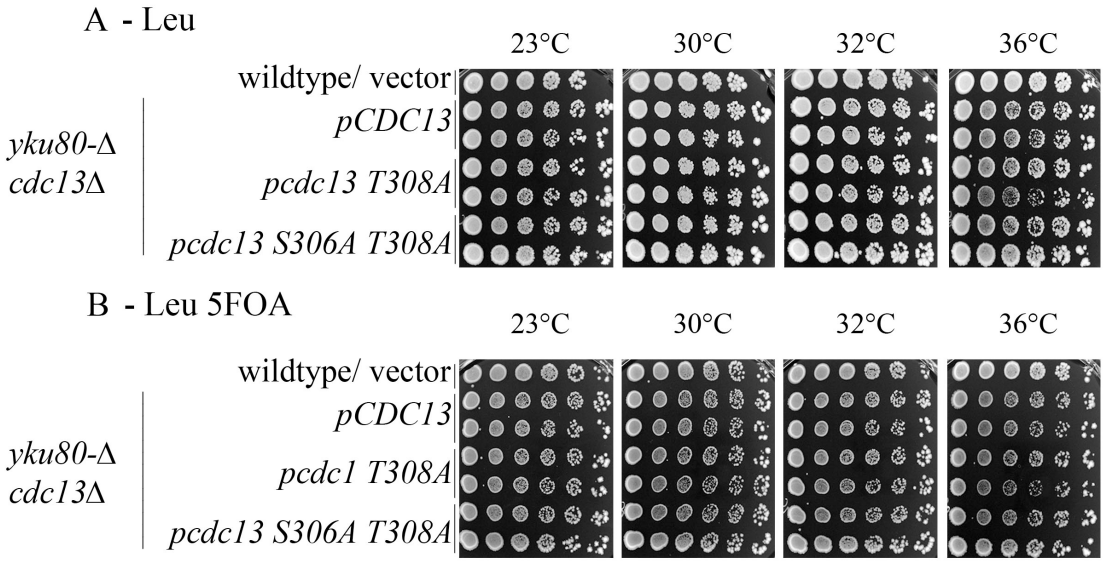

Figure 3-4 *cdc13* ^{T308A} does not decrease cell viability of *yku80Δ* mutants. *cdc13* phosphorylation mutants combined with *yku80Δ* retain normal viability at different temperatures. Cultures were grown to saturation in –Leu media at 23°C and used to prepare tenfold serial dilutions which were stamped onto -Leu plates, and incubated at indicated temperatures for three to five days. B. Strains used in A were stamped onto –Leu 5FOA plates to select for loss of the complementing *CDC13* plasmid. Strain: *yku80Δ cdc13Δ/pCDC13* (hC1165) was transformed with *pCDC13* (pVL1086), *pcdc13* ^{T308A} (pCN335), and *pcdc13* $^{S306A\ T308A}$ (pCN339). Wild-type was transformed with a -Leu vector plasmid (pRS415).

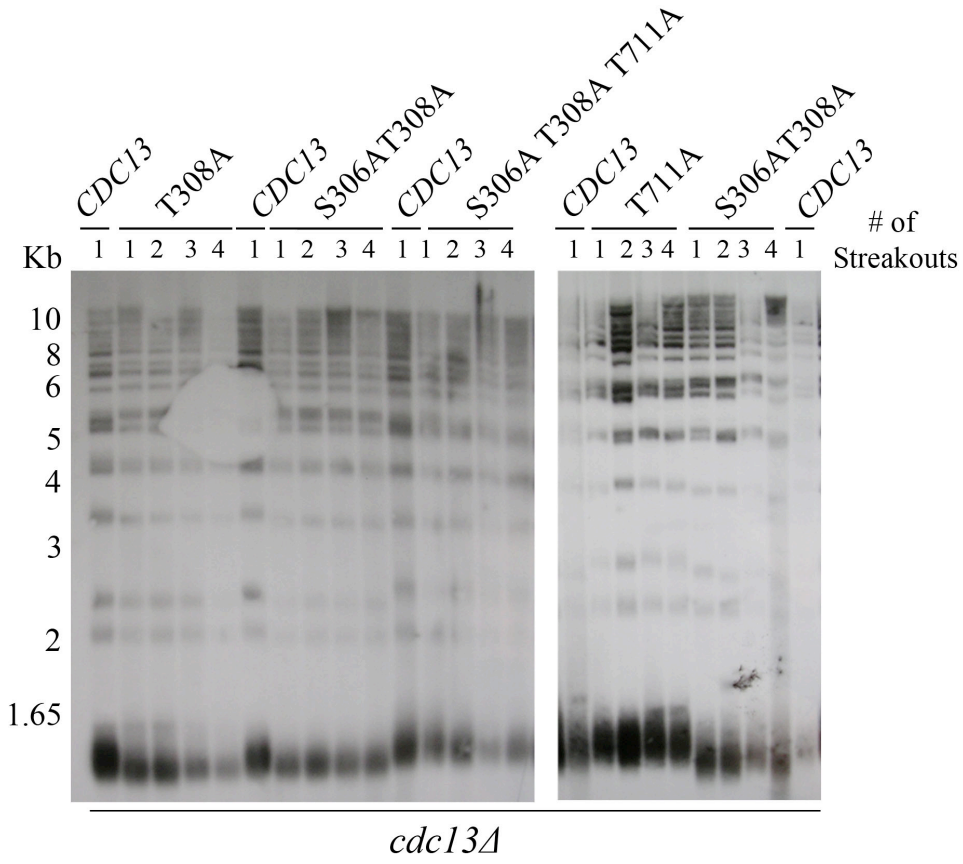

Figure 3-5 Loss of Cdc13 phosphorylation causes modest telomere shortening. Southern blot analysis comparing telomere restriction fragments from Cdc13 phosphorylation site mutant strains grown at 23°C. Yeast strains were struck out from single colonies after loss of *CDC13* complementing plasmid four successive times corresponding to approximately 25, 50, 75, and 100 generations. The blots shown are from two independent experiments and both blots were exposed to film for 1 day. Genomic DNA was prepared from the indicated yeast strains, digested with XhoI, fractionated through 1% agarose, transferred to a nylon membrane, hybridized with a [32P]-TG $_{1\text{-}3}$ probe, and exposed on film. Strains: *cdc13Δ::LYS2/ pCDC13* (hC1238), *cdc13Δ::LYS2/ pcdc13* ^{T308A} (hC1233), *cdc13Δ::LYS2/ pcdc13* $^{S306A\ T308A}$ (hC1245), *cdc13Δ::LYS2/ pcdc13*$^{S306A\ T308A\ T711A}$ (hC1936), *cdc13Δ::LYS2/ pcdc13* ^{T711A} (hC1937).

Figure 3-6 The interaction between Cdc13 and the 14-3-3 protein, Bmh1, is phosphorylation dependent. Yeast two-hybrid analysis demonstrates that the 14-3-3 protein, Bmh1 interacted with $Cdc13^{1-450}$ but not with the phosphorylation defective $Cdc13^{1-450\ T308A}$ or $Cdc13^{1-450\ S306A\ T308A}$ mutants. Bmh1 is fused to the Gal4 activation domain (AD) and expressed from the pACT2 vector. Cdc13 wild-type and phosphorylation mutants are fused to the Gal4 DNA-binding domain and expressed from pAS1 vectors. All fusions are under the control of the ADH1 promoter. A. Ten-fold serial dilutions of each strain were plated onto media selecting for the two plasmids (-Leu -Trp) or for the two-hybrid interaction (-Leu –Trp -Ade) or (-Leu –Trp –His+ 3AT). B. Extracts were produced from strains shown in panel A expressing $Cdc13^{1-450}$, $Cdc13^{1-450\ T308A}$ or $Cdc13^{1-450\ S306A\ T308A}$ and either the pAct2.2 vector alone or Bmh1. Data are the average of five independent β -galactosidase measurements from 5 different colonies tested. Error bars indicate standard deviation. Yeast two-hybrid reporter strain (PJ694a) was transformed with combinations of the following plasmids: pAS1 (Gal4 Binding Domain, GBD), pAct2.2 (Gal4 Activation Domain, GAD), pMN2 ($Sgs1^{434-792}$-GBD), pMN4 (Top2-GAD), pVL587 ($Cdc13^{1-450}$-GBD), pCN473 ($Cdc13^{1-450\ T308A}$-GBD), pCN474 ($Cdc13^{1-450\ S306A\ T308A}$ -GBD), pVL1389 (Bmh1-GAD).

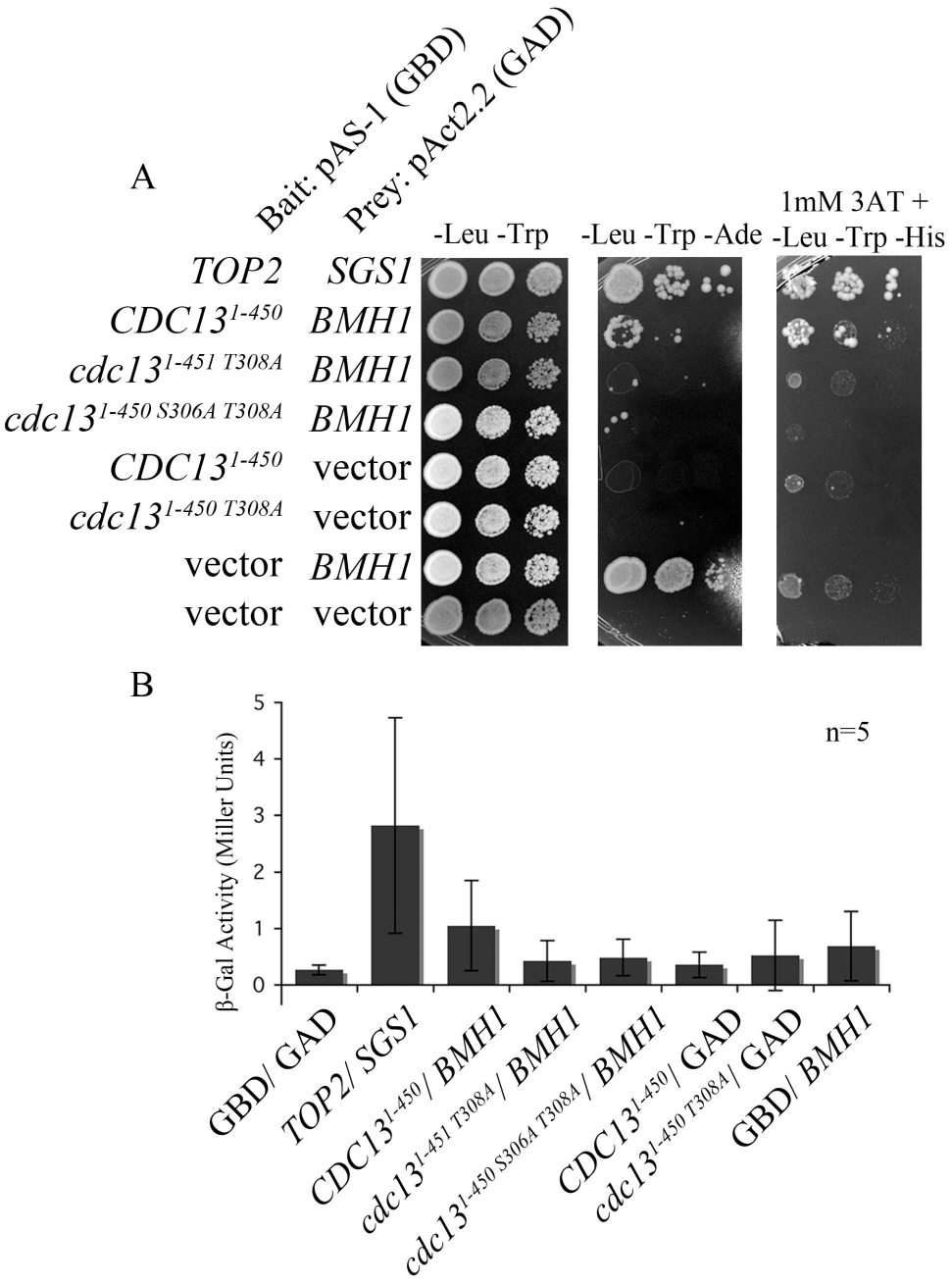
A
Bait: pAS-1 (GBD)
Prey: pAct2.2 (GAD)
-Leu -Trp
-Leu -Trp -Ade
1mM 3AT +
-Leu -Trp -His
TOP2 SGS1
CDC13 1-450 BMH1
cdc13 1-451 T308A BMH1
cdc13 1-450 S306A T308A BMH1
CDC13 1-450 vector
cdc13 1-450 T308A vector
vector BMH1
vector vector
B
β-Gal Activity (Miller Units)
n=5
0
1
2
3
4
5
GBD/ GAD
TOP2/ SGS1
CDC13 1-450/ BMH1
cdc13 1-451 T308A/ BMH1
cdc13 1-450 S306A T308A/ BMH1
CDC13 1-450/ GAD
cdc13 1-450 T308A/ GAD
GBD/ BMH1

Table 3-1 Yeast Strains used in chapter 3

Strain	Relevant Genotype	Reference
hC 1	*MATa cdc13-Δ::LYS2 / pVL438 (CDC13) ura3-52 ade2-101 lys2-801 leu2-Δ1 trp1-Δ1 his3-Δ200*	Nugent Lab
hC 5	*MATa CDC1318xmyc::HIS3 ura3-52 ade2-101 lys2-801 leu2-Δ1 trp1-Δ1 his3-Δ200*	Nugent Lab
hC 160	*MATa ura3-52 ade2-101 lys2-801 leu2-Δ1 trp1-Δ1 his3-Δ200*	Nugent Lab
hC 1165	*MATa yku80Δ::KANMX cdc13-Δ::LYS2/pVL438 (CDC13) ura3-52 ade2-101 lys2-801 leu2-Δ1 trp1-Δ1 his3-Δ200*	Nugent Lab
hC 1233	*MATa cdc13-Δ::LYS2 / pCN335 (cdc13^{T308A}) ura3-52 ade2-101 lys2-801 leu2-Δ1 trp1-Δ1 his3-Δ200*	HAE This study
hC 1236	*MATa cdc13-Δ::LYS2 / pCN336 (cdc13^{T308D}) ura3-52 ade2-101 lys2-801 leu2-Δ1 trp1-Δ1 his3-Δ200*	HAE This study
hC 1239	*MATα cdc13-Δ::LYS2 / pCN337 (cdc13^{S306A}) ura3-52 ade2-101 lys2-801 leu2-Δ1 trp1-Δ1 his3-Δ200*	HAE This study
hC 1238	*MATa cdc13-Δ::LYS2 / pVL438 ura3-52 ade2-101 lys2-801 leu2-Δ1 trp1-Δ1 his3-Δ200*	HAE This study
hC 1240	*MATα cdc13-Δ::LYS2 / pCN338 (cdc13^{S306D}) ura3-52 ade2-101 lys2-801 leu2-Δ1 trp1-Δ1 his3-Δ200*	HAE This study
hC 1245	*MATa cdc13-Δ::LYS2 / pCN339 (cdc13$^{S306A\ T308A}$) ura3-52 ade2-101 lys2-801 leu2-Δ1 trp1-Δ1 his3-Δ200*	HAE This study
hC 1936	*MATa cdc13-Δ::LYS2 / pCN475 (cdc13$^{S306A\ T308A\ T711A}$) ura3-52 ade2-101 lys2-801 leu2-Δ1 trp1-Δ1 his3-Δ200*	VS This study
hC 1937	*MATa cdc13-Δ::LYS2 / pCN461(cdc13^{T711A}) ura3-52 ade2-101 lys2-801 leu2-Δ1 trp1-Δ1 his3-Δ200*	VS This study
JBY12	*MATa CLB2:HA3 ade2-1 trp1-1 ura3-1 leu2-3,112 his3-11,15 can1-100*	Bachant lab
PJ694a	*trp1-901 leu2-3,112 ura3-52 his3-200 gal4Δ gal80Δ LYS2::GAL1-HIS3 GAL2-ADE2 met2::GAL7-lacZ*	James et.al Genetics, 1996

Table 3-2 Plasmids used in chapter 3

Plasmid	Gene	Reference
pVL438	*YCplac33-$_{NATIVE}$CDC13*	Lundblad
pVL587	*pAS1-$_{ADH}$ CDC13$^{1-451}$*	Nugent
pVL1086	*pRS415-$_{NATIVE}$CDC13myc18x*	Nugent
pVL1389	*pACT2.2-$_{ADH}$BMH1*	Nugent

pCN335	pRS415-$_{NATIVE}$ cdc13^{T308A} myc18x	HAE
pCN336	*pRS415-$_{NATIVE}$ cdc13^{T308D} myc18x*	HAE
pCN337	pRS415-$_{NATIVE}$ cdc13^{S306A} myc18x	HAE
pCN338	*pRS415-$_{NATIVE}$ cdc13^{S306D} myc18x*	HAE
pCN339	*pRS415-$_{NATIVE}$ cdc13$^{S306A\ T308A}$ myc18x*	HAE
pCN460	*pRS415-$_{NATIVE}$ cdc13^{S708A} myc18x*	VS
pCN461	pRS415-$_{NATIVE}$ cdc13^{T711A} myc18x	VS
pCN468	*pRS415-$_{NATIVE}$ cdc13$^{S306A\ T308A\ T711A}$ myc18x*	VS
pCN470	*pET101/D-TOPO–GST- cdc13^{T308A}*	VS
pCN473	pAS1-$_{ADH}$ CDC13$^{1\text{-}450\ T308A}$	VS
pCN474	pAS1-$_{ADH}$ CDC13$^{1\text{-}450\ S306A\ T308A}$	VS
pPC19	*pET101/D-TOPO–GST-CDC13*	Nugent Lab
pPC20	*pET101/D-TOPO–GST*	Petreaca et al.
pMN2	pAS1-$_{ADH}$ TOP2	Bachant Lab
pMN4	*p pACT2.2-$_{ADH}$SGS1$^{434\text{-}792}$*	Bachant Lab

Table 3-3 Primers used in chapter 3

Oligo	Sequence	Reference
CO191	CCTACATCCAGTCACAGGCGCCTGAAAGGAAAA CAAGC	HAE
CO192	AAATCCTACATCCAGTCACAGGATCCTGAAAGG AAAACAAGCGTAC	HAE
CO193	TCAAAATCCTACATCCAGGCCCAGACACCTGAA AGGAAAA	HAE
CO194	AGCTCAAAATCCTACATCCAGGACCAGACACCT GAAAGGAAAACAA	HAE

CO195	CAAAATCCTACATCCAGGCCCAGGCGCCTGAAAGGAAAACAAGC	HAE
CO215	GAATTTAAATGAATGGCC	HAE
CO217	ATGGCAAGGAAAGACCCCC	HAE
CO404	AAAAAGGCGCCCACTACACCAGCTC	VS
CO405	AGTGGGCGCCTTTTTTGGTTCATGC	VS
CO406	CCACGGCGCCAGCTCTCGCAGAAC	VS
CO407	CTGGCGCCGTGGGTGATTTTTTTG	VS

References

Bertuch, A., & Lundblad, V. (2003). Which end: dissecting Ku's function at telomeres and double-strand breaks. *Genes Dev, 17*(19), 2347-2350.

Boulton, S., & Jackson, S. (1996). Identification of a *Saccharomyces cerevisiae* Ku80 homologue: roles in DNA double strand break rejoining and in telomeric maintenance. *Nucleic Acids Res, 24*(23), 4639-4648.

Bruckmann, A., Hensbergen, P., Balog, C., Deelder, A., de Steensma, H., & van Heusden, G. (2007). Post-transcriptional control of the *Saccharomyces cerevisiae* proteome by 14-3-3 proteins. *J Proteome Res, 6*(5), 1689-1699.

Bruckmann, A., Steensma, H., Teixeira De Mattos, M., & Van Heusden, G. (2004). Regulation of transcription by *Saccharomyces cerevisiae* 14-3-3 proteins. *Biochem J, 382*(Pt 3), 867-875.

Chan, A., Boulé, J., & Zakian, V. (2008). Two pathways recruit telomerase to *Saccharomyces cerevisiae* telomeres. *PLoS Genet, 4*(10), e1000236.

Chandra, A., Hughes, T., Nugent, C., & Lundblad, V. (2001). Cdc13 both positively and negatively regulates telomere replication. *Genes Dev, 15*(4), 404-414.

de Bruin, D., Zaman, Z., Liberatore, R., & Ptashne, M. (2001). Telomere looping permits gene activation by a downstream UAS in yeast. *Nature, 409*(6816), 109-113.

Diede, S. J., & Gottschling, D. E. (1999). Telomerase-mediated telomere addition in vivo requires DNA primase and DNA polymerases alpha and delta. *Cell, 99*(7), 723-733.

Dionne, I., & Wellinger, R. (1996). Cell cycle-regulated generation of single-stranded G-rich DNA in the absence of telomerase. *Proc Natl Acad Sci U S A, 93*(24), 13902-13907.

Downey, M., Houlsworth, R., Maringele, L., Rollie, A., Brehme, M., Galicia, S., et al. (2006). A genome-wide screen identifies the evolutionarily conserved KEOPS complex as a telomere regulator. *Cell, 124*(6), 1155-1168.

Evans, S., & Lundblad, V. (1999). Est1 and Cdc13 as comediators of telomerase access. *Science, 286*(5437), 117-120.

Fisher, T., Taggart, A., & Zakian, V. (2004). Cell cycle-dependent regulation of yeast telomerase by Ku. *Nat Struct Mol Biol, 11*(12), 1198-1205.

Frank, C., Hyde, M., & Greider, C. (2006). Regulation of telomere elongation by the cyclin-dependent kinase *CDK1*. *Mol Cell, 24*(3), 423-432.

Gardner, R., Nelson, Z., & Gottschling, D. (2005). Degradation-mediated protein quality control in the nucleus. *Cell, 120*(6), 803-815.

Goudsouzian, L., Tuzon, C., & Zakian, V. (2006). *S. cerevisiae* Tel1p and Mre11p are required for normal levels of Est1p and Est2p telomere association. *Mol Cell, 24*(4), 603-610.

Grandin, N., & Charbonneau, M. (2008). Budding yeast 14-3-3 proteins contribute to the robustness of the DNA damage and spindle checkpoints. *Cell Cycle, 7*(17), 2749-2761.

Gravel, S., Larrivée, M., Labrecque, P., & Wellinger, R. (1998). Yeast Ku as a regulator of chromosomal DNA end structure. *Science, 280*(5364), 741-744.

James, P., Halladay, J., & Craig, E. (1996). Genomic libraries and a host strain designed for highly efficient two-hybrid selection in yeast. *Genetics, 144*(4), 1425-1436.

Kakiuchi, K., Yamauchi, Y., Taoka, M., Iwago, M., Fujita, T., Ito, T., et al. (2007). Proteomic analysis of in vivo 14-3-3 interactions in the yeast *Saccharomyces cerevisiae*. *Biochemistry, 46*(26), 7781-7792.
Larrivée, M., LeBel, C., & Wellinger, R. (2004). The generation of proper constitutive G-tails on yeast telomeres is dependent on the MRX complex. *Genes Dev, 18*(12), 1391-1396.
Li, S., Makovets, S., Matsuguchi, T., Blethrow, J., Shokat, K., & Blackburn, E. (2009). Cdk1-dependent phosphorylation of Cdc13 coordinates telomere elongation during cell-cycle progression. *Cell, 136*(1), 50-61.
Lin, J., & Zakian, V. (1996). The Saccharomyces *CDC13* protein is a single-strand TG1-3 telomeric DNA-binding protein in vitro that affects telomere behavior in vivo. *Proc Natl Acad Sci U S A, 93*(24), 13760-13765.
Loayza, D., & de Lange, T. (2004). Telomerase regulation at the telomere: a binary switch. *Cell, 117*(3), 279-280.
Lundblad, V., & Szostak, J. W. (1989). A mutant with a defect in telomere elongation leads to senescence in yeast. *Cell, 57*(4), 633-643.
Marcand, S., Brevet, V., Mann, C., & Gilson, E. (2000). Cell cycle restriction of telomere elongation. *Curr Biol, 10*(8), 487-490.
Marvin, M., Becker, M., Noel, P., Hardy, S., Bertuch, A., & Louis, E. (2009). The association of yKu with subtelomeric core X sequences prevents recombination involving telomeric sequences. *Genetics, 183*(2), 453-467, 451SI-413SI.
Marvin, M., Griffin, C., Eyre, D., Barton, D., & Louis, E. (2009). In *Saccharomyces cerevisiae,* yKu and subtelomeric core X sequences repress homologous recombination near telomeres as part of the same pathway. *Genetics, 183*(2), 441-451, 441SI-412SI.
Miller, M., & Cross, F. (2001). Cyclin specificity: how many wheels do you need on a unicycle? *J Cell Sci, 114*(Pt 10), 1811-1820.
Nugent, C., Bosco, G., Ross, L., Evans, S., Salinger, A., Moore, J., et al. (1998). Telomere maintenance is dependent on activities required for end repair of double-strand breaks. *Curr Biol, 8*(11), 657-660.
Nugent, C., Hughes, T., Lue, N., & Lundblad, V. (1996). Cdc13p: a single-strand telomeric DNA-binding protein with a dual role in yeast telomere maintenance. *Science, 274*(5285), 249-252.
Osterhage, J., Talley, J., & Friedman, K. (2006). Proteasome-dependent degradation of Est1p regulates the cell cycle-restricted assembly of telomerase in Saccharomyces cerevisiae. *Nat Struct Mol Biol, 13*(8), 720-728.
Peterson, S., Stellwagen, A., Diede, S., Singer, M., Haimberger, Z., Johnson, C., et al. (2001). The function of a stem-loop in telomerase RNA is linked to the DNA repair protein Ku. *Nat Genet, 27*(1), 64-67.
Polotnianka, R., Li, J., & Lustig, A. (1998). The yeast Ku heterodimer is essential for protection of the telomere against nucleolytic and recombinational activities. *Curr Biol, 8*(14), 831-834.
Porter, S., Greenwell, P., Ritchie, K., & Petes, T. (1996). The DNA-binding protein Hdf1p (a putative Ku homologue) is required for maintaining normal telomere length in Saccharomyces cerevisiae. *Nucleic Acids Res, 24*(4), 582-585.

Stellwagen, A., Haimberger, Z., Veatch, J., & Gottschling, D. (2003). Ku interacts with telomerase RNA to promote telomere addition at native and broken chromosome ends. *Genes Dev, 17*(19), 2384-2395.
Taggart, A., Teng, S., & Zakian, V. (2002). Est1p as a cell cycle-regulated activator of telomere-bound telomerase. *Science, 297*(5583), 1023-1026.
Tseng, S., Lin, J., & Teng, S. (2006). The telomerase-recruitment domain of the telomere binding protein Cdc13 is regulated by Mec1p/Tel1p-dependent phosphorylation. *Nucleic Acids Res, 34*(21), 6327-6336.
Tseng, S., Shen, Z., Tsai, H., Lin, Y., & Teng, S. (2009). Rapid Cdc13 turnover and telomere length homeostasis are controlled by Cdk1-mediated phosphorylation of Cdc13. *Nucleic Acids Res, 37*(11), 3602-3611.
Ubersax, J., Woodbury, E., Quang, P., Paraz, M., Blethrow, J., Shah, K., et al. (2003). Targets of the cyclin-dependent kinase Cdk1. *Nature, 425*(6960), 859-864.
van Hemert, M., Steensma, H., & van Heusden, G. (2001). 14-3-3 proteins: key regulators of cell division, signalling and apoptosis. *Bioessays, 23*(10), 936-946.
Vodenicharov, M., & Wellinger, R. (2006). DNA degradation at unprotected telomeres in yeast is regulated by the *CDK1* (Cdc28/Clb) cell-cycle kinase. *Mol Cell, 24*(1), 127-137.
Watt, P., Louis, E., Borts, R., & Hickson, I. (1995). Sgs1: a eukaryotic homolog of E. coli RecQ that interacts with topoisomerase II in vivo and is required for faithful chromosome segregation. *Cell, 81*(2), 253-260.
Wellinger, R., Wolf, A., & Zakian, V. (1993). Saccharomyces telomeres acquire single-strand TG1-3 tails late in S phase. *Cell, 72*(1), 51-60.

Chapter 4

Functional Analysis of Multiple Interactions between the C-S-T telomere capping complex and DNA polymerase α

Introduction

Telomeres must deal with specific challenges to ensure their efficient replication. These challenges include the passage of a unidirectional replication fork, the conservative synthesis of the C-strand that can occur after telomerase extends the telomere tract on newly made leading DNA strands, and regulation of telomere length. Thus, telomeres are crucial to the complete duplication of chromosome ends, which is necessary for the maintanence of intact chromosomes.

Specialized mechanisms may be employed to help ensure passage of the replication fork through telomere repeat sequences and promote complete replication of chromosome termini. At most genomic loci, the unreplicated DNA located on the side farthest away from a stalled replication fork can eventually be duplicated by a fork that approaches from the opposite direction. However, when a replication fork stalls near a telomere, telomere ends cannot be replicated by forks coming from the opposite direction since there is no evidence that yeast replication can initiate at the very end of a chromosome (Stevenson and Gottschling, 1999). The majority of telomeric repeats are replicated by conventional semi-conservative replication which initiates at origins internal to the telomeric repeats, with the C-strand being replicated by lagging-strand synthesis and the G-strand being replicated by leading strand synthesis. Telomerase uses its own internal RNA subunit as a template to catalyze the addition of telomeric repeats to the newly synthesized leading strand (Lingner et al., 1996, Lingner et al., 1997b). Telomere elongation by telomerase has been shown to occur in late S phase, the time when semi-conservative replication is replicating the terminal regions of chromosomes,

suggesting that complete telomere replication is a coordinated effort between DNA polymerase α and telomerase (Marcand et al., 2000, Diede and Gottschling, 1999, Wellinger et al., 1993b). Furthermore, analysis of yeast telomere replication intermediates demonstrated that the single-stranded G-rich 3' overhang is extended up to 30 bases in late S-phase, after the replication fork had reached the telomere, suggesting that the formation of extended G-tails requires the passage of the replication fork (Wellinger et al., 1993a, Wellinger et al., 1993b). Consistent with this idea, telomeres on a minichromosome containing an origin of replication were found to be elongated by telomerase, while telomeres on a minichromosome without an origin of replication were not elongated by telomerase, suggesting that replication fork passage promotes telomere extension by telomerase (Marcand et al., 2000, Dionne and Wellinger, 1998). Hence, it is possible that interactions between DNA polymerase and telomerase facilitate passage of the replication fork through telomere repeat sequences, and promote subsequent extension of telomere repeats on the newly synthesized leading strand by telomerase.

Interactions between components of DNA polymerase and telomerase subunits are proposed to facilitate fill-in synthesis of the complementary C-strand by DNA polymerase, although the exact mechanism is not completely understood. The hypothesis that telomere elongation is somehow coordinated with semi-conservative replication has been proposed in several different organisms. Analysis of telomere elongation in *Euplotes* has shown that an interaction between telomerase and DNA primase of the DNA polymerase α- primase complex exists (Fan and Price, 1997). Furthermore, inhibiting DNA polymerase function with aphidicolin during the time when bulk DNA

replication was complete and only telomeres were being extended resulted in lengthening of G-strands and an increase in heterogeneity of C-strand length. This result suggested that G-strand and C-strand synthesis are coordinated with each other, and this regulation involves DNA polymerase function (Fan and Price, 1997). In *S. cerevisiae*, analysis of mutations in the replication components Cdc17/Pol1, Pol12 and Cdc44/Rfc1 (large subunit of replication factor C) has been shown to result in the accumulation of ssDNA at the telomere and longer telomeres, suggesting that DNA polymerase fills in the complementary C-rich strand and inhibits further telomere elongation (Carson and Hartwell, 1985, Adams and Holm, 1996, Adams Martin et al., 2000). In *S. pombe,* the DNA polymerase catalytic subunit, DNA polymerase α has been shown to interact with telomerase during in S phase and G2 phase. In addition, the *polα-13* allele which disrupts the interaction with telomerase was shown to have long telomeres (Dahlen et al. 2003). Similarly, loss of DNA polymerase α in mouse cells using a temperature-sensitive allele of *polα* causes elongation of the G tail and lengthening of the telomere overall (Nakamura et al., 2005). Taken together, these data suggest that uncoupling the interactions between the DNA polymerase and telomerase affects telomere length and this coordination between telomerase with the conventional DNA replication machinery is evolutionarily conserved.

Cdc13 binds single-stranded telomeric DNA (ssDNA) in late S phase and functions in regulating telomerase activity (Taggart et al., 2002, Lin and Zakian, 1996, Nugent et al., 1996). The physical interaction between Cdc13 and Est1 facilitates recruitment of telomerase to telomeres, which activates telomere elongation in late S

phase (Chandra et al., 2001, Taggart et al., 2002, Chan et al., 2008, Evans and Lundblad, 1999, Bianchi et al., 2004). In addition to interaction with Est1, Cdc13 has been shown by yeast two hybrid assays and co-immunoprecipitation experiments to interact with Pol1 of DNA polymerase α (Qi and Zakian, 2000). *POL1* is an essential gene which encodes the conserved, catalytic subunit of the DNA polymerase α-primase complex and is required for proper DNA replication and cell cycle progression (Hartwell, 1973). Mutations in *CDC13* (*cdc13-50*) or *POL1* (*pol1-236*) that reduced their interaction, resulted in slight telomere lengthening, suggesting that the Cdc13-Pol1 interaction is involved in regulating telomere length (Qi and Zakian, 2000). Thus, since Cdc13 can interact with both a component of the DNA polymerase α complex, and a component of telomerase, it is possible that Cdc13 may be involved in the coordination between telomerase and DNA polymerase α at the telomere.

It is hypothesized that once telomerase has extended the newly synthesized 3' G-strand, DNA polymerase α is recruited to the telomere via the Cdc13-Pol1 to synthesize the complementary C-strand (Qi and Zakian, 2000). Cdc13 associates with the proteins Stn1 and Ten1 to form a complex at the telomere that maintains telomere capping (Grandin et al., 1997, Grandin et al., 2001). Stn1 has been shown to interact with the Pol12 component of DNA polymerase α (Grossi et al., 2004, Petreaca et al., 2006). Pol12 is the conserved, regulatory B subunit of the DNA polymerase α-primase complex. Pol12 does not contain enzymatic activity and has been implicated in stabilizing and regulating the catalytic subunit, Pol1 (Brooke et al., 1991). The *POL12* gene is essential and is required for DNA synthesis during DNA replication and correct progression

through S phase (Foiani et al., 1994). Both genetic and physical interactions between Pol12 and Stn1 suggest that the Stn1- Pol12 interaction is functionally important at telomeres (Grossi et al., 2004, Petreaca et al., 2006). Thus, the Cdc13-Pol1 and Stn1-Pol12 interactions could potentially serve to coordinate DNA polymerase and telomerase function at the telomere.

In order to determine the requirements for telomerase-dependent telomere synthesis, a system was developed by the Gottschling lab which separates telomere addition from normal semi-conservative replication during S-phase (Diede and Gottschling, 1999). These studies show that *in vivo* telomere addition was specifically dependent on *CDC17/POL1* (DNA polymerase α catalytic subunit), *POL2* (DNA polymerase δ catalytic subunit), and *PRI2* (DNA primase subunit), as loss of these genes eliminates the addition of telomere repeats *in vivo* (Diede and Gottschling, 1999). These results suggest that the DNA polymerase α-primase complex does indeed participate in telomerase-mediated telomere addition, and may be required for fill-in C-strand synthesis of newly synthesized telomeric repeats.

These observations lead to a particular problem that I have attempted to address in this chapter, namely whether the interaction between Cdc13 and Pol1 is direct and whether the Cdc13-Pol1 and Stn1-Pol12 interactions are required for telomere C-strand synthesis. Although the significance of the interactions between the telomere capping proteins, Cdc13 and Stn1, with the DNA polymerase α complex have been proposed, it has not been directly shown that these interactions are required for C-strand fill-in synthesis. Therefore, further characterization of the Cdc13-Pol1 and Stn-Pol12

interactions is required in order to test the hypothesis that these interactions serve to recruit the DNA polymerase α complex to the telomere following telomerase-mediated extension. Here, we analyze the interactions between the C-S-T complex and the DNA polymerase α complex. We determine that the Cdc13-Pol1 and Stn1-Pol12 associations are direct. We examine the functional significance of the Cdc13-Pol1 and Stn1-Pol12 interactions through use of alleles that disrupt them. Loss of these interactions using the *pol1-236 pol12-40* double mutant resulted in telomere lengthening. Thus, the data shown here provides additional insight as to the role of the Cdc13-Pol1 and Stn1-Pol12 interactions in the regulation of telomere length.

Materials and Methods

Protein Expression

GST-POL12 (pPC23), *GST-CDC13* (pPC19), or *GST* (pPC20) plasmid was transformed into BL21 *E. Coli* cells. BL21 chemically competent *E. coli* cells were thawed on ice and 1µl of the appropriate T7 based plasmid DNA was added to the cells. The cell mixture was placed on ice for 20 minutes. The cells were heat shocked at 42°C for 30 seconds, then placed on ice for 5 minutes. LB media was added to the cells and incubated at 37°C for 60 minutes. Transformations were then spread onto LB and ampicillin plates and incubated overnight at 37°C. 5 ml cultures of cells carrying each plasmid were grown at 37˚C overnight and inoculated into 50 ml fresh LB medium next day. After cells reached an O.D. of 0.3-0.4, GST protein expression was induced by 1mM IPTG (Fisher Scientific, Tustin, CA) and grown at 16˚C for 18 hours.

Bacterial cells were pelleted in a cold centrifuge at 3000g for 30 minutes. Pelleted cells were resuspended in 1.5 ml lysis buffer (50 mM potassium phosphate, pH7.8, 400 mM NaCl, 100 mM KCl, 10% glycerol, 0.5% Triton X-100 and 10 mM imidazole) with protease inhibitors followed by three freeze (-80˚C)/ thaw (37˚C) cycles. Samples were then sonicated 12 seconds for 10 times with 1 minute incubation on ice between each sonication. After sonication, samples were pelleted in the cold centrifuge at 12,000g for 20 minutes. Supernatants were transferred to a siliconized tube and stored at -20˚C.

To obtain Cdc13-myc protein, a 50 ml culture of yeast cells was grown to an OD of .6 and pelleted at 3000g for 5 minutes. Pellets were resuspended in 500 µl buffer A (25 mM HEPES at pH 7.5, 5 mM $MgCl_2$, 50 mM KCl, 10% glycerol and 1% Triton-X) supplemented with protease inhibitors (leupeptin, aprotinin, benzamidine, PMSF, and pepstatin). 500 µl glass beads were added to samples, and cells were lysed by 1 minute bead-beating 8 times with a 1 minute incubations on ice in between each beating (Biospec Products, Bartlesville, OK). Lysates were clarified by 2 minute centrifugation at 12,000g at 4°C. Crude extracts were transferred into new tubes and quantified using Bradford assay (Bio-Rad, Hercules, CA).

***in vitro* Translation Reactions**

TNT Quick Coupled transcription/translation system (Promega, Madison, WI) was used for *in vitro* protein transcription and translation. The *in vitro* reaction contained 1 µl plasmid DNA, 20 µl TNT Quick Master Mix, 2 µl nuclease-free water, 1ul PCR Enhancer and 1 µl ^{35}S-methionine (Amersham, Piscataway, NJ) and was incubated at 30˚C for 90 minutes.

GST Pull-down assays

One milliliter of clarified cell extracts containing bacterially expressed GST–Pol12, GST–Pol12-40, GST–Cdc13, or GST were incubated with 25 µl Glutathione Sepharose 4B (Amersham, Piscataway, NJ) at 4˚C for 30 min in LSBT buffer (20 mM HEPES–NaOH at pH 7.9, 100 mM NaCl, 2.5 mM $MgCl_2$, 0.1 mM EDTA, 0.05% NP-40 and 0.2% Triton X-100) and then washed with LSBT buffer. GST-Pol12 immobilized to GST beads was then incubated at 4°C for 2 hours with 1 mg yeast-cell lysates from Cdc13myc strain (hC1871).

in vitro interaction assays were conducted by incubating the GST-Pol12, GST-Cdc13, or GST proteins immobilized to GST beads with 5 µl of TNT reactions containing either ^{S35}Pol1 (pPC35), ^{S35}Cdc13 (pVL427), or ^{S35}Stn1 (pPC7) at 4°C for 2 hours. Reactions were washed once with LSBT buffer. Pull-down products were then subjected to SDS–PAGE and analyzed by exposure to a film for five days followed by Western blotting probed with anti-GST antibody (Amersham, Piscataway, NJ). ImageJ software was used to determine the ^{35}S-labelled protein signal present on the in the pull-down reactions. Background signal was measured on an area on the film where ^{35}S-signal was not present and was subtracted from all values. The percent recovery was determined by dividing the amount of ^{35}S -signal present in the pull downs by the ^{35}S-labelled protein input signal. Results from three independent experiments are shown.

Yeast manipulations

Standard techniques were followed in handling the yeast strains. Yeast strains used in this

study are listed in Table 4-1. Plasmids used in this study are listed in Table 4-2. To plate dilutions of yeast cells, serial ten-fold dilutions of equivalent starting concentrations of cell cultures were performed in microtiter dishes, "stamped" onto solid media, and grown at the indicated temperatures.

Viability Testing

Two milliliter cultures of the indicated strains were grown in YPD for 2 days. Serial ten-fold dilutions were stamped onto YPD plates and placed at the appropriate temperature for 2-3 days. *pol1-236 pol12Δ/pPol112* mutants were obtained from tetrad analysis of dCN526. Cells were then transformed with the *pol12-40* plasmid (pPC64) and plated on -His plates. Individual colonies were struck onto 5FOA to shuffle out *POL12* plasmid (pPC15) and obtain pol12Δ/ *pol12-40 pol1-236* double mutants. Strains: wildtype (hC160), *cdc17-1* (hC1199), *pol1-236* (hC1985), *pol12-40* (hC1740), *pol1-236 pol12-40* (hC2293). Three different transformants for the *pol1-236 pol12-40* were struck out and used for frogging. The first two are from transformants of dCN 526 1A, and the third is from dCN 526 10D.

p*cdc13-50* (Qi and Zakian 2000) marked with *TRP* was transformed into *cdc13-Δ pol12-Δ* cells carrying p*CDC13-URA3* (pVL438) and either p*POL12* (pPC65)or p*pol12-40* (pPC64) marked with *HIS3*. Transformed cells were grown in -trp-ura medium at 30˚C for 3 days. Serial 10-fold diluted cells were placed on -trp-ura or -trp 5-FOA plates. Plates were incubated at the indicated temperatures for 3-5 days.

Survival assays after transient exposure to HU

Cell survival was tested after HU exposure. Wild-type, *rad53–21, cdc17-1, pol12-40, pol1-236, pol1-236 pol12-40, pol12-216* , and *pol1-236 pol12-216* were exposed to 200mM hydroxyurea (HU). At the indicated times, the percentage of cells able to form colonies on plates lacking HU was determined. The average from 2 experiments is plotted.

Telomere Southern blot

Yeast genomic DNA was isolated according to the established protocols (Lundblad and Szostak, 1989). The DNA was digested overnight with *Xho*I. A conserved *Xho*I site is located within the subtelomeric Y' elements which release a terminal telomere fragment. After running the digested DNA on a 1.3% agarose gel and transferring to a nylon membrane (Hybond XL, Amersham), a [32P]- GT/dCA probe radiolabeled with 32P-dCTP was made from telomeric DNA cut from pRW41 digested with BamHI and XhoI and used to detect telomere fragments.

Results

Cdc13 directly interacts with Pol1, but not with Pol12, of the DNA polymerase α complex

Previous studies have shown that Cdc13 associates with Pol1 through two-hybrid interaction, as well as in co-immunoprecipitation assays (Qi and Zakian, 2000). These studies have demonstrated that a physical interaction exists between Cdc13 and Pol1, but does not address whether this association is direct, as both were *in vivo* experiments that could potentially include additional proteins. A study conducted by the Shore lab observed an association between the regulatory subunit of the DNA polymerase α complex**,** Pol12, and Stn1 using a GST pull-down biochemical assay. In this assay, GST-Pol12 fusion proteins were incubated with epitope tagged Stn1 proteins from yeast whole cell extracts, so the interaction could potentially have included additional proteins from yeast lysates (Grossi et al., 2004). A study conducted previously in our lab showed that the physical interaction that exists between Pol12 and Stn1 is direct, using an assay in which GST-Pol12 was incubated with radioactively labeled Stn1 that was produced in a rabbit reticulocyte lysate (Petreaca et al., 2006). Taken together, these data suggest that multiple interactions may exist between telomere binding proteins and components of the DNA polymerase α complex (Grossi et al., 2004, Petreaca et al., 2006). A summary of these interactions are shown in Figure 4-1.

It is possible that the reported interaction between Cdc13 and Pol1 is established via the direct interaction between Stn1 and Pol12 (Petreaca et al., 2006). In order to test the hypothesis that the observed interaction between Cdc13 and Pol1 is direct; we used an

in vitro transcription and translation system to produce radio-labeled Pol1 for use in GST pull-down reactions with Cdc13-GST. The presence of radio-labeled ^{S35}Pol1 signal in the Cdc13-GST pull-down products indicates that these two proteins can interact with each other directly *in vitro* (Figure 4-2a). The interaction between Pol1 and Pol12 was used as a positive control (Figure 4-2a). Approximately 30% of ^{35}S-Pol1 was observed in GST-Cdc13 pull-down products as compared with 15% in the GST pull down (Figure 4-2b). The difference in the amount of Pol1 in the GST-Cdc13 pull down compared with the amount of Pol1 in the GST pulldown was found to be significant using a student's t test, and indicates that the Cdc13-Pol1 direct interaction is authentic. For each reaction, we determined the amount of the GST proteins associated with the beads by probing the blot with anti GST antibody (Figure 4-2a, bottom panel). Obtaining high levels of soluble Cdc13-GST proved to be technically challenging, thus the amounts of Cdc13-GST protein and Pol12-GST protein are not equivalent. The amount of Cdc13-GST protein was reduced relative to the amount of Pol12-GST protein present in the assay (Figure 4-2a, bottom panel). Thus, these data demonstrate that the previously reported *in vivo* Cdc13-Pol1 interaction is indeed direct.

To test the hypothesis that additional interactions exist between Cdc13 and the components of the DNA polymerase α complex, we used a GST pull-down assay from yeast lysates to determine if there is an interaction between Cdc13 and Pol12. This assay will allow us to determine if Cdc13 and Pol12 associate in the same protein complex, however it does not address whether the interaction between Cdc13 and Pol12 is direct. We found that Cdc13myc from total yeast protein extracts was able to associate with

Pol12-GST (Figure 4-3a). This result suggested that Cdc13 is able to associate in a larger complex with Pol12 or that Cdc13 can also interact with Pol12. *pol12-40* possesses six mutations spread throughout the *POL12* gene (N86S, K235R, F416L, N651D, T681A, and N693S), and was characterized as having reduced interaction with both Stn1 and Pol1 (HC Chiu, Thesis Dissertation, Figure 4-4). Use of this allele which disrupts the direct interaction between Stn1 and Pol12 will allow us to determine whether any interaction we observe between Cdc13 and Pol12 is bridged by the Stn1 or Pol1 protein. The levels of Cdc13myc were diminished in the GST-Pol12-40 pull-down compared with the wild-type GST-Pol12 pull-down (Figure 4-3a). The result that Cdc13myc is not pulled down by GST- Pol12-40, suggests that the interaction between Cdc13 and Pol12 may be bridged through Cdc13's interaction with Stn1 or Pol1. To test the hypothesis that the observed interaction between Cdc13 and Pol12 is bridged, we used the *in vitro* transcription and translation system to produce ^{S35}Cdc13 for use in GST pull-down reactions with Pol12-GST. In these experiments Pol12-GST protein was incubated with the radio-labeled ^{S35}Cdc13 produced in rabbit reticulocyte lysate. The amount of Cdc13 able to associate with Pol12 was assessed by autoradiography. Approximately 10% of ^{S35}Cdc13 was observed in GST-Pol12 pull-down products, similar to the levels of Cdc13 observed when GST alone was used in the pull-down (Figure 4-3c). For each reaction, the amount of the GST protein present in each reaction was determined by probing with anti-GST antibody. The Western blot shows relatively equal Pol12 protein levels present in each lane (Figure 4-3b, bottom panel). Hence, these results indicate that any interaction

observed between Cdc13 and Pol12 was bridged through other proteins, and Cdc13 does not interact directly with Pol12 *in vitro*.

The *pol12-40* allele reduces direct interactions with both Pol1 and Stn1

It has been previously reported that the N-terminus of Pol12 interacts with Stn1 (Grossi et al., 2004) through yeast two hybrid and biochemical assays. Our lab has also observed that the N-terminus of Stn1 interacts with Pol12 directly (Petreaca et al., 2006). To test the hypothesis that the observed Stn1-Pol12 interaction is direct, we again employed the *in vitro* transcription and translation system to produce ^{S35}Stn1 for use in GST-pulldown reactions. As shown in Figure 4-4a, ^{S35}Stn1 was able to interact with GST-Pol12 robustly. About 70% of the ^{S35}Stn1 was observed in GST-Pol12 pull-down products, which is higher than the ~ 45% ^{S35}Pol1 observed in the GST-Pol12 pull-downs (Figure 4-4b). Stn1 exhibited non-specific binding and was able to associate with GST alone as well (Figure 4-4a, b). The *pol12-40* allele was used to further characterize known Pol12 interactions (HC Chiu, Thesis Dissertation). ^{S35}Stn1 was incubated with GST-Pol12-40, and it was found that Stn1 could interact with Pol12-40 (Figure 4-4a). However, compared with the efficiency of the pull-down by GST-Pol12, reduced amounts of ^{S35}Stn1 were pulled down by GST-Pol12-40, such that ^{S35}Stn1 recovery dropped from 70% to about 50%. (Figure 4-4 a, b). When Pol12-40 was used in the assay with Pol1, it was found that the Pol1-Pol12 interaction was also disrupted. Reduced levels of ^{35}S-Pol1 were observed in the GST-Pol12-40 pull-down compared to the wild-type GST-Pol12 pull-down, with ^{S35}Pol1 recovery being decreased from 40% to about 25%, indicating that Pol12-40 reduces association with Pol1 as well (Figure 4-4a, b). The

difference in the amount of Pol1 in the GST-Pol12 or in the GST-Pol12-40 pull down compared with the amount of Pol1 in the GST pulldown was not found to be significant using a student's t test, and most likely due to the limited sample size. Despite this, these observations suggests that Pol12-40 reduces direct associations with both Pol1 and Stn1, confirming previous results from our lab (HC Chiu, Thesis Dissertation). We expect that the *pol12-40* allele in combination with *pol1-236,* which disrupts interactions with Cdc13 (Qi and Zakian 2000), would substantially reduce the ability of the telomere capping proteins, Cdc13 and Stn1, to promote DNA polymerase α function at the telomere (Figure 4-1). Thus, our next approach was to characterize the *pol1-236 pol12-40* double mutant phenotypes to better understand the functional significance of the interactions between Cdc13 and Pol1 and between Stn1 and Pol12.

Characterization of *pol1-236 pol12-40* double mutant

Point mutations in either Cdc13 or Pol1 that disrupt the Cdc13-Pol1 interaction lead to a slight increase in average telomere length, but cause no other obvious phenotypes (Qi and Zakian, 2000). Our lab has characterized the *pol12-40* allele, as having normal cell viability, and slight telomere lengthening, but with no accumulation of telomeric single stranded DNA (HC Chiu, Thesis Dissertation). We introduced the *pol1-236* mutant into our *pol12-40* strain to create a *pol1-236 pol12-40* double mutant. If the Cdc13-Pol1 and Stn1-Pol12 associations are only necessary for filling in the telomeric C-strand after they are extended by telomerase, then the *pol1-236 pol12-40* double mutant may have a phenotype similar to, but not as strong as, a telomerase-deficient

strain due to gradual loss of telomere length. If, on the other hand, we find a more severe phenotype, this could indicate that the mutations are compromising DNA polymerase α function or that the Cdc13-Pol1 and Stn1-Pol12 interactions are needed to facilitate C-strand synthesis more generally.

To determine if perturbation of the Pol1-Cdc13 and Pol12-Stn1 interactions would reduce the ability of Cdc13 and Stn1 to promote DNA polymerase α function at the telomere we examined cell viability, and telomere structure in the *pol1-236 pol12-40* double mutant. Indicated strains were grown until saturated in YPD liquid media and serial dilutions were stamped onto YPD plates and grown at the indicated temperatures. The *pol1-236 pol12-40* strains did not exhibit a senescent phenotype and exhibited logs of growth similar to the wild-type strain (Figure 4-5). This result suggests that disruption of the Cdc13-Pol1 and Stn1-Pol12 interactions do not result in progressive loss of telomere sequence, since these cells maintained normal viability. This data also suggests that the essential function of DNA polymerase α is maintained in the *pol1-236 pol12-40* double mutant because the combination of both alleles is not lethal to cell viability. However, it remains possible that the *pol1-236* and *pol12-40* alleles compromise or alter DNA polymerase α activity, extending the time its takes cells to complete S phase. Thus, it would be of interest to conduct cell cycle progression experiments using FACS analysis on this double mutant strain. If bulk DNA replication is compromised, then progression of the *pol1-236 pol12-40* mutant through the cell cycle would likely be slower compared to wild-type cells. If bulk DNA replication is normal in *pol1-236 pol12-40*

cells, then cell cycle progression of the double mutant should be similar in timing compared to wild-type cells.

Although *pol1-236 pol12-40* cells maintain normal cell viability, it is possible that *pol1-236 pol12-40* cells may accumulate ssDNA due to defective C-strand fill in synthesis. In this case, we may expect the DNA damage checkpoint to be activated. In order to determine whether the DNA damage checkpoint was activated in the *pol1-236 pol12-40* double mutants, a budding analysis was conducted to look at cell cycle progression. Cells were arrested with in G_1 with α-factor and released to determine whether cells progressed normally through the cell cycle at 36°C or arrested at the DNA damage checkpoint. Cells from the *pol1-236, pol12-40,* and *pol1-236 pol12-40* appeared to leave G_1 and progress through S phase with kinetics similar to wildtype cells. *cdc17-1* is a temperature sensitive allele of *POL1* allele (Carson and Hartwell, 1985). As expected, about 60% of *cdc17-1* cells arrest as large-budded cells when grown at 36°C (compare Figure 4-6e and f, squares). A slightly higher percentage (~20%) of *pol1-236 pol12-40* cells were found to persist as large-budded cells compared to wildtype at 36°C (Figure 4-6f, circles). This slight delay in cell cycle progression suggested that the DNA damage checkpoint may be activated in the *pol1-236 pol12-40* mutants. As mentioned before, FACS analysis should be performed on the *pol1-236 pol12-40* double mutant. If the DNA damage checkpoint is being activated in these cells due to ssDNA accumulation, then *pol1-236 pol12-40* cells should arrest with 2N DNA content at G2/M phase when grown at 36°C compared to wild-type cells.

To further assess activation of the DNA damage checkpoint, we characterized cell growth of *pol1-236 pol12-40* cells in response to various DNA damaging agents. If the DNA damage checkpoint is being activated in *pol1-236 pol12-40* mutants due to accumulated DNA damage that remains unrepaired, then these cells may exhibit reduced viability. We examined the sensitivity of the wildtype, *pol1-236, pol12-40,* and *pol1-236 pol12-40,* to different types of DNA damage. We also used additional alleles to characterize the Cdc13-Pol and Stn1-Pol12 interactions. The *cdc13-50* allele disrupts the interaction with Pol1-Cdc13 interaction as characterized by yeast two hybrid (Qi and Zakian, 2000). The *pol12-216* mutation slightly reduced the Stn1-Pol12 interaction and displayed normal cell cycle progression, normal cell viability and telomere lengthening suggesting that the *pol12-216* allele may affect activities at the telomere (H.C. Chiu, Dissertation, Grossi et al., 2004). Thus the *cdc13-50, pol1-216, pol1-236 pol1-216* and *cdc13-50 pol12-40* mutant alleles were added to our analysis as well. These mutant strains were treated with the alkylating agent methyl methanesulfonate (MMS), and the ribonucleotide reductase inhibitor hydroxyurea (HU). Hydroxyurea treatment results in a depletion of dNTP pools during DNA replication, causing replication forks to slow down (Feng et al., 2006). We find that *pol1-236 pol12-40* mutants did not lose viability in response to MMS, suggesting the DNA damage checkpoint is functional and able to properly process and repair lesions caused by this type of damage. Interestingly, *pol1-236, pol12-40,* and *pol1-236 pol12-40* cells treated with hydroxyurea all displayed similar levels of sensitivity to the drug (Figure 4-7a). However, when these strains were transiently exposed to HU for two hours, only the *pol1-236 pol12-40* double mutant

exhibited poor recovery from temporary exposure, although not as severe as the lethality observed in the checkpoint defective *rad53-21* mutant (Figure 4-7b). When we examined the growth phenotype in *cdc13-50 pol12-40* cells, we found that the double mutant did not display any sensitivity to temperature or MMS (Figure 4-8a, b). Similar to the *pol1-236* strains, *cdc13-50* and *cdc13-50 pol12-40* cells treated with hydroxyurea displayed a slight sensitivity to the drug (Figure 4-8b). However, *cdc13-50* and *cdc13-50 pol12-40* cells transiently exposed to hydroxyurea were able to retain normal viability after removal from the drug, unlike the *pol1-236 pol12-40* strain (Figure 4-8c). In addition, *pol1-236 pol12-216* did not demonstrate any sensitivity to HU and retained normal cell viability as was previously reported (Grossi et al., 2004). The failure of the *pol1-236 pol12-40* cells to recover from HU exposure may suggest that the *pol1-236 pol12-40* double mutant has a defect in response to HU induced replication stress. The basis for the sensitivity in the *pol1-236 pol12-40* double mutant is unclear. It is possible that the *pol1-236 pol12-40* mutants acquire single-stranded DNA damage to due disrupted C-strand synthesis and exposure to HU leads to additional DNA damage which results in reduced cell growth. The difference in cell viability of the *pol1-236 pol12-40* and *cdc13-50 pol12-40* mutants in response to HU may be attributed to a difference in allele severity. Telomere length in *pol1-236* mutants is approximately a 100bp longer than telomeres in *cdc13-50* mutants, suggesting that *pol1-236* may be a slightly more severe allele than *cdc13-50* (Qi and Zakian, 2000). A direct way to test whether there is damage accumulating at telomeres in *pol1-236 pol12-40* cells would be to conduct an in-gel hybridization assay to determine the levels of terminal telomeric single-stranded

DNA present. If loss of the Cdc13-Pol1 and Stn1-Pol12 interactions result in ssDNA due to disrupted C-strand synthesis, then the level of ssDNA at telomeres should be higher in the *pol -236 pol12-40* strain relative to *pol -236, pol12-40 ,* or wildtype cells.

To further assess the growth phenotype of the *pol1-236 pol12-40* double mutants, a simple cell growth assay was conducted to compare the time it takes the yeast population to double in each of the mutant strains compared to wild-type cells. *POL1HA pol12Δ*/ p*POL12* or *pol1-236 pol12/* p*POL12* cells were transformed with p*POL12-HIS3* or p*pol12-40–HIS3*. In yeast, growth of cells expressing *URA3* is inhibited in the presence of the drug 5-Fluoroorotic acid, (5FOA). Therefore, transformed yeast strains were grown on plates containing 5FOA to select for loss of the wildtype *POL12* complementing plasmid. *POL1HA pol12Δ*/ p*POL12-HIS3*, *pol1-236 pol12Δ*/ p*POL12-HIS3, POL1HA pol12Δ*/ p*pol12-40-HIS3*, and *pol1-236 pol12Δ*/ p*pol12-40-HIS3* strains were struck out four times sequentially following loss of the complementing *POL12* plasmid. Figure 4-9a shows that *pol1-236 pol12-40* cells were slightly sensitive to extensive propagation, and cells appear to lose viability between the 2nd and 3rd streakout. However, cells recover and can resume normal growth by the fourth streakout, suggesting that if the observed loss of viability was due to accumulated DNA damage, cells are able to repair the damage and maintain cell viability (Figure 4-9a). Additional analysis was repeated with five independent colonies, and *pol1-236 pol12-40* cells did not exhibit a senescent phenotype. However, *pol1-236 pol12-40* cells did display heterogeneous growth and smaller colony size (Figure 4-9a). Cells from the first streak-out after 5FOA shuffle were inoculated into YPD media and the population doubling times were

monitored using a spectrophotometer. Figure 4-9b shows that *pol1-236 pol12-40* cells took approximately 3 hours to double the O.D. 600 reading compared with the approximately 2 hours needed for wild-type cells. Taken together, the results thus far suggest that *pol1-236 pol12-40* cells grow slower than wild-type cells, which may potentially be due to accumulated ssDNA damage at the telomere.

***pol1-236 pol12-40* double mutants acquire elongated telomeres**

If there is reduced recruitment in the *pol1-236 po112-40* double mutant due to disruption of both the Cdc13-Pol1 and Stn1-Pol12 interactions relative to either of the single mutants, then telomeres length in *pol1-236 pol12-40* cells should be elongated. To determine whether telomere lengthening occurred in the *pol1-236 pol12-40* mutant, DNA was prepared from wild-type and mutant cells, digested with *Xho*I, and analyzed by Southern blotting using a telomere probe (Figure 4-10). *pol1-236* cells had telomeres that were slightly longer compared wild type (Figure 4-10), consistent with what has been previously reported (Qi and Zakian, 2000, Grossi et al., 2004). *pol12-40* cells had telomeres that were longer than wild type but slightly shorter than telomeres in *pol1-236* cells (Figure 4-10, compare *pol1-236* and *pol12-40* lanes). *pol1-236 pol12-40* mutants had terminal telomere fragments that were longer than wild-type, but not longer than either *pol1-236* or *pol12-40* mutant alone. Since there was not additive telomere elongation in the *pol1-236 pol12-40* mutant, it is possible that the residual interaction between Cdc13-Pol1 and between Stn1-Pol12 in the *pol1-236 pol12-40* strain is sufficient for recruitment of DNA polymerase α to the telomere and inhibition of telomerase extension. Thus, the telomere lengthening in *pol1-236 pol12-40* mutant cells

is consistent with the established idea that the interactions between the telomere capping proteins and DNA polymerase provides negative regulation of telomerase activity.

If the telomere lengthening phenotype in *pol1-236 pol12-40* cells is due to loss of the negative regulation of telomerase, it is possible that telomeres would get progressively longer with increasing generations. Genomic DNA was analyzed from cells at four serial streak-outs after loss of the *POL12* complementing plasmid. The increase in telomere length seen in these mutants was not progressive, as telomeres were equally long after four rounds of sequential propagation (Figure 4-11). Taken together, these data indicate that telomere lengthening in the *pol1-236 pol12-40* is not dependent upon the number of generations and is likely that *pol1-236 pol12-40* do not completely lose negative regulation on telomerase.

Discussion

DNA polymerase α complex makes multiple direct contacts with telomere capping proteins

Studies have demonstrated that physical interactions exist between the C-S-T telomere capping complex and components of DNA polymerase α (Qi and Zakian, 2000, Grossi et al., 2004, Petreaca et al., 2006). Here, we find that a direct interaction does indeed exist between Cdc13 and Pol1. This work also confirms previous observations made by our lab which indicate that the Pol12 and Stn1 interaction is direct and the *pol12-40* mutant allele reduces direct associations between both Pol1 and Pol12 and Pol12 and Stn1 (Petreaca et al., 2006). We also determined Cdc13 can associate with

Pol12 in a larger complex, bridged through Stn1 or Pol1. However, this characterization of the interactions between telomere capping proteins and the DNA polymerase α-primase complex is not complete, and there are possibly new interactions to be identified. The ability of Ten1 to interact with Pol1 has been tested by our lab, and a direct interaction was not observed (HC Chiu, H. Gasparayan, unpublished data). DNA primase may play a role in the recruitment of the DNA polymerase α-primase complex to the telomere to participate in fill-in of the C-strand. Thus, experiments can be conducted to determine if Cdc13, Stn1 or Ten1 can interact with the Pri1 or Pri2 subunits. The Cdc13- Pol1 and Stn1-Pol12 interactions have both been proposed to function in the recruitment of DNA polymerase α to the telomere to facilitate synthesis of the C-strand after telomerase mediated extension. However, it still remains unclear as to whether these interactions actually serve this function. The multiple direct interactions between the C-S-T complex and the DNA polymerase α strengthens the idea that there are redundant pathways of recruiting DNA polymerase α to the telomere.

The *pol12-40* allele disrupts Pol1- Pol12 and Pol12-Stn1 direct interactions

pol12-40 is an allele of the essential *POL12* gene, which is required for DNA synthesis during DNA replication and correct progression through S phase (Foiani et al., 1994). Pol12 is the conserved, regulatory B subunit of the DNA polymerase α-primase complex, and has been implicated in stabilizing and regulating the catalytic subunit, Pol1 (Brooke et al., 1991). The *pol12-40* allele has been characterized as having slight telomere lengthening, but no accumulation of telomeric single stranded DNA (H.C. Chiu, Dissertation). Pol12-40 shows reduced interaction with Pol1, confirming previous results

(H.C. Chiu, Dissertation). It has been reported that the Pol12 N- terminus interacts with Stn1 in yeast two hybrid and biochemical assays (Grossi et al., 2004, Petreaca et al., 2006). The *pol12-40* allele contains two mutations in this region, and has reduced interactions with Stn1, as shown in Figure 4-4. To determine exactly which mutations in *pol12-40* disrupt the interaction with Stn1, the six missense mutations in *pol12-40* should be created individually and each mutant should be tested for Stn1 interaction. The mutations in the *pol12-40* allele reduce both the Pol1-Pol12 and Pol12-Stn1 interactions. It remains possible that the function of Pol12 may be affected by the missense mutations located throughout the protein, albeit in a subtle way. It would be useful to obtain alleles of *POL12* which more specifically and dramatically reduce the interaction with Stn1. Despite this, the *pol12-40* allele is of value in characterizing the significance of the Stn1-Pol12 interaction.

Characterization of *pol1-236 pol12-40* double mutant

The functional significance of the interactions between Cdc13 and Pol1 and between Stn1 and Pol12 is not well understood. Thus, we conducted an analysis of a *pol1-236 pol12-40* double mutant to determine the effect that loss of the Cdc13-Pol1 and Stn1-Pol12 interactions has on the cell. It is possible that loss of the Cdc13-Pol1 and Stn1-Pol12 associations in the *pol1-236 pol12-40* double mutant would reduce cell growth due to a progressive loss of telomere length. We did not observe any decrease in viability in the *pol1-236 pol12-40* double mutant that would be indicative of a senescent-like phenotype, suggesting that these interactions may not be the only interactions responsible for recruitment of DNA polymerase α to the telomere. Thus, further

characterization of interactions between the C-S-T complex with the DNA polymerase α complex is necessary. In addition, the loss of the associations between Cdc13 and Pol1 and between Stn1 and Pol12 did not result in a severe phenotype, which suggests that these interactions are not required to facilitate C strand synthesis more generally. The finding that the viability of the *pol1-236 pol12-40* mutant was not reduced, also suggested that the *pol1-236 pol12-40* double mutant maintained the essential function of DNA polymerase α. It still remains possible that the general function of the DNA polymerase α complex is perturbed in the double mutant, although it may be in a subtle way. Thus, further characterization of bulk DNA replication in the double mutant through FACS analysis would be necessary.

Loss of the Cdc13-Pol1 and Stn1-Pol12 interactions in *pol1-236 pol12-40* cells could result in ssDNA accumulation due to defective C-strand fill in synthesis and subsequent activation of the DNA damage checkpoint. Thus, budding analysis was conducted to look at cell cycle progression in *pol1-236 pol12-40* double mutants to determine whether the DNA damage checkpoint was activated. We found that a small percentage of cells *pol1-236 pol12-40* cells remained as large-budded cells after 4 hours compared to wildtype cells, suggesting that the *pol1-236 pol12-40* mutants may be activating the DNA damage checkpoint. However, the damage that may be activating the checkpoint was not lethal, as the majority of cells can progress through the cell cycle. Hence, it is possible that checkpoint activation in the *pol1-236 pol12-40* results in a slight delay in cell cycle progression compared to wildtype cells.

In order to further assess the DNA damage checkpoint response in *pol1-236 pol12-40* double mutants, cell viability in response to various DNA damaging agents was examined. We found that the *pol1-236 pol12-40* cells were sensitive to HU induced DNA replication stress specifically, as cells retained normal viability when exposed to MMS. This suggests that any damage in *pol1-236 pol12-40* mutant cells may get exacerbated in the presence of HU- induced replication stress. Analysis of the population doubling of *pol1-236 pol12-40* cells suggested that *pol1-236 pol12-40* cells may take a longer time to divide relative to wild-type cells, consistent with the idea that *pol1-236 pol12-40* cells may experience a delay in cell cycle progression. One way to directly test how long it takes for *pol1-236 pol12-40* cells to progress through the cell cycle, FACS analysis must be performed. If *pol1-236 pol12-40* cells take a longer time to divide, it is likely that the FACS profile would show that *pol1-236 pol12-40* double mutants would take more time to progress through S phase compared to wildtype cells.

In addition to facilitating synthesis of the C-rich strand, the Cdc13-Pol1 and Stn1-Pol12 interactions are thought to inhibit further telomere extension by telomerase. Accordingly, mutations that disrupt the Cdc13-Pol1 interaction result in slight telomere elongation (Qi and Zakian, 2000). We observe modest telomere lengthening in *pol1-236 pol12-40* double mutants, which is consistent with the idea that the Cdc13-Pol1 and Stn1-Pol12 interactions negatively regulate further telomerase-mediated extension. The terminal restriction pattern of telomeres in *pol1-236 pol12-40* cells do not look particularly rearranged compared to wildtype cells. However, it is possible that a recombination pathway was utilized to maintain the chromosome ends resulting in the

elongated telomeres we observed. If the associations between Cdc13-Pol1 and between Stn1-Pol12 interactions are needed to regulate telomerase extension, then one would expect to observe continue extension by an unregulated telomerase in *pol1-236 pol12-40* cells, resulting in extremely elongated telomeres. However, the fact that telomeres are not elongated as cells are continually propagated suggests that the residual association between C-S-T and DNA polymerase α that exists in the *pol1-236 pol12-40* double mutant may be sufficient to maintain some level of negative regulation on telomerase. It is also possible that the interactions between Cdc13 and Pol1 and between Stn1 and Pol12 do not provide the only means of negative regulation on telomerase, and perhaps in the absence of these interactions, uncontrolled telomerase extension is limited by another mechanism.

Further characterization of the *pol1-236 pol12-40* double mutant is required in order to address the whether the Cdc13-Pol1 and Stn1-Pol12 interactions are required for C-strand synthesis. An *in vivo* telomere addition assay has been developed that allows analysis of a specific telomere end that is created by enzyme digestion and monitored for telomerase addition of telomeric DNA repeats (Diede and Gottschling 1999). This assay separates out semi-conservative replication from telomerase-mediated extension because cells are arrested at G2/M; a time after DNA replication has been completed. The addition of telomere repeats to a telomere seed adjacent to an induced DSB requires the activity of telomerase, as well as DNA polymerase α (Diede and Gottschling 1999). Thus, use of the *pol1-236 pol12-40* mutant in the telomere addition assay, would determine if the the Cdc13-Pol1 and Stn1-Pol12 interactions are important for efficient *de*

novo telomere addition. If the *pol1-236 pol12-40* mutant is still be proficient for telomere healing in the telomere addition assay, then it would suggest that the residual interaction between Cdc13-Pol1 and between Stn1-Pol12 is sufficient to recruit DNA polymerase α to the telomere to participate in C-strand synthesis. However, it can also mean that the Cdc13-Pol1 and Stn1-Pol12 interactions are not the only associations utilized to recruit the DNA polymerase α complex to the telomere. Consistent with the idea that the residual interaction between Pol1-Cdc13 and Pol12-Stn1 would be sufficient to promote telomere addition, a *cdc13-50 pol12-40* double mutant was found to be proficient for telomere addition in this assay (H. Gasparayan, unpublished data). Despite being proficient for telomere addition, *cdc13-50 pol12-40* double mutants acquire ssDNA at their telomeres, suggesting that fill-in synthesis of the C-strand may still be disrupted in this mutant. Unquestionably, taking advantage of this *pol1-236 pol12-40* double mutant, as well as identifying alleles that completely abolish the Cdc13-Pol1 and Stn1-Pol12 interactions, will help us better understand the significance of the interactions between the C-S-T telomere capping complex and the DNA polymerase α complex.

Although the analysis described here was not complete and did not result in an absolute answer as to whether the interactions between telomere capping protein and the DNA polymerase α complex were required for synthesis of the complementary C-strand, further analysis of the *pol1-236 pol12-40* double mutant could provide more insight into the significance of these associations. It would be of interest to determine the levels of ssDNA in our *pol1-236 pol12-40* double mutant. An increase in ssDNA present at the telomere would suggest that C-strand synthesis is defective in the *pol1-236 pol12-40*

double mutant. It has been shown that a *cdc13-50 pol12-40* double mutant has a dramatic increase in ssDNA at the telomere, consistent with the idea that the Cdc13-Pol1 and Stn1-Pol12 interactions promote efficient fill-in synthesis (H. Gasparyan, unpublished data). Thus, it is possible that the *pol1-236 pol12-40* mutants will also exhibit an increase in the amount of ssDNA at the telomere, suggestive of defective C-strand synthesis.

The most direct way of testing the role of the Cdc13 – Pol1 and Stn1-Pol12 in Pol α-primase complex recruitment to the telomere would be through chromatin immuno-precipitation experiments using a tagged primase subunit. ChIP analysis could be used to determine if recruitment of the DNA polymerase α - primase complex to the telomere is affected if the Cdc13 – Pol1 and Stn1-Pol12 interactions are disrupted. This ChIP analysis should be conducted on cells that have been synchronized in G_1 phase with α-factor, with time-points taken as cells progress through the cell cycle. An increase in the levels of telomeric DNA associated with primase should be observed in wildtype cells as they progress into late S phase, approximately 45 minutes after release from the G_1 arrest. If the Cdc13-Pol1 and Stn1-Pol12 interactions are required for DNA polymerase α - primase recruitment to the telomere, then there should be a significant reduction in the amount of primase associated with telomeres in *pol1-236 pol12-40* cells compared to wild type cells in late S phase.

It is also possible that the Cdc13-Pol1 and Stn1-Pol12 interactions are required for normal semi-conservative replication of telomeres as well. The fission yeast doubled-stranded DNA binding protein Taz1 has been shown to be necessary for efficient replication of telomeres, since *taz1Δ* mutants have replication forks that stall at telomeres,

leading to replication fork collapse (Miller et al., 2006). It was concluded from these results that telomere DNA binding proteins may help with the passage of the replication fork through telomeres during semi-conservative replication (Miller et al., 2006). In order to analyze telomere replication separately from semi-conservative replication, ChIP analysis of the Cdc13-Pol1 and Stn1-Pol12 interactions would have to be conducted on a telomeric DNA seed adjacent to an induced DSB in the *de novo* telomere addition experimental system (Diede and Gottschling, 1999). In this ChIP analysis, cells would be synchronized in G_2/M phase with nocodazole, a time when semi-conservative replication is complete. Time-points would be taken after induction of the DSB. The amount *ADE2* sequence (which is located adjacent to the telomere DNA seed) associated with the primase subunit would be assessed by PCR amplification and compared with the amount of *ARO1* (a negative control) sequence associated the primase subunit at each timepoint. An increase in the levels of *ADE2* sequence associated with primase should be observed in wildtype cells as telomeres get extended. If the Cdc13-Pol1 and Stn1-Pol12 interactions are necessary for DNA polymerase α - primase recruitment to the telomere, then there should be a decrease in the amount of *ADE2* sequence associated with the primase subunit in *pol1-236 pol12-40* cells relative to wild type cells.

Interactions between the telomeric proteins and DNA polymerase α have been identified in organisms other budding yeast. The telomerase catalytic subunit, Trt1, coimmunoprecipitates with Polα, and indicates that a physical interaction exists between the DNA replication machinery and telomerase *in vivo* (Dahlen, et al., 2003). Although it is not known whether the interaction between Trt1 and Polα is direct, these results

suggest that G-strand extension and C-strand synthesis are coordinated in *S. pombe* as well. Two factors, initially named *AAF-132* and *AAF-44*, were found to stimulate the activity of mammalian DNA polymerase α -primase *in vitro*. The mammalian protein *CTC1* is identical to *AAF-132,* and is thought to be a distant homolog of *CDC13* (Casteel, et al., 2009, Surovtseva, et al., 2009). The *AAF-44* subunit is the mammalian ortholog of *STN1 (OBFC1*) (Casteel, et al., 2009, Martín, et al., 2007). The AAF complex was shown to facilitate DNA polymerase α-primase association with ssDNA, by allowing the enzyme to prime and extend DNA more processively (Casteel et al., 2009, Goulian and Heard, 1990). Taken together, these observations suggest that interactions between CST-like proteins and DNA polymerase α may also exist in mammalian cells. It is not known whether the interaction between telomerase and DNA polymerase α in *S. pombe* and the interactions between CST-like proteins with DNA Polymerase α in mammalian cells serve the same purpose, and further work is required in order to determine the exact function of these protein-protein interactions during telomere replication (Dahlen, et al., 2003, Casteel, et al., 2009, Martín, et al., 2007, Surovtseva, et al., 2009).

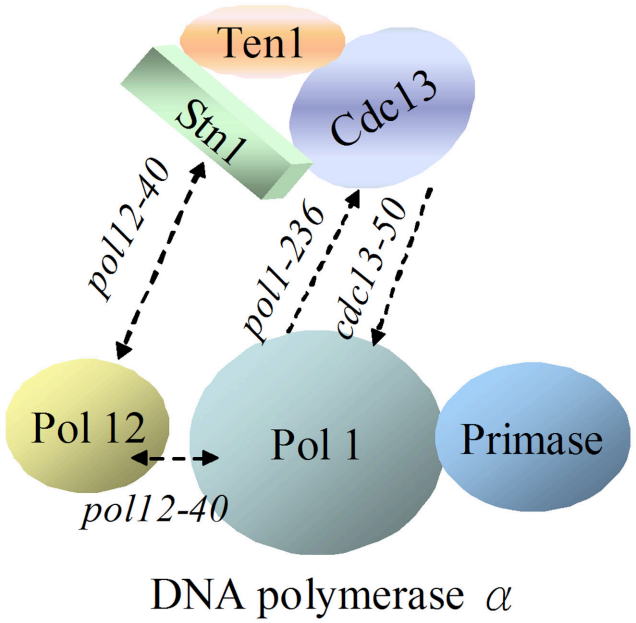

Figure 4-1 Multiple interactions exist between capping proteins and the DNA polymerase α complex
Cdc13 associates with Pol1 through two-hybrid interaction, as well as in co-immunoprecipitation assays. This interaction is disrupted in the *pol1-236* and *cdc13-50* mutations (Qi and Zakian, 2000). Stn1 and Pol1 interact directly (Petreaca et al., 2006). The *pol12-40* allele disrupts the interaction between Stn1 and Pol12. The interaction between Pol1 and Pol12 is also reduced by the *pol12-40* allele (HC Chiu, Thesis Dissertation, Figure 4-4).

Figure 4-2 Cdc13 directly interacts with Pol1, the catalytic subunit of DNA polymerase α A. Bacterially expressed GST-Pol12 (pPC23), GST-Cdc13 (pPC19) or GST alone (pPC20) was immobilized on GST beads, and then incubated with ^{35}S-methionine-labelled Pol1 that was generated in rabbit reticulocyte lysates using *POL1* (pPC35) plasmid. 20% of ^{35}S-labelled Pol1 reactions and the pull-down products from GST, GST-Pol12, and GST-Cdc13 incubations were subjected to SDS–PAGE on a 10% gel, transferred to a nitrocellulose membrane and analyzed by exposure to film for 5 days. The membrane was then probed with anti-GST to determine the amount of total GST protein present in each reaction. α- GST Western blot showing the amount of substrate proteins that went into the assay. Bottom left panel shows 4 minute exposure to film. Asterisks denote full length ^{35}S -Pol1 protein signal. Input shows the amount of ^{35}S -Pol1 protein that went into the assay. Arrow denotes full length Cdc13-GST protein and the caret denotes full length Pol12-GST present in this assay. All lanes are from the same experiment, on the same blot, and have the same exposure. B. To quantify the percent of ^{35}S-Pol1 present in the pull-downs, ImageJ software was used to measure the signal present on the films in the area corresponding to the full-length Pol1 protein. Background signal was subtracted from all values. The percent recovery was determined by dividing the amount of signal present in the pull downs by the ^{35}S-Pol1 input signal. The average of three independent experiments is shown with error bars representing standard deviations. P-values were determined using a student's t – test.

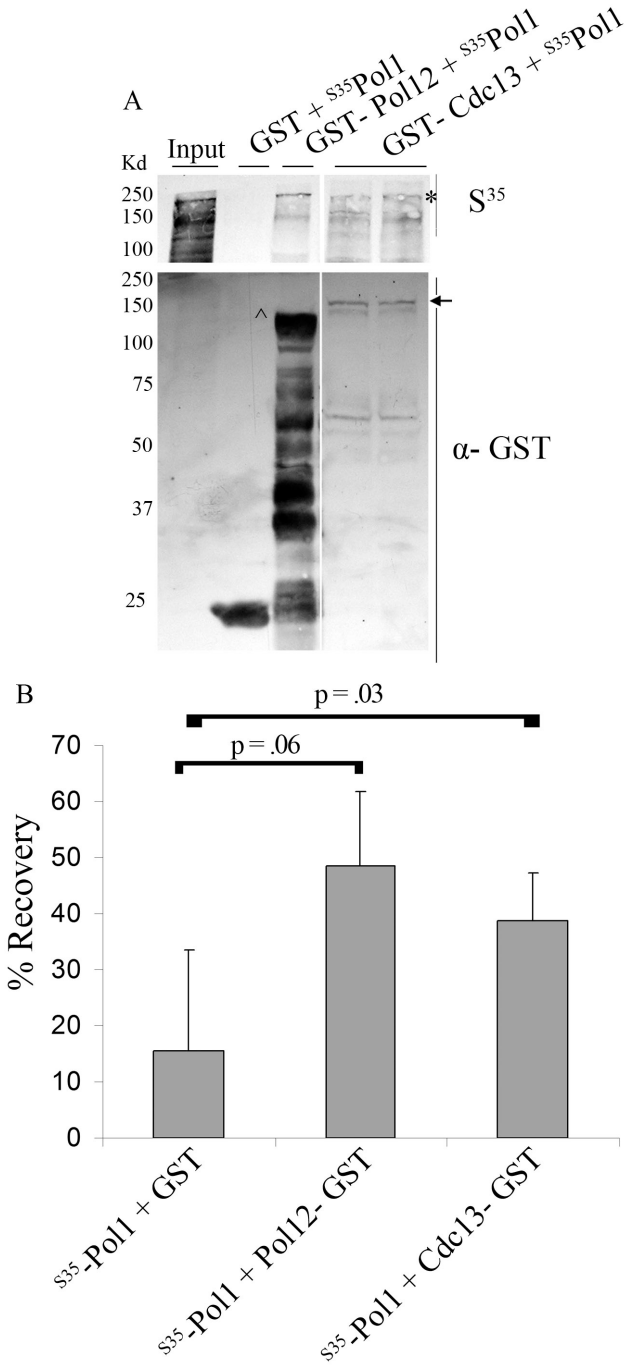
A
Input
GST + S35Pol1
GST- Pol12 + S35Pol1
GST- Cdc13 + S35Pol1
Kd
250
150
100
S35
*
250
150
100
75
50
37
25
^
α- GST
B
p = .03
p = .06
% Recovery
70
60
50
40
30
20
10
0
S35-Pol1 + GST
S35-Pol1 + Pol12- GST
S35-Pol1 + Cdc13- GST

Figure 4-3 Pol12 can associate indirectly with Cdc13.

A. Bacterially expressed GST-Pol12 (pPC23), GST-Pol12-40 (pPC52), or GST alone (pPC20) was immobilized on GST beads and incubated with yeast lysates from wildtype (hC160) or Cdc13myc (hC1871) strains. The presence of Cdc13myc associated with GST, GST-Pol12, or GST-Pol12-40, was analyzed by Western blotting using anti-MYC. The amount of GST, GST-Pol12, or GST-Pol12-40 was detected with anti-GST. Bottom left panel shows 4 minute exposure to film. All lanes are from the same experiment, on the same blot, and have the same exposure. *B*. Bacterially expressed GST, GST-Pol12, GST-Pol12-40, were immobilized on GST beads, and incubated with ^{35}S-methionine-labelled Cdc13 produced in rabbit reticulocyte lysates using *CDC13* (pVL427) plasmid. 20% of ^{35}S-labelled Cdc13 reactions and the pull-down products from GST, GST-Pol12, and GST-Pol12-40 were subjected to SDS–PAGE on a 10% gel, transferred to a nitrocellulose membrane and analyzed by exposure to film for 5 days. The membrane was then probed with anti-GST to determine the amount of total GST protein present in each reaction. C. To quantify the percent of ^{35}S-Cdc13 present in the pull-downs, ImageJ software was used to measure the signal present on the films in the area corresponding to the full-length Cdc13 protein. Background signal was subtracted from all values. The percent recovery was determined by dividing the amount of signal present in the pull downs by the ^{35}S-Cdc13 input signal. The average of three independent experiments is shown with error bars representing standard deviations. P-values were determined using a student's t – test. The data shown here are from the same experiment shown in Figure 4-1 and Figure 4-3, and included the same controls.

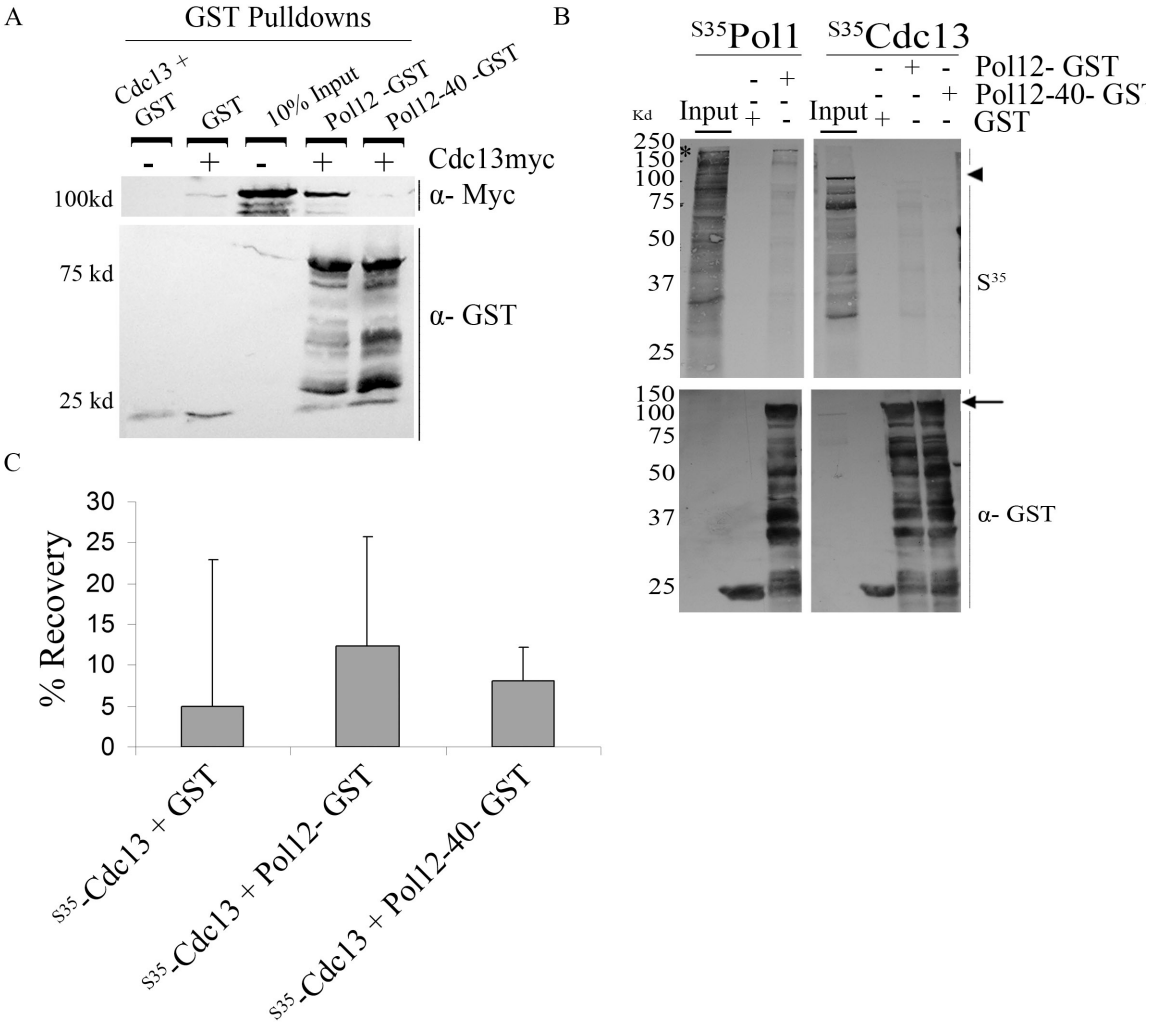
A
GST Pulldowns
Cdc13 + GST
GST
10% Input
Pol12 -GST
Pol12-40 -GST
Cdc13myc
100kd
α- Myc
75 kd
25 kd
α- GST
B
S35Pol1
S35Cdc13
Pol12- GST
Pol12-40- GST
GST
Kd
Input
250
150
100
75
50
37
25
S35
α- GST
C
% Recovery
30
25
20
15
10
5
0
S35-Cdc13 + GST
S35-Cdc13 + Pol12- GST
S35-Cdc13 + Pol12-40- GST

Figure 4-4 *pol12-40* allele reduces direct interactions with both Pol1 and Stn1

A. Bacterially expressed GST-Pol12 (pPC23), GST-Pol12-40 (pPC52) and GST alone (pPC20) were immobilized on GST beads, and incubated with ^{35}S-methionine-labelled Stn1 produced in rabbit reticulocyte lysates using an *STN1* (pPC7) plasmid. 20% of ^{35}S-labelled Stn1 reactions and the pull-down products from GST, GST-Pol12, and GST-Pol12-40 were subjected to SDS–PAGE on a 10% gel, transferred to a nitrocellulose membrane and analyzed by exposure to film for 5 days. The membrane was then probed with anti-GST to determine the amount of total GST protein present in each reaction. Bottom left panel shows 4 minute exposure to film. All lanes are from the same experiment, on the same blot, and have the same exposure. B. To quantify the percent of ^{35}S-Stn1 present in the pull-downs, ImageJ software was used to measure the signal present on the films in the area corresponding to the full-length Stn1 protein. Background signal was subtracted from all values. The percent recovery was determined by dividing the amount of signal present in the pull downs by the ^{35}S-Stn1 input signal. The average of three independent experiments with error bars representing standard deviations are shown for ^{35}S-Pol1+GST, ^{35}S-Pol1 + Pol12-GST , ^{35}S-Pol1 + Pol12-40-GST reactions. ^{35}S-Stn1 ^{35}S-Stn1 +GST, ^{35}S-Stn1 + Pol12-GST, and ^{35}S-Stn1 + Pol12-40-GST reactions were performed once and the results are shown. P-values were determined using a student's t – test. The data for the ^{35}S-Pol1+GST, and ^{35}S-Pol1 + Pol12-GST reactions are also shown in Figure 4-1. The data shown here are from the same experiment shown in Figure 4-1 and Figure 4-2, and included the same controls.

A

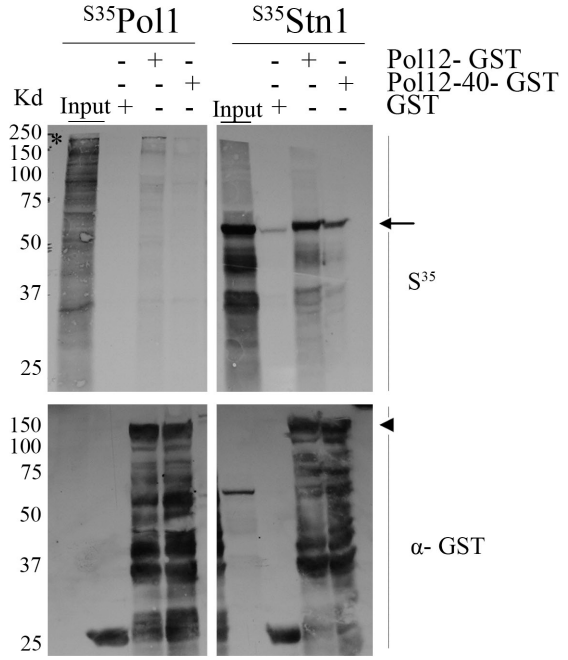
S35Pol1
S35Stn1
Pol12- GST
Pol12-40- GST
GST
Kd
Input
250
150
100
75
50
37
25
S35
α- GST

B

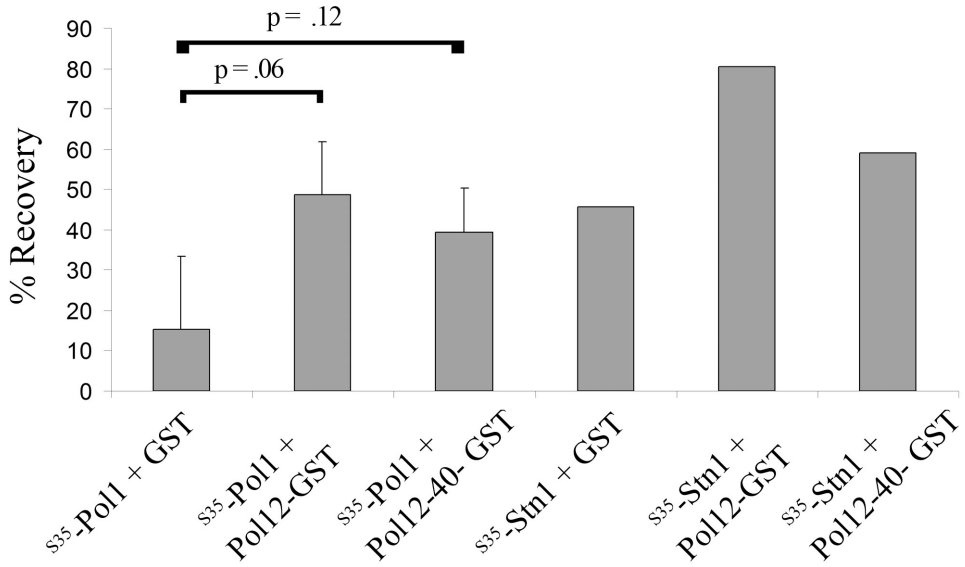
p = .12
p = .06
% Recovery
90
80
70
60
50
40
30
20
10
0
S35-Pol1 + GST
S35-Pol1 + Pol12-GST
S35-Pol1 + Pol12-40- GST
S35-Stn1 + GST
S35-Stn1 + Pol12-GST
S35-Stn1 + Pol12-40- GST

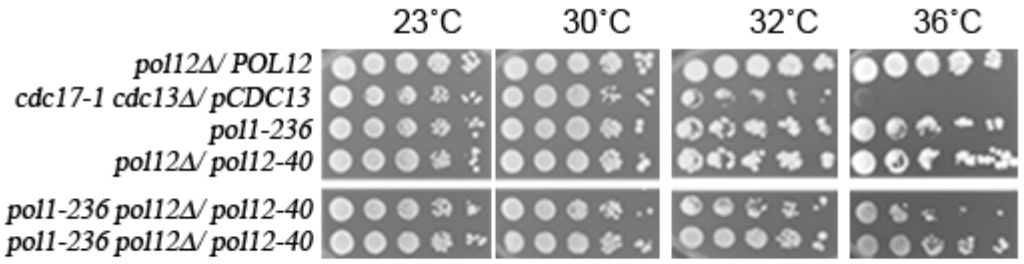

Figure 4-5 *pol1-236 pol12-40* double mutant does not have any apparent sensitivity to increased temperature. Cultures were grown to saturation in YPD liquid media at 23°C. Tenfold serial dilutions were prepared from liquid cultures, stamped onto YPD plates, and incubated at indicated temperatures for three to five days to test cell viability. Strains: *pol12Δ::KanMX/ pPOL12* (hC1750), *cdc17-1* (hC1199), *pol1-236* (hC1985), *pol12-40* (hC1740), *pol1-236 pol12Δ::KanMX/ ppol12-40* (hC2294), *pol1-236 pol12Δ::KanMX/ ppol12-40* (hC2332)

Err

Figure 4-6 Small percentage of *pol1-236 pol12-40* are held at a large budded cell cycle arrest *pol12Δ/ Pol12*, *pol12Δ/ pol12-40*, *pol1-236,* and *pol1-236 pol12-40* strains were arrested in G_1 with α-factor at 23°C. The cultures were then incubated at 23°C (panels A, C, and E), or shifted to 36°C (panels E, D, and F) for the indicated amount of time, and a 1ml sample was taken at each timepoint. One hundred cells were scored at each timepoint. Data shown is from one experiment. Each timepoint sample was counted twice and the averages are shown. Panel A and B shows percentage of unbudded cells. Panels C and D shows percentage of small budded cells. Panels E and F shows percentage of large budded cells. Strains: wild-type (hC160), *cdc17-1* (hC1199), *pol1-236* (hC1985), *pol12-40* (hC1740), *pol1-236 pol12Δ::KanMX/ ppol12-40* (hC2332).

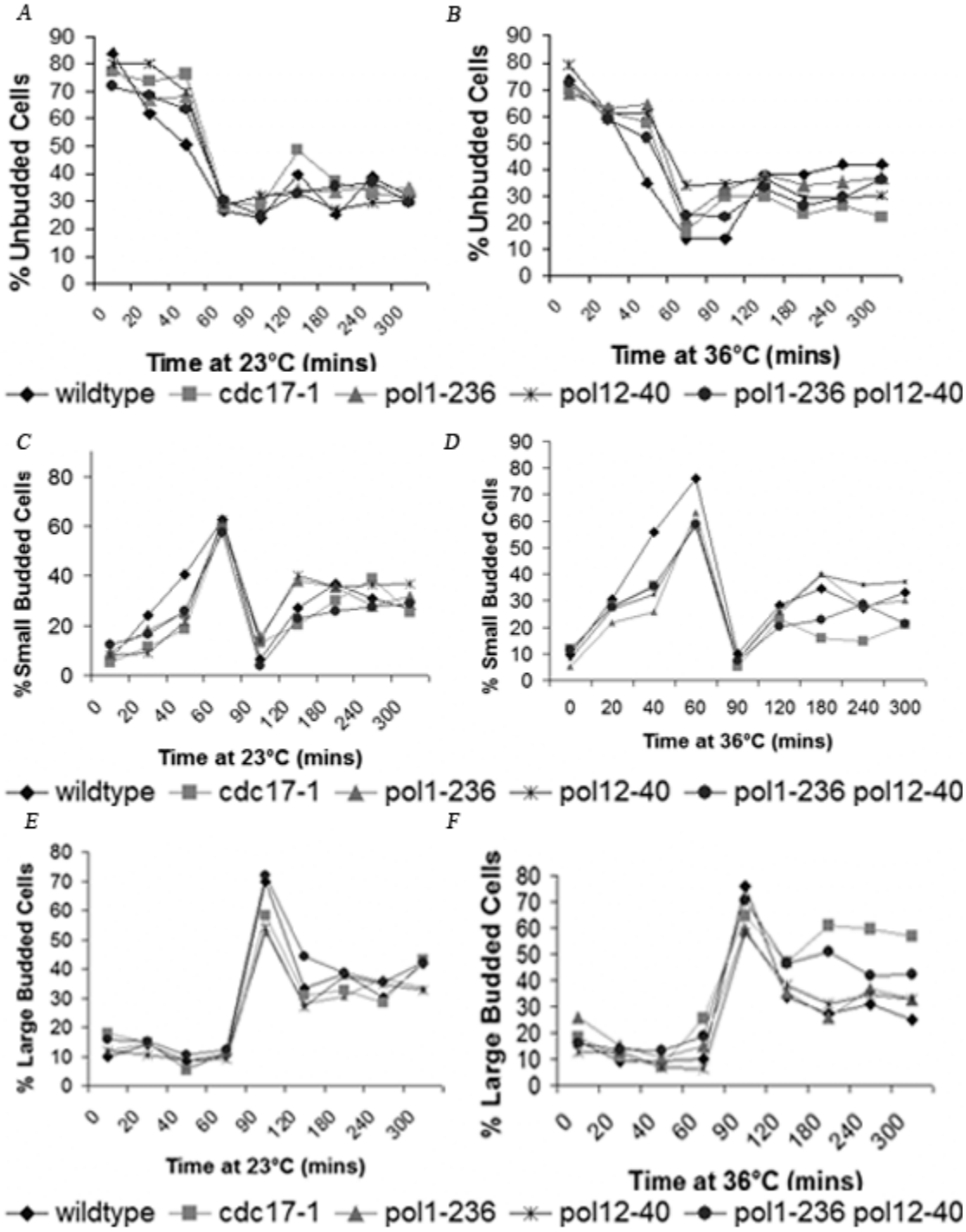
A
% Unbudded Cells
Time at 23°C (mins)
B
% Unbudded Cells
Time at 36°C (mins)
wildtype
cdc17-1
pol1-236
pol12-40
pol1-236 pol12-40
C
% Small Budded Cells
Time at 23°C (mins)
D
% Small Budded Cells
Time at 36°C (mins)
wildtype
cdc17-1
pol1-236
pol12-40
pol1-236 pol12-40
E
% Large Budded Cells
Time at 23°C (mins)
F
% Large Budded Cells
Time at 36°C (mins)
wildtype
cdc17-1
pol1-236
pol12-40
pol1-236 pol12-40

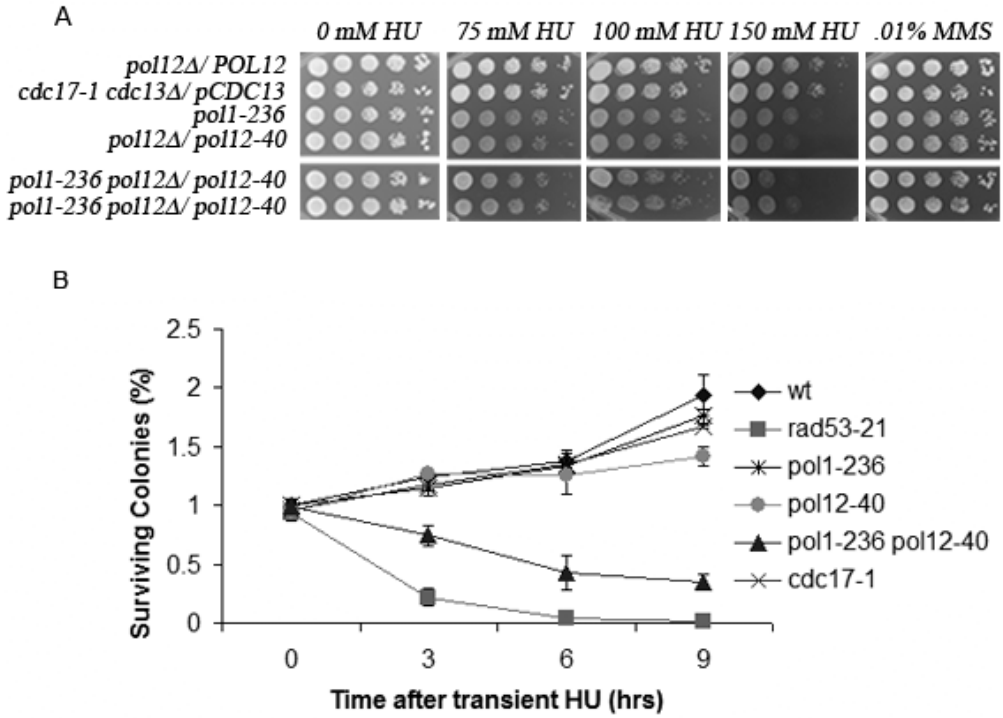

Figure 4-7 Sensitivity of *pol1-236 pol12-40* strains to HU

A. Strains were grown to saturation in YPD and ten-fold serial dilutions were spotted onto YPD or YPD media containing 75 mM, 100 mM, 150 mM hydroyurea, or .01% MMS and grown at 23°C for 4 days. Strains: *pol12Δ::KanMX/ pPOL12* (hC1750), *cdc17-1* (hC1199), *pol1-236* (hC1985), *pol12-40* (hC1740), *pol1-236 pol12Δ::KanMX/ ppol12-40* (hC2294), *pol1-236 pol12Δ::KanMX/ ppol12-40* (hC2332) B. *rad53-21*, *pol12Δ/ Pol12*, *pol12Δ/ pol12-40*, *pol1-236,* and *pol1-236 pol12-40* strains were arrested in G_1 with α-factor, incubated in 200 mM HU for the indicated times, and then plated on YPD dropout media lacking HU. Surviving colonies were counted after 3 days growth at 23°C. Strains: wild-type (hC160), *rad53-21* (JBY1275), *pol1-236* (hC1985), *pol12-40* (hC1740), *pol1-236 pol12Δ::KanMX/ ppol12-40* (hC2294), *cdc17-1* (hC1199). The average of two independent experiments is shown with error bars representing standard deviations.

Figure 4-8 Analysis of growth phenotypes in additional *pol12-40* mutant strains

A. Cultures were grown to saturation in YPD at 23°C and used to prepare tenfold serial dilutions which were stamped onto YPD plates, and incubated at indicated temperatures for three to five days to test for viability. Strains: *pol12Δ::KanMX/ pPOL12* (hC1750), *cdc17-1* (hC1199), *pol1-236* (hC1985), *cdc13-50 pol12-40* (hC1780), *cdc13-50 pol12-40* (hC1779), *pol1-236 pol12Δ::KanMX/ ppol12-216* (hC2388), *POL1HA pol12Δ::KanMX/ ppol12-216* (hC2389), *pol1-236 pol12Δ::KanMX/ ppol12-40* (hC2294). B. Strains were grown to saturation in YPD and ten-fold serial dilutions were spotted onto YPD (see A) or YPD media containing 75 mM, 100 mM, 150 mM hydroxyurea, or .01% MMS and grown at 23°C for 4 days. Strains: *pol12Δ::KanMX/ pPOL12* (hC1750), *cdc17-1* (hC1199), *pol1-236* (hC1985), *cdc13-50* (hC1780), *cdc13-50 pol12-40* (hC1779), *pol1-236 pol12Δ::KanMX/ ppol12-216* (hC2388), *POL1HA pol12Δ::KanMX/ ppol12-216* (hC2389), *pol1-236 pol12Δ::KanMX/ ppol12-40* (hC2294). C. *rad53-21*, *pol12Δ/ Pol12*, *pol12Δ/ pol12-40*, *pol1-236, pol12-216, pol1-236 pol12-216* and *pol1-236 pol12-40* strains were arrested in G_1 with α-factor, incubated in 200 mM HU for the indicated times, and then plated on YPD dropout media lacking HU. Surviving colonies were counted after 3 days growth at 23°C. Data shown is from one experiment. Strains: wild-type (hC160), *rad53-21* (JBY1275), *pol1-236* (hC1985), *pol12-40* (hC1740), *POL1HA pol12Δ::KanMX/ ppol12-216* (hC2389), *pol1-236 pol12Δ::KanMX/ ppol12-216* (hC2388), *pol1-236 pol12Δ::KanMX/ ppol12-40* (hC2294).

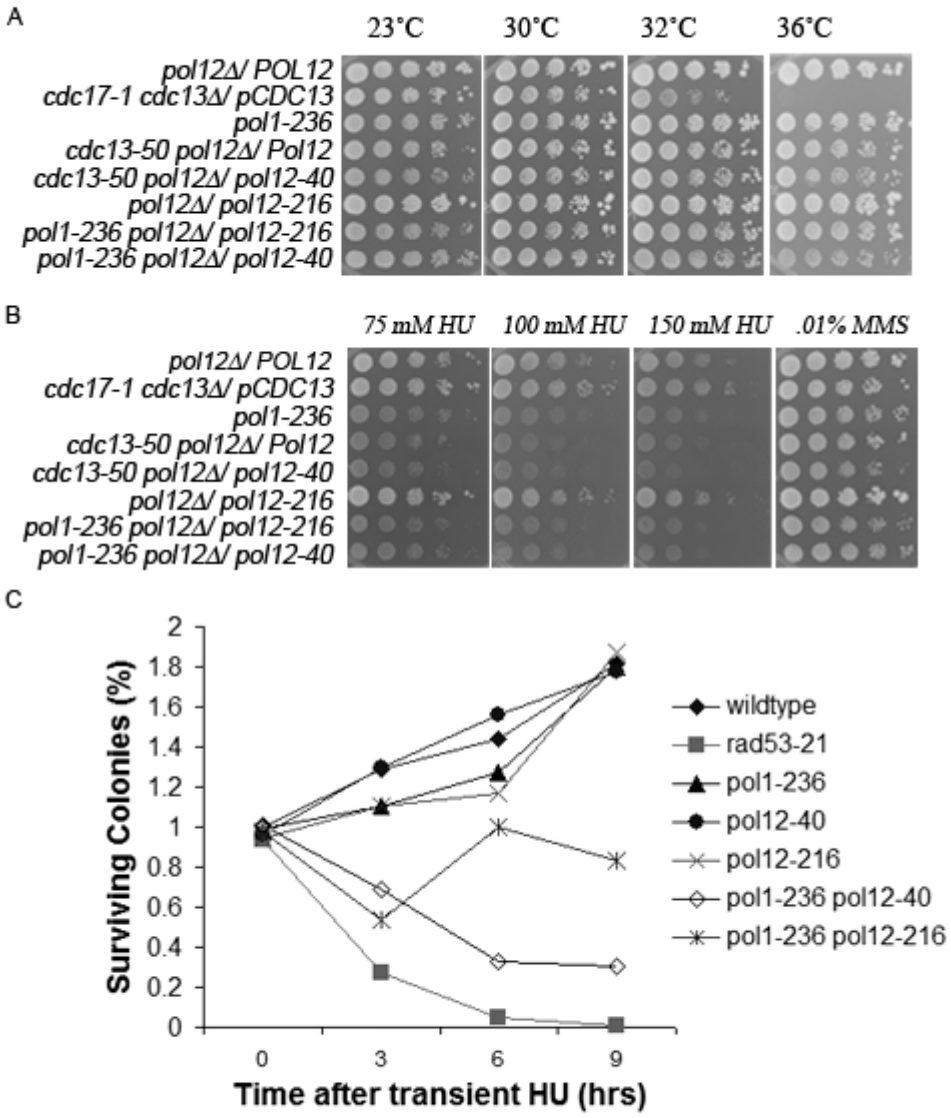
A
23°C
30°C
32°C
36°C
pol12Δ/ POL12
cdc17-1 cdc13Δ/ pCDC13
pol1-236
cdc13-50 pol12Δ/ Pol12
cdc13-50 pol12Δ/ pol12-40
pol12Δ/ pol12-216
pol1-236 pol12Δ/ pol12-216
pol1-236 pol12Δ/ pol12-40
B
75 mM HU
100 mM HU
150 mM HU
.01% MMS
pol12Δ/ POL12
cdc17-1 cdc13Δ/ pCDC13
pol1-236
cdc13-50 pol12Δ/ Pol12
cdc13-50 pol12Δ/ pol12-40
pol12Δ/ pol12-216
pol1-236 pol12Δ/ pol12-216
pol1-236 pol12Δ/ pol12-40
C
Survivlng Colonles (%)
2
1.8
1.6
1.4
1.2
1
0.8
0.6
0.4
0.2
0
0
3
6
9
Time after transient HU (hrs)
wildtype
rad53-21
pol1-236
pol12-40
pol12-216
pol1-236 pol12-40
pol1-236 pol12-216

Figure 4-9 *pol1-236 pol12-40* mutant strains grow slower than wildtype cells

A. Sequential streak-outs comparing the growth of single yeast colonies from the indicated strains are shown. Strains were transformed with *HIS3* plasmids encoding either *POL12* (pPC65) or *pol12-40* (pPC64) HIS plasmids, and plated for single colonies. Single colonies were then struck onto 5FOA plates to shuffle out the covering *URA3* marked *POL12* plasmid. After cells have lost the *URA3* marked plasmid, they are struck onto YPD plates. 1X , 2X, 3X, 4X refer to number of sequential streak-outs after 5FOA shuffle. Plates were then grown at 30°C for 3 days. Strains: *POL1HA pol12Δ::KanMX/ POL12* (hC2329), *POL1HA pol12Δ::KanMX/ ppol12-40* (hC2330), *pol1-236 pol12Δ::KanMX/ POL12* (hC2331), *pol1-236 pol12Δ::KanMX/ ppol12-40* (hC2332). B. Optical Density readings to compare population doubling times in the indicated strains are shown. Single colonies from the 1st streakout after 5FOA shuffle were inoculated into 5mls YPD and incubated at 23°C overnight. 5mls of fresh YPD was added to each culture to bring the O.D.600 reading of each strain to ~.1, and incubated at 30°C. O.D.600 readings were then taken at 1 hour timepoints for 9 hours. Strains: *POL1HA pol12Δ::KanMX/ POL12* (hC2329), *POL1HA pol12Δ::KanMX/ ppol12-40* (hC2330), *pol1-236 pol12Δ::KanMX/ POL12* (hC2331), *pol1-236 pol12Δ::KanMX/ ppol12-40* (hC2332). The average of two independent experiments is shown, with error bars representing standard deviations.

A

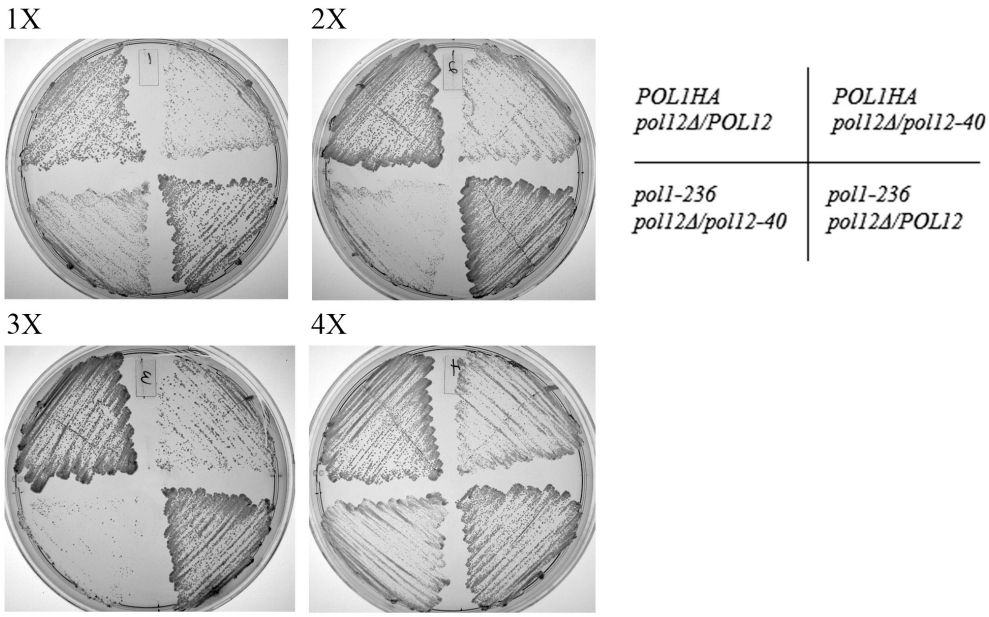
1X
2X
3X
4X
POL1HA pol12Δ/POL12
POL1HA pol12Δ/pol12-40
pol1-236 pol12Δ/pol12-40
pol1-236 pol12Δ/POL12

B

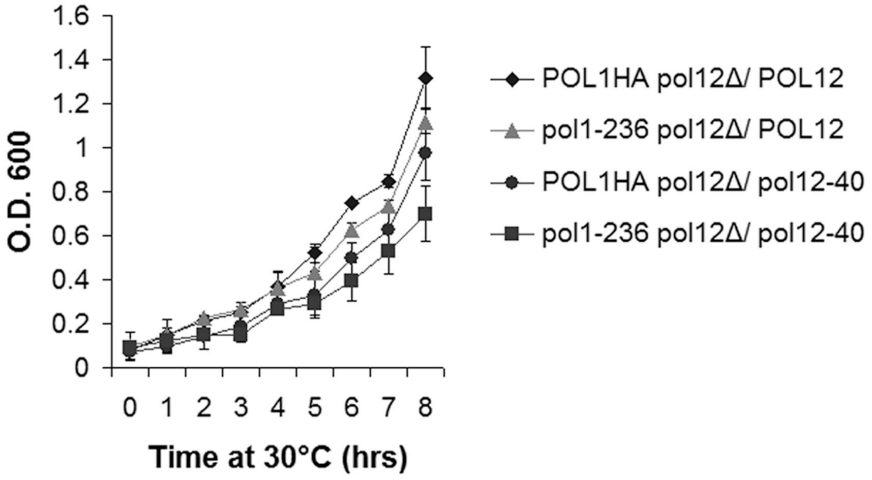
O.D. 600
Time at 30°C (hrs)
POL1HA pol12Δ/ POL12
pol1-236 pol12Δ/ POL12
POL1HA pol12Δ/ pol12-40
pol1-236 pol12Δ/ pol12-40

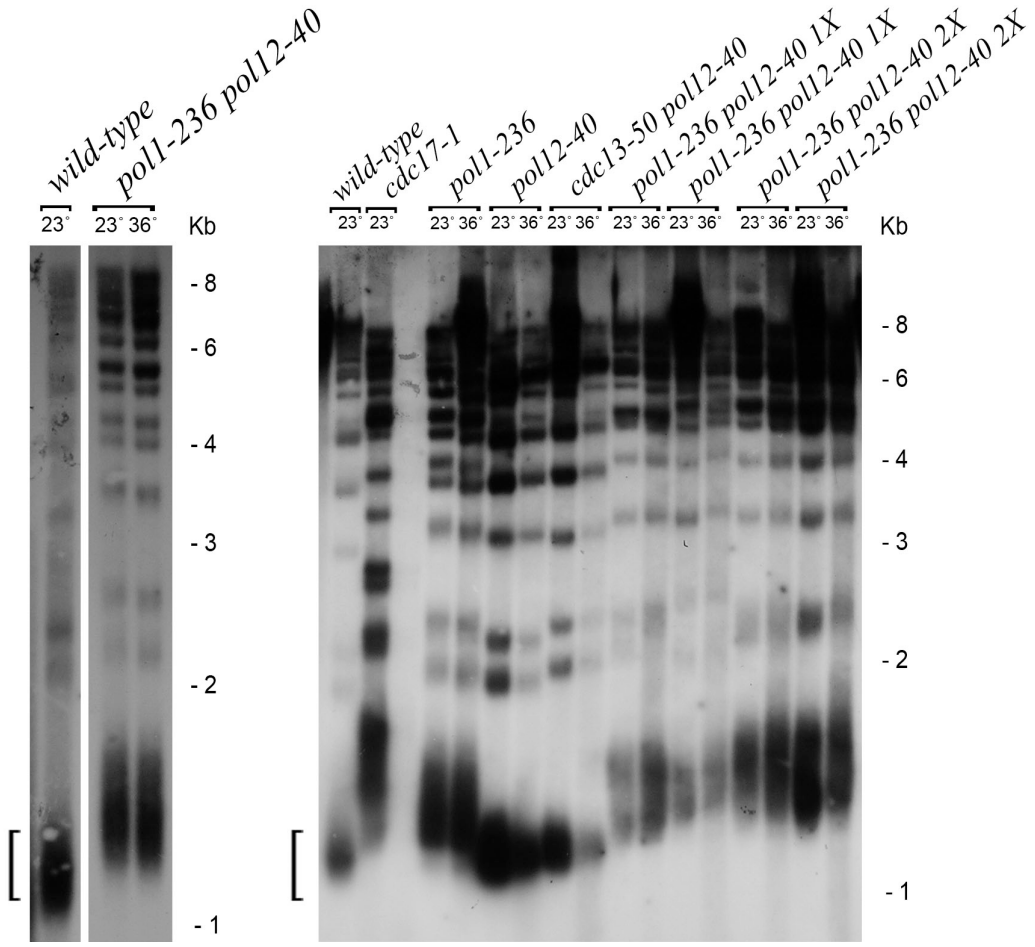

Figure 4-10 *pol1-236 pol12-40* mutant strains acquire elongated telomeres.
Southern Blot analysis comparing telomere restriction fragments from single and double *pol1-236 pol12-40* mutant strains grown at 23°C and 36°C. Genomic DNA was prepared from the indicated yeast strains, digested with *Xho*I, fractionated through 1% agarose, transferred to a nylon membrane, hybridized with a [32P]-GT/dCA probe, and exposed on film. Strains marked noted as 1X and 2X refer to number of sequential streakouts. The bracket indicates wild-type length of the telomere terminal restriction fragment. Strains: wild-type (hC160), *cdc17-1* (hC1199), *pol1-236* (hC1985), *pol12-40* (hC1740), *cdc13-50 pol12-40* (hC1779), *pol1-236 pol12Δ::KanMX/ ppol12-40* (hC2294).

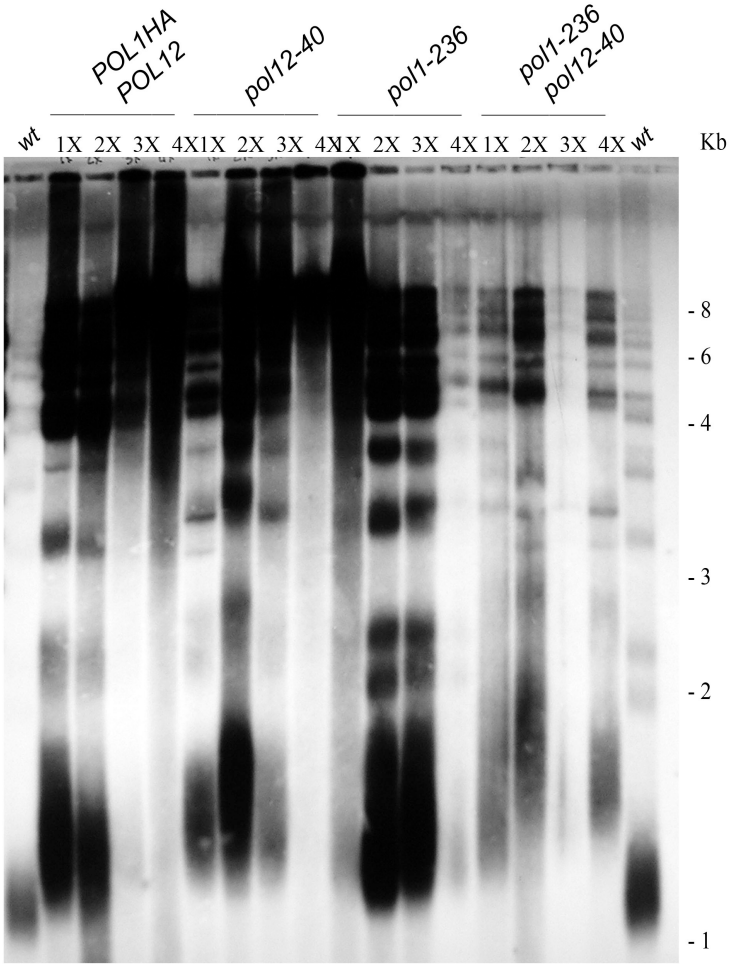

Figure 4-11 Telomere lengthening in *pol1-236 pol12-40* double mutant strains is not dependent on generation number. Southern Blot analysis comparing telomere restriction fragments from *pol1-236 pol12-40* strains from serial streak-outs after *pPOL12-URA3* plasmid loss, and grown at 23°C. Genomic DNA was prepared from the indicated yeast strains, digested with *Xho*I, fractionated through 1% agarose, transferred to a nylon membrane, hybridized with a [32P]- GT/dCA probe, and exposed on film. Strains marked noted as 1X, 2X, 3X, 4X refer to number of sequential streak-outs prior to DNA extraction. Strains: wild-type (hC160), *POL1HA pol12Δ::KanMX/ POL12* (hC2329), *POL1HA pol12Δ::KanMX/ ppol12-40* (hC2330), *pol1-236 pol12Δ::KanMX/ POL12* (hC2331), *pol1-236 pol12Δ::KanMX/ ppol12-40* (hC2332).

Table 4-1 Yeast Strains used in Chapter 4

Strain	Relevant Genotype
JBY1275	*MATa rad53-21* *ade2-1 trp1-1 ura3-1 leu2-3,112 his3-11,15 can1-100*
hC 160	*MATa* *ura3-52 ade2-101 lys2-801 leu2-Δ1 trp1-Δ1 his3-Δ200*
hC1199	*MATa cdc13Δ:: LYS2*/ p*CDC13-URA3 cdc17-1* *ura3-52 ade2-101 lys2-801 leu2-Δ1 trp1-Δ1 his3-Δ200*
hC1740	*MATa pol12Δ:: KAN*/ pPC64 *ura3-52 ade2-101 lys2-801 leu2-Δ1 trp1-Δ1 his3-Δ200*
hC1750	*MATa pol12Δ:: KAN* p*POL12-HIS3 cdc13Δ:: LYS2*/ pVL438 *ura3-52 ade2-101 lys2-801 leu2-Δ1 trp1-Δ1 his3-Δ200*
hC1779	*MATa pol12Δ:: KAN* p*pol12-40-HIS3 cdc13Δ:: LYS2*/ p*cdc13-50* *ura3-52 ade2-101 lys2-801 leu2-Δ1 trp1-Δ1 his3-Δ200*
hC1780	*MATa pol12Δ:: KAN* p*POL12-HIS3 cdc13Δ:: LYS2*/ p*cdc13-50* *ura3-52 ade2-101 lys2-801 leu2-Δ1 trp1-Δ1 his3-Δ200*
hC1871	*MATa POL1HA::TRP1 Cdc13myc-HIS3* *ade2-1 trp1-1 ura3-1 leu2-3,112 his3-11,15 can1-100*
hC1985	*MATa pol1-236*
hC2292	*MATα POL1HA::TRP1 pol12Δ:: KAN* pPC15
hC2293	*MATα pol1-236 pol12Δ:: KAN /* pPC15
hC2294	*MATα pol1-236 pol12Δ:: KAN/* pPC64
hC2329	*MATα POL1HA::TRP1 pol12Δ:: KAN* pPC65
hC2330	*MATα POL1HA::TRP1 pol12Δ:: KAN* pPC64
hC2331	*MATa pol1-236 pol12Δ:: KAN /* pPC65
hC2332	*MATa pol1-236 pol12Δ:: KAN/* pPC64
hC2388	*MATα pol1-236 pol12Δ:: KAN/* pPC53
hC2389	*MATα POL1HA::TRP1 pol12Δ:: KAN/* pPC53

Table 4-2 Plasmids used in chapter 4

Plasmid	Gene	Reference
pVL427	*pRSET –T7- CDC13*	Nugent Lab
pPC7	*pET101/D-TOPO–GST-STN1*	Phoebe Chiu
pPC15	*pYes2.1- GAL POL12*	Phoebe Chiu
pPC19	*pET101/D-TOPO–GST-CDC13*	Nugent Lab
pPC20	*pET101/D-TOPO–GST*	Phoebe Chiu
pPC23	*pET101/D-TOPO–GST-POL12*	Phoebe Chiu
pPC35	*pET101/D-TOPO–-POL1*	Phoebe Chiu
pPC52	*pET101/D-TOPO–GST- po112-40*	Phoebe Chiu
pPC53	*pRS413- CEN pol12-216*	Phoebe Chiu
pPC64	*pRS413- CEN pol12-40*	Phoebe Chiu
pPC65	*pRS413- CEN POL12*	Phoebe Chiu

References

Adams, A., & Holm, C. (1996). Specific DNA replication mutations affect telomere length in Saccharomyces cerevisiae. *Mol Cell Biol, 16*(9), 4614-4620.

Adams Martin, A., Dionne, I., Wellinger, R., & Holm, C. (2000). The function of DNA polymerase alpha at telomeric G tails is important for telomere homeostasis. *Mol Cell Biol, 20*(3), 786-796.

Bianchi, A., Negrini, S., & Shore, D. (2004). Delivery of yeast telomerase to a DNA break depends on the recruitment functions of Cdc13 and Est1. *Mol Cell, 16*(1), 139-146.

Carson, M., & Hartwell, L. (1985). CDC17: an essential gene that prevents telomere elongation in yeast. *Cell, 42*(1), 249-257.

Chakhparonian, M., & Wellinger, R. (2003). Telomere maintenance and DNA replication: how closely are these two connected? *Trends Genet, 19*(8), 439-446.

Chan, A., Boulé, J., & Zakian, V. (2008). Two pathways recruit telomerase to Saccharomyces cerevisiae telomeres. *PLoS Genet, 4*(10), e1000236.

Collins, K., Russo, A., Tseng, B., & Kelly, T. (1993). The role of the 70 kDa subunit of human DNA polymerase alpha in DNA replication. *EMBO J, 12*(12), 4555-4566.

Dahlén, M., Sunnerhagen, P., & Wang, T. (2003). Replication proteins influence the maintenance of telomere length and telomerase protein stability. *Mol Cell Biol, 23*(9), 3031-3042.

Diede, S. J., & Gottschling, D. E. (1999). Telomerase-mediated telomere addition in vivo requires DNA primase and DNA polymerases alpha and delta. *Cell, 99*(7), 723-733.

Dionne, I., & Wellinger, R. (1998). Processing of telomeric DNA ends requires the passage of a replication fork. *Nucleic Acids Res, 26*(23), 5365-5371.

Evans, S., & Lundblad, V. (1999). Est1 and Cdc13 as comediators of telomerase access. *Science, 286*(5437), 117-120.

Fan, X., & Price, C. (1997). Coordinate regulation of G- and C strand length during new telomere synthesis. *Mol Biol Cell, 8*(11), 2145-2155.

Feng, W., Collingwood, D., Boeck, M., Fox, L., Alvino, G., Fangman, W., et al. (2006). Genomic mapping of single-stranded DNA in hydroxyurea-challenged yeasts identifies origins of replication. *Nat Cell Biol, 8*(2), 148-155.

Foiani, M., Marini, F., Gamba, D., Lucchini, G., & Plevani, P. (1994). The B subunit of the DNA polymerase alpha-primase complex in Saccharomyces cerevisiae executes an essential function at the initial stage of DNA replication. *Mol Cell Biol, 14*(2), 923-933.

Grandin, N., Damon, C., & Charbonneau, M. (2001). Ten1 functions in telomere end protection and length regulation in association with Stn1 and Cdc13. *EMBO J, 20*(5), 1173-1183.

Grandin, N., Reed, S., & Charbonneau, M. (1997). Stn1, a new Saccharomyces cerevisiae protein, is implicated in telomere size regulation in association with Cdc13. *Genes Dev, 11*(4), 512-527.

Grossi, S., Puglisi, A., Dmitriev, P., Lopes, M., & Shore, D. (2004). Pol12, the B subunit of DNA polymerase alpha, functions in both telomere capping and length regulation. *Genes Dev, 18*(9), 992-1006.

Hartwell, L. (1973). Three additional genes required for deoxyribonucleic acid synthesis in Saccharomyces cerevisiae. *J Bacteriol, 115*(3), 966-974.

Ivessa, A., Zhou, J., Schulz, V., Monson, E., & Zakian, V. (2002). Saccharomyces Rrm3p, a 5' to 3' DNA helicase that promotes replication fork progression through telomeric and subtelomeric DNA. *Genes Dev, 16*(11), 1383-1396.
Larrivée, M., LeBel, C., & Wellinger, R. (2004). The generation of proper constitutive G-tails on yeast telomeres is dependent on the MRX complex. *Genes Dev, 18*(12), 1391-1396.
Lin, J., & Zakian, V. (1996). The Saccharomyces CDC13 protein is a single-strand TG1-3 telomeric DNA-binding protein in vitro that affects telomere behavior in vivo. *Proc Natl Acad Sci U S A, 93*(24), 13760-13765.
Lingner, J., Cooper, J., & Cech, T. (1995). Telomerase and DNA end replication: no longer a lagging strand problem? *Science, 269*(5230), 1533-1534.
Lundblad, V., & Szostak, J. (1989). A mutant with a defect in telomere elongation leads to senescence in yeast. *Cell, 57*(4), 633-643.
Makovets, S., Herskowitz, I., & Blackburn, E. (2004). Anatomy and dynamics of DNA replication fork movement in yeast telomeric regions. *Mol Cell Biol, 24*(9), 4019-4031.
Marcand, S., Brevet, V., Mann, C., & Gilson, E. (2000). Cell cycle restriction of telomere elongation. *Curr Biol, 10*(8), 487-490.
Nakamura, M., Nabetani, A., Mizuno, T., Hanaoka, F., & Ishikawa, F. (2005). Alterations of DNA and chromatin structures at telomeres and genetic instability in mouse cells defective in DNA polymerase alpha. *Mol Cell Biol, 25*(24), 11073-11088.
Nugent, C., Hughes, T., Lue, N., & Lundblad, V. (1996). Cdc13p: a single-strand telomeric DNA-binding protein with a dual role in yeast telomere maintenance. *Science, 274*(5285), 249-252.
Petreaca, R., Chiu, H., Eckelhoefer, H., Chuang, C., Xu, L., & Nugent, C. (2006). Chromosome end protection plasticity revealed by Stn1p and Ten1p bypass of Cdc13p. *Nat Cell Biol, 8*(7), 748-755.
Qi, H., & Zakian, V. (2000). The Saccharomyces telomere-binding protein Cdc13p interacts with both the catalytic subunit of DNA polymerase alpha and the telomerase-associated *est1* protein. *Genes Dev, 14*(14), 1777-1788.
Ray, S., Karamysheva, Z., Wang, L., Shippen, D., & Price, C. (2002). Interactions between telomerase and primase physically link the telomere and chromosome replication machinery. *Mol Cell Biol, 22*(16), 5859-5868.
Stevenson, J., & Gottschling, D. (1999). Telomeric chromatin modulates replication timing near chromosome ends. *Genes Dev, 13*(2), 146-151.
Taggart, A., Teng, S., & Zakian, V. (2002). Est1p as a cell cycle-regulated activator of telomere-bound telomerase. *Science, 297*(5583), 1023-1026.
Wellinger, R., Ethier, K., Labrecque, P., & Zakian, V. (1996). Evidence for a new step in telomere maintenance. *Cell, 85*(3), 423-433.
Wellinger, R., Wolf, A., & Zakian, V. (1993a). Origin activation and formation of single-strand TG1-3 tails occur sequentially in late S phase on a yeast linear plasmid. *Mol Cell Biol, 13*(7), 4057-4065.
Wellinger, R., Wolf, A., & Zakian, V. (1993b). Saccharomyces telomeres acquire single-strand TG1-3 tails late in S phase. *Cell, 72*(1), 51-60.

Chapter 5

Conclusions

Telomere maintenance plays an important role in the relationship between genome stability and cancer. The loss of the protective telomere function can result in large-scale chromosome rearrangements that can promote tumorigenesis. Telomeres are required for the overall stability of the genome by protecting chromosomes from the nucleolytic degradation and chromosome end-to-end fusions that are often associated with loss of genetic integrity, a hallmark of cancer cells. In addition to functioning as protective caps on chromosome ends, telomeres contribute to the accurate completion of DNA replication. The work presented here touches upon both these important function of telomeres.

Cdc13 is an important telomeric single stranded DNA binding protein in *S. cerevisiae* that is required for telomere end protection (Garvik et al., 1995, Lin and Zakian, 1996, Nugent et al., 1996a). Telomeres in temperature sensitive *cdc13-1* mutants become deprotected at restrictive temperatures and accumulate ssDNA damage, which is a potent activator of the DNA damage checkpoint and cells rapidly lose viability (Garvik et al., 1995, Lydall and Weinert, 1995, Nugent et al., 1996b). The exonuclease, Exo1 had been found to contribute to telomeric ssDNA accumulation in *cdc13-1* mutants (Maringele and Lydall, 2002, Zubko et al., 2004). In addition to this nuclease, Rad24 has also been implicated in contributing to the excessive single-stranded DNA accumulation in *cdc13-1* cells, since *cdc13-1 rad24Δ* exhibit lower levels of ssDNA (Lydall and Weinert, 1995). However, it has been previously shown that *cdc13-1 rad24Δ exo1Δ* cells still generated detectable levels of ssDNA at telomeres, suggesting that additional nuclease activity acted on uncapped telomeres in *cdc13-1* cells (Zubko et al., 2004). It

has since been proposed that the sliding clamp loaded by the Rad24 complex is required to anchor another unidentified exonuclease, termed ExoX (Zubko et al., 2004). In the second chapter of this thesis, we characterized two novel *RAD24* alleles that were recovered in a screen to identify nuclease activities degrading telomeres in *cdc13-1* cells. Interestingly, both alleles recovered from the screen were alleles of the *RAD24* gene. Rad24 has been previously shown to have a role in DNA processing, as *rad24Δ* cells did not successfully resect sequences located 1 kb away from a DSB using a HO endonuclease site to generate a single DSB (Aylon and Kupiec, 2003). Strains with a single DSB which can be repaired by either allelic (sequences at the same location on homologous chromosomes) or ectopic donor sequences (dispersed homologous sequences). It was shown that *rad24Δ* diploid yeast with homologous allelic donor sequence had 100% survival in response to a DSB, however, *rad24Δ/ rad24Δ* diploid cells did not perform ectopic recombination when allelic sequences were provided. In addition, when homology length was increased, the survival of *rad24Δ* cells also increased (Aylon and Kupiec, 2003). Taken together this data indicates that Rad24 is important for proper DNA processing, recombination partner choice and survival after repair (Aylon and Kupiec, 2003). Although the *rad24-2* allele did not strongly enhance recombination occurring at the telomere, the *rad24-2* allele did increase the frequency of obtaining *cdc13-1* temperature resistant colonies relative to *rad24-Δ*. Furthermore, *cdc13-1* cells have been shown to have increased mitotic recombination exclusively at the ends of chromosomes as measured by recombination events in the *CAN1* gene (Garvik et al., 1995). Since we observe significant telomere amplification in *cdc13-1 rad24-2* cells,

it is possible that the availability of telomere repeats allows more telomere donor sequences to be utilized during a rearrangement event, resulting in higher survival. The Rad24-2 protein may facilitate the acquisition of chromosomal alterations that promote temperature resistant *cdc13-1* growth. Thus, the protein fragments produced from the *rad24-2* allele could still potentially interfere with telomere processing and/or recombination pathways, though this has not been thoroughly tested.

It has been shown that telomeres in temperature resistant *cdc13-1 rad24-Δ exo1-Δ* or *cdc13-1 mec3- Δ* strains become rearranged, and exhibit with a pattern of restriction digest fragments indicative of TG_{1-3} repeat amplification (Zubko and Lydall, 2006, Grandin et al., 2001a). The initial *cdc13-1 rad24-2* strain from our screen acquired similar telomeric TG_{1-3} repeat amplification, with additional subtelomeric Y' elements observed as well. This amplification contributed to the ability of these cells to remain viable at increased temperatures. Interestingly, we also find that the telomere rearrangement alone was sufficient to promote growth of *cdc13-1* cells at 28°C. Consistent with this idea, *cdc13-Δ* cells which displayed telomere amplification characteristic of type-II survivor cells also acquired extra chromosomal Y'-circles. These extra chromosomal circular DNA have been proposed to be a supply of telomeric sequences to promote telomere-telomere recombination- based telomeric repeat maintenance (Larrivée et al., 2006). It is possible that these alternate telomere structures could serve as a protective capping structure similar to the protection provided by the terminal t-loop structure found at mammalian telomeres. These extra chromosomal circles could also provide a physical impediment to block nuclease access to the

telomere. Thus, the observed telomere amplification may itself provide an epigenetic contribution to the ability of *cdc13-1* cells to maintain growth at elevated temperatures.

Unfortunately our screen did not result in the identification of the nuclease we had attempted to uncover. A subsequent genetic screen has been conducted to identify suppressors of *cdc13-1* temperature sensitivity. This screen has identified some interesting new suppressors of *cdc13-1* temperature sensitivity including genes encoding proteins involved in protein degradation, chromatin architecture, and histone modification, but this screen has not uncovered any new nuclease activities at unprotected telomeres in *cdc13-1* cells. Hence, the response to the unprotected telomeres in *cdc13-1* mutants appears to be affected by diverse cellular pathways and processes. Further analyses will be necessary to understand how these pathways and processes interact to maintain protected telomeres (Addinall et al., 2008).

The cell not only needs to control the formation of the ssDNA on the 3' G-rich strand, but also needs to regulate telomere length, since critically short telomeres lose their protective function. As a central player in telomere protection and replication processes, it is crucial to understand at a molecular level how Cdc13 itself is regulated. In our studies, we have found that Cdc13 is phosphorylated at residue T308 by the primary cyclin-dependent kinase (Cdk1) driving cell cycle transitions. The third chapter of this thesis focused on determining whether this phosphorylation is relevant to how Cdc13 functions to protect telomere integrity during the cell cycle. Our observation that telomere length is decreased in the $cdc13^{T308A}$ mutant suggested a role for the phosphorylation at T308 in telomere length regulation. Our finding that lack of Cdk1-

mediated phosphorylation at T308 caused shorter telomeres is consistent with what has been published by two other groups (Li et al., 2009, Tseng et al., 2009). Decreased association of Est1 and Est2 with telomeres was observed in *cdc13*^{T308A} mutants, suggesting that Cdc13 phosphorylation promotes telomerase association with the telomere (Li et al., 2009). The phosphorylation of Cdc13 by Cdk1 was proposed to play a central role in regulating telomerase's access to telomeres by promoting association Cdc13 with Est1 when Cdc13 is phosphorylated. In addition, it was also proposed that Cdc13's association with Stn1 is promoted when Cdc13 is un-phosphorylated during telomere elongation (Li et al., 2009). This role for Cdc13 phosphorylation is very attractive and could provide a molecular switch by which processing events at the telomere can be coordinated.

The phosphorylation on Cdc13 was also found to mediate an interaction with the 14-3-3 protein, Bmh1. 14-3-3 proteins play a role in various cellular processes such as signal transduction, cell cycle regulation, apoptosis, stress response, and cytoskeleton organization by associating with the phosphorylated versions of their interacting proteins (Kakiuchi et al., 2007, Bruckmann et al., 2007). Bmh1 has been found to be involved with the post-transcriptional regulation of several *S. cerevisiae* proteins and these studies suggest a role for Bmh1 binding in protein synthesis and degradation (Bruckmann et al., 2004, Bruckmann et al., 2007). We found that Cdc13 could interact with Bmh1 in a yeast two hybrid assay, but the interaction was abolished when the *cdc13*^{T308A} mutant was used in the two hybrid assay. Cdc13 phosphorylation has been implicated in regulating Cdc13 protein stability, since *cdc13*^{T308A} cells treated with cycloheximide (to turn off the

production of Cdc13) maintained a longer protein half life relative to wild-type or *cdc13*^{T308D} strains (Tseng et al., 2009). To determine whether the Cdc13-Bmh1 interaction regulates protein stability, an experiment could be perform in which the production of Cdc13 is turned off using cycloheximide and the protein half life of Cdc13 in *CDC13 bmh1Δ* cells versus *cdc13*^{T308A} *bmh1Δ* cells is evaluated. If the Cdc13-Bmh1 interaction decreases protein stability, then the amount of Cdc13 protein and Cdc13^{T308A} protein should remain at a steady state level, since phosphorylated Cdc13 is not being bound by Bmh1 and targeted for degradation. It is possible that the interaction between Cdc13 and Bmh1 serves to regulate the levels of phosphorylated Cdc13 protein at the telomere, with the association of phosphorylated Cdc13 with Bmh1 promoting Cdc13's degradation. Loss of phosphorylated Cdc13 could allow for the association of unphosphorylated Cdc13 with the telomere, thereby facilitating subsequent Cdc13 association with Stn1.

In Chapter 4, we examine whether the interactions between Cdc13 -Pol12 and between Stn1-Pol12 are direct. These interactions are proposed to recruit the DNA polymerase α complex to the telomere to synthesis the C-strand after telomerase has extended G-strand (Qi and Zakian, 2000, Grossi et al., 2004). This would presumably inhibit further extension of the telomere by telomerase. However, there has been no direct evidence for this model, and the Cdc13-Pol1 and Snt1-Pol12 interactions may not be directly promoting DNA polymerase recruitment.

Here, we confirm the previous results from our lab that the Stn1-Pol12 interaction is direct and that the *pol12-40* mutant allele reduces the direct associations between both

Pol1 and Pol12 and between Pol12 and Stn1 (Petreaca et al., 2006, H.C. Chiu Dissertation). Use of the *pol12-40* allele in combination with *pol1-236* resulted in a *pol1-236 pol12-40* double mutant strain whose telomeres were elongated, consistent with the idea that the idea that the interactions between the telomere capping proteins and DNA polymerase provides negative regulation of telomerase.

To test the model that the interactions between Cdc13 and Pol1 and between Stn1 and Pol12 are important for recruitment of DNA polymerase α-primase to the telomere, chromatin immunoprecipitation experiments using a tagged primase subunit should be conducted. This experiment can provide information about the contribution these interactions make to the recruitment of the DNA polymerase α-primase complex to the telomere. If the Cdc13-Pol1 and Stn1-Pol12 interactions are responsible for recruitment of DNA polymerase α to the telomere, then the amount of the polymerase complex associated with the telomere should be reduced in the *pol1-236 pol12-40* double mutant in late S-phase, the time during which telomere replication is expected to occur. In addition, telomerase recruitment to the telomere can be assessed by performing ChIP experiments using a tagged Est2 protein. ChIP analysis through the cell cycle can provide valuable insight into the timing of the telomere replication. Comparing the timing of DNA polymerase α-primase recruitment with telomerase recruitment to the telomere, will allow the sequential ordering of events involved in complete telomere replication to be determined. If the DNA-polymerase α complex is required to complete telomere replication after semi- conservative replication, then following an initial increase of DNA-polymerase association in late S-phase due to semi-conservative replication, an

increase in the amount telomerase associated with telomeres should be observed, indicative of post-replication telomere extension. The increase in telomerase association should then be followed by an increase in DNA polymerase α-primase association with the telomere, corresponding to synthesis of the complementary C-strand.

The C-S-T complex was initially thought to be unique to budding yeast. However, recent studies have reported identification of Stn1 and Ten1 homologs in several organisms that contain *POT1* complexes, and have suggested a role for Stn1 and Ten1 in telomere capping (Martín et al., 2007, Song et al., 2008). In fact, a mammalian *CTC1* (conserved telomere maintenance component 1), *STN1* and *TEN1* complex has been identified which was shown to bind to single-stranded DNA as a trimeric complex and localize to telomeres in Hela cells (Miyake et al., 2009). Loss of telomere protection as measured by DNA damage foci demonstrated that Stn1/Pot-knockdown cells had an increase in DNA damage foci compared to either single knockdown, suggesting that Pot1 and CST play redundant roles in telomere protection (Miyake et al., 2009). The human ortholog of STN1, initially identified as OBFC1 (OB Fold-containing Protein 1), was found to associate with telomeric DNA and the shelterin component, TPP1 (Wan et al., 2009, Déjardin and Kingston, 2009). Furthermore, Stn1 protein orthologs necessary for proper telomere-capping have been discovered in both plants and fission yeast, suggesting that these proteins are evolutionarily conserved (Martín et al., 2007, Song et al., 2008).

Interestingly, the mammalian CTC1 and STN1 (OBFC1) proteins were found to be identical to proteins originally termed AAF-132 and AAF-44, respectively (Casteel et

al., 2009). AAF is a heterodimeric protein that was initially identified as an accessory factor that stimulated DNA polymerase α-primase activity *in vitro*. It was shown that the AAF complex facilitated DNA polymerase α-primase association with ssDNA, by allowing the enzyme to prime and extend DNA in a more processive manner (Casteel et al., 2009, Goulian and Heard, 1990). It is not yet known whether the CST-like protein make direct contacts with DNA Polymerase α subunits in mammalian cells. The interactions between the mammalian CTC1 and STN1 proteins with DNA Polymerase α -primase may be similar to the interactions observed between the CST complex and DNA Polymerase α -primase in *S. cerevisiae,* however, it remains possible that CST-like complexes in other species do not serve the same purpose as CST proteins in yeast. Although mammalian CTC1 and STN1 have been shown to localize to telomeres, these CST-like proteins have not been shown to telomere specific and the exact function of CTC1 and STN1 at mammalian telomeres is not completely understood (Miyake et al., 2009). Thus, additional functional studies on CST-like complexes from different organisms should be conducted to elucidate the functional relevance of the interactions between CST-like proteins and the DNA replication machinery.

The mammalian CTC1 and STN1 proteins contain OB folds similar to OB folds found in RPA, which is consistent with the structural similarity found between CST and RPA in budding yeast (Miyake et al., 2009, Gao et al., 2007). Replication protein A (RPA) is a heterotrimeric single-stranded DNA binding protein complex. RPA promotes processivity and fidelity of primer extension by the DNA polymerase α – primase, in addition to it's many other roles in DNA processing (Fanning et al., 2006). Although it

has not been shown, it is possible that the human and yeast CST proteins function as specialized RPA complexes. Hence, additional characterization of CTC1 and STN1 function is necessary to determine whether these CST-like proteins form an alternative specialized RPA complex that contributes to telomere capping and telomere replication (Miyake et al., 2009, Gao et al., 2007). In addition, further work is necessary in order to determine the exact the composition of proteins present at telomeres during telomere replication. Identification of the interactions between the telomere capping proteins and DNA polymerase α is encouraging, but pinpointing the significance for these interactions will contribute to understanding the mechanisms required to properly maintain telomere length.

References

Addinall, S., Downey, M., Yu, M., Zubko, M., Dewar, J., Leake, A., Hallinan, J., Shaw, O., James, K., Wilkinson, D., Wipat, A., Durocher, D. & Lydall, D. 2008. A Genomewide Suppressor And Enhancer Analysis Of Cdc13-1 Reveals Varied Cellular Processes Influencing Telomere Capping in *Saccharomyces Cerevisiae*. *Genetics,* 180**,** 2251-66.

Aylon, Y. & Kupiec, M. 2003. The Checkpoint Protein Rad24 Of *Saccharomyces Cerevisiae* Is Involved In Processing Double-Strand Break Ends And In Recombination Partner Choice. *Mol Cell Biol,* 23**,** 6585-96.

Bruckmann, A., Hensbergen, P., Balog, C., Deelder, A., De Steensma, H. & Van Heusden, G. 2007. Post-Transcriptional Control Of The *Saccharomyces Cerevisiae* Proteome By 14-3-3 Proteins. *J Proteome Res,* 6**,** 1689-99.

Bruckmann, A., Steensma, H., Teixeira De Mattos, M. & Van Heusden, G. 2004. Regulation Of Transcription By *Saccharomyces Cerevisiae* 14-3-3 Proteins. *Biochem J,* 382**,** 867-75.

Garvik, B., Carson, M. & Hartwell, L. 1995. Single-Stranded DNA Arising At Telomeres In Cdc13 Mutants May Constitute A Specific Signal For The Rad9 Checkpoint. *Mol Cell Biol,* 15**,** 6128-38.

Grandin, N., Damon, C. & Charbonneau, M. 2001a. Cdc13 Prevents Telomere Uncapping And Rad50-Dependent Homologous Recombination. *Embo J,* 20**,** 6127-39.

Grandin, N., Damon, C. & Charbonneau, M. 2001b. Ten1 Functions In Telomere End Protection And Length Regulation In Association With Stn1 And Cdc13. *Embo J,* 20**,** 1173-83.

Grandin, N., Reed, S. & Charbonneau, M. 1997. Stn1, A New *Saccharomyces cerevisiae* Protein, Is Implicated In Telomere Size Regulation in Association With Cdc13. *Genes Dev,* 11**,** 512-27.

Grossi, S., Puglisi, A., Dmitriev, P., Lopes, M. & Shore, D. 2004. Pol12, The B Subunit Of DNA Polymerase Alpha, Functions in Both Telomere Capping And Length Regulation. *Genes Dev,* 18**,** 992-1006.

Kakiuchi, K., Yamauchi, Y., Taoka, M., Iwago, M., Fujita, T., Ito, T., Song, S., Sakai, A., Isobe, T. & Ichimura, T. 2007. Proteomic Analysis Of In Vivo 14-3-3 Interactions In The Yeast Saccharomyces Cerevisiae. *Biochemistry,* 46**,** 7781-92.

Larrivée, M. & Wellinger, R. 2006. Telomerase- and Capping-Independent Yeast Survivors With Alternate Telomere States. *Nat Cell Biol,* 8**,** 741-7.

Li, S., Makovets, S., Matsuguchi, T., Blethrow, J., Shokat, K. & Blackburn, E. 2009. Cdk1-Dependent Phosphorylation of Cdc13 Coordinates Telomere Elongation During Cell-Cycle Progression. *Cell,* 136**,** 50-61.

Lin, C., Chang, H., Wu, K., Tseng, S., Lin, C., Lin, C. & Teng, S. 2005. Extrachromosomal Telomeric Circles Contribute To Rad52-, Rad50-, And Polymerase Delta-Mediated Telomere-Telomere Recombination in *Saccharomyces Cerevisiae*. *Eukaryot Cell,* 4**,** 327-36.

Lin, J. & Zakian, V. 1996. The Saccharomyces Cdc13 Protein Is A Single-Strand Tg1-3 Telomeric DNA-Binding Protein In Vitro That Affects Telomere Behavior In Vivo. *Proc Natl Acad Sci U S A,* 93**,** 13760-5.

Lydall, D. & Weinert, T. 1995. Yeast Checkpoint Genes In DNA Damage Processing: Implications For Repair And Arrest. *Science,* 270**,** 1488-91.
Maringele, L. & Lydall, D. 2002. Exo1-Dependent Single-Stranded DNA At Telomeres Activates Subsets Of DNA Damage and Spindle Checkpoint Pathways In Budding Yeast Yku70delta Mutants. *Genes Dev,* 16**,** 1919-33.
Martín, V., Du, L., Rozenzhak, S. & Russell, P. 2007. Protection Of Telomeres By A Conserved Stn1-Ten1 Complex. *Proc Natl Acad Sci U S A,* 104**,** 14038-43.
Miyake, Y., Nakamura, M., Nabetani, A., Shimamura, S., Tamura, M., Yonehara, S., Saito, M. & Ishikawa, F. 2009. Rpa-Like Mammalian Ctc1-Stn1-Ten1 Complex Binds To Single-Stranded DNA And Protects Telomeres Independently Of The Pot1 Pathway. *Mol Cell,* 36**,** 193-206.
Nugent, C., Hughes, T., Lue, N. & Lundblad, V. 1996. Cdc13p: A Single-Strand Telomeric DNA-Binding Protein With A Dual Role In Yeast Telomere Maintenance. *Science,* 274**,** 249-52.
Petreaca, R., Chiu, H., Eckelhoefer, H., Chuang, C., Xu, L. & Nugent, C. 2006. Chromosome End Protection Plasticity Revealed By Stn1p And Ten1p Bypass Of Cdc13p. *Nat Cell Biol,* 8**,** 748-55.
Qi, H. & Zakian, V. 2000. The Saccharomyces Telomere-Binding Protein Cdc13p Interacts With Both The Catalytic Subunit Of DNA Polymerase Alpha And The Telomerase-Associated Est1 Protein. *Genes Dev,* 14**,** 1777-88.
Song, X., Leehy, K., Warrington, R., Lamb, J., Surovtseva, Y. & Shippen, D. 2008. Stn1 Protects Chromosome Ends In Arabidopsis Thaliana. *Proc Natl Acad Sci U S A,* 105**,** 19815-20.
Tseng, S., Shen, Z., Tsai, H., Lin, Y. & Teng, S. 2009. Rapid Cdc13 Turnover And Telomere Length Homeostasis Are Controlled By Cdk1-Mediated Phosphorylation Of Cdc13. *Nucleic Acids Res,* 37**,** 3602-11.
Wan, M., Qin, J., Songyang, Z. & Liu, D. 2009. Ob Fold-Containing Protein 1 (Obfc1), A Human Homolog of Yeast Stn1, Associates With Tpp1 And Is Implicated In Telomere Length Regulation. *J Biol Chem,* 284**,** 26725-31.
Zubko, M., Guillard, S. & Lydall, D. 2004. Exo1 and Rad24 Differentially Regulate Generation Of Ssdna At Telomeres Of *Saccharomyces cerevisiae cdc13-1* Mutants. *Genetics,* 168**,** 103-15.
Zubko, M. & Lydall, D. 2006. Linear Chromosome Maintenance In The Absence Of Essential Telomere-Capping Proteins. *Nat Cell Biol,* 8**,** 734-40.

Appendix

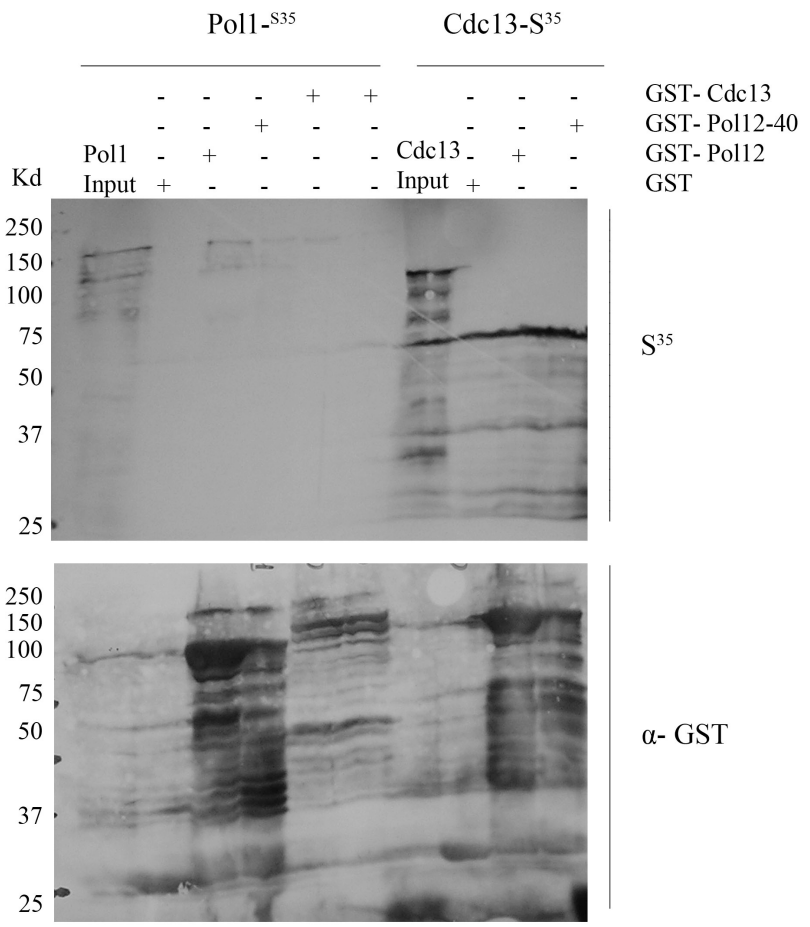

Appendix Figure 1 *in vitro* binding of Cdc13 and Pol1. Bacterially expressed GST, GST-Pol12, GST-Pol12-40, were immobilized on GST beads, and incubated with ^{35}S-methionine-labelled Cdc13 produced in rabbit reticulocyte lysates using *CDC13* (pVL427) plasmid. Parallel experiments were performed with *E. coli* produced GST that was immobilized on beads and incubated with the same amount of ^{35}S- labeled Cdc13. 20% of ^{35}S-labelled Cdc13 reactions and the pull-down products from GST, GST-Pol12, and GST-Pol12-40 were subjected to SDS–PAGE on a 10% gel, transferred to a nitrocellulose membrane and analyzed by exposure to film for 5 days. The membrane was then probed with anti-GST to determine the amount of total GST protein present in each reaction. Experiment conducted on 6/9/09.

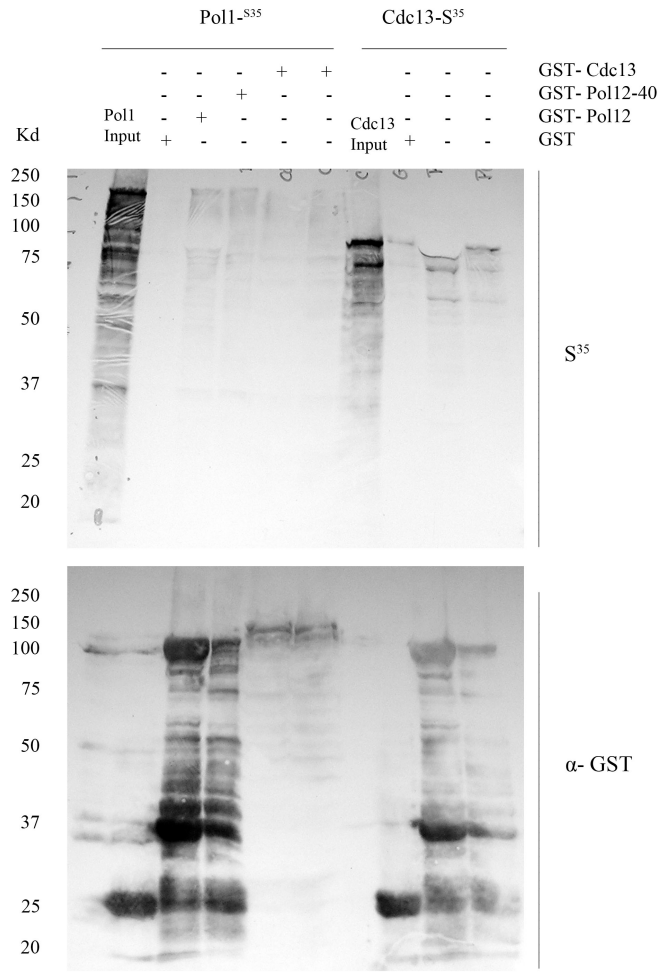

Appendix Figure 2 *in vitro* binding of Cdc13 and Pol1. Bacterially expressed GST, GST-Pol12, GST-Pol12-40, were immobilized on GST beads, and incubated with ^{35}S-methionine-labelled Cdc13 produced in rabbit reticulocyte lysates using *CDC13* (pVL427) plasmid. Parallel experiments were performed with *E. coli* produced GST that was immobilized on beads and incubated with the same amount of ^{35}S- labeled Cdc13. 20% of ^{35}S-labelled Cdc13 reactions and the pull-down products from GST, GST-Pol12, and GST-Pol12-40 were subjected to SDS–PAGE on a 10% gel, transferred to a nitrocellulose membrane and analyzed by exposure to film for 5 days. The membrane was then probed with anti-GST to determine the amount of total GST protein present in each reaction. Experiment conducted on 6/26/09.

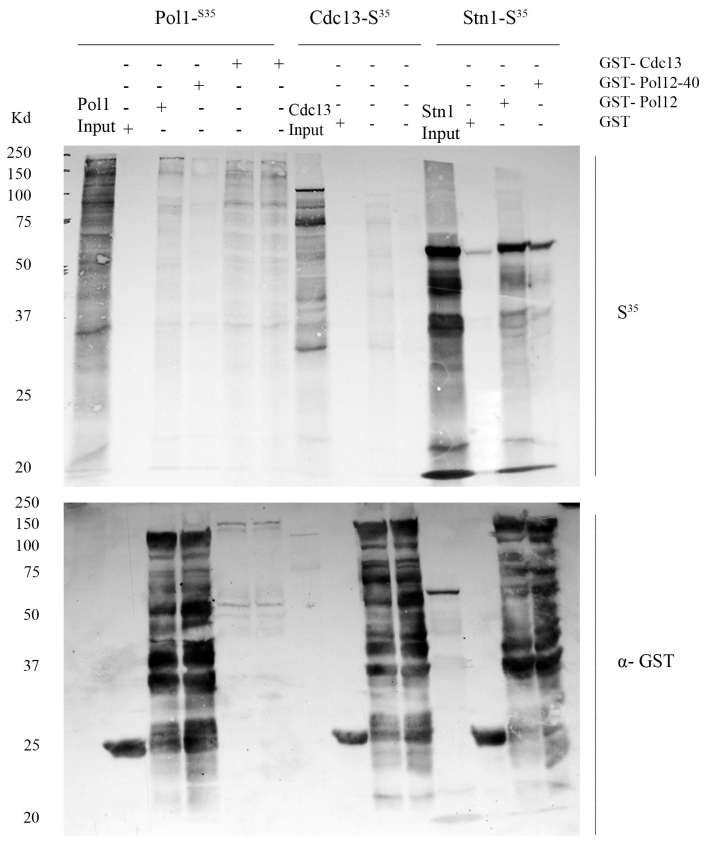

Appendix Figure 3 *in vitro* binding of Cdc13 and Pol1. Bacterially expressed GST-Pol12, GST-Pol12-40, or GST-Cdc13 were immobilized on GST beads, and then incubated with 35S-methionine-labelled Pol1 that was generated in rabbit reticulocyte lysates using POL1 (pPC35) plasmid. Parallel experiments were performed with E. coli produced GST that was immobilized on beads and incubated with the same amount of 35S- labeled Pol1. 20% of 35S-labelled Pol1 reactions and the pull-down products from GST, GST-Pol12, GST-Pol12-40, and GST-Cdc13 incubations were subjected to SDS–PAGE on a 10% gel, transferred to a nitrocellulose membrane and analyzed by exposure to film for 5 days. The membrane was then probed with anti-GST to determine the amount of total GST protein present in each reaction. Parallel experiments were conducted with 35S-methionine-labelled Cdc13 (pVL 427) and Stn1 (pPC7) produced from plasmid DNA incubated with GST-Pol12 and GST-Pol12-40. Experiment conducted on 8/26/09.